Altuna Ruiz de Eguino, Amaia (2016) *Polymer microspheres: synthesis, characterisation and post-functionalisation by olefin metathesis.* PhD thesis.

https://theses.gla.ac.uk/7712/

POLYMER MICROSPHERES:
Synthesis, Characterisation and Post-Functionalisation by Olefin Metathesis

Amaia Altuna Ruiz de Eguino

A thesis submitted in fulfilment of the requirements for the Degree of Doctor of Philosophy in Chemistry.

School of Chemistry

College of Science and Engineering

University of Glasgow

June 2016

I declare that, except where explicit reference is made to the contribution of others, the content of this thesis is the result of my own work and has not been submitted for any other degree at the University of Glasgow or any other institution.

Signed:

Date:

ACKNOWLEDGEMENTS

First, I would like to express my deep gratitude to Dr. Joëlle Prunet for sharing her knowledge and for all the support, encouragement and guidance that she has given to me during my stay in Glasgow. Thank you also to Prof. Peter Cormack for all his support, guidance and for sharing his knowledge with me.

I would also like to thank to Prof. Stephen Wimperis and Nicole Faure for the solid-state NMR analysis.

Needless to say that without the support of the technical staff of both universities, many of the analyses would not have been possible; thank you very much to Alex Clunie, Lindsay McCulloch, Gavin Bain, Kim Wilson, David Adams and James Gallagher.

A huge thank you to all members of both of the Cormack and the Prunet group, past and present, and to the members of the organic section in the University of Glasgow for all of their support and for making my time such an enjoyable and memorable experience. I would also like to especially thank to Alex and Stephen from the Prunet group for all their help and the great moments that we spend together in the lab and outside the lab.

A big thank you as well to Tim, Jen, Kim, Omer, Ain, Ali, Daniela, Mariam, Maitane and Danny for all their help and all the long talks in the office as well as the Stirling lab weekend away because it was “very emotional” and we had a great time there.

I would also like to thank to all my Glasgow friends; Irene M., Marc, Mimmo, Javi, Arrate, Rubén, Rurru and Fra for all the good times and parties that we have had together. I would like to thank to Loretta because she has become in a good friend and she gave me a lot of support and encouragement. A mi gran amiga Irene que nos conocimos la primera semana y hemos pasado por todo (tanto bueno como malo) juntas y ha sido un gran apoyo para mí. Eskerrik asko nire betiko lagunei; Xabi, Eneko, Jaione, Amaia, Uxue, Ren, Irene, Lili, Iker, Raúl, Jurgi, Marijo eta Ido beti hor izan zaretelako bueltatu naizenean.

Me gustaría agradecer enormemente a Luis por todo lo que me ha aguantado, tranquilizado, ayudado y animado durante todo este tiempo. También agradezco a toda mi familia, por la cual siempre me he sentido animada y arropada.

Nire ahizpari ere izugarri eskertzea gustatuko litzaidake munduko ahizparik hoberena delako eta hemen egon naizen udara guztitean nirekin egoteko etorri delako.

Finalmente me gustaría agradecer de todo corazón a mis padres que siempre me han animado y me han ayudado en todo para que esto haya sido posible.

Eskerrik asko guztioi!!

Nire gurasoei eta nire ahizpari,

beraiek gabe hau ez litzatekeelako posible izango.

ABSTRACT

Porous polymer particles are used in an extraordinarily wide range of advanced and everyday applications, from combinatorial chemistry, solid-phase organic synthesis and polymer-supported reagents, to environmental analyses and the purification of drinking water. The installation and exploitation of functional chemical handles on the particles is often a prerequisite for their successful exploitation, irrespective of the application and the porous nature of the particles. New methodology for the chemical modification of macroreticular polymers is the primary focus of the work presented in this thesis.

Porous polymer microspheres decorated with a diverse range of functional groups were synthesised by the post-polymerisation chemical modification of beaded polymers *via* olefin cross metathesis. The polymer microspheres were prepared by the precipitation polymerisation of divinylbenzene in porogenic (pore-forming) solvents; the olefin cross-metathesis (CM) functionalisation reactions exploited the pendent (polymer-bound) vinyl groups that were not consumed by polymerisation. Olefin CM reactions involving the pendent vinyl groups were performed in dichloromethane using second-generation Grubbs catalyst (Grubbs II), and a wide range of coupling partners used. The results obtained indicate that high quality, porous polymer microspheres synthesised by precipitation polymerisation in near-θ solvents can be functionalised by olefin CM under very mild conditions to install a diverse range of chemical functionalities into a common polydivinylbenzene precursor.

Gel-type polymer microspheres were prepared by the precipitation copolymerisation reaction of divinylbenzene and allyl methacrylate in neat acetonitrile. The unreacted pendent vinyl groups that were not consumed by polymerisation were subjected to internal and external olefin metathesis-based hypercrosslinking reactions. Internal hypercrosslinking was carried out by using ring-closing metathesis (RCM) reactions in toluene using Grubbs II catalyst. Under these conditions, hypercrosslinked (HXL) polymers with specific surface areas around 500 m^2g^{-1} were synthesised. External hypercrosslinking was attempted by using CM/RCM in the presence of a multivinyl coupling partner in toluene using second-generation Hoveyda-Grubbs catalyst. The results obtained indicate that no HXL polymers were obtained. However, during the development of this methodology, a new type of polymerisation was discovered with tetraallylorthosilicate as monomer.

ABBREVIATIONS

Abs.	Absorbance
Ac	Acetyl
AIBN	2,2'-Azo*bis*(isobutyronitrile)
AMA	Allyl methacrylate
AMI	Allyl maleimide
AOI	2-(Acryloyloxy)ethylisocyanate
ATRA	Atom-transfer radical addition
ATRP	Atom-transfer radical polymerisation
A.U.	Arbitrary units
Av.	Average
BET	Brunauer-Emmett-Teller
BCMBP	4,4'-*Bis*(chloromethyl)-1,1'-biphenyl
BOC	*tert*-butyloxycarbonyl
b.p.	Boiling point
BPO	Benzoyl peroxide
BrS	Bromostyrene
CED	Cohesive energy density
CI	Chemical ionisation
CM	Cross Metathesis
CME	Chloromethyl ether
CTA	Control transfer agent
CuAAC	Copper-catalysed azide/alkyne cycloaddition

CV	Coefficient of variation
Def.	Deformation
DIAD	Diisopropyl azodicarboxylate
DMA	Dimethylacetamide
DMAP	4-(Dimethylamino)pyridine
DMF	Dimethylformamide
DVB	Divinylbenzene
DMAEMA	*N*-*N*-Dimethylaminoethyl methacrylate
DMPA	Dimethylolpropionic acid
DMSO	Dimethyl sulfoxide
EDX	Energy-dispersive X-ray analysis
ESI	Electrospray ionisation
Et	Ethyl
FDA	Formaldehyde dimethyl acetal
Fmoc	9-Fluorenylmethoxycarbonyloxy
Fmoc-allylgly-OH	Fmoc-*L*-allylglycine
Fmoc-O-Su	Fmoc-hydroxysuccinimide
FRP	Free radical polymerisation
FT-IR	Fourier-Transform Infrared
GA	Glycidyl acrylate
GMA	Glycidyl methacrylate
GII/Grubbs II	Second-generation Grubbs catalyst
HDA	Hetero Diels-Alder

HEMA	Hydroxyethyl methacrylate
HGII	Second-generation Hoveyda-Grubbs catalyst
HPLC	High performance liquid chromatography
HRMS	High-resolution mass spectrometry
HXL	Hypercrosslinked
Hz.	Hertz
IEC	Ion-exchange capacity
MA	Maleic anhydride
Max.	Maximum
Me	Methyl
MEK	Methyl ethyl ketone
MI	Maleimide
Min.	Minimum
Mon.	Monomer
m.p.	Melting point
MVI	Methylvinylisocyanate
NAS	*N*-acryloxysuccinimide
NHS	*N*-hydroxysuccinimide
NMAS	*N*-methacryloxysuccinimide
NMO	4-Methylmorpholine *N*-oxide
NMP	Nitroxide-mediated polymerisation
NMR	Nuclear magnetic resonance
PDMS	Poly(dimethylsiloxane)

PE	Petroleum ether
PFP	Pentafluorophenyl
PP	Precipitation polymerisation
RAFT	Reversible addition-fragmentation chain transfer
RCM	Ring-closing metathesis
Ref.	Reference
Rf	Retention factor
RO(M)P	Ring-opening (metathesis) polymerisation
RRM	Ring-rearrangement metathesis
r.t.	Room temperature
SAX	Strong anion-exchanger
SCX	Strong cation-exchanger
SD	Standard deviation
SEM	Scanning electron microscopy
SMANCS	Poly(styrene-co-MA) conjugated neocarzinostatin
Solv.	Solvent
SPE	Solid-phase extraction
Str.	Stretching
T	Transmittance
TAOSi	Tetraallylorthosilicate
TAPSi	Tris(allyloxy)(phenyl)silane
TBP	*N*,*N*-dimethyl-*S*-thiobenzoyl-thiopropionamide
TEA	Triethylamine

TEG	triethylene glycol
TFA	Trifluoroacetic acid
THF	Tetrahydrofuran
TLC	Thin layer chromatography
Tol.	Toluene
TT	Thiazoleidine-2-thione
TVSi	Tetravinylsilane
UV	Ultraviolet
VBC	Vinylbenzylchloride
VDM	2-Vinyl-4,4-dimethyl-5-oxazoline
Vol.	Volume
WAX	Weak anion-exchanger
WCX	Weak cation-exchanger

CONTENTS

CHAPTER 1

CHAPTER 2

CHAPTER 3

CHAPTER 4

CHAPTER 5

CHAPTER 6

CHAPTER 1

INTRODUCTION

1.1 POLYMER MODIFICATION

In polymer chemistry, a polymerisation is a process in which monomer molecules react together in a chemical reaction to give long polymer chains. Some of the polymerised monomers however, do not have any functional groups and therefore cannot be functionalised to either improve the properties of the formed polymers or to be used for different scopes. In order to install functionality in an easy and straightforward way, direct copolymerisation reactions were developed. This new polymerisation technique was carried out between two different monomers wherein one contains a functional or pendent functional group. One of the most common examples is the copolymerisation between styrene and maleic anhydride (MA) which generates poly(styrene-*alt*-MA) polymer.(1) Another example of the formation of functional polymers is the direct copolymerisation of α olefins (Polyethylene and polypropylene) with functional monomers such as glycidyl methacrylate (GMA) or MA, by using a Ziegler-Natta catalyst or similar catalysts. Difficulties started with the use of this kind of catalysts as they exhibit intolerance to Lewis bases, which led to the deactivation of these highly oxophilic catalysts. As a result, very stable complexes between the catalyst and the heteroatoms present in the monomers were obtained.(2-4)

Living polymerisation was then used to form functionalised polymers by direct copolymerisation, as it allows control over the molecular weight, the architecture and the composition of the polymer. Traditional living cationic or anionic polymerisation techniques offer very limited possibilities for the formation of functionalised polymers *via* direct copolymerisation reaction. Nevertheless, this situation was improved due to the combination between the advances in catalytic copolymerisation and the development of controlled (living) radical polymerisation, as functional group tolerance was increased. In spite of these improvements, with this kind of polymerisation there is a broad range of side-chains functionalities that cannot be introduced directly during the polymerisation. Such functional groups will interfere during the polymerisation reaction as they can participate in side-chain reactions that lead to the loss of control or the prevention of a controlled polymerisation reaction.(5)

More recently, functionalisation-grafting techniques have been used in order to install functionality directly during the polymerisation. Polymer grafting can be carried out in three different ways (Figure 1.1); by grafting *in situ* the polymers or copolymers containing functional groups located along the polymer backbone (grafting-from), by interchanging the labile atoms of the polymer backbone (grafting through) and by grafting functional polymer chains, which have affinity to some species of the polymer backbone (grafting onto). However, in many of the previously mentioned techniques, post-polymerisation or post-grafting modification reactions are needed.(1)

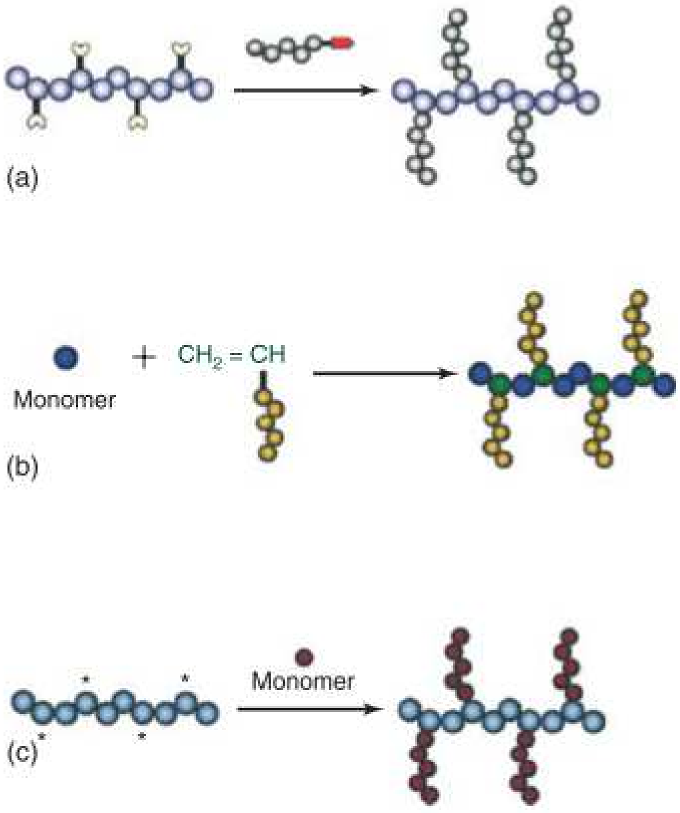

Figure 1.1 Schematic representation of; a) grafting-onto, b) grafting-through, and c) grafting-from methods.(1)

Post-polymerisation modification reactions offer a more attractive approach for the synthesis of functionalised polymers, as it allows access to a broad range of functionalised polymers that cannot be prepared by direct copolymerisation of the corresponding monomers. With this method, apart from installing the desired functionality onto the graft polymers, the difficulties encountered with Ziegler-Natta type catalysts and the limited functional groups tolerance of living polymerisation can be solved.

1.2. POLYMER ANALOGOUS MODIFICATION

The history of post-polymerisation modification or polymer analogous modification is as long as the history of polymer science. In 1833 the term “polymer” was coined by Jöns Jakob Berzelius who worked in the area that nowadays is called polymer science. A few years later, in 1840, the first post-polymerisation functionalisations were performed by Hanock and Ludsdorf who independently reported the discovery of a tough and elastic material by the addition of sulfur to natural raw rubber. In 1847 Schönbein discovered the nitrocellulose by exposing cellulose to nitric acid. In 1865, Schüzenberg modified cellulose with acetic anhydride in a sealed tube to obtain cellulose acetate, which is used as photographic film, artificial silk, membrane materials etc. However, the nature of these materials and their modifications were not completely understood in the late nineteenth and early twentieth centuries until Staudinger coined the term macromolecule. In the 1920s Staudinger demonstrated the existence of macromolecules, and studied the polymer analogous reactions for the obtainment of functionalised materials, which increased the use of post-polymerisation modification reactions.(6)

Serniuk *et al.*(7) reported in 1948 butadiene-based polymer functionalisation with aliphatic thiols *via* thiol-ene addition. In the 1950s Merrifield(8) used chlorinated polystyrene-divinylbenzene beads to develop solid-state polymer synthesis. In the 1960s modification of halogenated or lithiated poly(meth)acrylates was studied and later, Iwakura *et al.*(9) studied the modification of polymers bearing pendent epoxide groups. Although several post-polymerisation modifications were successfully carried out in those years, there were not many chemical modification reactions until the 1990s, when living/controlled radical polymerisation was discovered. The controlled radical polymerisation techniques discovered were: atom-transfer radical polymerisation (ATRP), reversible addition-fragmentation chain transfer (RAFT) and nitroxide-mediated polymerisation (NMP). These techniques are more tolerant of distinct functional groups in comparison to regular polymerisation reactions, and their mild reaction conditions prevent undesirable side-reactions.(6)

The development of controlled radical polymerisation techniques coincided with the discovery/revival of the so-called click reactions (copper-catalysed azide/alkyne cycloaddition (CuAAC), thiol-ene addition among others). These reactions have prompted an exponential growth in the versatility of post-polymerisation reactions since 1990s. There are nine main classes of polymer analogous modifications (Figure 1.2), which modify the functional groups in a single reaction step after polymerisation, in high yield, and with enough chemoselectivity and independence to form polymer analogues with different functional groups.(5)

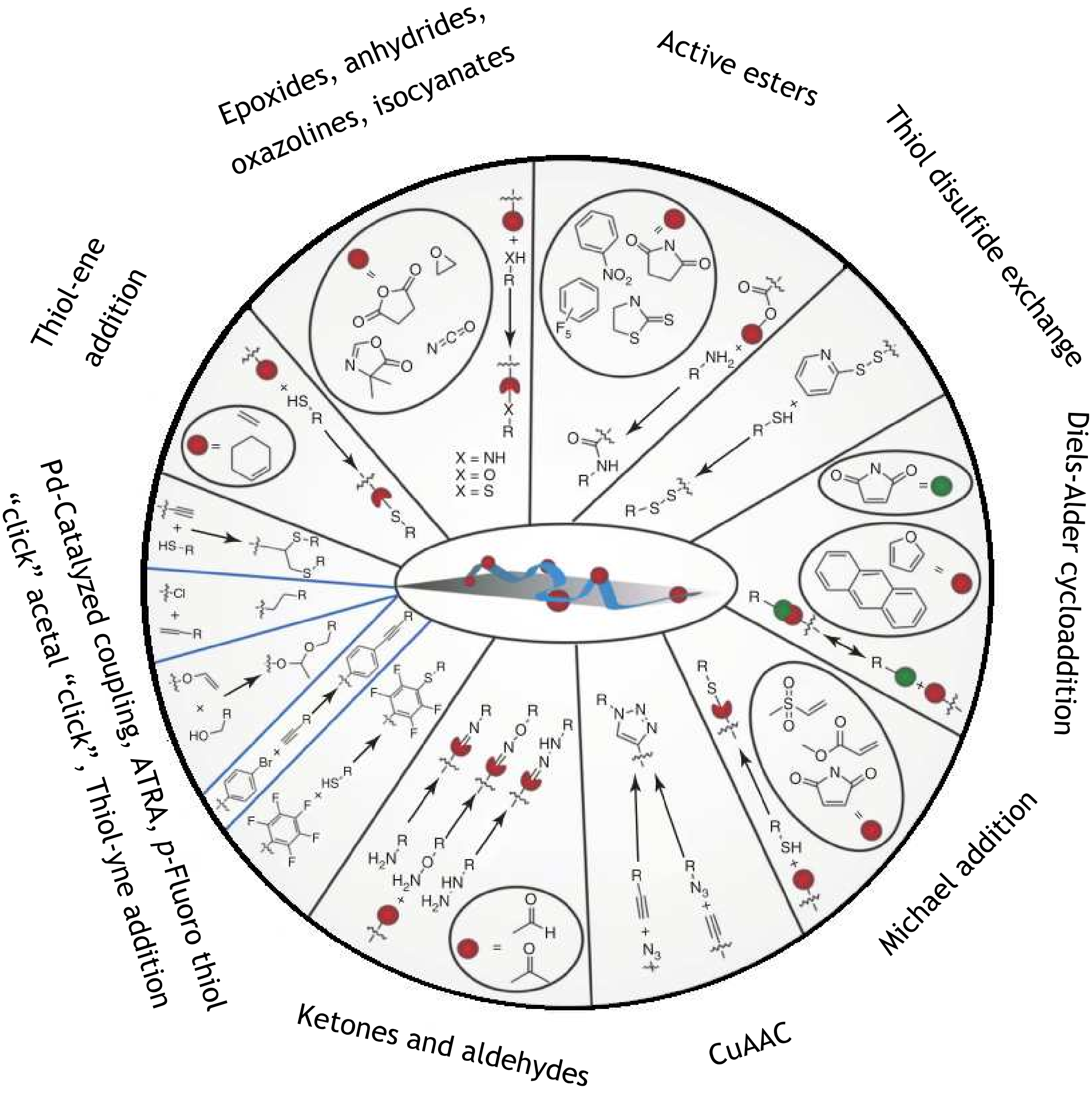

Figure 1.2 Nine different classes of functionalisation reactions.(6)

1.2.1. *Post-polymerisation modification via thiol-ene addition*

The radical addition of thiols to polymeric alkenes such as poly(1,2-butadiene) as post-polymerisation modification was reported by Serniuk and coworkers in 1948. The addition was carried out by a radical source or by ultraviolet (UV) and followed the anti-Markovnikov addition rule.(7) They proposed and later on this was confirmed by Romani and coworkers(10) that the pendent vinyl groups generated after the radical polymerisation of poly(1,2-butadiene) were functionalised by 1,2-addition of the thiols. In 2004, Justynska and Schlaad demonstrated the versatility of this post-polymerisation modification reaction by functionalising poly(1,2-butadiene) with a wide range of functional groups such as carboxylic acids, amines and alcohols among others (Figure 1.3).(11)

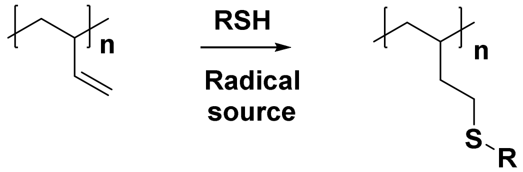

Figure 1.3 Radical thiol-ene addition to poly(1,2-butadiene).(12)

Due to the proximity of other double bonds, the radical formed after the addition of the thiol may attack another double bound to form a six-membered cyclic structure rather than undergoing an intermolecular reaction with a molecule of thiol (Figure 1.4a). To avoid this cyclisation reaction, Schlaad and coworkers(13) carried out the post-polymerisation modification at high concentrations and at low temperature. Gress *et al.*(14) also demonstrated that by increasing the distance between the neighbouring double bonds, the cyclisation was eliminated (Figure 1.4b).

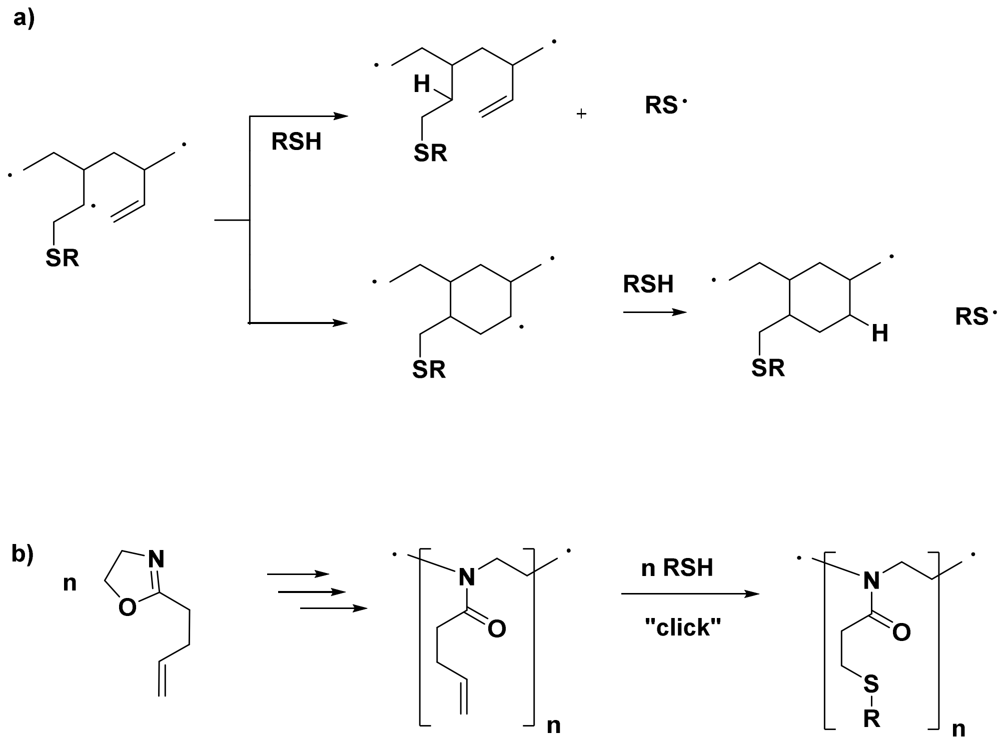

Figure 1.4 a) Possible cyclisation reaction of poly(1,2-butadiene).b) Synthesis and click modification of poly(2-(3-butenyl)-2-oxazoline).⁽¹⁴⁾

Different kinds of initiators can be used in order to form radicals *via* thiol-ene post-polymerisation modification. Hawker and coworkers studied the initiation step of the reaction by using photochemical and thermal initiators. They reported that in both cases a complete conversion was obtained, but milder conditions and shorter reaction times could be applied when a photoinitiator was used (Figure 1.5).(15)

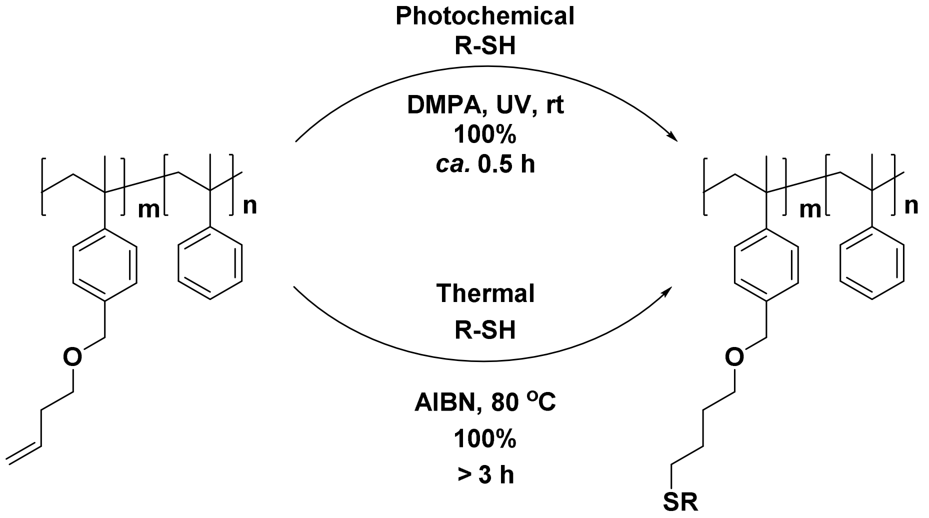

Figure 1.5 Comparison between photochemical and thermal initiations.(15)

Some years later, in 2011, Ates *et al.* reported the synthesis of an unsaturated polyester *via* enzymatic ring-opening polymerisation (ROP) of the corresponding cyclic ester with backbone alkene groups. They proved that those alkenes could undergo post-polymerisation modification *via* thiol-ene addition (Figure 1.6). However, an excess of thiol had to be used in order to obtain near-quantitative yields, as the disubstituted alkenes were less reactive than pendent vinyl groups.(16)

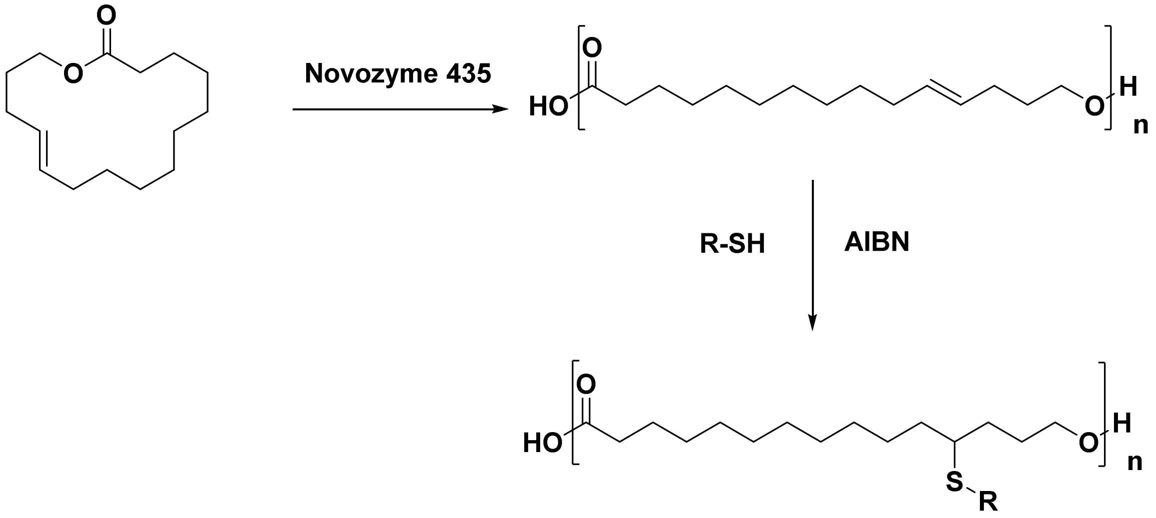

Figure 1.6 Enzymatic ROP and subsequent thiol-ene addition reactions.(16)

Most recently, in 2015, Boyer and coworkers presented a photoredox thiol-ene reaction in which polymers such as poly(butadiene) or poly(allylmethacrylate), were post-functionalised in less than 20 min under aerobic conditions with a wide range of functional thiols. They also reported that the use of *N*-methyl-2-pyrrolidone as solvent and *p*-toluidine redox mediator improved the reaction rates and avoided the formation of by-products.(17)

1.2.2. Post-polymerisation modification of epoxides, anhydrides, oxazolines and isocyanates

Epoxides, anhydrides, oxazolines and isocyanates have a relative long history in polymer chemistry. The extensive use of these functional groups in post-polymerisation modification reactions is due to their tolerance toward radical-based polymerisation techniques. The first study of post-polymerisation modification of polymers containing epoxides was carried out in the 1960s by Iwakura and coworkers. They modified polyglycidyl acrylate (polyGA) and polyGMA with secondary amines such as di-*n*-butylamine, obtaining low to moderate yields of the functionalised polymer.(9) Later, Kalal *et al.*(18) illustrated that the opening of the epoxide could be performed with primary amines using tertiary amines as catalysts. Barbey and Klok exploited the catalytic effect of the tertiary amine groups on epoxide ring-opening by preparing polyGMA-*co*-polyDMAEMA brushes, which contained pendent tertiary amines groups (Figure 1.7). They observed that the presence of these tertiary amines accelerated the post-polymerisation modification reaction with primary amines achieving higher conversions.(19) A drawback of using primary amines with epoxide-functionalised polymers is that they can be crosslinked by further reaction of the resulting secondary amine with another unreacted epoxide group. However, the epoxide functionalised polymers represent a versatile platform as they can react with a wide range of functional groups including carboxylic acids, alcohols, thiols, amines and anhydrides. Recently, Yan *et al.* carried out epoxy-amine post-polymerisation modifications on non-toxic glycopolymers in order to inhibit the adhesion of *Escherichia coli* in cells, but further analysis is required.(20)

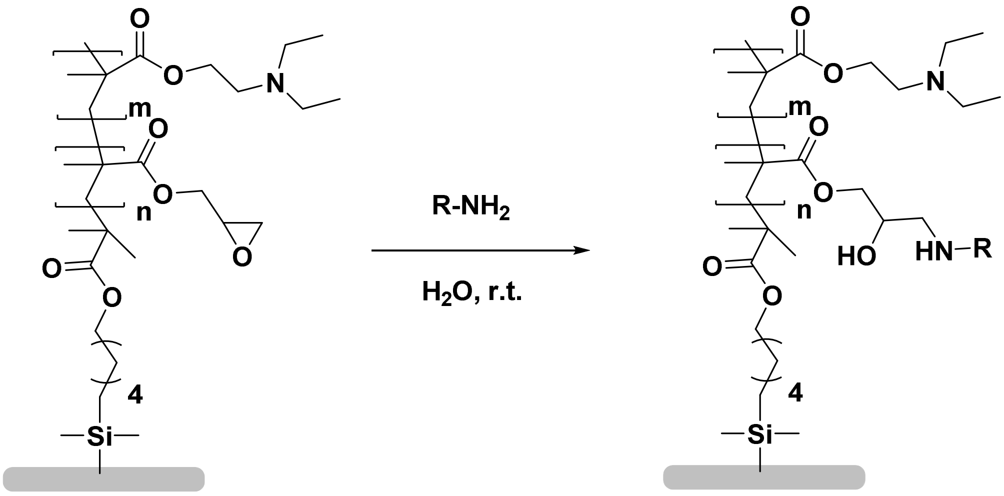

Figure 1.7 Post-polymerisation *via* epoxide ring-opening modification reaction.(19)

Post-polymerisation functionalisation reactions on MA have attracted significant attention since Maeda and coworkers prepared the anticancer agent poly(styrene-*co*-MA) conjugated neocarzinostatin (SMANCS) in the early 1980s.(21) Functionalisation of MA polymers were carried out by using amines and almost full conversion was achieved at room temperature.(22) However, high temperatures are required in order to achieve the closure of the ring and form *N*-substituted maleimides (MI) (Figure 1.8).(23)

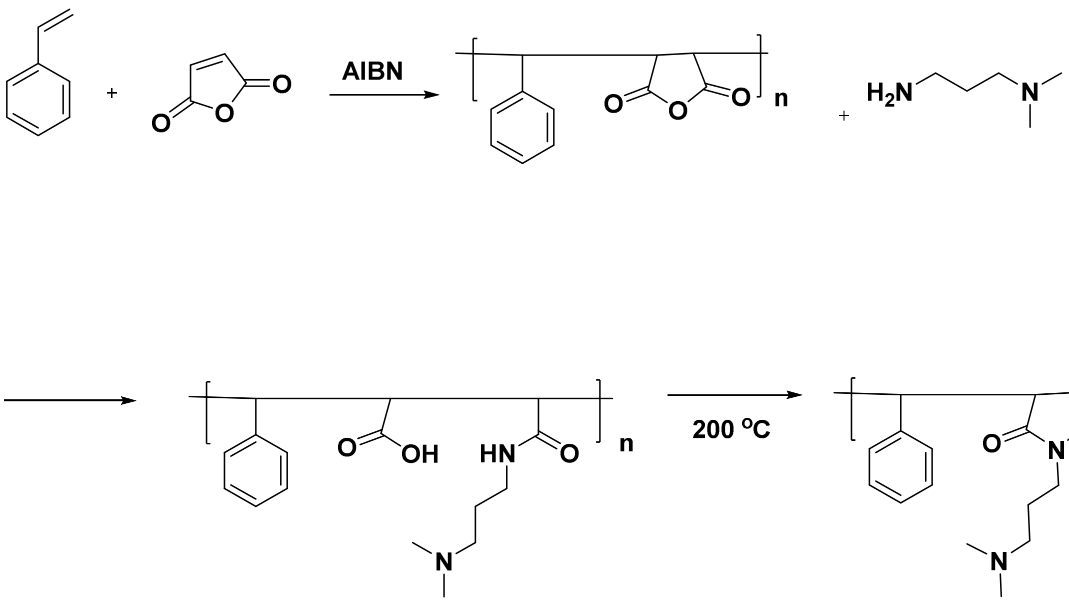

Figure 1.8 Post-polymerisation modification on maleic anhydride.(23)

Post-polymerisation modifications on oxazoline groups were carried out by Taylor and coworkers. They modified the pendent oxazoline groups from the polymer 2-vinyl-4,4-dimethyl-5-oxazoline (VDM) with amines at room temperature (Figure 1.9).(24,25) However, VDM-containing polymers react rapidly and quantitatively with amines such as benzylamine at room temperature. Furthermore, modifications of oxazoline with amines can be performed in aqueous media without any side reactions, which renders them suitable for protein immobilisation.(25)

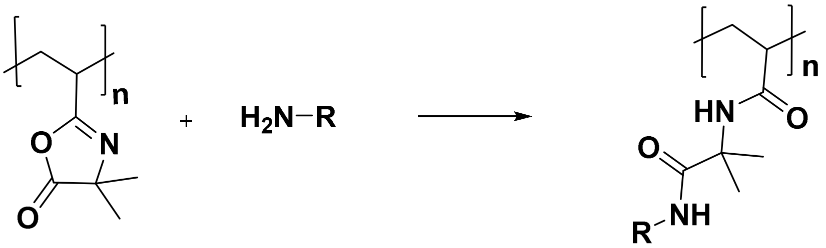

Figure 1.9 Ring-opening reaction of dimethyl azlactone with amines.(25)

Isocyanates are another group that can be easily and quantitatively modified with thiols and amines. The use of a catalyst such as dibutyltin dilaurate is required for quantitative conversions with alcohols.(26) Copolymerisation between MA and 1-methylvinylisocyanate (MVI) monomers gives alternating microstructure and two different functionalisation handles.(27) Beyer and coworkers(26) reported that poly(MVI-*alt*-MA) modified isocyanate and anhydride groups reacted sequentially with an alcohol and amine, respectively (Figure 1.10a). Flores *et al.*(28) reported that 2-(acryloyloxy)ethylisocyanate (AOI) could be homopolymerised by RAFT polymerisation and Hensarling and coworkers demonstrated that polyAOI could be modified in minutes with thiols (Figure 1.10b).(29) Seto *et al.* recently reported that the product obtained from radical copolymerisation between styrene and 2-propenyl isocyanate was stable in water and at room temperature. Modification reactions with amines in water were carried out and they found that primary amines readily reacted in water depending on the hydrophobicity and steric hindrance of the amine (Figure 1.10c).(30)

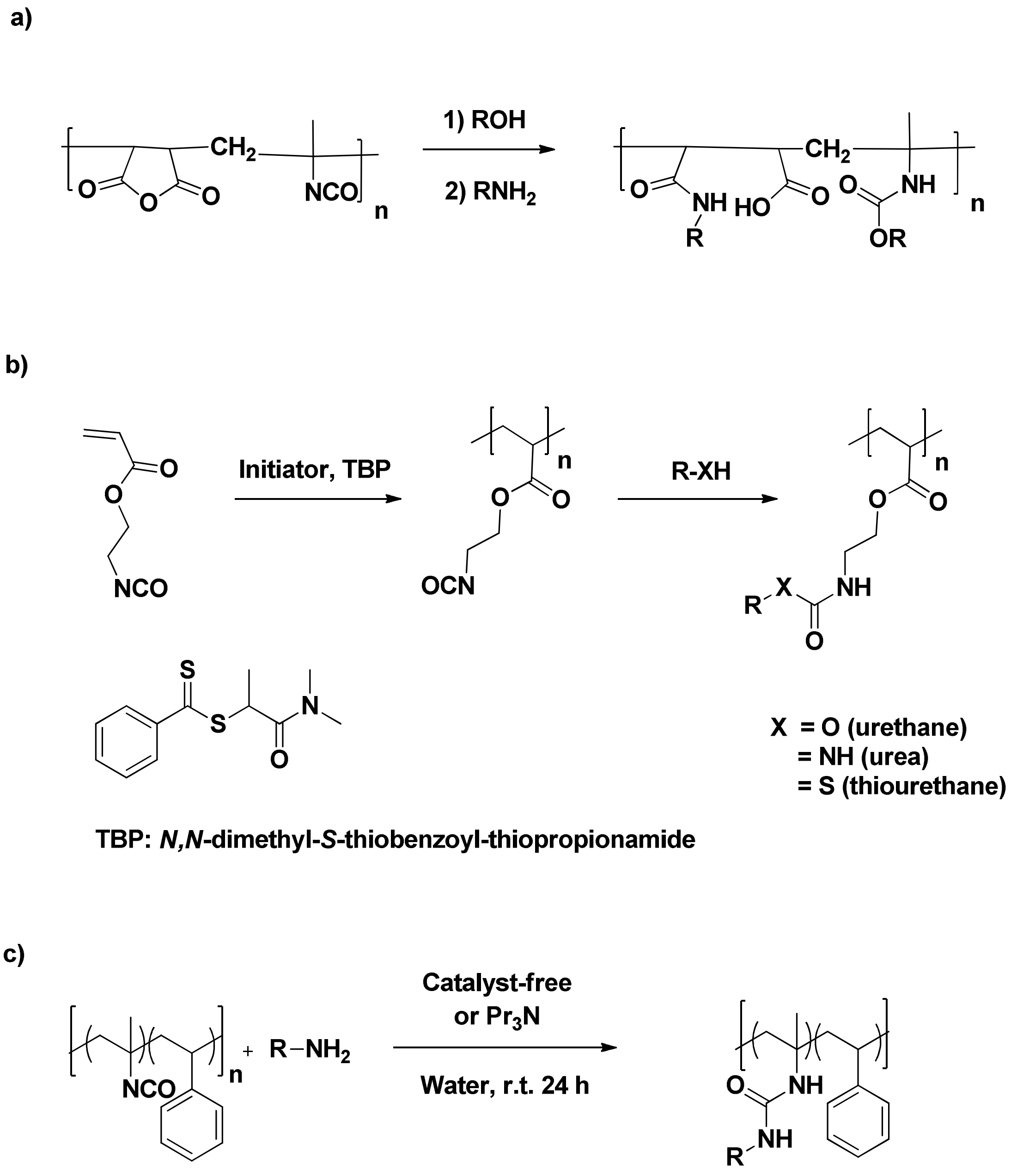

Figure 1.10 a) Sequential modification of the isocyanate and the anhydride of poly(MVI-alt-MA).(26) b) Direct RAFT polymerisation of AOI and isocyanate post-functionalisation with thiols, alcohols and amines.(28) c) Addition of primary amine to isocyanate in water.(30)

1.2.3. Post-polymerisation modification of active esters

The synthesis and post-polymerisation modification of active esters was introduced by Ferruti and Ringsdorf in 1972.(31,32) Since then, active esters have become the most used polymers for post-polymerisation modification as they can be synthesised by both (controlled) radical polymerisation and metal-catalysed polymerisation techniques. On the other hand, due to their reactivity, amines are the most used reagents for post-polymerisation modifications.

N-hydroxysuccinimide (NHS) derivatives such as poly(*N*-acryloxysuccinimide) (polyNAS) and poly(*N*-methacryloxysuccinimide) (polyNMAS) are some of the most frequently used active esters.(31) However, those polymers can only be dissolved in DMF and DMSO and side reactions can take place (Figure 1.11).(33) Wong *et al.* reported a method where side reactions were eliminated by using an excess of amine (TEA) or a proton acceptor (DMAP).(34)

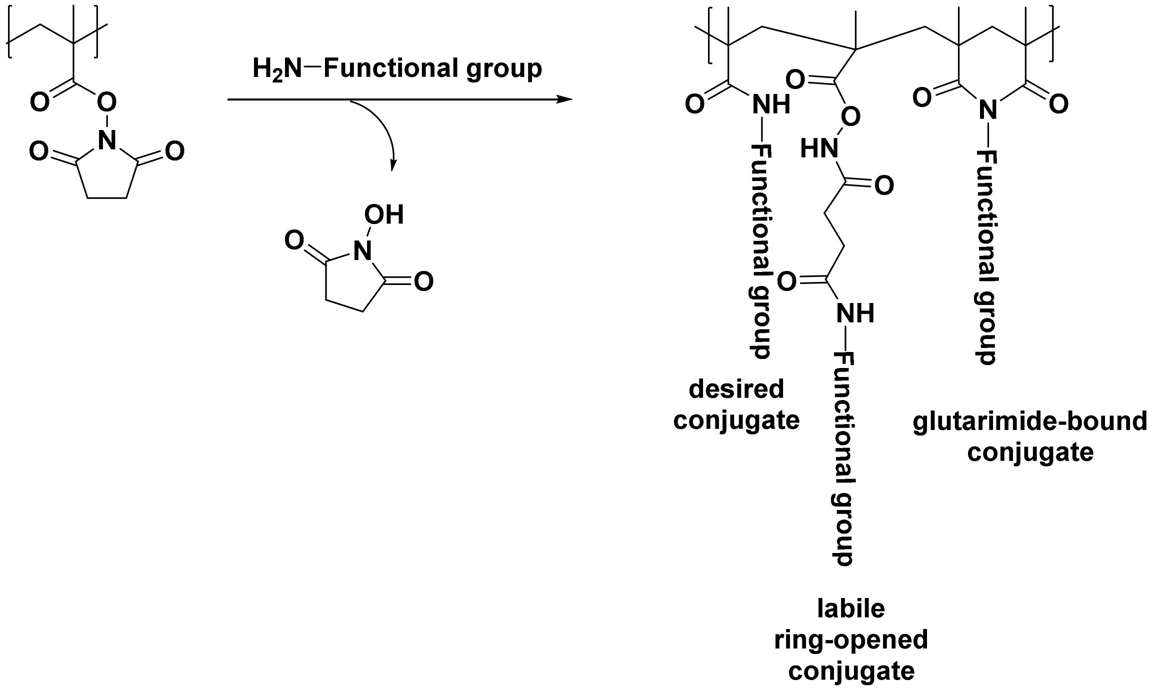

Figure 1.11 PolyNMAS post-polymerisation modification reaction with possible side reactions.(33)

Poly pentafluorophenyl (polyPFP) derivatives such as poly pentafluoro methacrylate(35) or poly pentafluoro acrylate(36) are good alternatives to poly(NHS) derivatives. These polyPFP derivatives can be dissolved in a wide range of solvent comparing to poly(NHS), and they present higher reactivity and better hydrolytic stability. However, ester homopolymers cannot be functionalised in aqueous media as they are not soluble in water.(35) Hoenders *et al.* recently reported the synthesis of diblock copolymers with incompatible groups such as amine and active ester by RAFT polymerisation and further functionalisation of the active ester with another amine to obtain dual functionality compounds (Figure 1.12).(37)

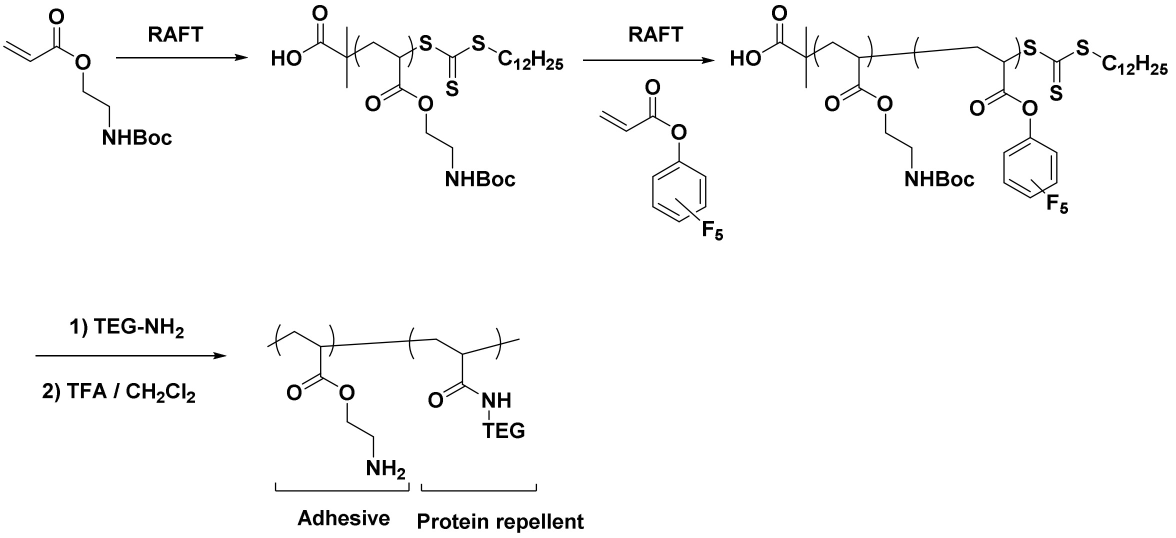

Figure 1.12 RAFT polymerisation of incompatible groups and post-polymerisation modification with amines.(37)

1.2.4. Post-polymerisation modification via thiol-disulfide exchange

Thiol-disulfide exchange is an easy and quick post-polymerisation modification technique used in biological processes such as enzyme activity modulation among others.(38) Pyridyldisulfide-containing polymers can be synthesised by conventional free-radical polymerisation (FRP) or ATRP and their functionalisation is strongly dependent on the pH. Wang(39) and coworkers and Bulmus *et al.*(40) reported two different studies of thiol-disulfide exchange modifications at pH 6 and pH 10. They found that higher conversions were obtained at pH 6, as the protonated pyridine is a better leaving group. Further studies revealed that post-polymerisation modifications *via* thiol-disulfide exchange have to be carried out at pH below 8 to obtain the functionalised product selectively and quantitatively. An advantage of this method is that the thiol exchange generates 2-pyridine-thione, which is inert to pyridyldisulfide functionalities. Furthermore, the disulfide bond formed after the modification reaction can easily be cleaved by reduction or by exchange with another thiol (Figure 1.13).(40)

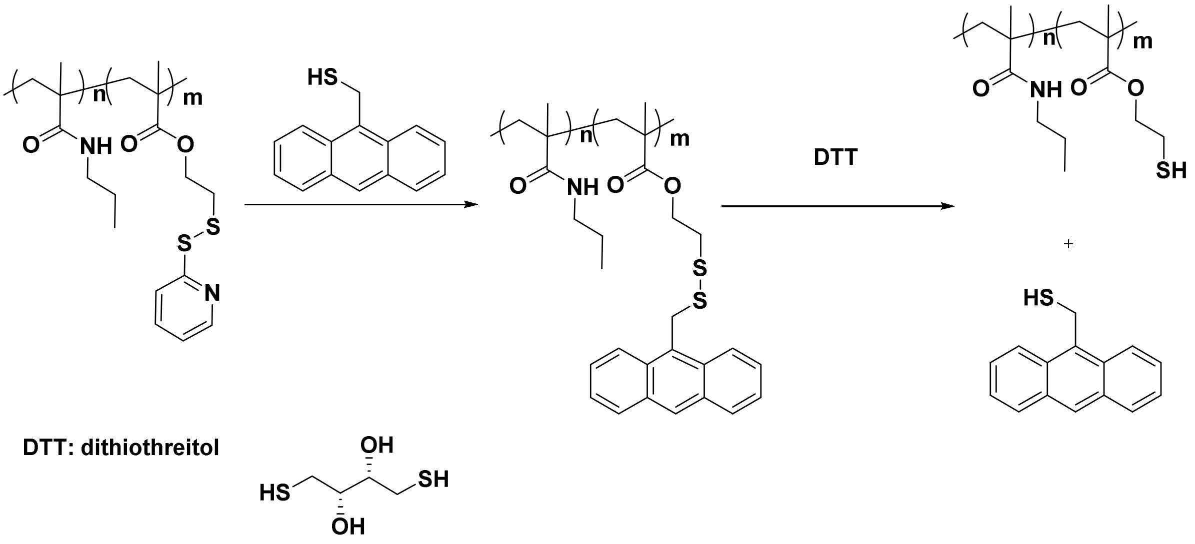

Figure 1.13 Post-polymerisation modification *via* thiol-disulfide exchange and disulfide bond cleavage.(39,40)

In 2006, Ghosh *et al.* reported the copolymerisation of NMAS and 2-(2-pyridylthio)ethyl methacrylate by ATRP, and the resulting polymer contained two orthogonal handles for modifications with amines and thiols (Figure 1.14).(41) More recently, in 2014, Chen *et al.*, managed to synthesise disulfide-linked glycol-nanoparticles that can deliver anticancer drugs into the hepatocellular carcinoma cells, by using thiol-disulfide exchange post-polymerisation modification.(42)

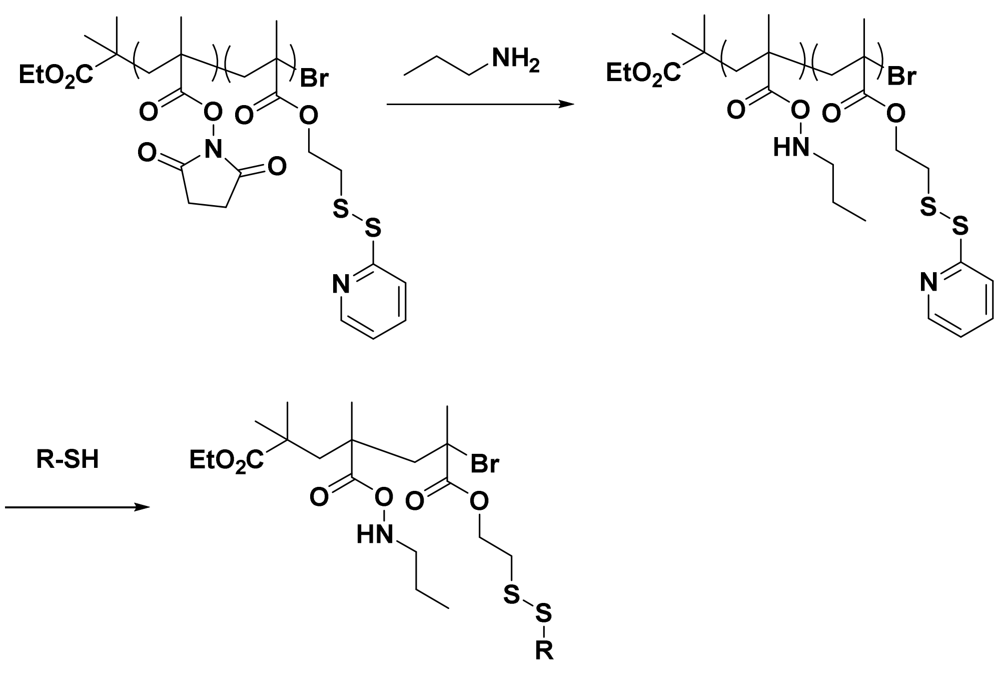

Figure 1.14 Modification of 2-(2-pyridylthio)ethyl methacrylate and NMAS copolymer with thiols and amines.(41)

1.2.5. Post-polymerisation modification via Diels-Alder reactions

The modification *via* Diels-Alder reaction fulfils the “click” criteria as it can be used with a broad range of functional groups, it gives quantitative yields and it does not form any side products.(43) Furthermore, the Diels-Alder reaction can be reversible and the starting diene can be recovered by increasing the temperature in comparison to the temperature of the forward reaction. Due to the resistance to high temperatures, this methodology is being used for the synthesis of thermoresponsive polymers; gels, dendrimers and smart copolymers among others.(44,45)

Using hetero Diels-Alder (HDA) reactions can be a very attractive idea since the heterodienophile can also act as a CTA in RAFT polymerisation.(46) Ravoo and coworkers synthesised a HDA product able to act as CTA for RAFT polymerisation of different acrylates, and molecular weight between 1500 and 6000 gmol^{-}1 were obtained (Figure 1.15).(47)

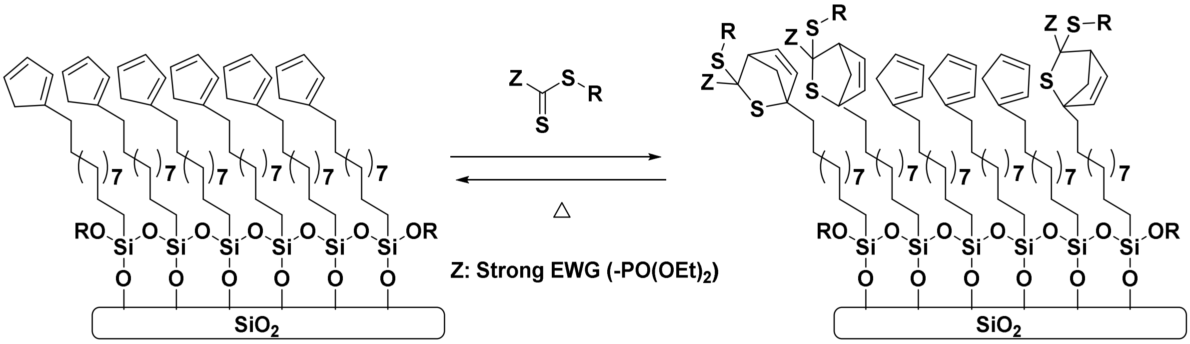

Figure 1.15 Reversible HDA reaction between cyclopentadiene and a RAFT agent as dienophile.(47)

1.2.6. Post-polymerisation modification via Michael-type addition

The Michael addition reaction was developed in 1887 and it has been used in organic chemistry since then. However, it was not until 1965 that Michael addition reactions were used as post-polymerisation modification reactions for the formation of dendrimers and cross-linked networks.(48) Friedman *et al.* reported the quantitative and selective post-polymerisation modification of polymers bearing Michael acceptors such as acrylates, MI and vinyl sulfones with thiols in aqueous media and at room temperature. It was also found that at neutral pH values Michael addition of thiols took place faster than that of amines, generating bifunctional polymers, which contains both amine and thiol groups.(49)

Rieger *et al.* synthesised acrylate-bearing polyethers *via* Michael addition (Figure 1.16a).(50) They obtained high conversions without damaging the backbone structure of the polymer by using an excess of thiols and pyridine in THF at room temperature. ROP can be also used to prepare polyesters with acrylate chains but unfortunately, the functional groups that can act as Michael acceptors are incompatible with radical and ionic polymerisation. Weck and coworkers discovered that monomers bearing MI groups were compatible with ring-opening metathesis polymerisation (ROMP) conditions and therefore, MI containing polymers susceptible to Michael-type post-polymerisation modifications were synthesised (Figure 1.16b).(51)

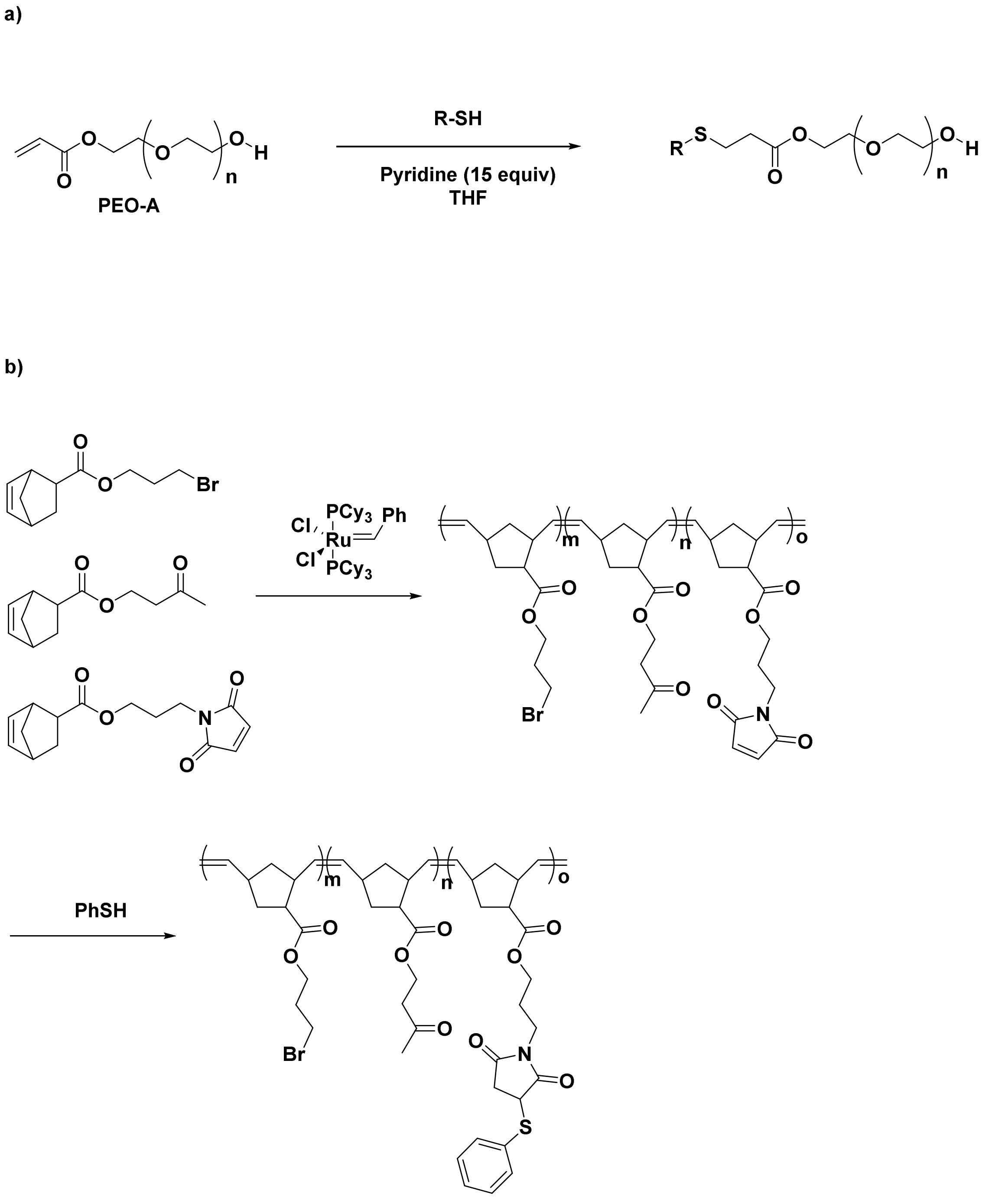

Figure 1.16 a) PEO-A modification with thiols via Michael addition.(50) b) ROMP polymerisation and further post-polymerisation modification by Michael addition.(51)

Michael addition of amines, thiols, alkenes and dicarbonyl groups to polyesters have been recently reported by Castle and coworkers (Figure 1.17a).(52) The conditions used for the Michael addition were highly efficient, solventless and heating using low power microwaves, which allows the reaction to take place in 5 min. Narayanan *et al.* also reported the post-polymerisation modification of chiral amino acids with pendent amine groups *via* aza-Michael addition reaction for the formation of thermostable polymers (Figure 1.17b). They also made a study on the reactivity of Michael acceptors for this addition reaction and it was observed that acrylates were the most reactive species and methacrylates the less reactive ones.(53)

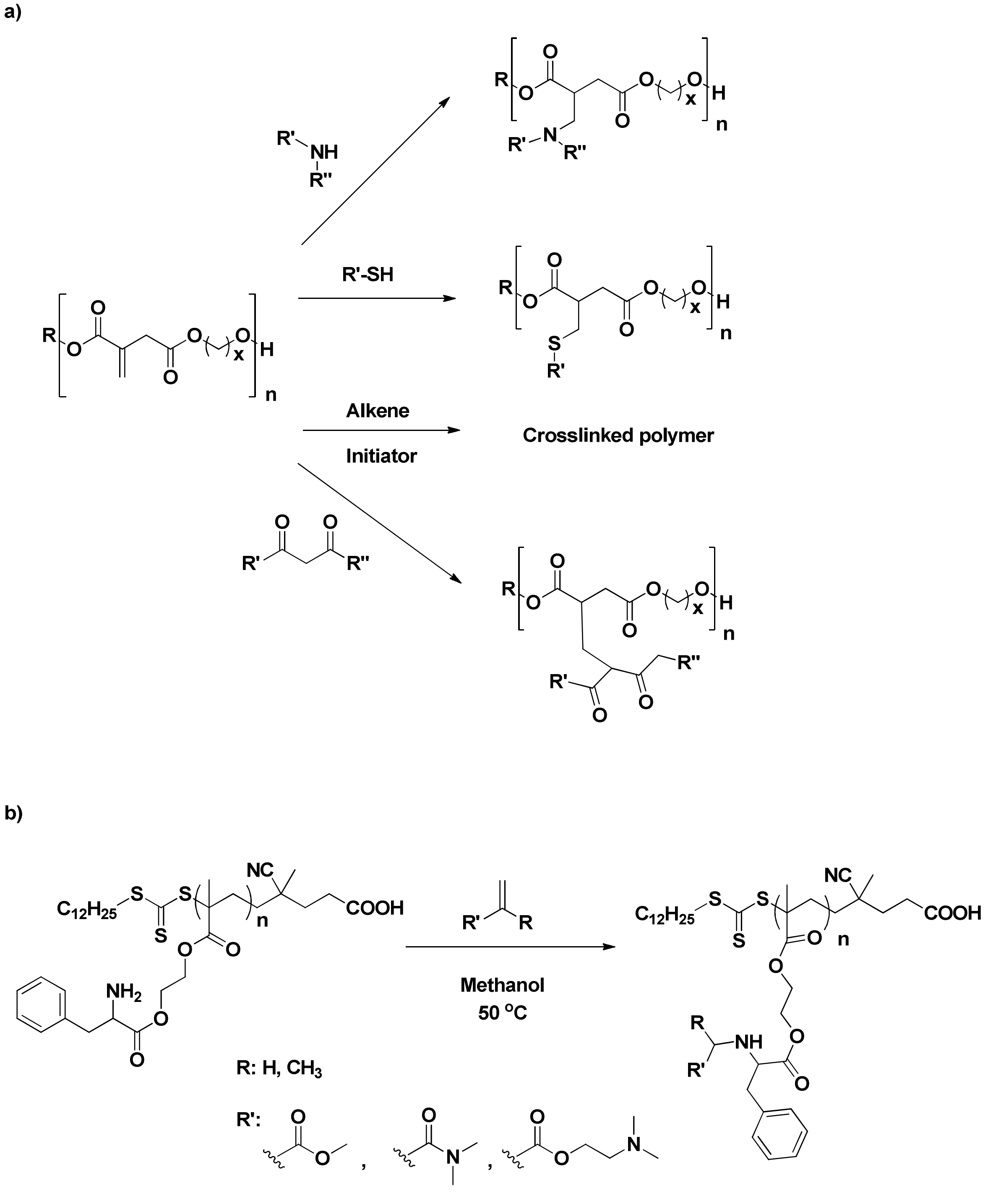

Figure 1.17 a) Michael addition of amines, thiols, akenes and dicarbonyl groups to polyesters.(52) b) Post-polymerisation modification of chiral amino acids *via* aza-Michael addition reaction.(53)

1.2.7. Post-polymerisation modification via azide alkyne cycloaddition reaction

When it was discovered that Huisgen 1,3-dipolar cycloaddition (CuAAC) reaction between azides and alkynes was catalysed by Cu(I) salts, giving quantitative yields in both organic and aqueous media and under mild conditions, the use of this technique grew exponentially. However, ROMP of oxynorbornenes with pendent alkyne groups could not be performed as the alkyne groups reacted with the ROMP catalyst.(54) Matyjaszewski *et al.* showed that azide-containing monomers could undergo ATRP reaction and further functionalisations could be carried out in the presence of CuBr at room temperature. However, polymerisation with propargyl methacrylate proceeded with poor control as side reactions involving the pendent acetylene group occurred.(55) These problems can be solved by protecting the alkynyl monomer by a trimethylsilyl group.(56)

A drawback of CuAAC post-polymerisation modification reaction is that, besides the toxicity of the copper, its removal can be far from trivial as it can complex with the triazole ring and hamper the solubility of the functionalised product. In order to eliminate copper and to use this modification reaction in biological media, a copper-free strategy was developed (Figure 1.18).(57) Zentel and coworkers carried out the functionalisation of the pendent azide groups of polysarcosine *via* strain promoted azide/alkyne cycloaddition in quantitative yields, short reaction times and low amount of equivalents of the cyclooctyne used.(58)

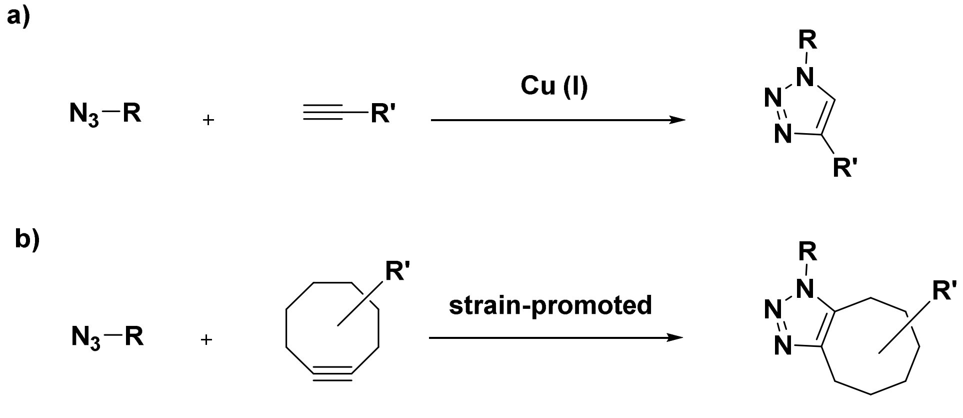

Figure 1.18 a) Cu (I) catalysed Huisgen cycloaddition ("click" chemistry). b) Strain-promoted [3+2] cycloaddition of azides and cyclooctynes.(57)

1.2.8. Post-polymerisation modification of ketones and aldehydes

Polymers bearing pendent ketone groups were reported in the 1960s but it was not until 2006 that Bertozzi and coworkers carried out post-polymerisation modification reactions. They synthesised copolymers containing vinylmethylketone and isopropenyl methyl ketone *via* FRP and RAFT polymerisation techniques and quantitative modification of the pendent ketones was carried out with aminoxy-functionalised sugars (Figure 1.19a).(59) Barret and coworkers worked upon the modification of poly(ketoesters) with ketones as part of the backbone of the polymer to form wide range of oximes (Figure 1.19b).(60) More recently, Ntoukam and coworkers synthesised a polymer bearing an activated ester and ketones and demonstrated the sequential multi-functionalisation in high yield (Figure 1.19c).(61)

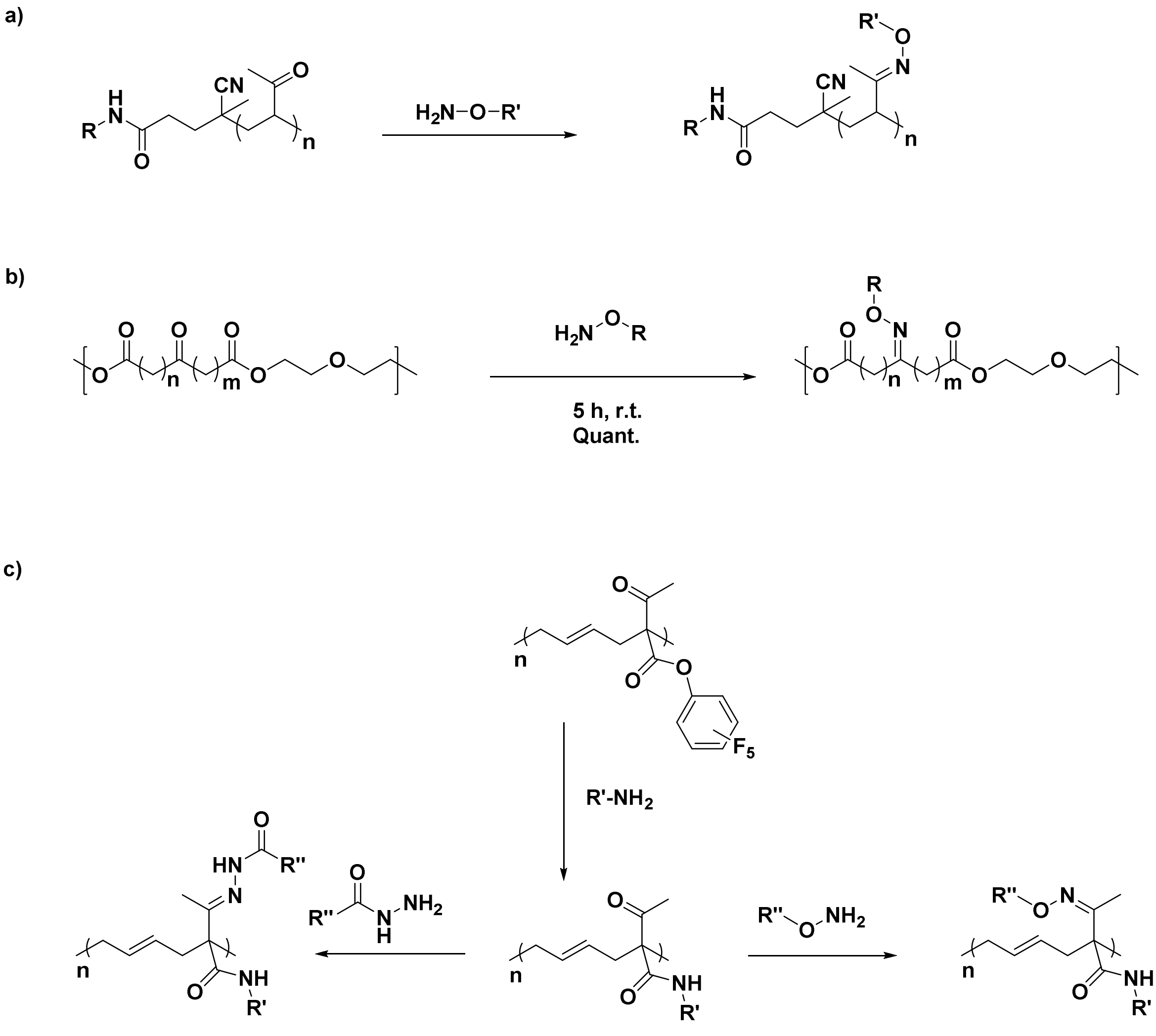

Figure 1.19 a) PolyMVK modification of the ketone with amines.(59) b) Post-polymerisation modification of poly(ketoesters).(60) c) Sequential multifunctionalisation of ketones and active esters.(61)

On the other hand, polymers bearing aldehydes were synthesised and modified after polymerisation in the 1950s. Schulz *et al.* presented the first post-polymerisation modifications on poly(acrolein), which was synthesised *via* redox polymerisation (Figure 1.20a).(62) Taton and coworkers studied the versatility of non-protected aldehyde-functionalised poly(2-oxazoline) for post-polymerisation modification with different amines (Figure 1.20b).(63) Wooley *et al.* reported the direct RAFT polymerisation of aldehyde-containing monomers and Fulton reported in 2008 further functionalisation reactions using an excess of acylhydrazides, obtaining quantitative yields (Figure 1.20c).(64,65)

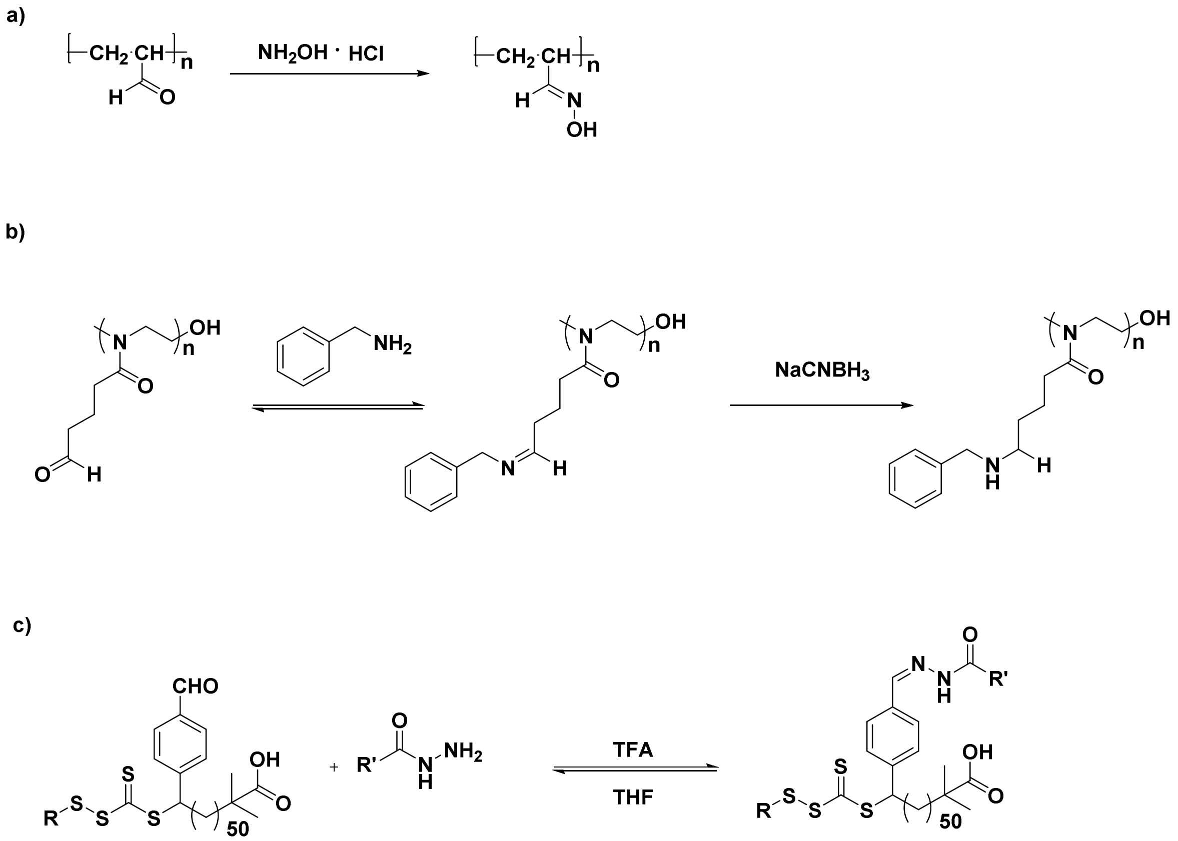

Figure 1.20 Post-polymerisation modification reaction with aldehydes.(62-64)

1.2.9. Post-polymerisation modification via other highly efficient reactions

The previously mentioned post-polymerisation modification techniques are the most used techniques in polymer chemistry for polymer functionalisation. However, there are many more techniques that can be used for functionalisation purposes, although they are relatively new or they are not as used as the others.

The discovery of organopalladium chemistry for the formation of C-C bonds in high yields and milder conditions than the previously used coupling reactions revolutioned organic synthesis as well as polymer chemistry. Albeit the high tolerance that palladium-catalysed coupling reactions have with many functional groups; halide, alkenes and alkynes among others, Sonogashira coupling has been the most used reaction for polymer modification between pendent phenyl halide groups and alkynes.(66) Grubbs and coworkers demonstrated near-quantitative functionalisation of low-molecular-weight poly(bromostyrene) (polyBrS) at room temperature using $[PdCl_2(PhCN)_2]$ as catalyst (Figure 1.21).(67) Kub *et al.* applied this palladium catalysed chemistry to hyperbranched copolymers(68) and Smith and coworkers to conjugated polymers to form stimuli responsive materials.(69)

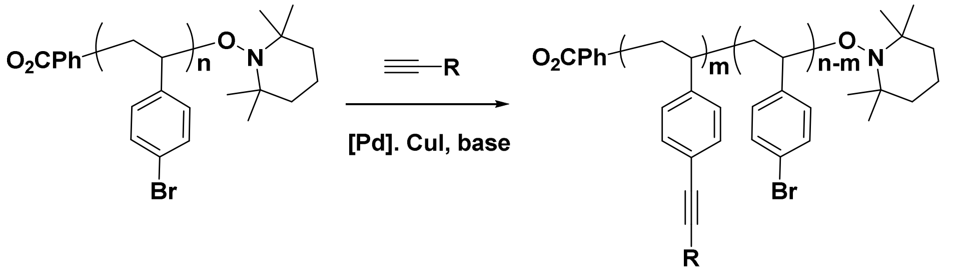

Figure 1.21 Sonogashira coupling modification on polyBrS.(67)

Post-polymerisation modification by using atom-transfer radical addition (ATRA) between alkyl halides and alkenes in the presence of a transition-metal catalyst was studied by Riva *et. al.* (Figure 1.22). They reported different modification reactions using alcohols, esters, epoxides and carboxylic acids. However, the extent of the reaction was limited as C-Cl bonds were reduced to C-H bonds during the modification reaction.(70)

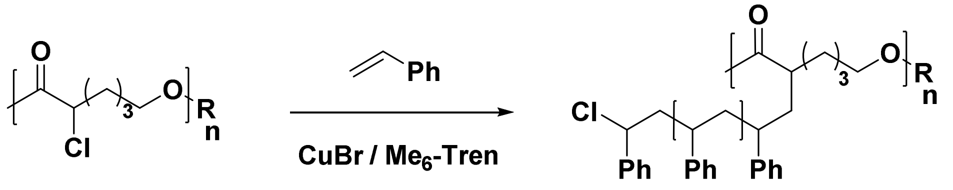

Me_6-Tren: Tris[(2-dimethylamino)ethyl]amine

Figure 1.22 Post-polymerisation modification *via* ATRA.(70)

After the development of CuAAC “click” reactions, alternative “click” reactions that proceed rapidly, quantitatively and under mild conditions have been reported. Schubert and coworkers studied the post-polymerisation modification of polyPFS copolymers *via* PFP click reactions. They showed that the para position of PFS could be rapidly and quantitatively modified by amines and thiols (Figure 1.23a).(71) On the other hand, Wurm and coworkers used the acetal click reaction to modify the pendent vinyl ether side-chains of polyether derivative.

They found that acetal formation with alcohols resulted in an acid-labile bond, which was attractive for biomedical applications that require slow and controlled release of a drug (Figure 1.23b).(72) Although chemical reaction between alkynes and thiols was developed in the 1930s, it was recently rediscovered and it has been used widely in the last few years for the fabrication of macromolecular architectures. Thiol-yne click chemistry offers a metal-free reaction and therefore, it is of benefit for medical use. Van Hensbergen *et al.* synthesised a series of copolymers *via* ROMP containing trimethylsilyl-protected alkynes that were further functionalised by thiol-yne modification. Unfortunately no full conversion was obtained (Figure 1.23c).(73) Nottelet and coworkers prepared some biodegradable crosslinked materials *via* photoradical thiol-yne reaction in high yields, short times and high efficiency.(74) The same group reported thiol-yne photografting reaction for the amphiphilic control of poly(ε-caprolactone)-*g*-poly(ethyleneglycol) copolymers.(75)

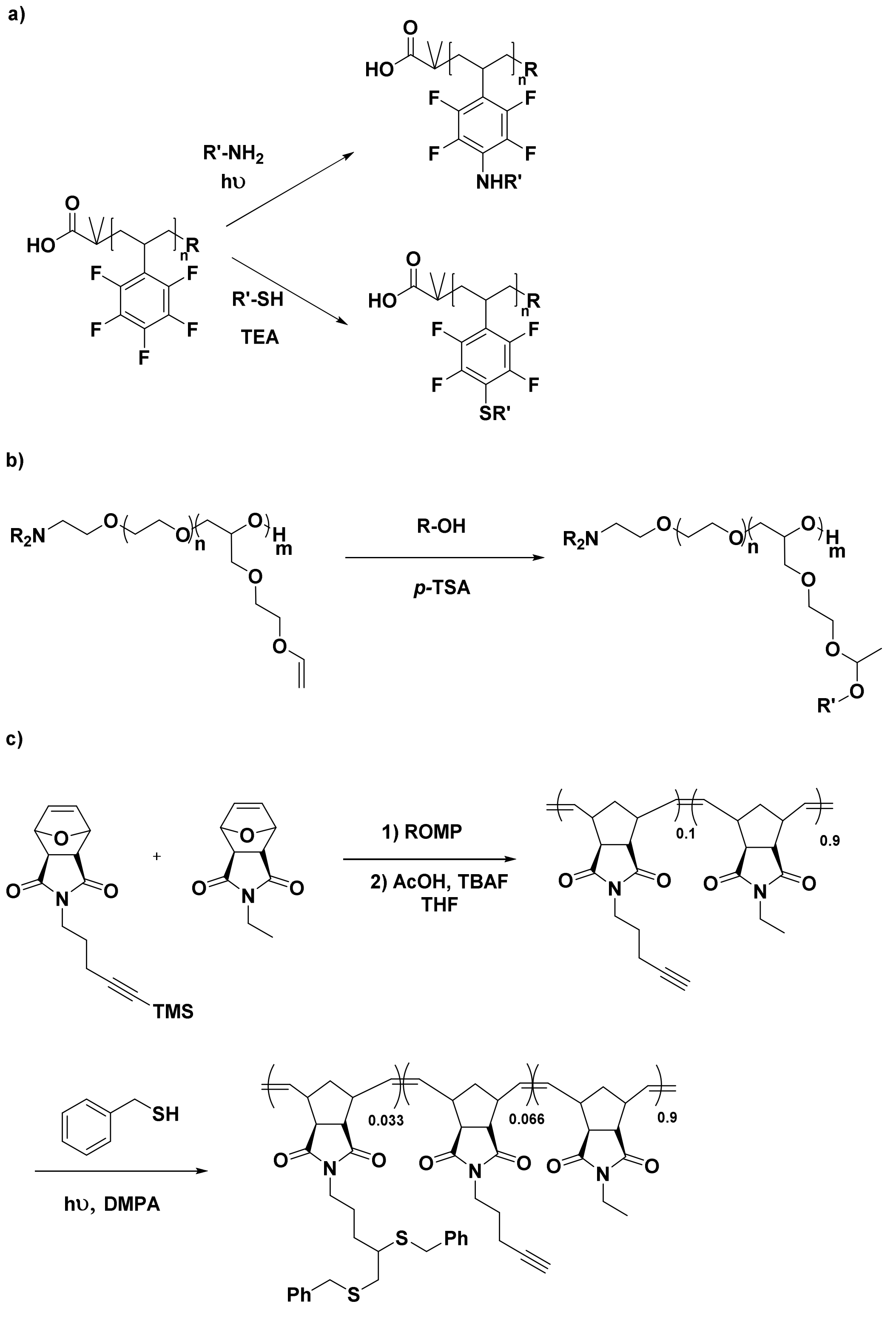

Figure 1.23 a) PFP click reaction,(71) b) acetal click reaction,(72) c) thiol-yne click reaction.(73)

1.3. CHEMICAL MODIFICATION ON POLYMER MICROSPHERES

The use of crosslinkers such as divinylbenzene (DVB) often results in the formation of polymer particles, which generally are spherically shaped as it is the geometric form that has lowest surface to volume ratio with the lowest interfacial tension. Different polymerisation techniques can be followed in order to obtain polymer beads of defined sizes. Particles smaller than 1 μm will be obtained by emulsion polymerisation, between 0.1 and 10 μm by precipitation polymerisation, between 0.1 and 20 μm by dispersion polymerisation and between 5 and 2000 μm by suspension polymerisation.(76)

Functionalisation can be installed into these particles by introducing a functional co-monomer or by post-polymerisation modification reactions. However, it is not usually possible to use direct copolymerisation modifications as some functional groups of the co-monomers have compatibility problems with polymerisation solvents. On the other hand, several post-polymerisation modification reactions can be carried out with DVB-based polymer microspheres. The electron-rich aromatic π-system on DVB rings will rapidly undergo different electrophilic aromatic substitutions, and these were studied by many groups.(77)

DVB reacts *via* FRP and as with many other divinyl monomers, not all the vinyl groups are reacted during the polymerisation, which can be used to install different functionalities on the network. Stranix *et al.* were one of the first groups which modified the pendent unreacted vinyl groups of polyDVB microspheres, by using a library of different addition reactions (Figure 1.24).(77)

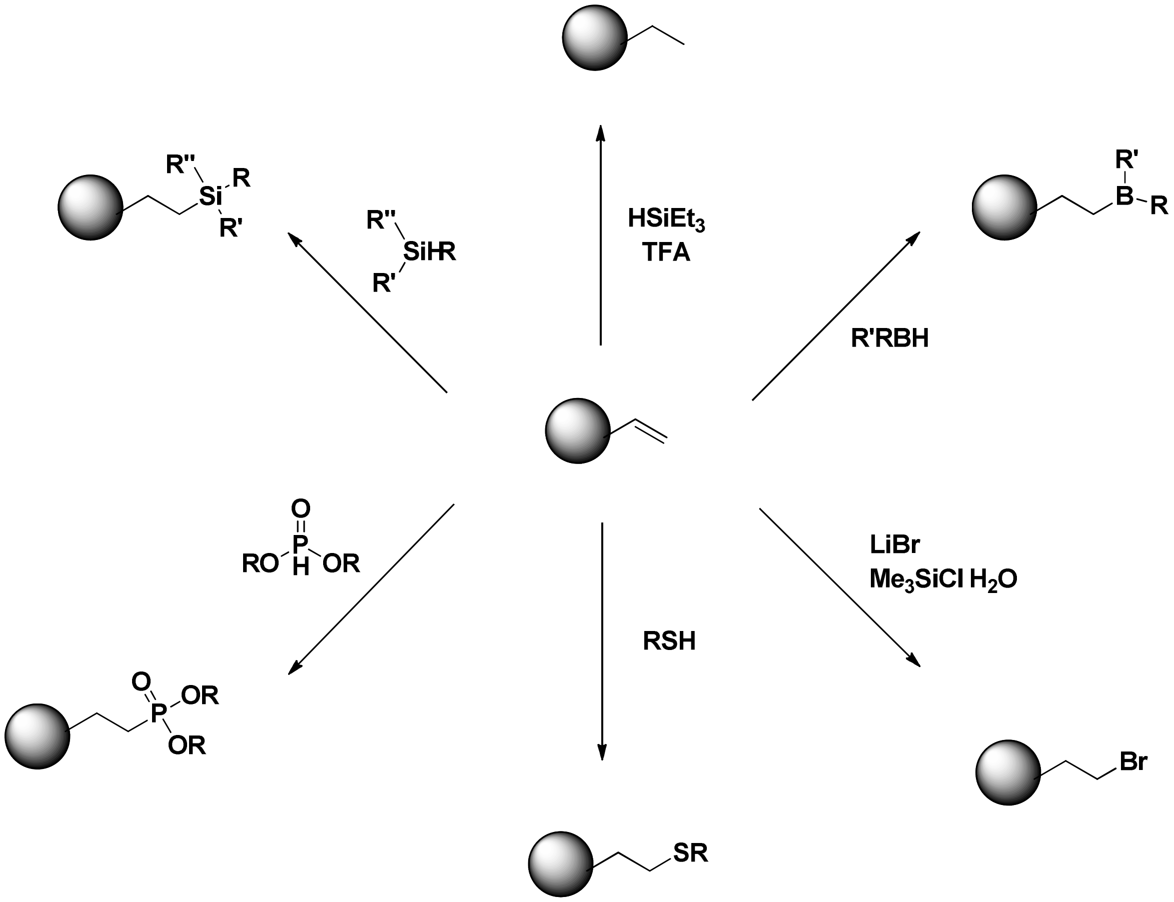

Figure 1.24 Modification reactions on polyDVB.(77)

Both azide-alkyne click chemistry and thiol-ene reactions are the most used post-polymerisation modifications for polymer microspheres. Breed *et al.* prepared polymer microspheres by copolymerising divinylbenzene with vinylbenzyl chloride and subsequently utilised the pendent chlorovinyl groups for functionalisation with sodium azide (Figure 1.25a).(78) Goldmann *et al.* modified polyDVB microspheres by thiol-ene reaction with 1-azidoundecanethiol installing an azide group at the end of the chain, which was further functionalised by azide-alkyne click reaction, with alkyne-end functionalised poly(hydroxyethyl methacrylate) (Figure 1.25b).(79)

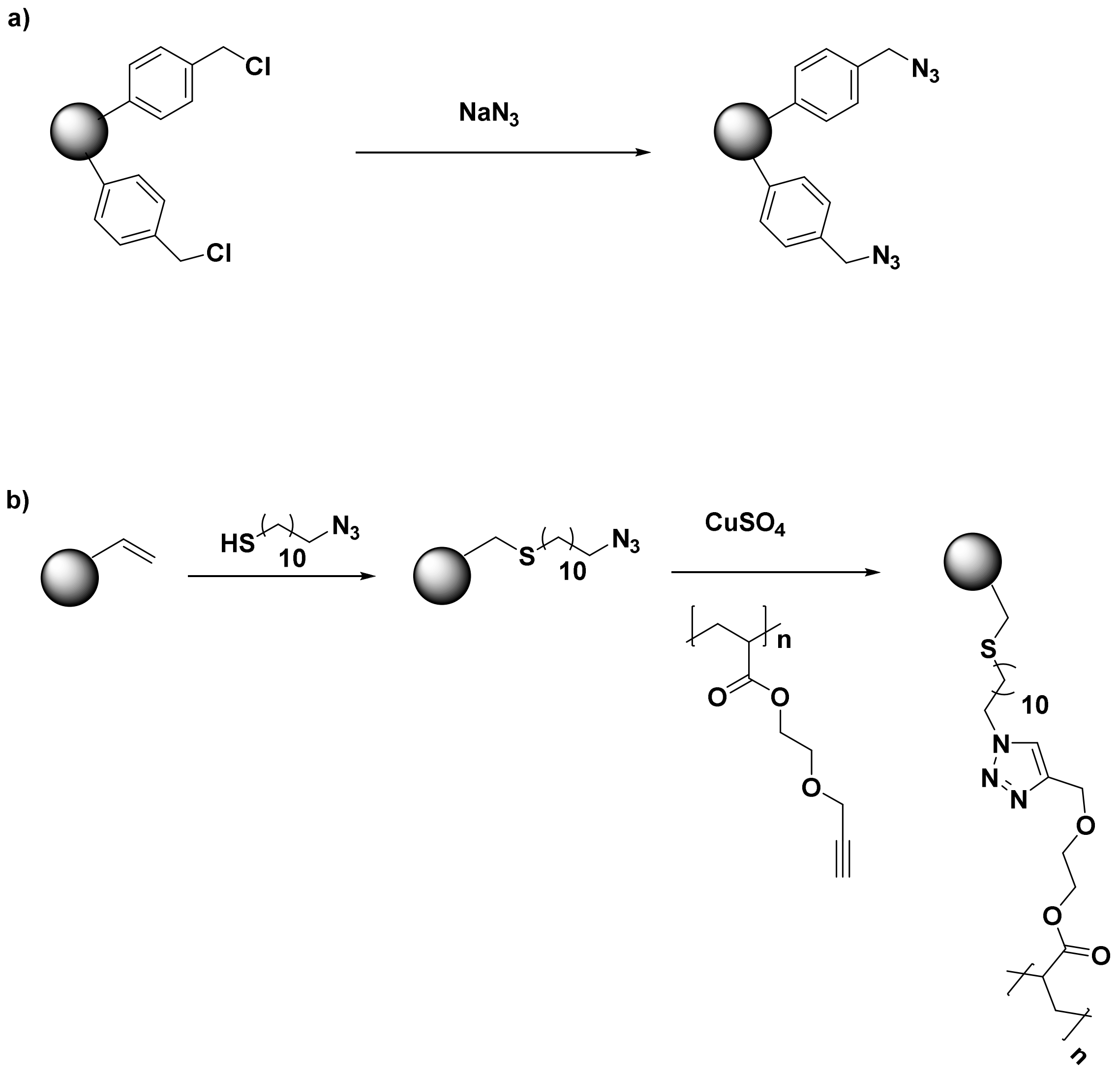

Figure 1.25 Modification of polyDVB-based microspheres by azide-alkyne click chemistry.(78,79)

Gokmen *et al.* also reported the functionalisation of thiol-containing microspheres not only with thiol click chemistry but also with many other post-polymerisation modification reactions (Figure 1.26a).(80) More recently, Cormack *et al.* reported the post-polymerisation modification of hypercrosslinked partilces by using acetyl sulfate for the obtainment of strong-cation exchange resins (Figure 1.26b).(81)

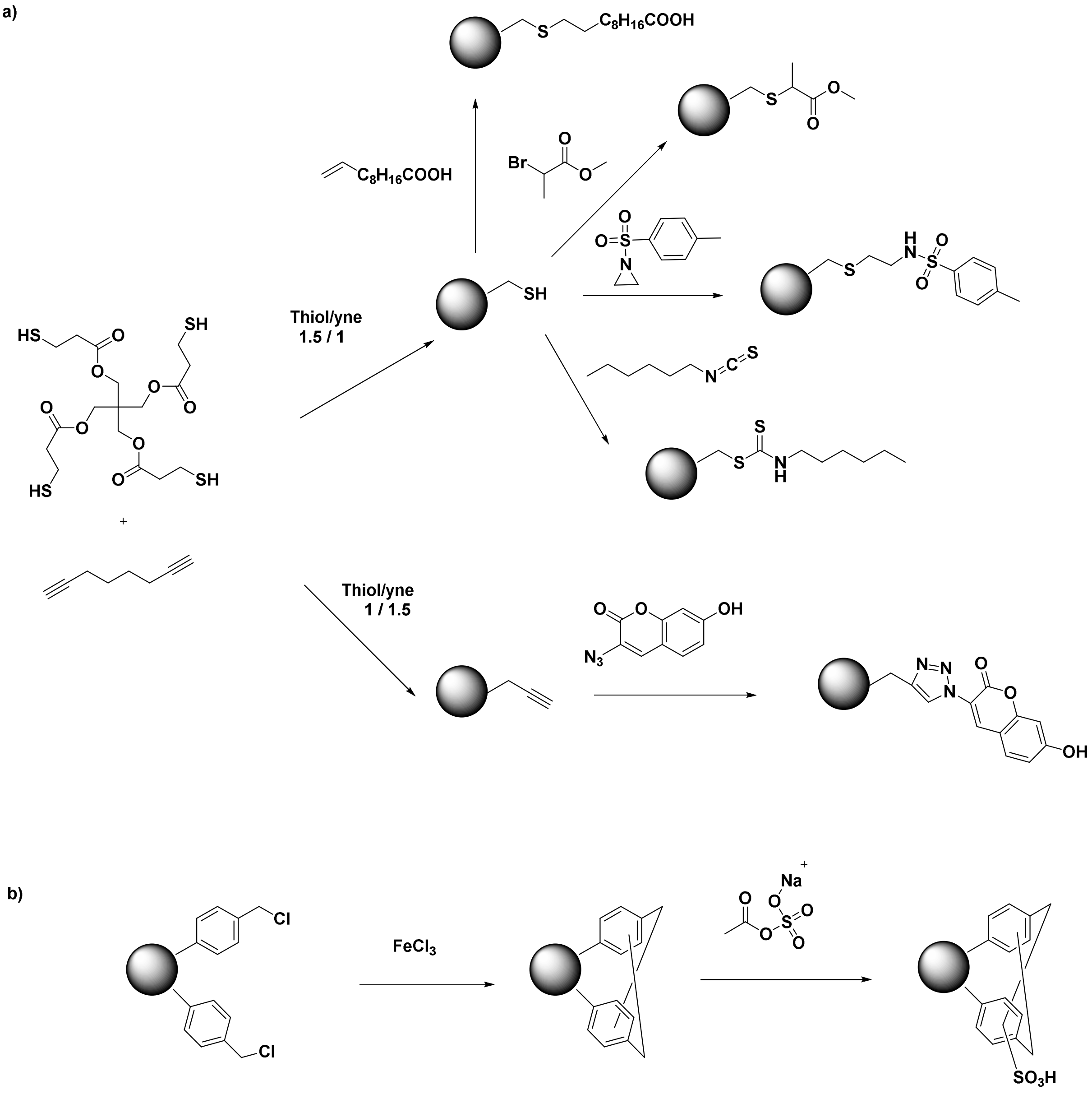

Figure 1.26 a) Functionalisation of thiol containing microspheres.(80) b) Functionalisation of hypercrosslinked microspheres.(81)

1.4. OLEFIN CROSS METATHESIS

As it has been reported before, there are many post-polymerisation modification techniques that can introduce functionality in different polymer architectures either linear, branched or even crosslinked. However, when these modifications are carried out, the selectivity of the reactions is quite limited and in some cases harsh conditions are used. Since many pendent side chains contain masked or unmasked alkene groups, olefin cross-metathesis can be an attractive technique to obtain functionalised polymers. With this technique, a wide range of polar functional groups could be installed on the polymer under mild conditions, different polymers are obtained from the same precursor and the olefin remains on the polymer, which can be further functionalised.

Olefin metathesis is a commonly used technique in the field of organic synthesis that entails the distribution of alkenes by the cleavage and the regeneration of the carbon-carbon double bond. In 2005, Yves Chauvin, Richard Schrock and Robert Grubbs received the Nobel Prize for the elucidation of the mechanism (Figure 1.27) and the development of the highly selective and efficient catalysts. Chauvin's proposed mechanism involves a metallocarbene undergoing a [2+2] cycloaddition with the olefin substrate to form a metallacyclobutane. This intermediate will then decompose, releasing a small molecule usually ethylene, and forming a new metallocarbene, which will react either intramolecularly (for ring closing metathesis (RCM)) or with another alkene (cross metathesis (CM)). The CM product can also undergo secondary metathesis reactions, resulting in an equilibrium system of olefin products, which leads to selectivity issues in CM reaction. The dimerisation of certain alkenes can be more favourable than CM, and even though metathesis reaction favours the formation of the *E* product, *E*/*Z* isomerism has to be taken in consideration. The isomerism is controlled by thermodynamics and therefore, a more stable olefin is less likely to undergo secondary metathesis favouring the formation of the *E* alkene. It is worth mentioning that the [2+2] cycloaddition of two alkenes in absence of any transition metal alkylidenes is symmetry forbidden as it has a high activation energy. However, the reaction can occur in presence of a metal catalyst, in which the the d orbital interactions lower the activation energy enough for the reaction to proceed.(82)

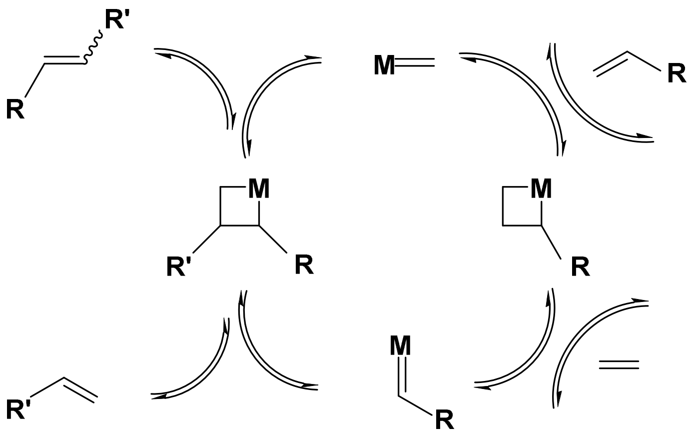

Figure 1.27 Olefin cross-metathesis mechanism.

A lot of work has been reported in the areas of ring-closing metathesis (RCM) or ring-opening metathesis polymerisation (ROMP) that overshadowed the olefin cross metathesis (CM). There are three main factors that make CM less attractive and less useful in organic synthesis: First, low activity of the metathesis catalysts to effect a reaction without a strong enthalpic driving force (such as ring-strain release in ROMP) or entropic advantage of intramolecular reactions (such as RCM), second, low product selectivity for the CM product, and third, poor stereoselectivity in the newly formed olefin. However, this route can produce highly functionalised alkenes, being the most flexible of the three reactions.(83)

Cross metathesis has recently gained prominence due to the availability of new catalysts (Figure 1.28) that mainly solved the drawbacks of CM. The Schrock catalyst was one of the first catalysts to be synthesised for the use in olefin metathesis. However, this catalyst is based on molybdenum and it is extremely sensitive to light and moisture. Furthermore, this catalyst can react violently with some functional groups making its use very difficult. Then Grubbs *et al.* synthesised the first ruthenium-based alkylidene catalyst (Grubbs 0). However, this catalyst shows very low activity and is only effective in the ROMP of highly strained olefins. Grubbs *et al.*, in order to increase the activity of the catalyst, modified his first catalyst and synthesised the Grubbs I catalyst, which shows much better functional group compatibility and thermal stability. Later, Grubbs *et al.* modified one of the tricyclohexylphosphine ligands with an *N*-heterocyclic carbene (Grubbs II and Grubbs-Nolan catalyst), which improved the catalytic activity, and maintained the functional group tolerance and thermal stability. By replacing the second tricyclohexylphosphine group by a bidentate alkylidene (HGI, HGII, Grela and Zhan 1b catalysts), the thermal stability was highly improved.(82-84)

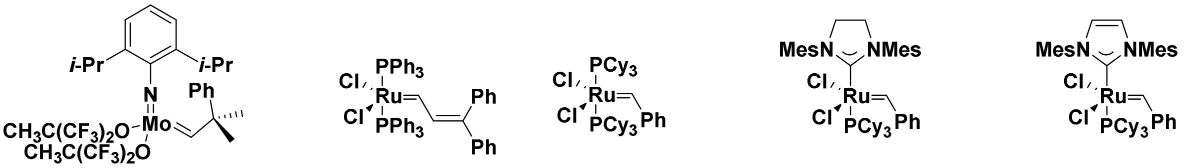

Schrock catalyst

Grubbs 0

First-generation Grubbs catalyst (Grubbs I)

Second-generation Grubbs catalyst (Grubbs II)

Grubbs-Nolan catalyst

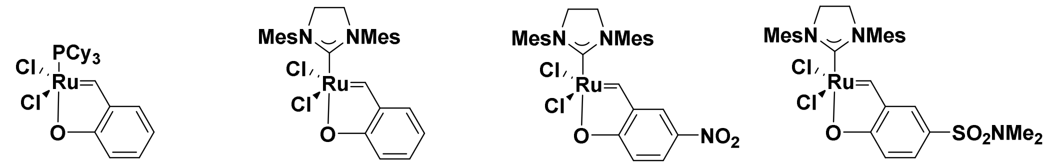

First-generation Hoveyda-Grubbs catalyst (HGI)

Second-generation Hoveyda-Grubbs catalyst (HGII)

Grela catalyst

Zhan-1B catalyst

Figure 1.28 Different catalysts used in olefin metathesis organised according to its reactivity and thermal stability.(84)

Another factor that has to be taken in consideration during the CM reaction to keep the control over the stereoselectivity is the reactivity of the reacting olefins. Grubbs and coworkers reported a categorisation of the olefins (Table 1.1) according to their ability to undergo homodimerisation with a metathesis catalyst and to the subsequent reactivity of their homodimers. Type I olefins, such as terminal olefins, are categorised as the ones that rapidly undergo homodimerisation and their homodimers can participate in CM reactions. Type II olefins on the other hand, have a slow homodimerisation rate and the formed dimers barely take part in the CM reactions. Type III olefins, such as vinyl phosphonates, do not homodimerise but can participate in CM reactions, and very hindered Type IV olefins act as spectators in CM reactions.(83)

Type of olefin	*Description*	*Examples*
I	Rapid homodimerisation, homodimers consumable	Terminal olefins, styrenes (no large ortho substituents), allyl halides, protected allyl amines, 1° allyl alcohols…
II	Slow homodimerisation, homodimers barely consumable	Styrenes (large ortho substituents), acrylates, acrylic acid, 2° allyl alcohols…
III	No homodimerisation	Vinyl phosphonates, 3° allyl alcohols…
IV	Olefins inert to CM, but do not deactivate catalyst (spectators)	Vinyl nitro olefins, trisubstituted allyl alcohols (protected)

Table 1.1 Categorisation of the olefins with Grubbs II catalyst. (83)

CM reactions can be carried out either in a selective or nonselective way. When two Type I olefins react together, their rates of homodimerisation are similar and their homodimers present high reactivities to undergo a secondary CM reaction. The formed cross products will be equilibrated with various homodimers by a secondary CM that will result in a statistical product mixture (Figure 1.29). In other words, when two olefins of the same type react together, mixtures of the products are obtained.(83)

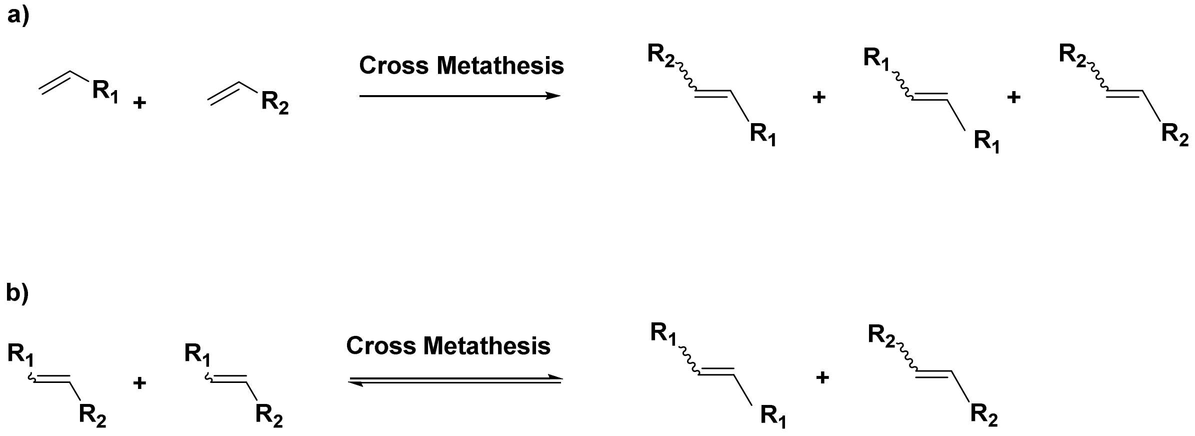

Figure 1.29 a) Nonselective statistical distribution of CM products b) Equilibration of cross products by secondary CM reaction.(83)

To avoid the statistical product distributions, selective CM reactions between two different types of olefins can be carried out. Although Type I olefins may homodimerise rapidly, the product distribution is driven towards the desired cross product as ethylene is driven from the system (preventing the regeneration of terminal olefins) and the Type I homodimer undergoes a secondary CM with the Type II/III olefins. In this case, the obtained cross product will not give a statistical product mixture as it does not undergo secondary metathesis (Figure 1.30). If CM occurs between Type II and Type III olefins, an excess of the Type III olefin has to be used to readily undergo the CM reaction with Type II olefin.(83)

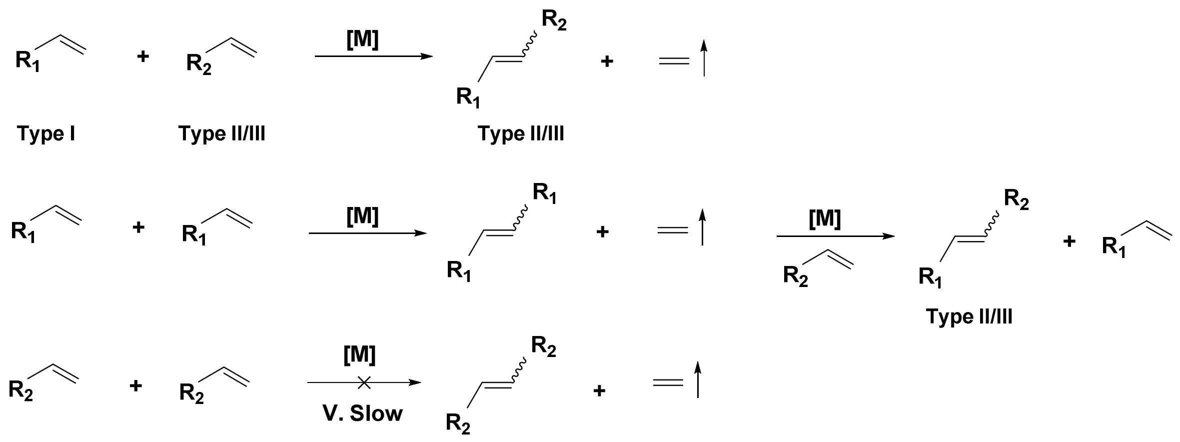

Figure 1.30 Cross product formation possibilities between Type I and Type II/III olefins.(83)

1.4.1. Post-polymerisation modification via olefin metathesis

Although CM is a versatile method requiring only mild conditions, there are very few examples of its use for post-polymerisation modification. Blechert and coworkers reported in 1997 the synthesis of 1% DVB crosslinked allyldimethylsilyl polystyrene and CM with a wide range of functional groups and Grubbs I as catalyst (Figure 1.31).(85) In this instance, the polymer is used to immobilise olefins, which are released from the resin after the functionalisation by CM.

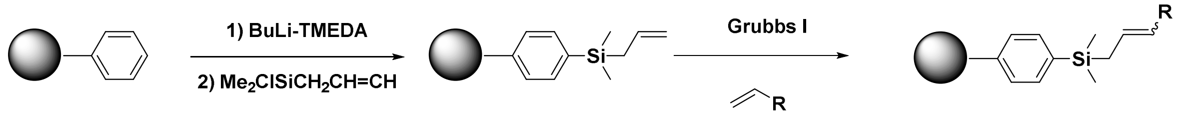

Figure 1.31 Post-polymerisation modification *via* olefin metathesis with Grubbs I.(85)

Some years later, Coates and coworkers reported the synthesis of different polyolefins by using a living titanium catalyst, and the functionalisation of the olefin side chains by CM reaction.(86) Meier and coworkers reported the quantitative modification of poly(oxazoline) by using HGII catalyst in the presence of a wide variety of acrylates (Figure 1.32a). The possible self-metathesis of the polymer was avoided by using an excess of cross-metathesis partner and 5 mol% of the catalyst.(87) The same conditions were recently used by Prunet, Thomas and coworkers for the functionalisation of the side chains of their tailor-made polyesters (Figure 1.32b).(88)

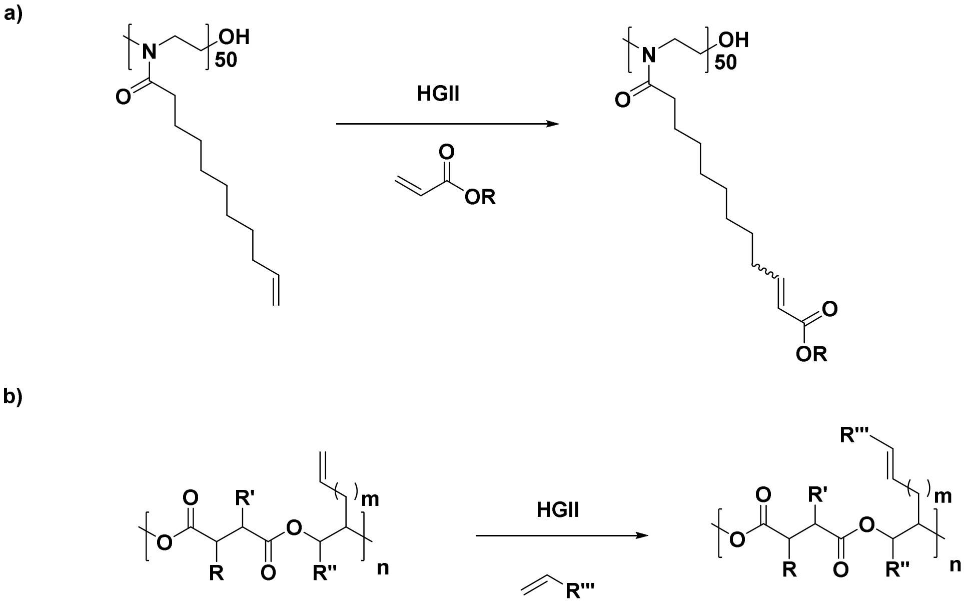

Figure 1.32 Post-polymerisation modification by CM reaction of polyoxazolines (a) and polyesters (b).(87,88)

Although several groups have used CM to modify the side chains of polymers, Guan and coworkers used a ring-rearrangement metathesis (RRM) reaction in order to modify the network topology of cross-linked polybutadiene (Figure 1.33). Furthermore, as the amount of crosslinks and average functionality remained constant, the mechanical integrity and strength of the network was maintained and thus malleable polymer networks were achieved.(89)

Figure 1.33 Malleable polybutadiene network obtained *via* RRM reaction.(89)

1.5. PHD HYPOTHESIS AND AIMS

Different functionalisation methodologies for different polymer architectures have been reported in this chapter. However, despite the easy functionalisation techniques used for polymer functionalisation, a general method suitable for a wide range of functional groups has not been reported yet. In this study, we focused upon the development of olefin metathesis-based methods for the functionalisation of polymer microspheres.

The main aims are as follows:

1- To prepare polyDVB-based porous polymer microspheres and install a wide range of functional groups on the unreacted pendent double bonds by CM reaction.
2- To prepare non-porous polymer microspheres and to use RCM in order to install porosity on the polymer as hypercrosslinking method.
3- To hypercrosslink the polymer network by using an external crosslinker *via* CM/RCM in order to install porosity on the polymer microspheres and obtain ultra-high specific surface areas.

1.6. REFERENCES

(1) Bonilla-Cruz, J.; Dehonor, M.; Saldivar-Guerra, E.; Gonzalez-Montiel, A. In *Handbook of Polymer Synthesis, Characterization, and Processing*; Saldivar-Guerra, E., Vivaldo-Lima, E., Eds.; John Wiley & Sons, Inc., 2013; pp 205–223.

(2) Zambelli, A.; Ammendola, P. *Prog. Polym. Sci.* **1991**, *16*, 203–218.

(3) Marques, M. M.; Correia, S. G.; Ascenso, J. R.; Ribeiro, A. F. G.; Gomes, P. T.; Dias, A. R.; Foster, P.; Rausch, M. D.; Chien, J. C. W. *J. Polym. Sci. Part A Polym. Chem.* **1999**, *37*, 2457–2469.

(4) Kawahara, N.; Saito, J.; Matsuo, S.; Kaneko, H.; Matsugi, T.; Kashiwa, N. *Polym. Bull.* **2010**, *64*, 657–666.

(5) Gauthier, M.; Gibson, M.; Klok, H.-A. *Angew. Chem. Int. Ed.* **2009**, *48*, 48–58.

(6) Günay, K. A.; Theato, P.; Klok, H. A. In *Functional Polymers by Post-Polymerization Modification: Concepts, Guidelines, and Applications*; Theato, P., Klok, H. A., Eds.; Wiley-VCH Verlag GmbH & Co. KGaA, 2013; pp 1–44.

(7) Serniuk, G. E.; Banes, F. W.; Swaney, M. W. *J. Am. Chem. Soc.* **1948**, *70*, 1804–1808.

(8) Merrifield, R. B. *J. Am. Chem. Soc.* **1963**, *85*, 2149–2154.

(9) Iwakura, Y.; Kurosaky, T.; Ariga, N.; Ito, T. *Makromol. Chem.* **1966**, *97*, 128–138.

(10) Romani, F.; Passaglia, E.; Aglietto, M.; Ruggeri, G. *Macromol. Chem. Phys.* **1999**, *200*, 524–530.

(11) Justynska, J.; Schlaad, H. *Macromol. Rapid Commun.* **2004**, *25*, 1478–1481.

(12) Justynska, J.; Hordyjewicz, Z.; Schlaad, H. *Polymer* **2005**, *46*, 12057–12064.

(13) Brummelhuis, N. Ten; Diehl, C.; Schlaad, H. *Macromolecules* **2008**, *41*, 9946–9947.

(14) Gress, A.; Vo, A.; Schlaad, H. *Macromolecules* **2007**, *40*, 7928–7933.

(15) Campos, L. M.; Killops, K. L.; Sakai, R.; Paulusse, J. M. J.; Damiron, D.; Drockenmuller, E.; Messmore, B. W.; Hawker, C. J. *Macromolecules* **2008**, *41*, 7063–7070.

(16) Ates, Z.; Thornton, P. D.; Heise, A. *Polym. Chem.* **2011**, *2*, 309–312.

(17) Xu, J.; Boyer, C. *Macromolecules* **2015**, *48*, 520–529.

(18) Kalal, J.; Svec, F.; Marousek, V. *J. Polym. Sci. Polym. Symp.* **1974**, *47*, 155–166.

(19) Barbey, R.; Klok, H. A. *Langmuir* **2010**, *26*, 18219–18230.

(20) Yan, X.; Sivignon, A.; Barnich, N.; Gouin, S. G.; Bouckaert, J.; Fleury, E.; Bernard, J. *Polym. Chem.* **2016**, *7*, 2674–2683.

(21) Maeda, H.; Takeshita, J.; Kanamaru, R. *Int. J. Pept. Protein Res.* **1979**, *14*, 81-87.

(22) Henry, S. M.; El-Sayed, M. E. H.; Pirie, C. M.; Hoffman, A. S.; Stayton, P. S. *Biomacromolecules* **2006**, *7*, 2407–2414.

(23) Lee, W.; Lee, C. *Polymer* **1997**, *38*, 971–979.

(24) Taylor, L.D., Chiklis, C.K., Platt, T. E. *J. Polym. Sci. Polym. Lett.* **1971**, *9*, 187–190.

(25) Coleman, P. L.; Walker, M. M.; Milbrath, D. S.; Stauffer, D. M.; Rasmussen, J. K.; R. Krepski, L.; Heilmann, S. M. *J. Chromatogr. A* **1990**, *512*, 345–363.

(26) Beyer, D.; Paulus, W.; Seitz, M.; Maxein, G.; Ringsdorf, H.; Eich, M. *Thin Solid Films* **1995**, *271*, 73–83.

(27) Barner, L.; Pereira, S.; Sandanayake, S.; Davis, T. P. *J. Polym. Sci. Part A-Polymer Chem.* **2006**, *44*, 857–864.

(28) Flores, J. D.; Shin, J.; Hoyle, C. E.; McCormick, C. L. *Polym. Chem.* **2010**, *1*, 213-220.

(29) Hensarling, R. M.; Rahane, S. B.; LeBlanc, A. P.; Sparks, B. J.; White, E. M.; Locklin, J.; Patton, D. L. *Polym. Chem.* **2011**, *2*, 88.

(30) Seto, R.; Matsumoto, K.; Endo, T. *J. Polym. Sci. Part A Polym. Chem.* **2015**, *53*, 1934–1940.

(31) Ferruti, P.; Bettelli, A.; Fere, A. *Polymer* **1972**, *13*, 462–464.

(32) Batz, H. G.; Franzmann, G.; Ringsdorf, H. *Angew. Chem. Int. Ed. Engl.* **1972**, *11*, 1103–1104.

(33) Devenish, S. R. A.; Hill, J. B.; Blunt, J. W.; Morris, J. C.; Munro, M. H. G. *Tetrahedron Lett.* **2006**, *47*, 2875–2878.

(34) Wong, S. Y.; Putnam, D. *Bioconjugate Chem.* **2007**, *18*, 970–982.

(35) Eberhardt, M.; Mruk, R.; Zentel, R.; Théato, P. *Eur. Polym. J.* **2005**, *41*, 1569-1575.

(36) Son, H.; Jang, Y.; Koo, J.; Lee, J.-S.; Theato, P.; Char, K. *Polym. J.* **2016**, *48*, 487–495.

(37) Hoenders, D.; Tigges, T.; Walther, A. *Polym. Chem.* **2015**, *6*, 476–486.

(38) Gilbert, H. *J Biol Chem* **1982**, *257*, 12086–12091.

(39) Wang, L.; Kristensen, J.; Ruffner, D. E. *Bioconjug. Chem.* **1998**, *9*, 749–757.

(40) Bulmus, V.; Woodward, M.; Lin, L.; Murthy, N.; Stayton, P.; Hoffman, A. *J. Control. Release* **2003**, *93*, 105–120.

(41) Ghosh, S.; Basu, S.; Thayumanavan, S. *Macromolecules* **2006**, *39*, 5595–5597.

(42) Chen, W.; Zou, Y.; Meng, F.; Cheng, R.; Deng, C.; Feijen, J.; Zhong, Z. *Biomacromolecules* **2014**, *15*, 900–907.

(43) Durmaz, H.; Dag, A.; Altintas, O.; Erdogan, T.; Hizal, G.; Tunca, U. *Macromolecules* **2007**, *40*, 191–198.

(44) Gregoritza, M.; Brandl, F. P. *Eur. J. Pharm. Biopharm.* **2015**, *97*, 438–453.

(45) Ochi, R.; Nishida, T.; Ikeda, M.; Hamachi, I. *J. Mater. Chem. B* **2014**, *2*, 1464–1469.

(46) Bousquet, A.; Barner-kowollik, C.; Stenzel, M. *J. Polym. Sci. Part A Polym. Chem.* **2010**, *48*, 1773–1781.

(47) Vonhören, B.; Langer, M.; Abt, D.; Barner-Kowollik, C.; Ravoo, B. J. *Langmuir* **2015**, *31*, 13625–13631.

(48) Mather, B. D.; Viswanathan, K.; Miller, K. M.; Long, T. E. *Prog. Polym. Sci.* **2006**, *31*, 487–531.

(49) Friedman, M.; Cavins, J. F. F.; Wall, J. S. S. *J. Am. Chem. Soc.* **1965**, *87*, 3672–3682.

(50) Rieger, J.; Van Butsele, K.; Lecomte, P.; Detrembleur, C.; Jérôme, R.; Jérôme, C. *Chem. Commun.* **2005**, 274–276.

(51) Yang, S. K.; Weck, M. *Soft Matter* **2009**, *5*, 582–585.

(52) Farmer, T. J.; Clark, J. H.; Macquarrie, D. J.; Ogunjobi, J. K.; Castle, R. L. *Polym. Chem.* **2016**, *7*, 1650–1658.

(53) Narayanan, A.; Maiti, B.; De, P. *React. Funct. Polym.* **2015**, *91–92*, 35–42.

(54) Binder, W. H.; Kluger, C. *Macromolecules* **2004**, *37*, 9321–9330.

(55) Wu, D.; Hui, C. M.; Dong, H.; Pietrasik, J.; Ryu, H. J.; Li, Z.; Zhong, M.; He, H.; Kim, E. K.; Jaroniec, M.; Kowalewski, T.; Matyjaszewski, K. *Macromolecules* **2011**, *44*, 5846–5849.

(56) Ladmiral, V.; Mantovani, G.; Clarkson, G. J.; Cauet, S.; Irwin, J. L.; Haddleton, D. M. *J. Am. Chem. Soc.* **2006**, *128*, 4823–4830.

(57) Agard, N. J.; Prescher, J. A.; Bertozzi, C. R. *J. Am. Chem. Soc.* **2004**, *126*, 15046–15047.

(58) Fokina, A.; Klinker, K.; Braun, L.; Jeong, B. G.; Bae, W. K.; Barz, M.; Zentel, R. *Macromolecules* **2016**, *49*, 3663–3671.

(59) Rabuka, D.; Parthasarathy, R.; Goo, S. L.; Chen, X.; Groves, J. T.; Bertozzi, C. R. *J. Am. Chem. Soc.* **2007**, *129*, 5462–5471.

(60) Barrett, D. G.; Yousaf, M. N. *Biomacromolecules* **2008**, *9*, 2029–2035.

(61) Seuyep Ntoukam, D. H.; Luinstra, G. A.; Theato, P. *J. Polym. Sci. Part A Polym. Chem.* **2014**, *52*, 2841–2849.

(62) Schulz, V. R. C.; Fauw, H. *Makromol. Chem.* **1956**, *19*, 161–167.

(63) Legros, C.; De Pauw-Gillet, M. C.; Tam, K. C.; Lecommandoux, S.; Taton, D. *Eur. Polym. J.* **2015**, *62*, 322–330.

(64) Sun, G.; Cheng, C.; Wooley, K. L. *Macromolecules* **2007**, *40*, 793–795.

(65) Fulton, D. A. *Org. Lett.* **2008**, *10*, 3291–3294.

(66) Sonogashira, K.; Tohda, Y.; Hagihara, N. *Tetrahedron Lett.* **1975**, *16*, 4467–4470.

(67) Sessions, L. B.; Cohen, B. R.; Grubbs, R. B. *Macromolecules* **2007**, *40*, 1926–1933.

(68) Kub, C.; Tolosa, J.; Zucchero, A. J.; McGrier, P. L.; Subramani, C.; Khorasani, A.; Rotello, V. M.; Bunz, U. H. F. *Macromolecules* **2010**, *43*, 2124–2129.

(69) Buelt, A. A.; Conrad, C. A.; Mackay, W. D.; Shehata, M. F.; Smith, V. D.; Smith, R. C. *Polym. Int.* **2015**, *64*, 730–739.

(70) Riva, R.; Jerome, R.; Lecomte, P. *J. Polym. Sci. Part A Polym. Chem.* **2006**, *44*, 6015–6024.

(71) Becer, C. R.; Babiuch, K.; Pilz, D.; Hornig, S.; Heinze, T.; Gottschaldt, M.; Schubert, U. S. *Macromolecules* **2009**, *42*, 2387–2394.

(72) Mangold, C.; Dingels, C.; Obermeier, B.; Frey, H.; Wurm, F. *Macromolecules* **2011**, *44*, 6326–6334.

(73) Van Hensbergen, J. A.; Burford, R. P.; Lowe, A. B. *Polym. Chem.* **2014**, *5*, 5339–5349.

(74) Leroy, A.; Al Samad, A.; Garric, X.; Huger, S.; Noël, D.; Coudane, J.; Nottelet, B. *RSC Adv.* **2014**, *4*, 32017–32023.

(75) Al Samad, A.; Bakkour, Y.; Fanny, C.; El Omar, F.; Coudane, J.; Nottelet, B. *Polym. Chem.* **2015**, *6*, 5093–5102.

(76) Gokmen, M. T.; Prez, F. E. Du. *Prog. Polym. Sci.* **2012**, *37*, 365–405.

(77) Stranix, B. R.; Gao, J. P.; Barghi, R.; Salha, J.; Darling, G. D. *J. Org. Chem.* **1997**, *62*, 8987–8993.

(78) Breed, D. R.; Thibault, R.; Xie, F.; Wang, Q.; Hawker, C. J.; Pine, D. J. *Langmuir* **2009**, *25*, 4370–4376.

(79) Goldmann, A. S. A.; Walther, A.; Nebhani, L.; Joso, R.; Ernst, D.; Loos, K.; Barner-Kowollik, C.; Earner, L.; Müller, A. H. E. *Macromolecules* **2009**, *42*, 3707–3714.

(80) Gokmen, M. T.; Brassinne, J.; Prasath, R. A.; Du Prez, F. E. *Chem. Commun.* **2011**, *47*, 4652–4654.

(81) Cormack, P. A. G.; Davies, A.; Fontanals, N. *React. Funct. Polym.* **2012**, *72*, 939–946.

(82) Vougioukalakis, G. C.; Grubbs, R. H. *Chem. Rev.* **2010**, *110*, 1746–1787.

(83) Chatterjee, A. K.; Choi, T. L.; Sanders, D. P.; Grubbs, R. H. *J. Am. Chem. Soc.* **2003**, *125*, 11360–11370.

(84) Grela, K.; Harutyunyan, S.; Michrowska, A. *Angew.Chem. Int. Ed.* **2002**, *41*, 4038–4040.

(85) Schuster, M.; Lucas, N.; Blechert, S. *Chem. Commun.* **1997**, 823–824.

(86) Mathers, R. T.; Coates, G. W. *Chem. Commun.* **2004**, 422–423.

(87) Espinosa, L. M. De; Kempe, K.; Schubert, U. S.; Hoogenboom, R.; Meier, M. A. R. *Macromol. Rapid Commun.* **2012**, *33*, 2023–2028.

(88) Fournier, L.; Robert, C.; Pourchet, S.; Gonzalez, A.; Williams, L.; Prunet, J.; Thomas, C. M. *Polym. Chem.* **2016**, *7*, 3700–3704.

(89) Lu, Y.; Tournilhac, F.; Leibler, L.; Guan, Z. *J. Am. Chem. Soc.* **2012**, *134*, 8424–8427.

CHAPTER 2

SYNTHESIS, CHARACTERISATION AND FUNCTIONALISATION BY OLEFIN CROSS METATHESIS OF POLYDIVINYLBENZENES

2.1. INTRODUCTION

2.1.1. Precipitation polymerisation

Precipitation polymerisation (PP) is a surfactant- and stabiliser-free heterogeneous polymerisation method used to synthesise polymer microspheres of uniform size and shape. The polymerisation begins as a homogeneous mixture of initiator, monomer and solvent. During polymerisation, the growing polymer chains separate from the continuous phase by enthalpic precipitation, in cases of unfavourable polymer-solvent interactions or entropic precipitation, in cases where the crosslinking prevents the polymer and solvent from freely mixing.(1)

Bulk polymerisations of vinyl chloride and acrylonitrile are classic examples of enthalpic precipitation polymerisations where the propagating chains grow beyond their solubility limit in the organic medium, which may be the monomer itself, and precipitate. The resulting nuclei typically aggregate into larger, polydisperse particles that continue to grow by capturing other particles or newly formed polymer chains, or by adsorption and polymerisation of monomer. In good solvents these polymerisations will often produce turbid macroscopic or microscopic gels, depending largely on the original monomer concentration. In poorer solvents, precipitation polymerisation normally produces micrometre-sized particles. Their size distribution is often broad due to a lack of colloidal stability.

Stöver and coworkers(2) reported the formation of highly crosslinked and monosized polydivinylbenzene (polyDVB) microspheres by the precipitation polymerisation of divinylbenzene (DVB) in neat acetonitrile with AIBN as radical initiator. Since the process is free of surfactants or steric stabilisers, the resulting particles had clean, stabiliser-free surfaces and no ionic charges were carried.

Similar, but porous, monodisperse polymer microspheres were formed by polymerisation in a mixture of acetonitrile and toluene.(3) The narrow particle size distributions observed resembled those found in dispersion polymerisations, suggesting that the particles become colloidally stable early on in the polymerisation.

Downey *et al.*(4) focused their research towards entropic precipitation polymerisations; monodisperse styrenic microspheres were formed in the presence of a crosslinker and a solvent but without adding steric stabilizer for the polymer. They proposed the hypothesis that the particles were formed in two steps. The first step consists of a nucleation process through aggregation of soluble oligomers to form swollen microgels which internally desolvate to produce colloidally stable particle nuclei. The second step is the growth stage which involves the entropic capture of soluble oligomers by surface vinyl groups, followed by desolvation (Figure 2.1).

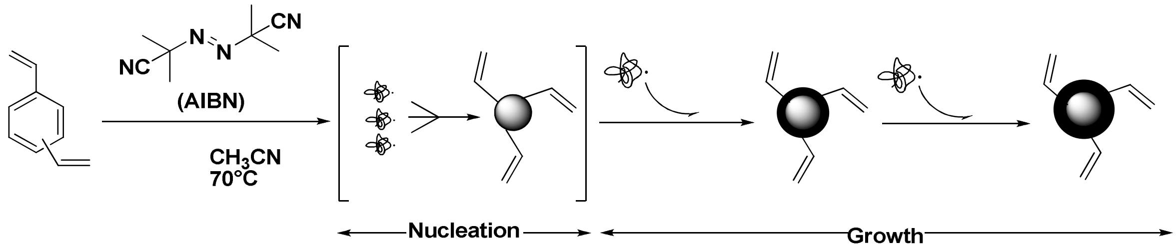

Figure 2.1 Particle formation and growth hypothesis for precipitation polymerisation.

This growth hypothesis was tested using seed particles which had been modified to eliminate the surface vinyl groups (Figure 2.2), by comparing the results to the data resulting from the use of unmodified seed particles with their vinyl groups intact. The surface modification reactions carried out transforms the surface vinyl groups into allyl groups on a master batch of seed particles, to form inert seed particles. Two different methods were used: the first method involved alkylation using an excess of *n*-BuLi in a mixture of toluene and THF (9:1) giving inert hexyl groups. The second method involved hydrogenation in the presence of Wilkinson's catalyst to give ethyl groups.(4)

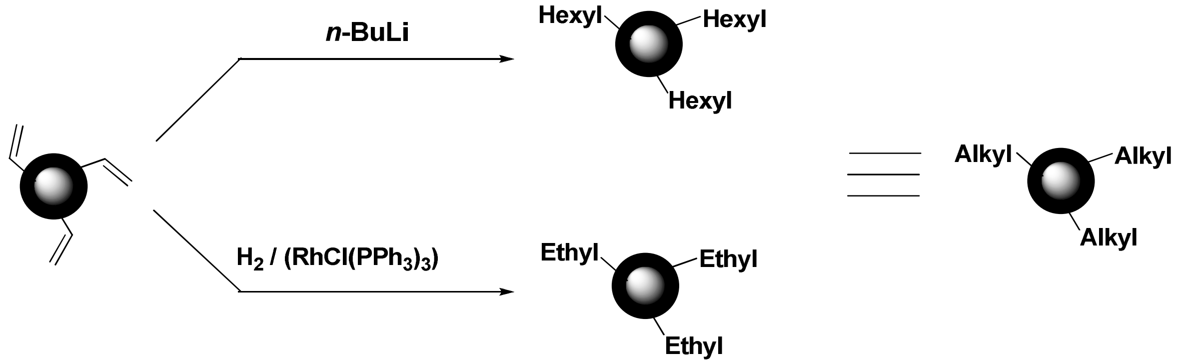

Figure 2.2 Surface Modification of polyDVB particles synthesised via precipitation polymerisation.

In the subsequent seeded growth reactions involving DVB and AIBN, only the unmodified seed particles grew uniformly by capturing oligomers (Figure 2.3a). Under the same conditions, the modified inert seed particles did not grow. Instead, in these reactions the oligomers which formed aggregated into polydisperse secondary particles (Figure 2.3b). This finding indicates that the presence of surface vinyl groups is essential for particle growth and it supports the hypothesis that particle growth is an entropic precipitation driven by radical reactions.

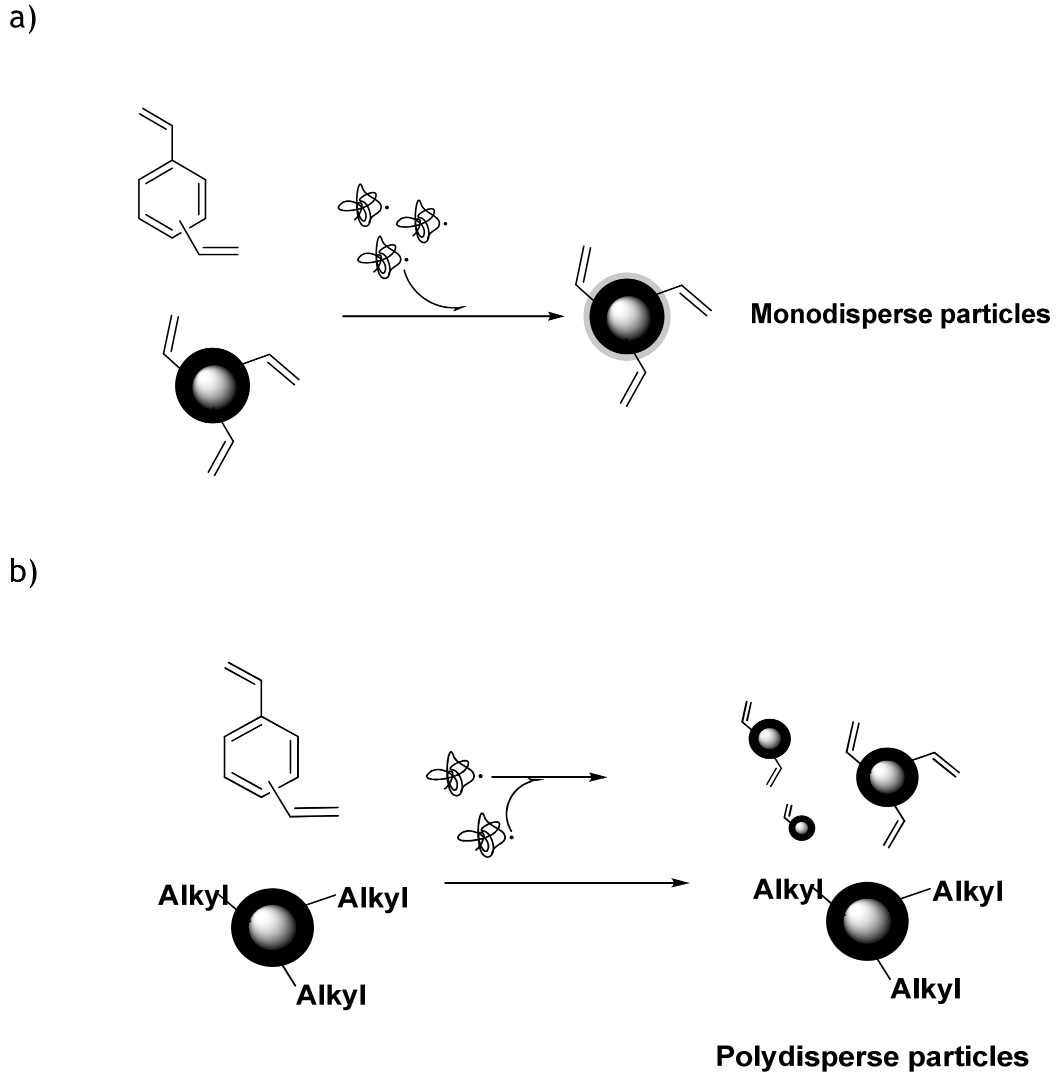

Figure 2.3 Growth reaction of: a) unmodified seed particles, and b) inert seed particles.

As a consequence of the particle growth mechanism, the surfaces of the microspheres must continuously capture swollen oligomers from the reaction medium. This suggests that the particles' surfaces must be swollen with solvent and be a partially crosslinked gel layer at any moment during the polymerisation. The surface gel layer stabilises the particles during their growth stage by auto-steric stabilisation. The particles formed have narrow size distributions and are quite similar to those formed in dispersion polymerisations. Nevertheless, they are formed in the absence of stabilisers.

Solvent effect

The selection of an appropriate solvent is an important step in precipitation polymerisation. The polymerisation requires a solvent in which the monomer is soluble, but then the polymer formed must be insoluble and precipitate. In order to deliver high quality polymer microspheres, a solvent known as near-θ solvent is required.

In a polymer solution, a solvent is called a θ solvent when the polymer coils act like ideal chains, assuming exactly their random walk coil dimensions. *e.g.*, acetonitrile for DVB-based polymerisations.

To define a near-θ solvent, it is very important to look at the solvency characteristics of solvents and also at the effect of a polymer in solution. There are two different kinds of solubility parameters: the Hildebrand solubility parameter and Hansen solubility parameters.(5)

- The one-dimensional Hildebrand solubility parameter (δ) corresponds to the cohesive energy density of solvents and polymers. It is an indicator of the affinity of a solute for a solvent, reflecting only the overall solvent properties.
- The three-dimensional Hansen solubility parameters are an attempt to break the overall interactions between a solute and a solvent into dispersive (δ_d), polar (δ_p), and hydrogen-bonding interactions (δ_h).

The latter parameters are related by the following equation (Figure 2.1):

$$\delta^2 = \delta_p^2 + \delta_d^2 + \delta_h^2$$

Equation 2.1 Relation of the three-dimensional Hansen solubility parameters relation. δ_d: the energy from dispersion forces between molecules, δ_p: the energy from dipolar intermolecular force between molecules and δ_h: the energy from hydrogen bonds between molecules.

The Hildebrand solubility parameter of a given solvent is a measure of its solvency behaviour, *i.e.*, its affinity for solutes. The Hildebrand solubility parameter is the square root of the cohesive energy density (Figure 2.2):

$$\delta = \sqrt{\frac{\Delta H_v - RT}{V_m}}$$

Equation 2.2 The Hildebrand solubility parameter. Where, ΔH_v is the heat of vaporisation, R is the ideal gas constant, T is the temperature and V_m is the molar volume.

The cohesive energy density (CED) is the energy needed to remove a given molecule from its nearest neighbours. This is equal to the heat of vaporisation (ΔH_v) of the compound divided by its molar volume (V_m) in the condensed phase. In order for a material to dissolve, these same interactions need to be overcome as the molecules are separated from each other and surrounded by the solvent.

This approach cannot be used for polymers as they exhibit negligible vapour pressure (they will decompose before the heat of vaporisation can be determined). This problem has been solved using the swelling behaviour to assign the Hildebrand value for polymers.

Hansen Solubility Parameters were developed as a way of predicting if a material will dissolve in another and form a solution. The three Hansen parameters are:

δ_d : The energy from dispersion forces between molecules.

δ_p : The energy from dipolar intermolecular force between molecules.

δ_h : The energy from hydrogen bonds between molecules.

As mentioned previously, these three parameters can be treated as coordinates for a point in three dimensions also known as the Hansen space. The nearer two molecules are in this three-dimensional space, the more likely they are to dissolve into each other. In good solvents, the polymer chains will expand in order to increase the favourable interactions with the solvent. In poor solvents, the chains will contract so the unfavourable interactions will be reduced. As a result, polymers tend to aggregate or precipitate in poor solvents.(6,7) According to this, the θ solvent will be at the limit between a good and a bad solvent.

In precipitation polymerisation, Stöver and coworkers(2) found that acetonitrile is the only solvent which can produce monodisperse particles on its own. They studied the formation of monodisperse particles using a mixture of acetonitrile and *n*-butanol or *n*-propanol as co-solvent up to 7:3 v/v ratio. Since those co-solvents have very similar Hildebrand parameter values, they attempted the polymerisation in neat *n*-propanol and neat *n*-butanol but irregular particles were formed. They also tried precipitation polymerisation with a solvent which has the same δ as acetonitrile, DMF, but a gel was formed. Although they have similar Hildebrand parameter values, they have very different Hansen parameters (Table 2.1). Comparing the Hansen parameters of *n*-propanol or *n*-butanol with acetonitrile, the only Hansen parameter which differs significantly is δ_p. Due to the large differences in the polar interaction between different solvents, this would suggest that the solvent polarity is a very important factor in particle formation.

Solvent	*Hildebrand parameter (δ) [(cal/cm^3)$^{1/2}$]*	*Hansen parameters [(cal/cm^3)$^{1/2}$]*		
		δ_d	δ_p	δ_h
***n*-butanol**	10.8	7.8	2.8	7.7
***n*-propanol**	12.2	7.8	3.3	8.5
Acetonitrile	12.1	7.5	8.8	7.5
THF	9.5	8.2	2.8	3.9
DMF	12.1	8.5	6.7	5.5
Toluene	8.9	8.8	0.7	1.0

Table 2.1 Hildebrand and Hansen parameters of selected solvents.

2.1.2. Ion-exchange resins

Ion-exchange resins, or ion-exchange polymers, are insoluble porous matrices that have functional sites/groups that can trap and release ions. Such resins trap ions with a simultaneous release of other ions. The ion-exchange character is provided in the resin by acids and bases. Sulfonic acids are the most widely used groups to provide resins with strong cation-exchange (SCX) capacity, while carboxylic acids are the most used as weak cation-exchangers (WCX). In the case of anions, quaternary ammonium salts are used in strong anion-exchange (SAX) resins and amine moieties in weak anion-exchangers (WAX)·(8)

The ion-exchange capacity (IEC) of a cation/anion-exchange resin is the total number of equivalents of hydroxyl/hydrogen ions per unit weight of resin that can be replaced by another anion/cation. The IEC is an important factor that has a controlling effect on the retention of cations/anions.

In cation-exchange resins, the acidic protons (H^+) from the sulfonic or carboxylic acids can be exchanged with other cations (M^+). The equilibrium can be shifted to the left by increasing the concentration of H^+, or to the right by increasing the M^+ concentration (Figure 2.4). The difference between strong and weak cation-exchange resins is the range of pH in which they can be used. The strong exchangers are used in a range of pH between 1 and 14, whereas the weak exchangers are used between pH 5 and 14. Weak exchangers do not work at low pH therefore they cannot be used to remove the cations of weak bases. SCX resins cannot, however, be used to remove the cations from amino acids or peptides as they will strongly retain those analytes and thus the separation process will be hindered.

$$\text{R-X}^-\text{H}^+ \;+\; \text{M}^+\text{B}^- \;\rightleftharpoons\; \text{R-X}^-\text{M}^+ \;+\; \text{H}^+ \;+\; \text{B}^-$$

Figure 2.4 Equilibrium for cation-exchange resins.

In the case of anion-exchange resins, the hydroxyl (HO^-) groups of ammonium or charged amine groups can be exchanged for other anions (B^-). The equilibrium in this case can also be shifted to the left by increasing the concentration of HO^-, or to the right by increasing the concentration of B^- (Figure 2.5). The difference between strong and weak anion-exchange resins is also the range of pH in which they are used. The strong exchangers are used in a range of pH between 0 and 12 and the weak exchangers are used between pH 0 and 9. In this case, the weak exchangers are used to remove strong acids which the SAX cannot remove.

$$\mathrm{R\text{-}X^+HO^-} + \mathrm{M^+B^-} \rightleftharpoons \mathrm{R\text{-}X^+B^-} + \mathrm{HO^-} + \mathrm{M^+}$$

Figure 2.5 Equilibrium for anion-exchange resins.

2.2. AIM OF THE RESEARCH

Macroreticular polymers are very useful in synthetic organic chemistry as they are easy to remove from the reaction medium due to their rigid, insoluble character suitable for filtration. Furthermore, their pore size offers little hindrance to the diffusion of reactants and the reactive groups are more accessible and easy to functionalise. However, despite the easy functionalisation methods used for these materials, a general functionalisation method suitable for several different functional groups is still lacking, and in some cases the presence of a co-monomer is required for functionalisation.

To tackle the chemical functionalisation requirements described above, we focused upon the development of olefin metathesis-based methods for the functionalisation of porous organic polymer networks, with a special focus upon porous polymer microspheres with low mean particle diameters and narrow particle size distributions, since such materials are very appealing from an applications perspective.(9) Blechert and coworkers(10) in 1996 reported, for the first time, olefin cross-metathesis (CM) reactions on resin-bound substrates. However, porous particles where the crosslinker serves simultaneously as a crosslinking agent and reactive handle for CM has never been described previously. Herein, we report the functionalisation of porous polyDVB under very mild conditions where the polydivinylbenzenes were prepared by PP.(1,11) One of the goals was to demonstrate the ease with which a broad range of diverse chemical functionalities could be installed into beaded polystyrenes by the appropriate choice of coupling partner for the polymer-bound vinyl groups.

2.3. RESULTS AND DISCUSSION

2.3.1. Synthesis of porous polymer microspheres by precipitation polymerisation

Monodisperse microspheres can be obtained by PP of a multivinyl crosslinker. The most used monomer for PP is DVB, which is used normally as a mixture of the *meta*- and *para*- isomers in either 55% or 80% grade. The remaining percentage content is made up of *meta*- and *para*- isomers of ethyl styrene. Polymers prepared from DVB-55 have fewer vinyl groups therefore they are less crosslinked and lower yields of insoluble products are obtained (Table 2.2).

Polym. ref.	*DVB*	*Mon./solv. (%wt./v)*	*AIBN (g)*	*CH_3CN (%)*	*Toluene (%)*	*Time (h)*	*Yield (g)*	*Yield (%)*
II-1$_a$	80	2	0.45	100	0	48	0.31	3
II-1$_b$	55	2	0.39	100	0	48	2.43	24
II-1$_c$	80	3	0.45	75	25	48	3.71	36
II-1$_d$	55	3	0.39	75	25	48	3.30	32
II-1$_e$	80	4	0.45	75	25	48	6.03	58
II-1$_f$	55	4	0.39	75	25	48	5.29	51
II-1$_g$	80	4	0.45	60	40	48	7.06	68
II-1$_h$	55	4	0.39	60	40	48	4.66	45

Table 2.2 Different conditions used for the synthesis polyDVB.

Table 2.2 shows that the greater the amount of crosslinker used in the polymerisation, the higher the yields are. The use of toluene as porogenic solvent in combination with acetonitrile results in the installation of porosity into the polymer, phase separation occurs later and higher yields and more mechanically robust particles are obtained.

Polymer ref.	*Elemental microanalysis (wt.%)*		
	C	*H*	*N*
Expected poly(DVB-80)	91.2	8.1	0.7
II-1$_g$	90.3	7.8	0.4
Expected poly(DVB-55)	91.0	8.4	0.6
II-1$_h$	90.2	8.0	0.3

Table 2.3 Elemental microanalysis results for polymers II-1$_g$ and II-1$_h$.

Table 2.3 shows the elemental microanalysis results for the poly(DVB-80) isolated in the highest yield (**II-1$_h$**) and its homologue starting with DVB-55 as monomer. The small differences between the expected and the experimental results confirm that the polymers obtained are polyDVB. The traces of nitrogen found in the microanalysis were attributed to the presence of AIBN-derived fragments in the polymers. FT-IR spectroscopic analysis was also used to show that the polymers formed were polyDVB. The spectrum below (Figure 2.6) shows a band at 900 cm^{-1}, which verifies the presence of the residual double bonds from the DVB. Similar elemental microanalysis and FT-IR spectroscopic data were collected for the other poly(DVB-80) and poly(DVB-55) materials in the series.

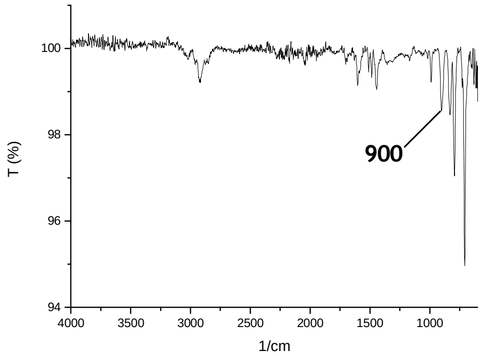

Figure 2.6 FT-IR spectrum of a polyDVB.

The shape, size and size distribution of the particles were determined using scanning electron microscopy. SEM micrographs of the poly(DVB-80) and poly(DVB-55) materials are presented in Figure 2.7. The SEM micrographs show that the polymer beads obtained were not monodisperse. This could be due to the amount of toluene used during the polymerisation. Since the porogenic solvent swells the particle nuclei, the reaction medium becomes less rich limiting the growth of some particles and therefore larger differences in size are observed. Comparing particles **II-1$_e$** and **II-1$_f$** with particles **II-1$_g$** and **II-1$_h$** respectively, an increase in the size of the particles can be appreciated, due to the higher amounts of toluene used. Figure 2.7 also shows evidence of some physical aggregation of the particles.

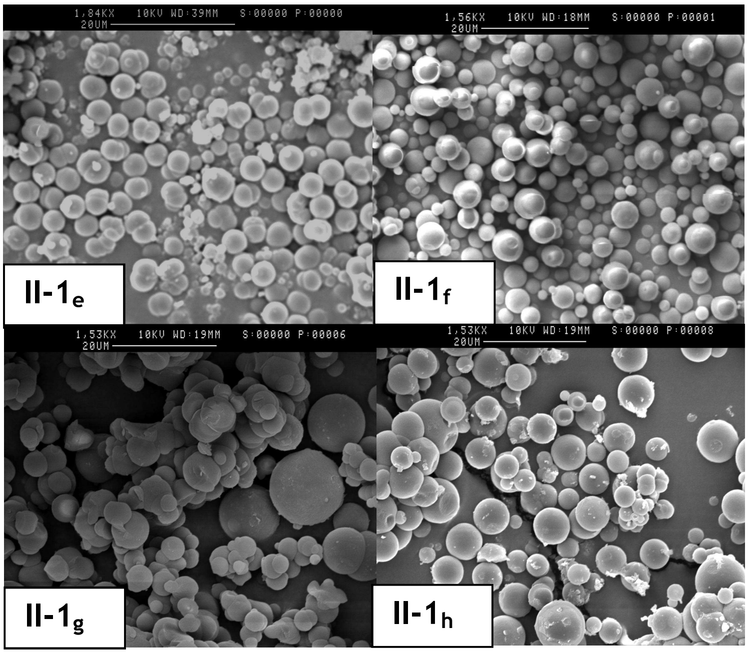

Figure 2.7 SEM micrographs of poly(DVB-80) and poly(DVB-55) with 4% wt./v monomer concentration.

Statistical analysis of the above micrographs was carried out using Image J (an image analysis program) by measuring carefully the diameters of at least 100 beads. The coefficient of variation (CV) is used as a measure of the dispersity of the particles as follows;

- CV < 3% monodisperse particles
- 3% < CV < 16% quasi-monodisperse particles
- > 16% polydisperse particles

Table 2.4 shows that the particles obtained were polydisperse as the CV value was above 16% in all cases. The high dispersity level could be attributed to the amount of toluene used. As it was mentioned previously, toluene swells the particle nuclei, which makes the media less rich in the porogenic solvent and some other simultaneously formed particles could have precipitated earlier.

Polym. ref.	*Mean diameter (μm)*	*SD (μm)*	*Min (μm)*	*Max (μm)*	*CV (%)*
II-1$_e$	2.9	1.0	0.7	4.9	33
II-1$_f$	3.3	1.2	1.2	6.2	36
II-1$_g$	4.3	2.2	1.3	14.8	52
II-1$_h$	4.6	1.9	0.9	9.6	42

Table 2.4 Image J analysis of poly(DVB-80) and poly(DVB-55) materials.

Nitrogen sorption analysis was another technique used to analyse these beaded products, with the specific surface area being calculated using the Brunauer-Emmet-Teller (BET) method. Smaller pore diameters and surface areas were obtained for polymers **II-1$_e$** and **II-1$_f$** (Table 2.5), due to the amount of toluene used during the polymerisation. By using less amount of the porogenic solvent, the particle nuclei will not capture the oligomers in a fully swollen state and therefore more crosslinked material will be obtained. Polymer **II-1$_f$** shows a non-porous character confirming that the amount of porogenic solvent used during the polymerisation was not enough. Thus, because of the big average pore diameters, and the high surface areas, polymers **II-1$_g$** and **II-1$_h$** were used for the preliminary tests of CM reactions.

Polymer ref.	*Specific surface area (m^2/g)*		*Specific pore vol. (cm^3/g)*	*Av. pore diameter (nm)*
	BET	*Langmuir*		
II-1$_e$	-	775	0.305	2.1
II-1$_f$	5	-	-	-
II-1$_g$	815	-	0.445	2.2
II-1$_h$	165	-	0.105	2.6

Table 2.5 Nitrogen sorption analysis data for poly(DVB-80) and poly(DVB-55) materials with 4% wt./v monomer concentration.

2.3.2. Quantification of the residual double bonds in polyDVB

In 1997, Law *et al.* reported upon a quantitative study of the level of residual unreacted vinyl groups by integration of the appropriate signals in the ^{13}C solid state NMR spectra of DVB resins prepared by suspension polymerisation. They found that for resins prepared with the 55% grade of commercial divinylbenzene, around 32% of the vinyl groups remained unreacted after the polymerisation and for resins made by DVB-80, around 45%.(12)

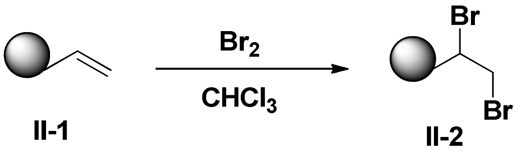

Figure 2.8 Bromination reaction of polyDVB.

Bromination reactions (Figure 2.8) were carried out to quantify the number of residual double bonds in polyDVB after precipitation polymerisation, by elemental microanalysis of bromine. Unfortunately, the orange colour of both polymers (**II-1**$_g$ and **II-1**$_h$) suggested that bromine was trapped inside the pores and therefore the elemental microanalysis results were not reliable.

2.3.3. Functionalisation of porous polymer microspheres by olefin cross metathesis

Functionalisation of porous polymer microspheres was carried out *via* CM reactions. With these reactions, the functionalisation is performed under very mild conditions and a wide range of coupling partners can be used whilst retaining the integrity of the polymer beads. A noteworthy advantage of this method is the retention of olefin functionality in the functionalised polymers, which can be used potentially for further functionalisation.

Methyl acrylate

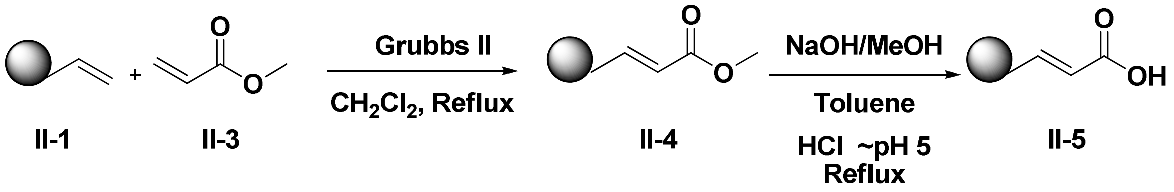

Figure 2.9 CM reaction of polyDVB with methyl acrylate followed by a hydrolysis reaction.

CM reactions involving **II-1$_g$** and **II-1$_h$** were first tested using 4 equiv (relative to the amount of double bonds available of the polymer, assuming that only one of the double bonds reacted during PP) of methyl acrylate (**II-3**) as the coupling agent (Figure 2.9), since this compound is a good CM partner for styrene in solution,[9] and its hydrolysed product could be a potential weak cation-exchanger. Figure 2.10 shows the FT-IR spectra of both polymers after a CM reaction with methyl acrylate (**II-4$_g$** and **II-4$_h$**), in which the appearance of a band at 1735 cm^{-1} confirms the success of the functionalisation reaction.

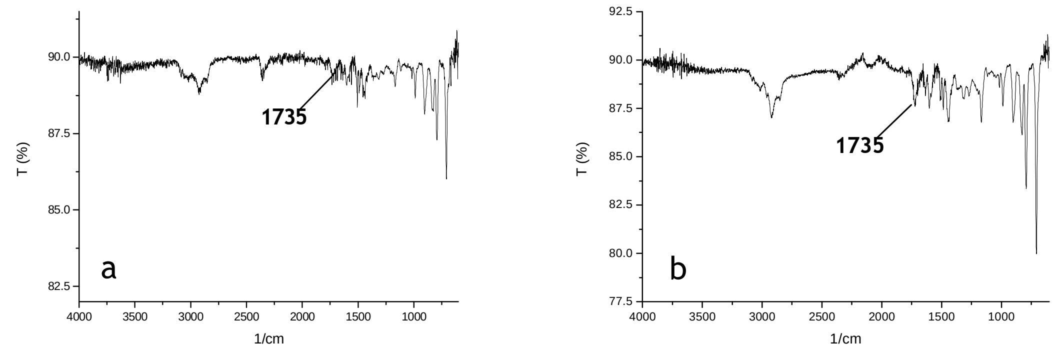

Figure 2.10 FT-IR spectra of: a) II-4$_g$ (poly(DVB-80)), and b) II-4$_h$ (poly(DVB-55)).

SEM analysis of the particles after CM (Figure 2.11) showed that the particle quality was still good after the reaction, but not as good as it could have been. This is probably due to the use of a magnetic stirrer bar during the reaction. As a consequence of this problem, it was decided to not use a magnetic stirrer bar in further functionalisation reactions.

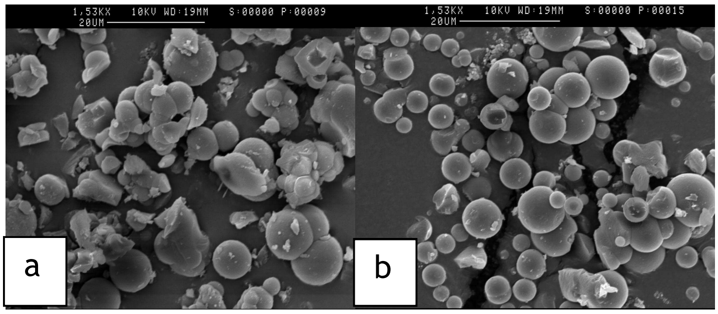

Figure 2.11 SEM images of: a) poly(DVB-80) and b) poly(DVB-55) after CM reactions with methyl acrylate.

Elemental microanalysis of **II-4$_g$** (*89.6% C, 7.8% H, 0.4% N*) and **II-4$_h$** (*88.9% C, 7.9% H, 0.3% N*) presents a small variation in comparison with the polymers **II-1$_g$** (*90.3% C, 7.8% H, 0.4% N*) and **II-1$_h$** (*90.2% C, 8.0% H, 0.3% N*). By using methyl acrylate as coupling partner, oxygen moieties are introduced on the polymer and therefore, the overall amount of carbon and hydrogen is reduced. The differences in the carbon contents may indicate that the modifications were performed successfully and methyl acrylate was potentially immobilised.

Solid state NMR was also carried out to verify the insertion of methyl acrylate. Figure 2.12 shows the solid state ^{13}C NMR spectra of polymers **II-1$_g$** and **II-1$_h$** as well as the polymers functionalised with methyl acrylate (**II-4$_g$** and **II-4$_h$**). The ^{13}C NMR spectra of the polymers (Figure 2.12a and b) show evidence of the residual double bonds of the precursor polymers. The appearance of a signal at 65 ppm (Figure 2.12c and d) after CM reaction with methyl acrylate indicates the presence of the methoxy group belonging to the immobilised ester. This confirms the CM reactions and illustrates the potential of CM as a novel, easy and efficient functionalisation technique.

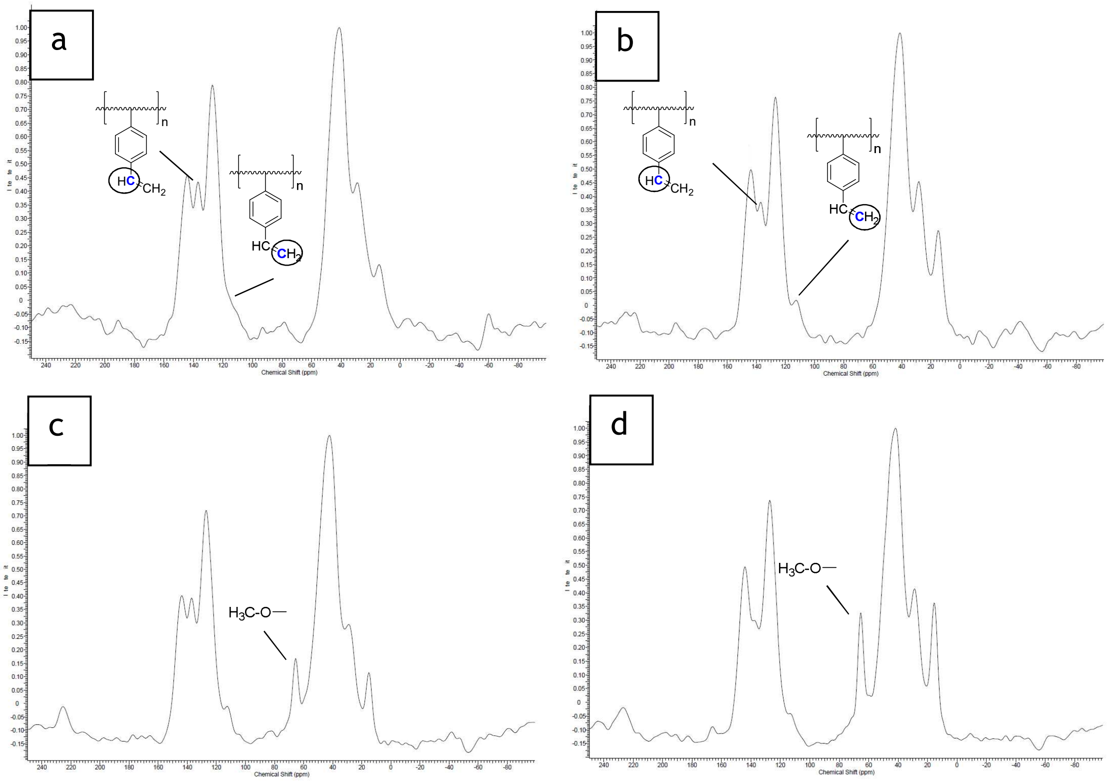

Figure 2.12 ^{13}C NMR spectra of: a) poly(DVB-80), b) poly(DVB-55),c) functionalised poly(DVB-80) and d) functionalised poly(DVB-55).

Due to the higher amount of *meta*- and *para*- ethyl styrene in poly(DVB-55) compared to poly(DVB-80), the particle nuclei swell more than the nuclei of poly(DVB-80). The higher the amount of DVB in the monomer, the more crosslinked the microspheres will be. Figure 2.12 also shows that the residual vinyl group signals at 138 and 112 ppm of **II-1$_g$** (Figure 2.12a) is less intense than the corresponding signals at 138 and 112 ppm for **II-1$_h$** (Figure 2.12b). This could be because the first polymer is more crosslinked and therefore it has less unreacted double bonds remaining. As a consequence, the ester or the acid immobilisations seem to be less efficient for **II-4$_g$** than for **II-4$_h$**.

Hydrolysis reactions were carried out after CM in order to obtain ion-exchange resins (**II-5$_g$** and **II-5$_h$**). The FT-IR spectra of these polymers (Figure 2.13) show the shift of the carbonyl peak from 1735 cm^{-1} to 1705 cm^{-1} and the appearance of a broad band in the OH region of the FT-IR spectra. This indicates that the hydrolysis reactions were successful and that weak cation-exchangers were obtained.

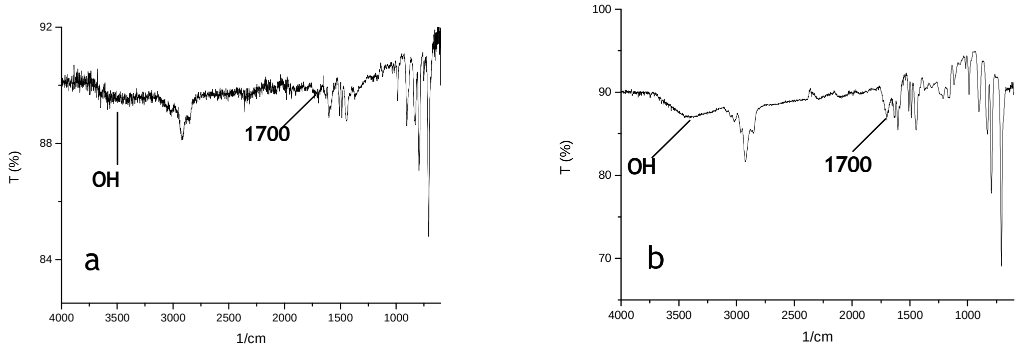

Figure 2.13 FT-IR spectra of: a) II-5$_g$ and b) II-5$_h$.

As mentioned previously, the quality of the beads as seen in the SEM micrographs (Figure 2.14) was not the best due to the use of a magnetic stirrer bar during the reactions. Elemental microanalysis results of **II-5$_g$** (*87.4% C, 7.6% H, 0.4% N*) and **II-5$_h$** (*84.1% C, 7.2% H, 0.3% N*) show a great decrease in the carbon amount in comparison with the results of methyl acrylate functionalised polymers (**II-4$_g$** and **II-4$_h$**), which suggests that the hydrolysis reactions occurred.

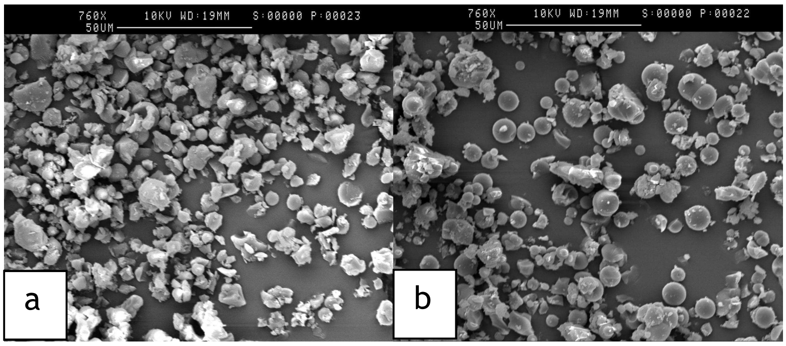

Figure 2.14 SEM micrographs of: a) II-5$_g$ and b) II-5$_h$.

Acrylic Acid

CM reactions (Figure 2.15) involving **II-1$_g$** and **II-1$_h$** were tested with acrylic acid (**II-6**) for a direct synthesis of weak cation-exchange resins. SEM micrographs of the functionalised polymers obtained are not shown as a magnetic stirrer bar was used and some particles were destroyed.

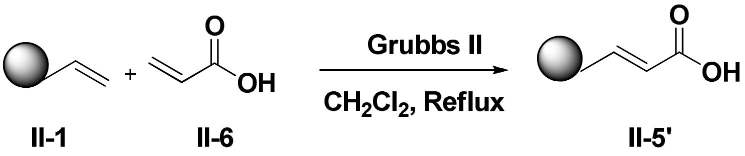

Figure 2.15 CM reaction of polyDVB with acrylic acid.

Figure 2.16 shows the FT-IR spectra of the polymers (**II-1$_g$** and **II-1$_h$**) after CM reaction with acrylic acid (**II-5$_g$'** and **II-5$_h$'**). These spectra confirm the success of the CM reaction with acrylic acid and also show that the carbonyl peak of the acid appears at the same wavenumber as it appeared after the hydrolysis reaction in Figure 2.13.

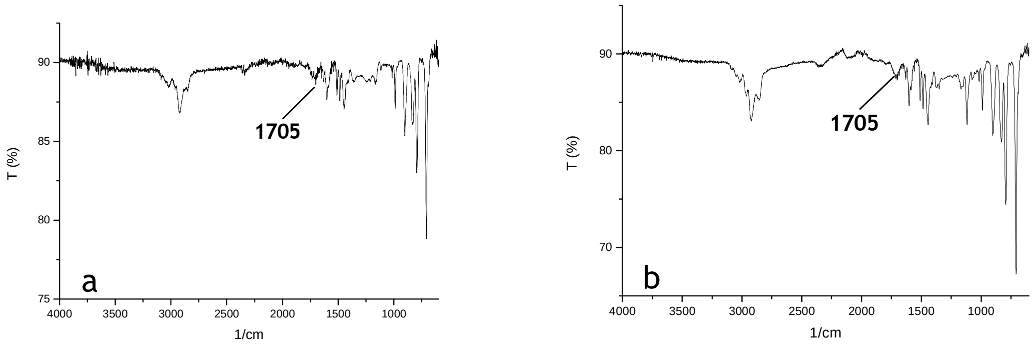

Figure 2.16 FT-IR spectra of: a) II-5$_g$' and b) II-5$_h$'.

As mentioned previously, the quality of the SEM micrographs was not the best due to the use of a magnetic stirrer bar during the reaction. Elemental microanalysis results of **II-5$_g$'** (*89.5% C, 7.8% H, 0.4% N*) and **II-5$_h$'** (*87.1% C, 7.6% H, 0.3% N*) show decrease in the carbon amount in comparison with the starting polymers polymers (**II-1$_g$** and **II-1$_h$**), which probes the success of the CM with acrylic acid. The carbon amounts of both elemental microanalyses also suggest that polymer **II-1$_h$** underwent the functionalisation reactions more efficiently than **II-1$_g$** as lower amount of carbon was observed.

To sum up, due to all the reasons mentioned before, and because polymer **II-1$_h$** has a multilayer adsorption of the nitrogen and has a larger pore-size than the others, it was selected for further functionalisation reactions.

Control experiment

A catalyst-free reaction was carried out as control experiment. The reaction was performed to study whether the methyl acrylate was coupled to the polymer *via* olefin cross metathesis or if it was physically entrapped inside the polymer network as happened with bromine. The lack of the carbonyl or the ester peak in the FT-IR spectrum (Figure 2.17a) in the isolated product confirmed the success in the ester immobilisation by olefin metathesis.

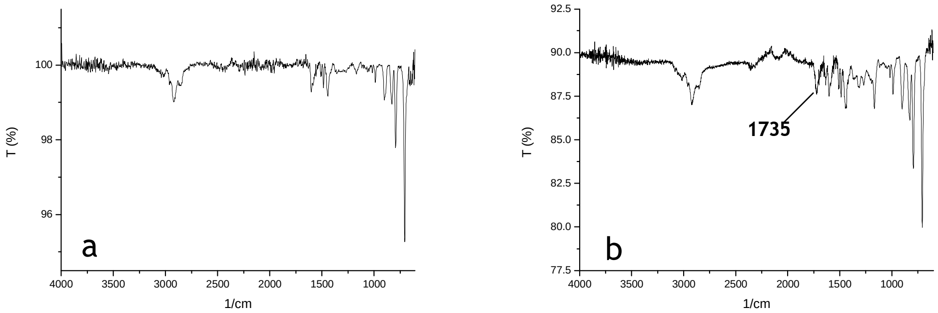

Figure 2.17 FT-IR spectrum of: a) polymer II-1$_h$ after the control experiment with methyl acrylate and b) polymer II-1$_h$ after CM with methyl acrylate.

Dimethyl vinylphosphonate

A CM reaction of polymer **II-1$_h$** with dimethyl vinylphosphonate (**II-7)** as coupling partner (Figure 2.18) was carried out to yield a strong cation-exchanger after subsequent hydrolysis of the phosphonate.

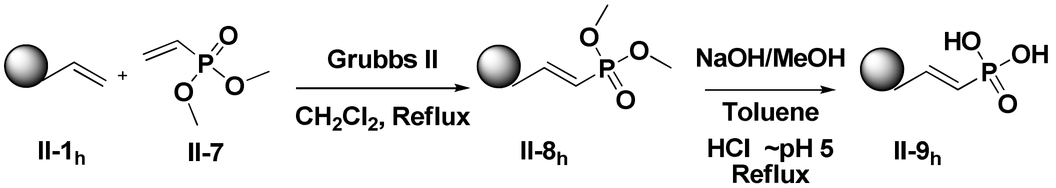

Figure 2.18 CM reaction with dimethyl vinylphosphonate and followed by hydrolysis reaction of the phosphonate.

Figure 2.19a shows the FT-IR spectrum of polymer **II-1$_h$** after CM with **II-7** (**II-8$_h$**). The appearance of the peaks at 1370 cm^{-1} (O-P-O str.), 1255 cm^{-1} (P=O str.) and 1180 cm^{-1} (C-O-P str.) confirms that the immobilisation of the phosphonate moiety was successful. On the other hand, Figure 2.19b shows the FT-IR spectrum of the functionalised polymer after the hydrolysis reaction (**II-9$_h$**). The appearance of the broad band at 3400 cm^{-1} (OH str.) suggests the presence of the phosphonic acid. Also, the presence of the peaks at 1370 cm^{-1} (O-P-O str.) and 1190 cm^{-1} (P=O str.) combined with the disappearance of the band at 1180 cm^{-1} (C-O-P str.) indicates that the hydrolysis was successful and complete.

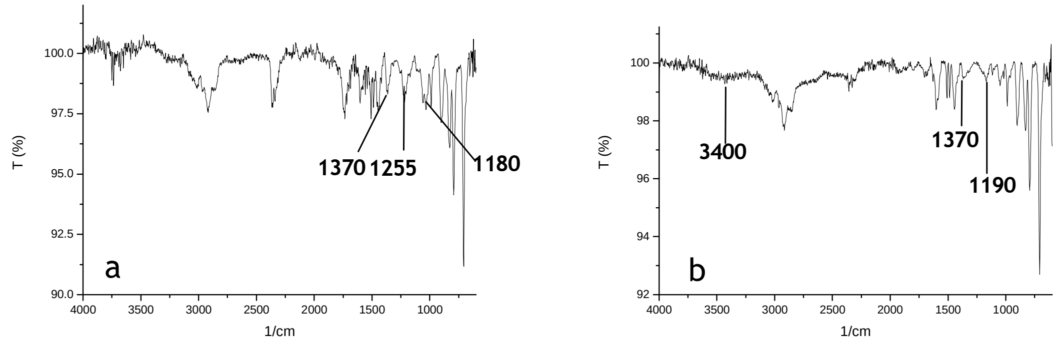

Figure 2.19 FT-IR spectra of: a) polymer II-1$_h$ after CM reaction with dimethyl vinylphosphonate and b) polymer II-9$_h$.

SEM micrographs (Figure 2.20) show that with no magnetic stirring of the reaction media, the microspheres kept the spherical shape. Thus, they were not damaged by the conditions used during the functionalisation or hydrolysis reactions.

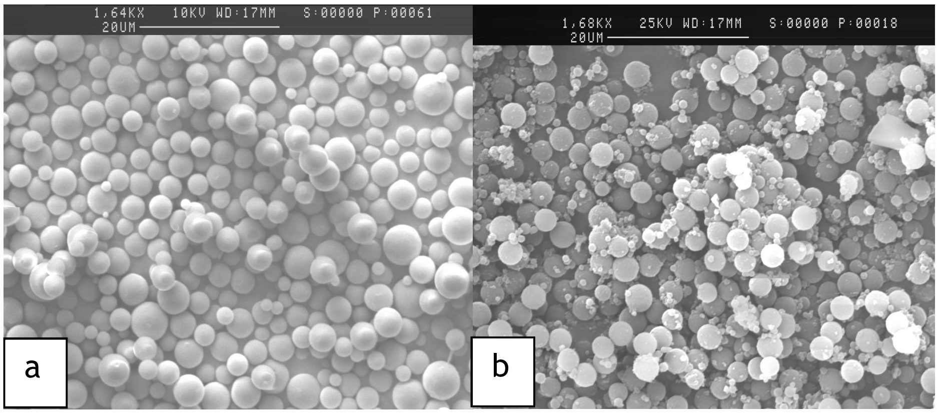

Figure 2.20 SEM micrograph of: a) II-8$_h$ and b) II-9$_h$.

Fmoc-homoallylamine

Fmoc-homoallylamine was chosen to be used as anion-exchanger after the removal of the Fmoc group. The synthesis began with the commercially available butenol, **II-10**, (Figure 2.21). A Mitsunobu(13) reaction was carried out to give homoallylphthalimide (**II-11**), followed by a Gabriel synthesis.(14)

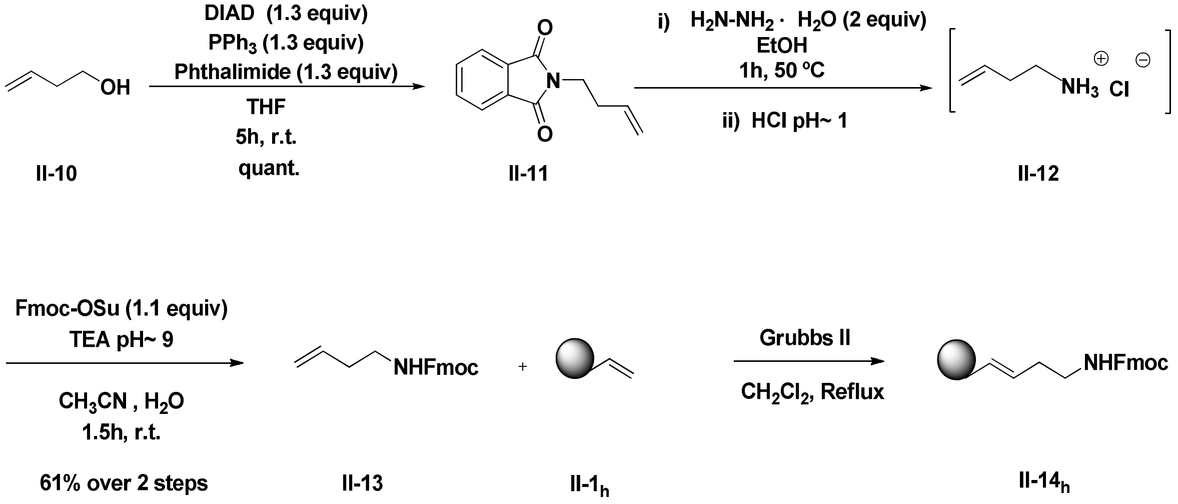

Figure 2.21 Synthesis and CM of Fmoc-homoallylamine.

Different conditions were attempted to obtain product **II-11**. Some of them are summarised in Table 2.6. The first attempt was carried out using CH_2Cl_2 as solvent, giving a yield of 74%. Changing the solvent to THF improved the yield of the reaction, which was optimised further by leaving the reaction stirring for one extra hour. These changes in the protocol led to the isolation of the product in a quantitative yield. Compound (**II-11**) was deprotected but the obtained product (**II-12**) was insoluble in organic solvents and could therefore not be characterised fully. This intermediate (**II-12**) was treated with Fmoc-OSu to impart fluorescence character to the product (**II-13**).(15) The last step was the metathesis, in which the obtained product (**II-14$_h$**) shows weak fluorescence under UV light. This fluorescence given by the Fmoc group confirms the success of the functionalisation reaction.

Attempt	*Solvent*	*Time (h)*	*Yield (%)*
1	CH_2Cl_2	4	74
2	THF	4	80
3	THF	5	quant.

Table 2.6 Some conditions used to synthesise compound II-11.

FT-IR spectrum (Figure 2.22a) shows the appearance of new bands at 3335 cm^{-1} (NH str.), 1685 cm^{-1} (C=O str.) and 1260 cm^{-1} (C-O str.). However, the intensity of the bands is higher than the intensity of the polymer bands, which suggests that the polymer needed to be washed. The polymer was washed several times with dichloromethane, methanol, water and acetone but the FT-IR spectrum looked similar to the one shown before (Figure 2.22a). This may suggest that some Fmoc protected homoallylamine was trapped inside the polymer. An SEM micrograph (Figure 2.22b) revealed that the shape of the beads was not changed but some aggregation was found as the purification was incomplete.

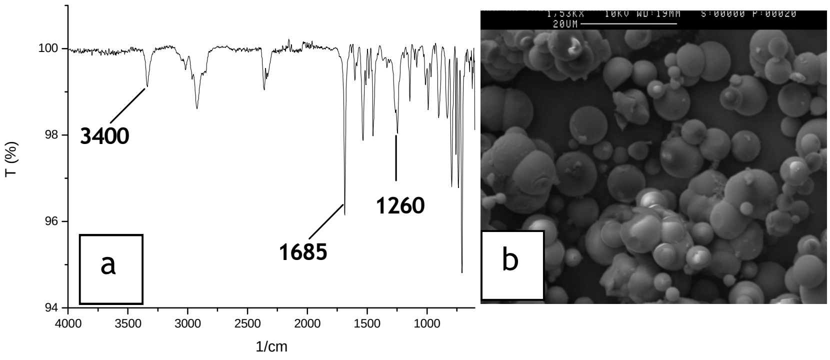

Figure 2.22 a) FT-IR spectrum and b) SEM micrograph of II-14$_h$.

Fmoc-allylglycine

CM involving **II-1$_h$** and Fmoc protected allylglycine, **II-15**, (Figure 2.23) was carried out to obtain polymer **II-16$_h$**. Allylglycine was selected as coupling partner as it is a zwitterionic species which can potentially form chromatographic surfaces for hydrophilic interaction liquid chromatography separations and pH sensitive resins to be used as WAX and SAX, but also for amino acid or even protein immobilisation. An Fmoc group was used to give fluorescence to the coupled polymer.

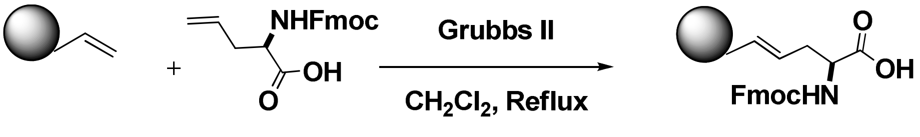

II-1$_h$ **II-15** **II-16$_h$**

Figure 2.23 CM reaction with Fmoc protected allylglycine.

The FT-IR spectrum of the product (Figure 2.24a) confirms the success of the reaction as the appearance of the different peaks at 3390 cm^{-1} (OH str.), 1690 (C=O) cm^{-1} and 1100 cm^{-1} (C-O str.) confirms that the amino acid has been immobilised onto the polymer. The SEM micrograph (Figure 2.24b) shows that the particles retained their integrity and no chemical aggregation was apparent after functionalisation.

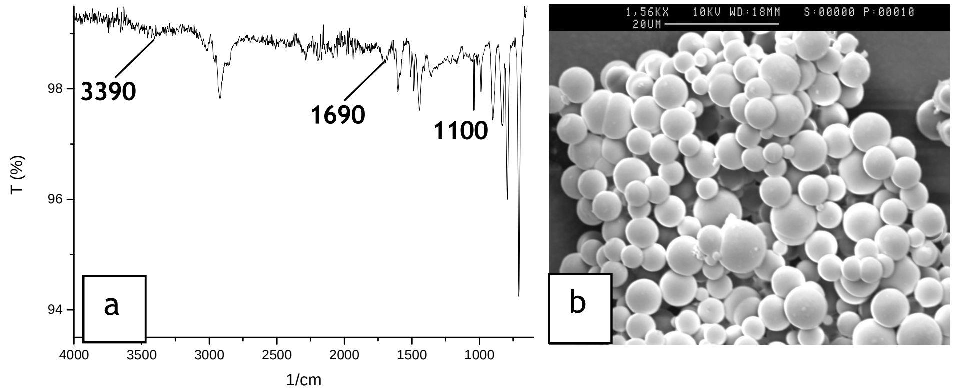

Figure 2.24 a) FT-IR spectrum and b) SEM micrograph of II-16$_h$.

Fmoc-4-allyloxyproline

The aim of this reaction was to perform a CM with compound **II-19** to synthesize a supported organocatalyst. In the first step of the synthesis, *trans*-4-hydroxyproline was protected with Fmoc hydroxysuccinimide(15) (Figure 2.25). The reaction gave the product **II-18** in good yield. Then, **II-18** was diallylated,(16) followed by a hydrolysis. Firstly, basic hydrolysis(17) was carried out, but unfortunately, the Fmoc moiety was also removed from the compound. To avoid

Fmoc deprotection, acidic hydrolysis(18) was performed, which gave product **II-19**. The last step was the metathesis, in which the obtained product showed weak fluorescence because of the Fmoc group.

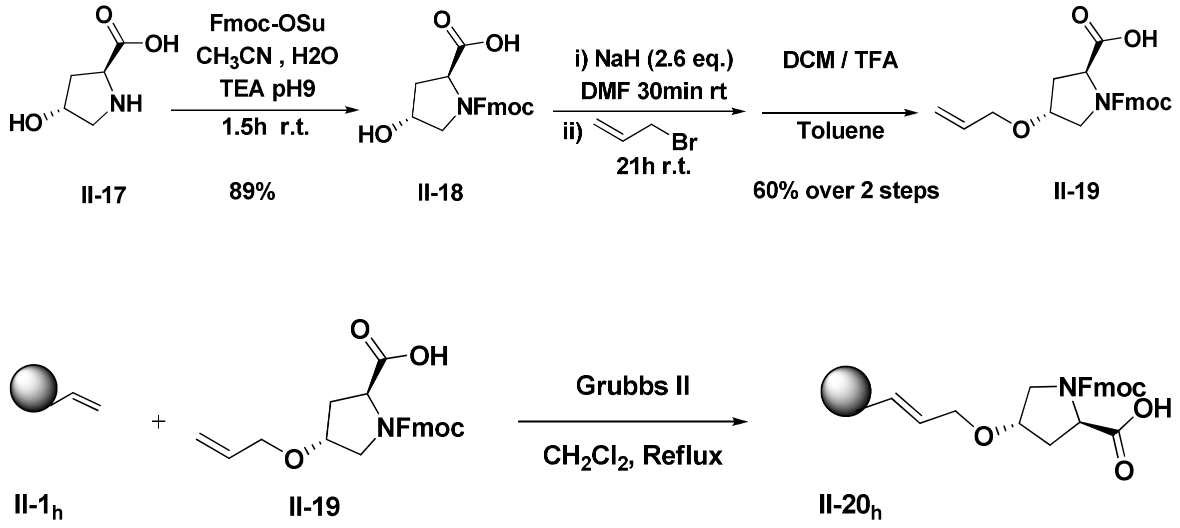

Figure 2.25 Synthesis and CM of Fmoc-4-allyloxyproline.

The appearance of the broad band in the FT-IR spectrum at 3400 cm^{-1} (OH str.) and a broad peak in the carbonyl region (1700 cm^{-1}) confirms the success of the reaction (Figure 2.26a). The peak in the carbonyl region represents the two different carbonyl peaks of the acid and the Fmoc protecting group. The SEM micrograph (Figure 2.26b) shows that when employing CM as a functionalisation technique, the particles were not damaged; well-shaped particles are still present and no chemical aggregation could be observed.

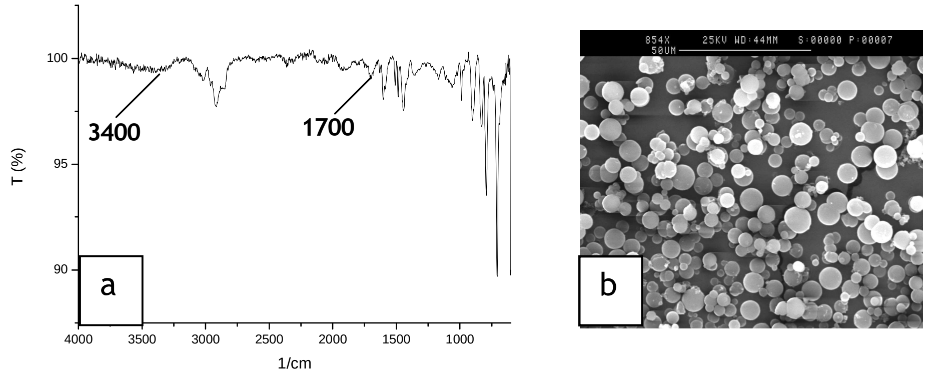

Figure 2.26 a) FT-IR spectrum and b) SEM micrograph of II-20$_h$.

Fmoc-allylcysteine

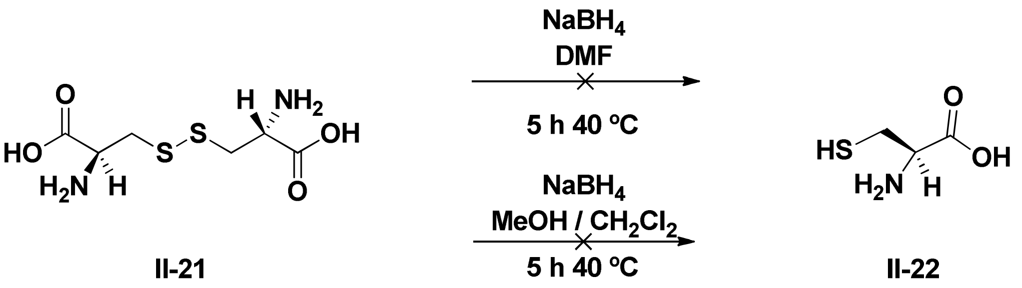

Figure 2.27 Attempt at disulfide cleavage to form II-18.

The aim of this reaction was to carry out the CM with Fmoc-protected allylcysteine (**II-26**) to measure the ion-exchange capacity of the corresponding deprotected zwitterionic species. The synthesis started from *L*-Cystine (**II-21**), attempting to reduce the disulfide bond to obtain cysteine (**II-22**). However, this reaction was unsuccessful (Figure 2.27) because the disulfide bond could not be cleaved.

A new strategy was followed. The synthesis started from **II-23** and the first reaction was the cleavage of the trityl group, forming **II-24** in good yield. Unfortunately, the allylation step was not successful (Figure 2.28). The allylation was carried out but the diallylated product was obtained (**II-25**).

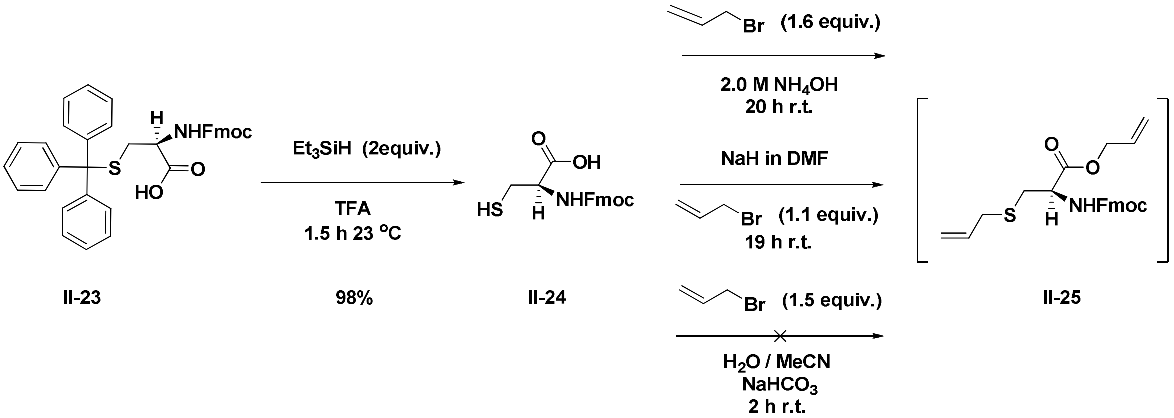

Figure 2.28 Trityl deprotection and dillylation reaction.

The hydrolysis of the resulting ester was carried out under basic conditions; however, both allyl groups were removed, as well as the Fmoc group (**II-22**). In order to not deprotect the Fmoc group, hydrolysis conditions were changed and the reaction was carried out in acidic media. Using an acidic hydrolysis, the final product **II-26** was obtained once, but it was not possible to isolate it pure. When acidic hydrolysis was used again, both allyl groups were deprotected (**II-27**). Different allylation conditions were also used in order to get the monoallylated product in one step rather than in two (diallylation plus hydrolysis). However, no monoalylated or diallylated products were obtained (Figure 2.29).

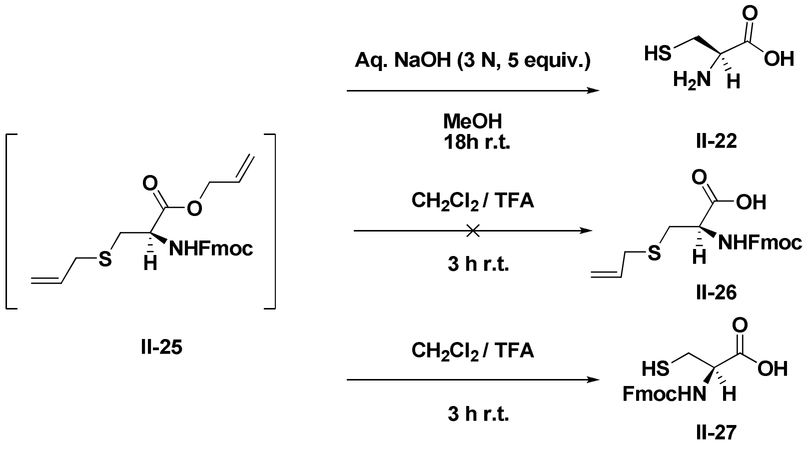

Figure 2.29 Hydrolysis reactions for the synthesis of Fmoc-allylcysteine.

Since the synthesis of **II-26** proved to be problematic, and taking in consideration that other reactions with zwitterionic species were previously carried out successfully, it was decided to abandon the synthesis of **II-26**.

2.3.4. Dispersity study of particles formed by precipitation polymerisation

Results with toluene as porogenic co-solvent

In order to obtain particles that were monodisperse, the monomer and initiator concentrations were varied. Table 2.7 shows the different polymerisation conditions carried out with DVB-80 and DVB-55 as monomers. As was mentioned before, polymers made by DVB-55 have fewer vinyl groups and therefore they are less crosslinked, which means lower yields are obtained (Table 2.7). The monomer concentration was reduced to 2% wt./v in order to supress particle aggregation. However, the decrease in monomer concentration gave lower yields. It can also be observed that when increasing the proportion of toluene, higher yields were obtained, as toluene delayed the phase separation. The amount of initiator used was also changed to ascertain if it will affect the total yield of the polymerisation but, similar yields were obtained in all cases.

Polym. ref.	*DVB*	*Mon. conc. (%wt./v)*	*AIBN (g)*	*CH_3CN (%)*	*Toluene (%)*	*Time (h)*	*Yield (g)*	*Yield (%)*
II-1$_i$	55	4	0.39	80	20	48	3.85	37
II-1$_j$	80	2	0.45	80	20	48	6.55	59
II-1$_k$	55	2	0.39	80	20	48	5.00	48
II-1$_l$	80	2	0.20	80	20	48	5.65	55
II-1$_m$	55	2	0.20	80	20	48	3.90	38
II-1$_n$	80	2	0.45	70	30	48	5.65	56
II-1$_o$	55	2	0.39	60	40	48	4.10	46

Table 2.7 Precipitation polymerisation results and conditions.

The shape, size and size distribution of the particles were determined using SEM. SEM micrographs of poly(DVB-80) and poly(DVB-55) are presented in Figure 2.30.

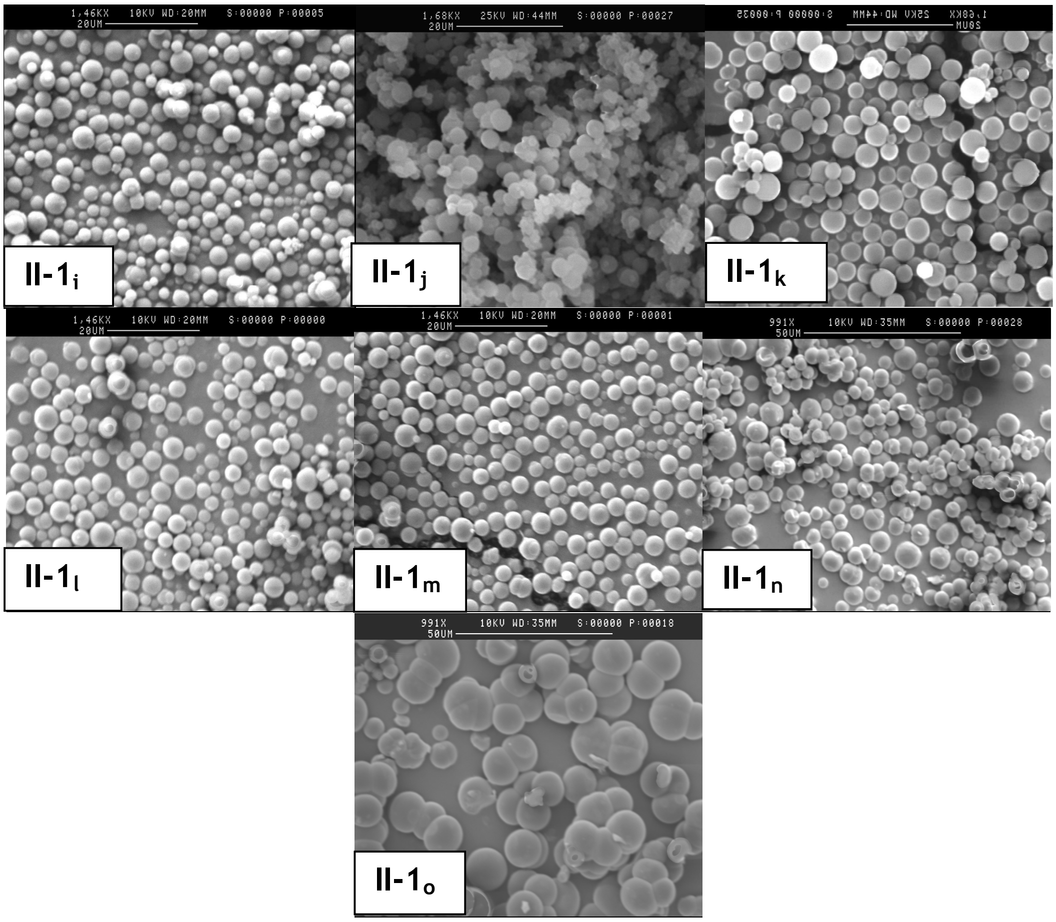

Figure 2.30 SEM micrographs of different polymers using toluene as co-solvent.

Table 2.8 shows that quasi-monodisperse particles were obtained for polymer **II-1$_{i}$** (CV < 16%). The only difference between polymer **II-1$_{i}$** and polymer **II-1$_{h}$** was the proportion of toluene co-solvent used, 40% for polymer **II-1$_{h}$** and 20% for polymer **II-1$_{i}$** (Table 2.8). Unfortunately, when polymer **II-1$_{i}$** was tested in CM with methyl acrylate, the cross-metathesis reaction was unsuccessful; no evidence of an ester group was observed in the FT-IR spectrum of the product after functionalisation. When the monomer concentration was reduced for the formation of polymers **II-1$_{j}$** and **II-1$_{k}$**, polydisperse particles were obtained. In addition, these polymers did not undergo CM reaction with methyl acrylate either. By changing the initiator amount from 2 mol% to 2 wt.% (Polymer **II-1$_{l}$** and **II-1$_{m}$**) not very spherical particles in shape were obtained and they did not undergo a CM reaction with methyl acrylate. The final attempt to prepare monodisperse and functionalisable particles was carried out when the amount of toluene was increased. It was thought that by increasing the proportion of this porogenic solvent, the resulting polymers could undergo the CM reaction as the pore formation will be favoured with large amounts of toluene. However, the increment of toluene led to the aggregation of the particles and the formation of some coagulum (**II-1$_{n}$** and **II-1$_{o}$**).

Polym. ref.	*Mean diameter (μm)*	*SD (μm)*	*Min (μm)*	*Max (μm)*	*CV (%)*
II-1$_{i}$	3.5	0.27	2.9	4.0	8
II-1$_{j}$	3.6	0.67	2.1	5.3	19
II-1$_{k}$	4.1	0.94	1.9	5.8	23
II-1$_{l}$	3.6	0.69	1.6	5.0	19
II-1$_{m}$	2.8	0.66	1.5	4.4	24
II-1$_{n}$	4.1	1.5	1.0	8.3	38
II-1$_{o}$	9.8	3.3	2.4	17	34

Table 2.8 Statistical analysis of different polymers using toluene as porogenic co-solvent.

Another aspect that has to be considered according to the potential use of the polymers as SPE sorbents is the size of the particles. Small particle diameters of 5-10 μm have been reported as the optimum particle size for efficient SPE.(19) Small particles promote better contact with the analytes during sample loading. An SPE column packed with larger particles will decrease the efficiency of the column as poorer retention of the analytes are obtained as the sample has larger pathways to flow between the particles. On the other hand, particle sizes much below 5 µm are often undesirable for SPE as higher pressures are required to pass samples through a column packed with small particles and longer retention times are obtained making the column less efficient.[20]

The Van Deemter equation (Equation 2.3) was the result of the first application of rate theory to the chromatography elution process. This equation (Equation 2.3) predicts the optimum velocity at which there will be the minimum variance per unit column length and hence, maximum efficiency. The A term describes Eddy diffusion. This relates to the flow and paths taken by the mobile phase through the sorbent and poorly packed SPE columns may result in band broadening. The effect of Eddy diffusion may be minimised by using particles with a low diameter, and a narrow particle size distribution. A small particle diameter decreases the distance that is required for an analyte to access and diffuse through its pores, therefore decreasing the diffusion time. Sorbents with a narrow distribution of particle size achieve a more homogeneous elution of analytes from the sorbent, resulting in an improved and narrower profile to minimise band broadening.(21) A short column of a few millimetres of sorbent is optimum; smaller columns may result in channelling and incomplete retention of analytes.(20)

$$HETP = A + \left(\frac{B}{u}\right) + (C \times u)$$

HETP: height equivalent to a theoretical plate, a measure of the resolving power of the column.

A: Eddie-diffusion parameter related to channeling through a non-ideal packing.

B: diffusion coefficient of the eluting particles in the longitudinal direction, resulting in dispersion.

C: resistance to mass transfer coefficient of the analyte between mobile and stationary phase.

u: linear velocity.

Equation 2.3 Van Deemter equation.

Nitrogen sorption analysis (Table 2.9) was carried out on these polymers in an attempt to understand why they did not undergo CM reactions. Studying the pore size, it is likely that none of the new polymers have undergone the CM reaction because all of them have smaller pores or they are not as porous as polymer **II-1$_h$**. It is not surprising that the pore size changes with the amount of toluene added, having greater pore size with larger amount of toluene used. As the SEM results (Table 2.9) have shown, the amount of toluene needs to be kept low for the formation of monodisperse particles. On the other hand, nitrogen sorption analysis shows that high amounts of toluene are needed in the synthesis of polymers that can undergo CM reactions. Therefore, another solvent was required to obtain monodisperse polymer beads with a narrow size distribution that could be functionalised by CM.

Polymer ref.	*Specific surface area (m^2/g)*		*Specific pore vol. (cm^3/g)*	*Av. pore diameter (nm)*
	BET	*Langmuir*		
II-1$_i$	-	5	-	-
II-1$_j$	-	520	0.20	2.0
II-1$_k$	-	70	-	-
II-1$_l$	440	-	0.24	2.2
II-1$_m$	-	80	-	-
II-1$_n$	715	-	0.40	2.1
II-1$_o$	-	110	0.03	1.4

Table 2.9 Nitrogen sorption analysis of the polymers prepared using toluene as porogenic co-solvent.

Results with THF as porogenic co-solvent

Irgum and coworkers(22) reported that using THF as a porogenic co-solvent results in an increase in the pore size and the pore volume, since THF has the solubility parameters (Hildebrand and Hansen) closer to the θ solvent than toluene. Table 2.10 shows that with THF as co-solvent, the yields of the reactions increased. THF decreases the solvency of the polymer in the media, which means that the polymers tend to precipitate faster in THF than in toluene, leading to better yields.

Polym. ref.	*DVB*	*Mon. conc. (%wt./v)*	*AIBN (g)*	*CH_3CN (%)*	*THF (%)*	*Time (h)*	*Yield (g)*	*Yield (%)*
II-1$_p$	80	4	0.39	80	20	48	8.05	78
II-1$_q$	55	4	0.45	80	20	48	7.00	68
II-1$_r$	80	2	0.39	60	40	48	6.00	58
II-1$_s$	55	4	0.20	60	40	48	6.35	62

Table 2.10 Precipitation polymerisation results and conditions of polymers using THF as co-solvent.

The SEM micrographs (Figure 2.31) show that when using THF as solvent, spherical shaped polymers were obtained. The particles obtained have a narrow size distribution in comparison with particles obtained using toluene as porogenic solvent (Figure 2.30). Due to the poor stability of the microspheres of polymer **II-1**$_r$ as consequence of the high solvency of the continuous phase, coagulums were obtained.

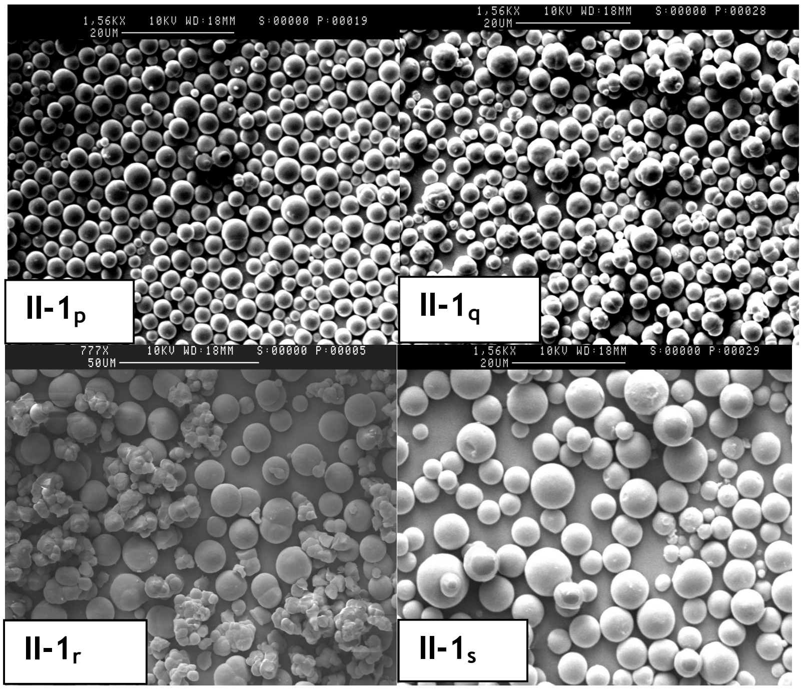

Figure 2.31 SEM micrographs of polymers prepared using THF as porogen.

Table 2.11 shows the statistical analysis of the particles, which indicates that polydisperse polymer microspheres were obtained as no CV below 16% was observed.

Polym. ref.	*Mean diameter (μm)*	*SD (μm)*	*Min (μm)*	*Max (μm)*	*CV (%)*
II-1$_p$	2.65	0.55	1.39	4.17	21
II-1$_q$	2.81	0.69	1.42	4.70	25
II-1$_r$	6.02	2.47	1.10	11.19	41
II-1$_s$	4.74	1.50	1.28	9.15	32

Table 2.11 Statistical analysis of polymers using THF as porogenic co-solvent.

In order to predict whether the metathesis reaction would be successful or not, nitrogen sorption analysis was carried out (Table 2.12). Taking into consideration previous results (Table 2.9), polymers with Langmuir surface area would not undergo the CM reaction so polymer **II-1$_p$** was not tested. Polymers **II-1$_q$** and **II-1$_r$** were not tested either since the **II-1$_q$** was not porous, and coagulums were formed for **II-1$_r$**. Polymer **II-1$_s$** has lower average pore size than polymer **II-1$_h$**, but larger pore volume and better particle quality, so polymer **II-1$_s$** was selected to perform functionalisation reactions.

Polymer ref.	*Specific surface area (m^2/g)*		*Specific pore vol. (cm^3/g)*	*Av. pore diameter (nm)*
	BET	*Langmuir*		
II-1$_p$	-	230	0.06	1.5
II-1$_q$	0.2	-	-	-
II-1$_r$	830	-	0.53	2.6
II-1$_s$	250	-	0.13	2.1

Table 2.12 Nitrogen sorption analysis of polymers prepared using THF as porogenic co-solvent.

2.3.5. Functionalisation of narrow particle size distribution polymer microspheres by olefin metathesis

After the careful synthesis of porous polymer microspheres with narrow size distribution, polymer **II-1$_s$** was chosen to be functionalised with the wide range of coupling partners used before with polymer **II-1$_h$**. Due to the increase in the pore volume, it was believed that CM would be more effective than it was previously giving larger IEC (Section 2.3.3). Furthermore, the narrow size distribution of polymer **II-1$_s$** makes it a good candidate to be used as an ion-exchange resin.

*Bromination reaction with polymer **II-1$_s$***

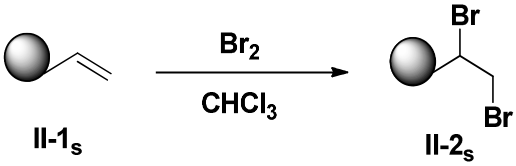

Figure 2.32 Bromination reaction of polyDVB.

Bromination reaction (Figure 2.32) was carried out to quantify the number of residual double bonds in polyDVB after precipitation polymerisation, by elemental microanalysis of bromine. After a careful washing process, elemental microanalysis of bromine shows (*63.9% C, 5.4% H, 0.3% N, 25.2% Br*) that around 38% of the double bonds remained unreacted after precipitation polymerisation. According to Law and Sherrington,$^{(12)}$ the amount of unreacted vinyl groups of DVB resins prepared by suspension polymerisation was around 32%. As it is well known, polymer beads obtained by suspension polymerisation have larger surface areas and pore sizes than by precipitation polymerisation. Due to the light yellow colour of polymer **II-2$_s$**, it was believed that bromine was trapped inside the pores and therefore microanalysis results were not reliable.

CM reactions with simple molecules

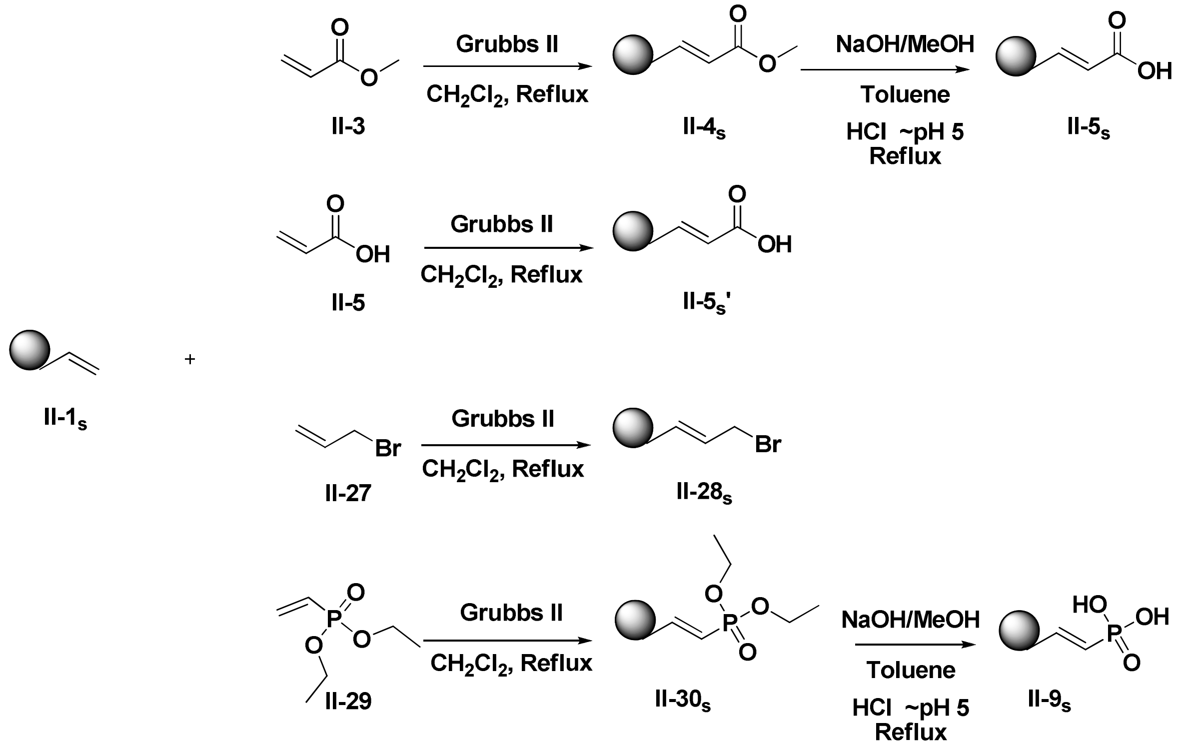

Figure 2.33 CM reactions of polymer II-1$_s$ using simple coupling partners.

CM and subsequent hydrolysis reactions involving polymer **II-1$_s$** were carried out using different coupling partners (Figure 2.33). These coupling partners were simple molecules which were tested previously with polymer **II-1$_h$.** Elemental microanalysis results suggest the success of the CM reaction with the different coupling partners, as a decrease in the carbon and hydrogen contents of the functionalised polymers can be observed (Table 2.13). In the case of polymer **II-28$_s$**, the choice of a halogenated coupling partner was made in order to be able to quantify the amount of available double bonds that can undergo the CM reaction *via* bromine elemental analysis. Elemental microanalysis confirmed the insertion of bromine and enabled the functional group loading level to be established (0.1 mmolg^{-1}). The insertion of the phosphorous moiety of polymer **II-30$_s$** was also analysed by elemental microanalysis indicating that the polymer underwent the CM reaction and establishing a functional group loading level of 0.3 mmolg^{-1}. The differences of the loading levels are probably derived from the reactivity of the metathesis partner. Allyl bromide, a Type I olefin, tends to homodimerise rapidly and it is the dimer that reacts with the polymer. Due to the big size of the formed dimer, only the vinyl groups of the surface can be functionalised since the dimer cannot go through the pores to reach the internal pendent double bonds. However, the phosphonate is a Type III olefin, which does not homodimerise but reacts directly with the polymer having a higher reactivity and thus giving a higher loading value in the post-functionalisation reaction. In the case of the hydrolysis reactions, elemental microanalysis suggests that both polymers, **II-4$_s$** and **II-30$_s$** were hydrolysed as the carbon amount increased after the elimination of the methyl and ethyl groups of their respective esters.

Polymer ref.	*Elemental microanalysis (wt.%)*				
	C	*H*	*N*	*Br*	*P*
II-1$_s$	90.8	8.2	0.3	-	-
II-4$_s$	88.3	8.0	0.3	-	-
II-5$_s$	87.2	7.9	0.3	-	-
II-5$_s$'	90.0	8.1	0.3	-	-
II-28$_s$	89.1	8.0	0.3	0.8	-
II-30$_s$	88.6	8.2	0.3	-	1.0
II-9$_s$	87.9	8.1	0.3	-	0.7

Table 2.13 Elemental microanalysis of the functionalised polymers with simple molecules.

The FT-IR spectra of the functionalised polymers (Figure 2.34a and c) indicate that functionalisation reactions worked well, as the peaks at 1740 cm^{-1} (Figure 2.34a) and 1705 cm^{-1} (Figure 2.34c) confirmed the methyl acrylate and acrylic acid immobilisation. Figure 2.34b also confirmed the success of the hydrolysis reaction since the carbonyl peak was shifted to a lower wavelength (1705 cm^{-1}) which coincides with the carbonyl peak of polymer **II-5$_s$'**. In the case of Figure 2.34d, the appearance of different bands at 1365 cm^{-1} (O-P-O str.), 1260 cm^{-1} (P=O str.) and 1160 (C-O-P str.) cm^{-1} confirmed the success of the reaction. Furthermore, to ensure the success of the reaction ^{15}P solid state NMR spectroscopy (Figure 2.34f) of polymer **II-30$_s$** was carried out in which the appearance of the peak at 18 ppm confirmed the success of the CM reaction.

Finally, in Figure 2.34e, the appearance of bands at 3600 cm^{-1} (OH str.), 2320 cm^{-1} (P-OH str.), 1370 cm^{-1} (O-P-O) and 1140 cm^{-1} (P=O) confirmed the hydrolysis of the phosphonate into a phosphonic acid.

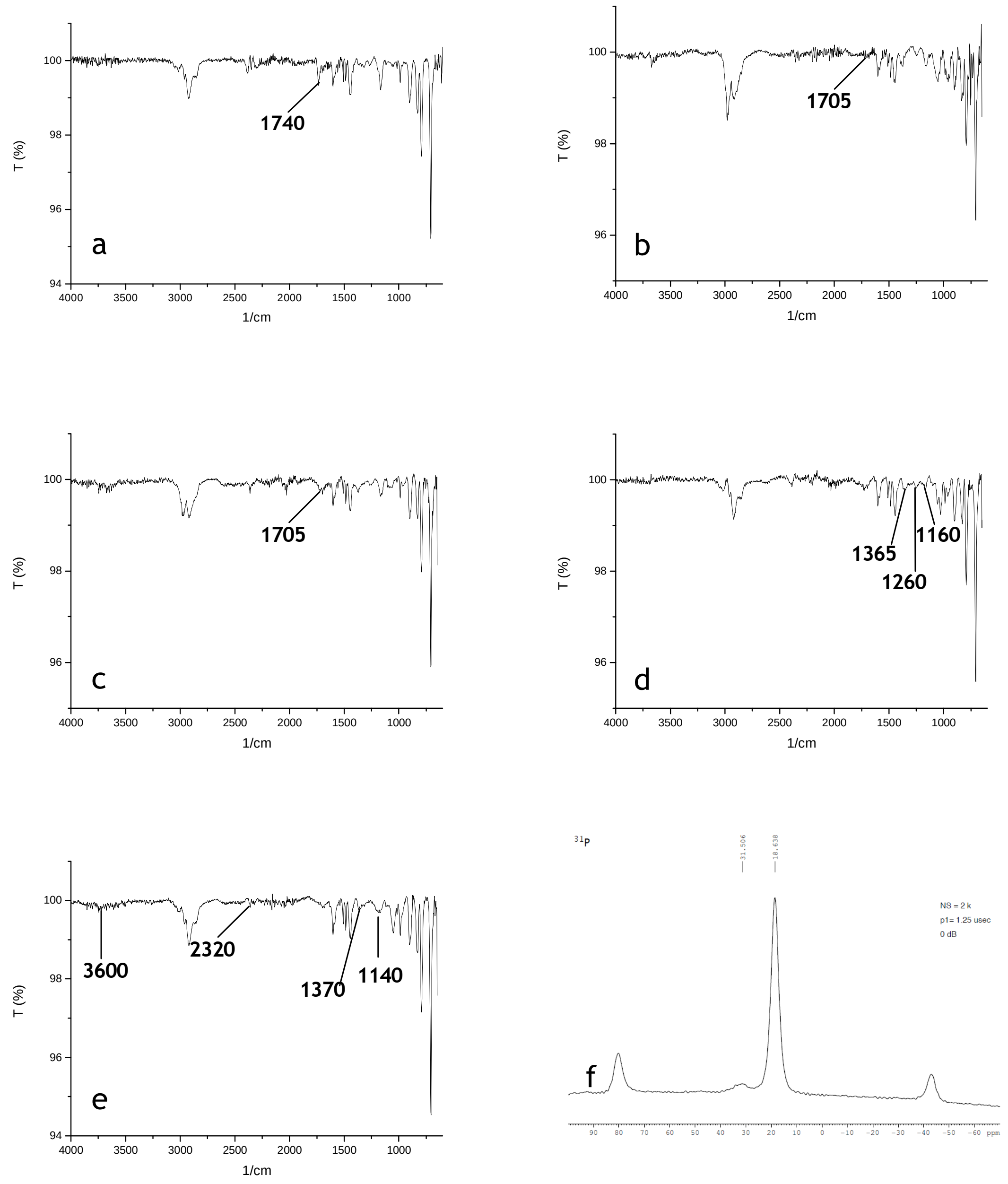

Figure 2.34 FT-IR spectra of polymers a) II-4$_s$, b) II-5$_s$, c) II-5$_s$', d) II-30$_s$ and e) II-9$_s$ and d) ^{15}P solid state NMR spectrum polymer II-30$_s$.

SEM micrographs (Figure 2.35) of the products show that the particles were not damaged after the functionalisation reactions. The micrographs also show that chemical aggregation is not an issue during CM or hydrolysis reactions. However, the size of the particles appeared to increase after the functionalisation reactions, as can be observed in Table 2.14.

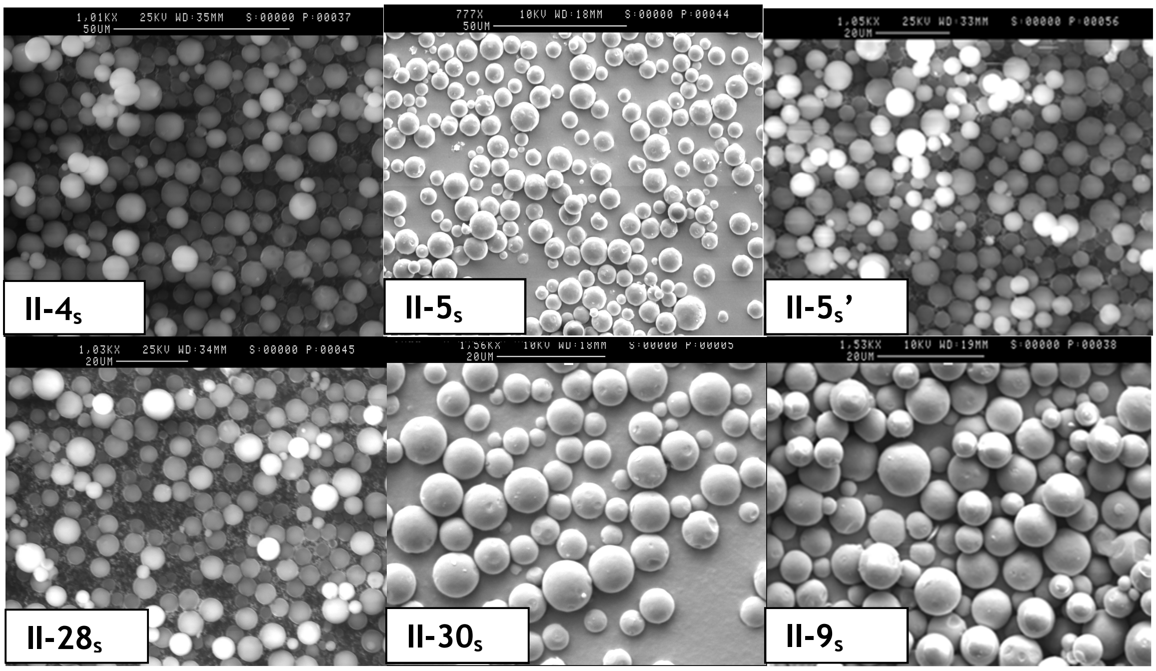

Figure 2.35 SEM micrographs of polymers II-4$_s$, II-5$_s$, II-5$_s$', II-28, II-30$_s$ and II-9$_s$'.

The statistical analysis of the particles (Table 2.14), describes the polymers as polydisperse. However, in comparison with polymer **II-1$_s$**, the size of the functionalised polymers increased and therefore the CV value decreased after CM reactions, suggesting that CM occurred. The increase of the size of the particles was due to metathesis reaction occurring through the pores of the particles with internal vinyl monomers. This leads to a lower difference between the SD and the mean diameter and thus, the CV value decreases. In the case of polymers **II-5$_s$** and **II-9$_s$**, due to the loss of the methyl group the particles shrank and the mean diameter of particles was lower than in polymers **II-4$_s$** and **II-30$_s$**.

Polym. ref.	*Mean diameter (μm)*	*SD (μm)*	*Min (μm)*	*Max (μm)*	*CV (%)*
II-1$_s$	4.8	1.5	1.3	9.1	32
II-4$_s$	5.8	1.4	2.6	9.2	25
II-5$_s$	5.2	1.5	2.2	8.6	29
II-5$_s$'	5.7	1.4	2.3	8.5	25
II-28$_s$	5.8	1.5	2.2	9.4	27
II-30$_s$	6.4	1.6	1.9	10.1	25
II-9$_s$	5.5	1.8	1.5	9.6	33

Table 2.14 Statistical analysis of polymer particles.

Nitrogen sorption analysis was performed for all the functionalised polymers. Table 2.15 shows that in some cases (polymers **II-5**$_s$, **II-28**$_s$ and **II-30**$_s$), the nitrogen is adsorbed onto the surface in a single layer as the pore volume has been greatly reduced suggesting a partial obstruction of the pores, caused by steric hindrance of the coupled product. Table 2.15 also shows that the values of the specific surface areas, which follow the BET method, are greater after the functionalisation. The change is due to the success of the CM reaction, which happened through the pores inside the beads, opening the pores and thus increasing the specific surface area. In the case of polymer **II-9**$_s$ no BET data was obtained as less than 2 points of the isotherm could not be measured.

Polymer ref.	*Specific surface area (m^2/g)*		*Specific pore vol. (cm^3/g)*	*Av. pore diameter (nm)*
	BET	*Langmuir*		
II-1$_s$	250	-	0.13	2.1
II-4$_s$	340	-	0.20	2.4
II-5$_s$	-	5	-	-
II-5$_s$**'**	270	-	0.15	2.1
II-28$_s$	-	50	-	-
II-30$_s$	-	145	0.06	2.2

Table 2.15 Nitrogen sorption analysis of the functionalised polymers with simple molecules.

CM reactions with Fmoc protected amines

Following the success of the CM reactions of polymer II-1s with simple and small molecules, functionalisation reactions involving bulkier molecules were carried out. Commercially available Fmoc-allylglycine (**II-16s**), or in-house synthesised molecules such as Fmoc homoallylamine (**II-14s**) and Fmoc-4-allyloxyproline (**II-20s**), were used as coupling partners for the metathesis reaction (Figure 2.36).

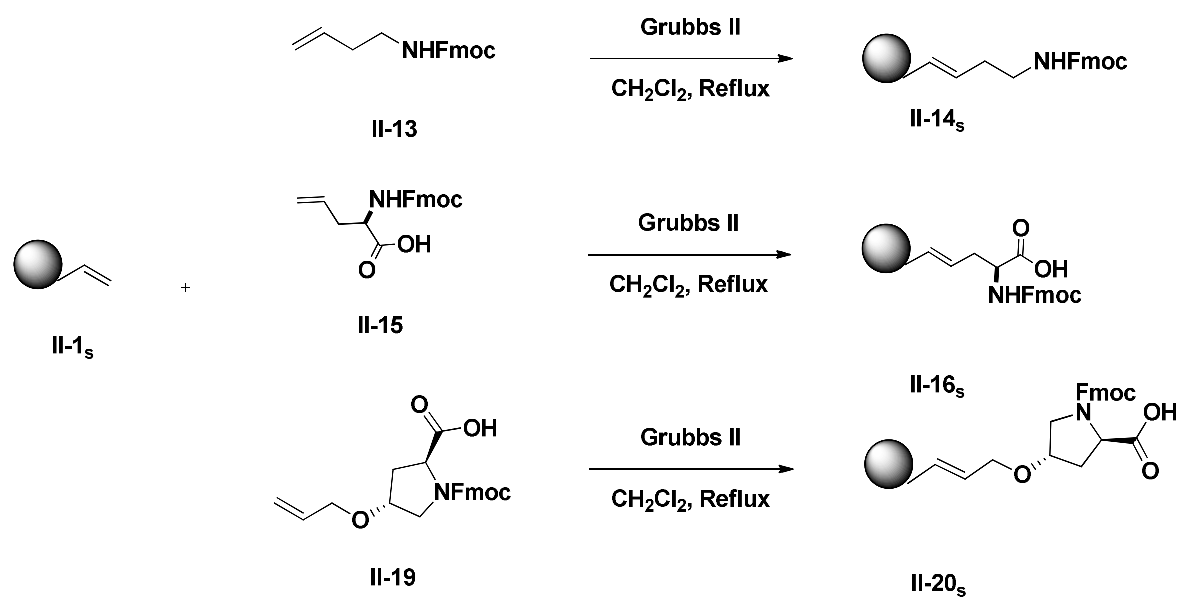

Figure 2.36 CM reactions involving coupling partners with nitrogen moieties.

Table 2.16 shows the elemental microanalysis of polymers functionalised with the Fmoc-protected coupling partners. The increase of the nitrogen amount between the functionalised polymers (**II-14**$_s$, **II-16**$_s$ and **II-20**$_s$) and the polymer **II-1**$_s$ suggests the immobilisation of the coupling partners on the polymer. The different values obtained in the amount of nitrogen could be due to the reactivity of the coupling partners during the CM reaction. Unfortunately, due to the presence of AIBN in the polymer **II-1**$_s$, the calculation of the loading level of the functional group was not carried out.

Polymer ref.	*Elemental microanalysis (wt.%)*		
	C	*H*	*N*
II-1$_s$	90.8	8.2	0.3
II-14$_s$	90.2	7.9	0.6
II-16$_s$	89.9	8.0	0.7
II-20$_s$	87.9	7.8	0.9

Table 2.16 Elemental microanalysis of nitrogen containing functionalised polymers.

Figure 2.37 shows the FT-IR spectra of the functionalised polymers. The appearance of a band at 1700 cm^{-1} (C=O str.) in Figure 2.37a indicates the presence of the Fmoc group in polymer **II-14$_S$**. Figure 2.37b shows the appearance of two peaks at 1715 cm^{-1} and 1695 cm^{-1}. The peaks, which belong to the carbonyl group of the acid and the carbamate of the Fmoc group (**II-16$_S$**), suggesting that the immobilisation occurred. However, in the case of polymer **II-20$_S$** (Figure 2.37c), only the peak of the acid can be observed at 1710 cm^{-1}, due to the broadness of the carbonyl peak, which also suggests the success of the reaction.

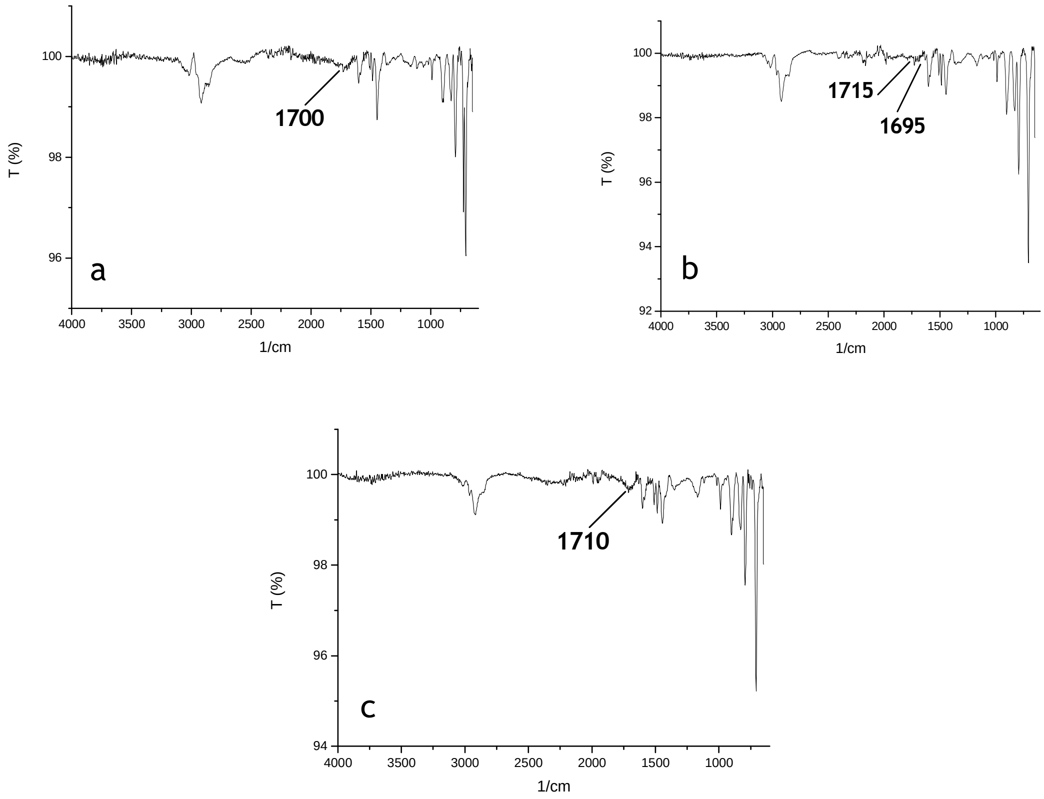

Figure 2.37 FT-IR spectra of a) II-14$_S$, b) II-16$_S$ and c) II-20$_S$.

SEM analysis was carried out in order to verify if the particles obtained after the CM reaction were damaged. SEM micrographs (Figure 2.38) showed no evidence of chemical aggregation during the CM reaction, and the particles were not destroyed. In order to see if the particles increased their size after functionalisation reaction, statistical analysis was carried out (Table 2.17).

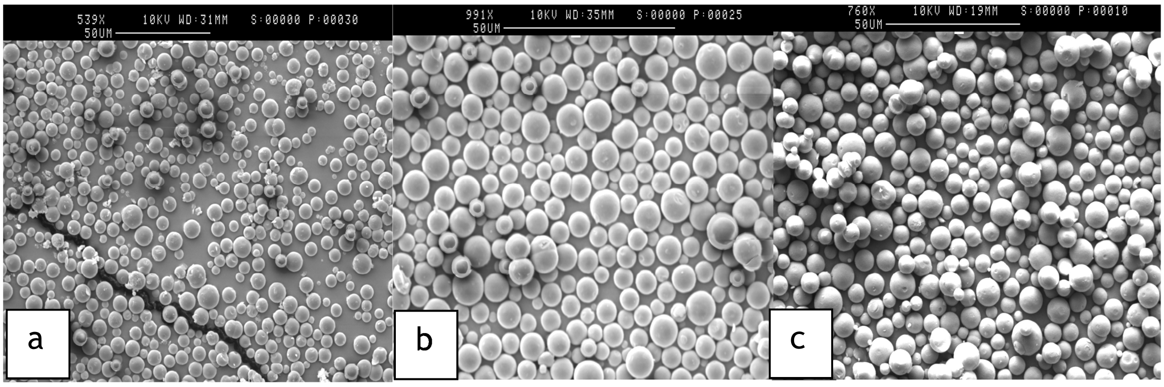

Figure 2.38 SEM micrographs of a) II-14$_s$ b) II-16$_s$ and c) II-20$_s$.

The statistical analysis of the particles, shown in Table 2.17, describes the polymers as polydisperse. As was mentioned before, due to metathesis reaction occurring through the pores of the particles with internal vinyl monomers, the size of the particles increased and as consequence of that, the CV decreased.

Polym. ref.	*Mean diameter (μm)*	*SD (μm)*	*Min (μm)*	*Max (μm)*	*CV (%)*
II-1$_s$	4.8	1.5	1.3	9.1	32
II-14$_s$	6.2	1.6	3.2	11	26
II-16$_s$	5.2	1.2	2.9	7.5	23
II-20$_s$	6.2	1.8	2.7	11	28

Table 2.17 statistical analysis of polymer particles.

Nitrogen sorption analysis was performed on the functionalised polymers. Table 2.18 shows that in polymer **II-20**, nitrogen was adsorbed in a single layer and the Langmuir isotherm must be used to calculate the specific surface area. The pore volume in polymer **II-20** has been greatly reduced, which suggested a partial obstruction of the pores, caused by steric hindrance of the coupled product. Therefore, the amount of nitrogen that can access each pore has been reduced and consequently it can only form a single layer in the space provided. Table 2.18 also shows that the values of the specific surface areas, which follow the BET method, are greater after the functionalisation. The change is due to the success of the CM reaction, which also happened through the pores inside the beads, opening the pores and thus increasing the specific surface area.

Polymer ref.	*Specific surface area (m^2/g)*		*Specific pore vol. (cm^3/g)*	*Av. pore diameter (nm)*
	BET	*Langmuir*		
II-1$_s$	250	-	0.13	2.1
II-14$_s$	294	-	0.18	2.4
II-16$_s$	252	-	0.15	2.1
II-20$_s$	-	120	0.05	2.0

Table 2.18 Nitrogen sorption porosimetry analysis of the functionalised polymers.

To further prove the successful insertion of the amine and the amino acids in polymer **II-1$_s$** the Fmoc protecting group was removed with piperidine in CH_2Cl_2 (Figure 2.39). The deprotection was also carried out to measure the absorbance of the fulvene-piperidine adducts at 301 nm (**II-31$_s$**: 0.09 A.U., **II-32$_s$**: 0.2 A.U.and **II-33$_s$**: 0.07 A.U.) The loading of the functional groups immobilised (**II-31$_s$**: 0.1 mmolg^{-1}, **II-32$_s$**: 0.2 mmolg^{-1} and **II-33$_s$**: 0.1 mmolg^{-1}) were calculated by using the Beer-Lambert Law.

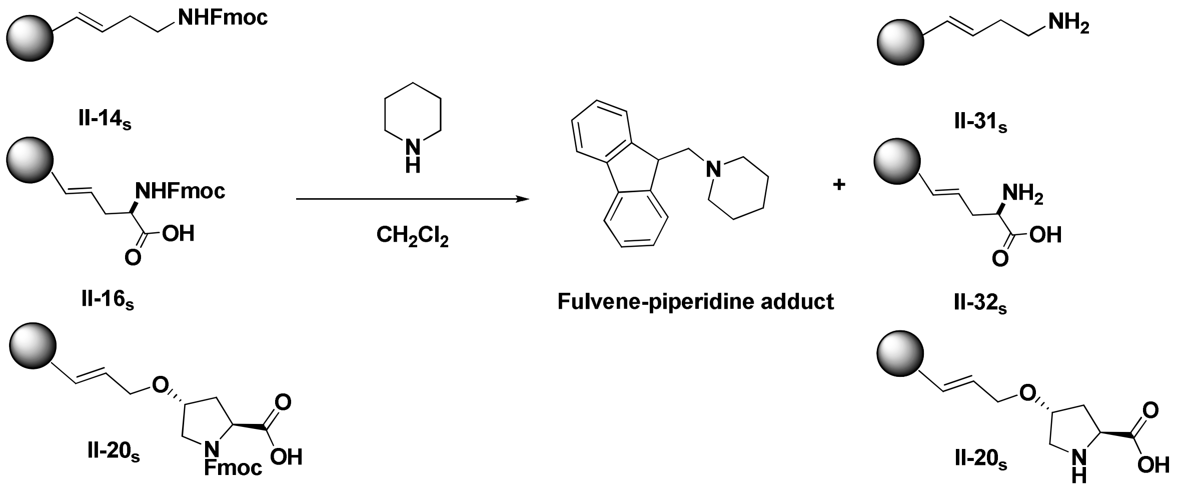

Figure 2.39 Fmoc deprotection of polymers II-14$_s$, II-16$_s$ and II-20$_s$.

After the Fmoc removal, two different tests were performed to verify the presence of free amines in the unprotected polymers. The first experiment was a ninhydrin test (Figure 2.40) in which a change of colour from colourless (polymer **II-14**$_s$) to purple (polymer **II-31**$_s$), brown (**II-32**$_s$) and red (**II-33**$_s$) proved the existence of amines in the polymer.

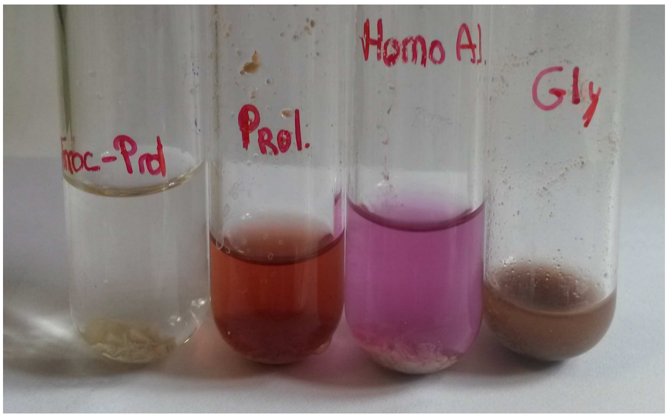

Figure 2.40 Ninhydrin test of polymers, from left to right: II-20$_s$, II-33$_s$, II-31$_s$ and II-32$_s$.

The second experiment was a bromophenol blue test, in which the particle beads went from colourless in their protected state to blue after the Fmoc group was removed, confirming the presence of amines in the polymers (Figure 2.41).

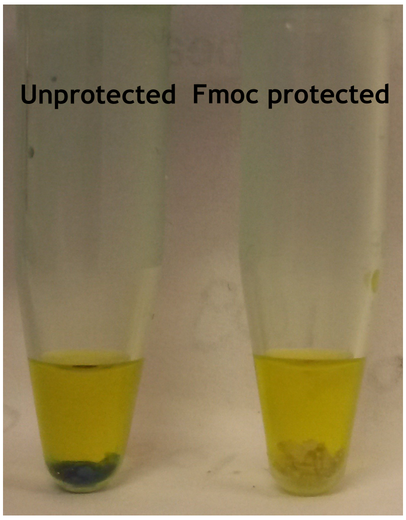

Figure 2.41 Bromophenol blue test change of colour. On the left: polymer II-32$_s$, on the right: polymer II-16$_s$.

2.4. CONCLUSIONS

Conventional precipitation polymerisation using toluene as porogenic co-solvent produced quality particles. However, in order to form functionalisable polymer microspheres, a high proportion of toluene had to be used, which led to an increase in the size dispersity of the particles; broad particle size distribution were obtained.

Porous polymer microspheres with narrow size distributions were obtained by precipitation polymerisation of DVB-55 in a solvent mixture of acetonitrile and THF.

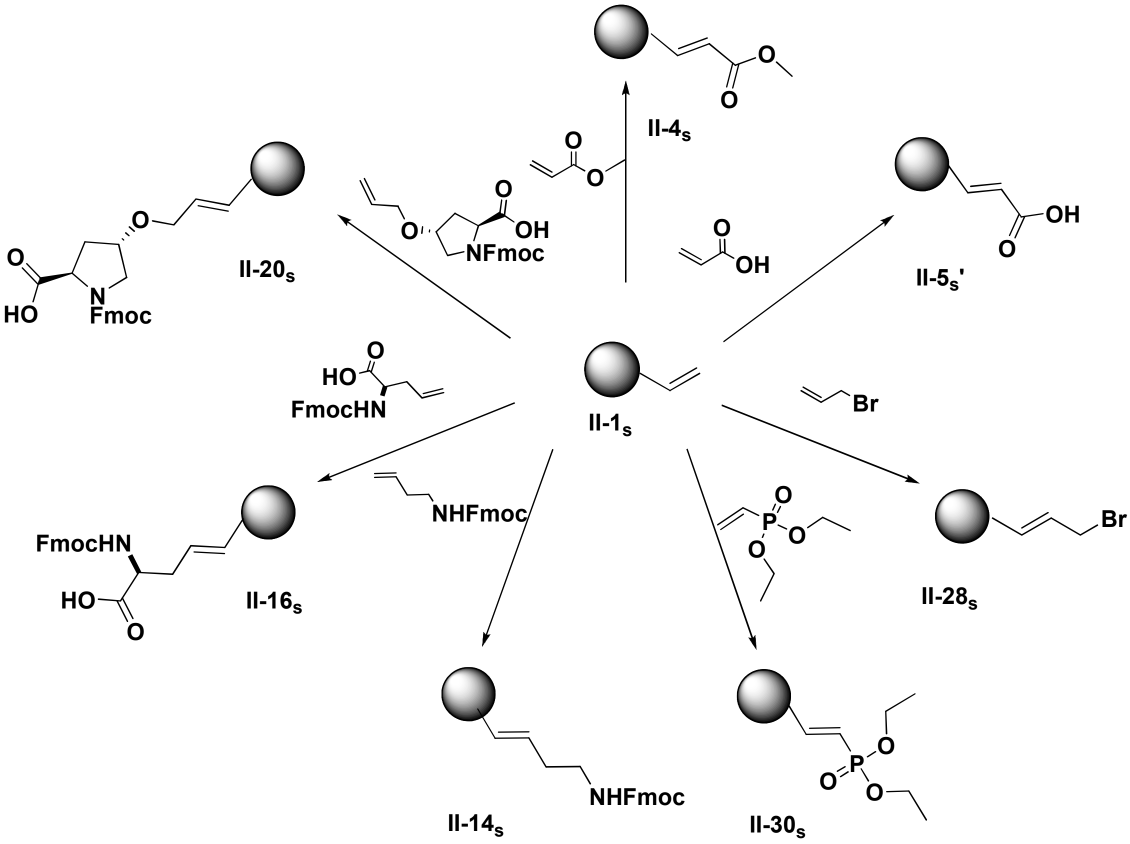

Figure 2.42 Different CM reactions of polymer II-1_s.

The pendent vinyl groups in the poly(DVB-55) product, derived from the incomplete consumption of the vinyl groups in DVB-55, were subjected to cross metathesis. A range of interesting and useful functional groups were installed into the polymer (Figure 2.42), under mild reaction conditions and maintaining the unsaturation for possible further functionalisation.

Through this work, porous polymer microspheres have been synthesised *via* a facile and versatile chemical functionalisation route which does not require the use of functional co-monomers. The intrinsic porosity and well-defined physical format of the microspheres renders them eminently suitable for a range of potential applications such as ion exchangers or heterogeneous organocatalysis.

2.5. FUTURE WORK

A novel methodology for the functionalisation of porous polymer microspheres has been developed successfully. In the future, these polymers could be tested as SPE sorbents in order to study the scope of the CM reaction as a functionalisation technique in the context of high performance separation science. A group of interesting analytes are pharmaceuticals, since they are dispersed in the environment by common human use.(23,24) For example, one possible application for these polymers could be for the preconcentration, fractionation and purification of analytes from environmental water samples.

Due to the traces of nitrogen in the polymers coming from the AIBN, the loading of the nitrogen moieties in polymers **II-14**$_s$, **II-16**$_s$ and **II-20**$_s$ were measured by absorbance analysis of the fulvene-piperidine adduct. In the future, precipitation polymerisation reactions could be carried out using (nitrogen-free) benzoyl peroxide as initiator. Elemental microanalysis could be used for easy measurement of the nitrogen amount, providing a more accurate loading of the immobilised amino groups.

2.6. EXPERIMENTAL

2.6.1. Materials

For the synthesis of porous polymer particles, divinylbenzene-80 (mixture of isomers, 80.0% grade) and divinylbenzene-55 (mixture of isomers, 55.0% grade) were purchased from Sigma Aldrich and purified prior to use through a column of neutral alumina. 2,2'-Azo*bis*(isobutyronitrile), AIBN, (97.0%) was purchased from BDH and was recrystalised from acetone at low temperature. HPLC grade acetonitrile was purchased from Rathburn Chemicals and was used as received. Methyl acrylate, Fmoc-*L*-allylglycine, phthalimide, trifluoroacetic acid and second-generation Grubbs catalyst were all purchased from Sigma Aldrich and were used as received. Diisopropyl azodicarboxylate, triphenylphosphine, sodium hydride, allylbromide, 4-*trans*-hydroxyproline and Fmoc-hydroxysuccinimide were all purchased from Acros Organics and were also used as received. Acrylic acid, dimethyl vinylphosphonate, diethyl vinylphosohonate and hydrazine monohydrate were purchased from Fisher Scientific and were all of high purity, so were used as received.

The solvents employed (toluene, acetone, methanol, tetrahydrofuran, ethanol, petroleum ether [b.p. 30-40 ^{o}C], ethyl acetate, diethyl ether and chloroform) were purchased from Sigma Aldrich as standard laboratory reagent grade.

Dry solvents were obtained from an in-house purification system. Column chromatography sorbent EMD Guduran silica gel 60 was used and Merk silica 60 covered with aluminium sheets were used as TLC plates.

2.6.2. Equipment

Precipitation polymerisations were carried out using a Stuart Scientific S160 incubator (Surrey, UK) and a Stovall low profile roller system (NC, USA). The polymerisations were performed in Nalgene® plastic bottles. When required, samples were dried in Townson & Mercer Limited (England) vacuum ovens set to either 40 °C or 70 °C, at ~ 60 mbar pressure.

Elemental microanalysis was performed by the University of Strathclyde Elemental Microanalysis service. C, H and N elemental microanalyses were carried out simultaneously using a Perkin Elmer 2400 Series II analyser, while halogen and phosphorous contents were determined by standard titration methods.

Scanning electron microscopy (SEM) was carried out using a Cambridge Instruments Stereoscan 90. Samples were coated in gold prior to SEM imaging. SEM statistical data was obtained by Image J.

Fourier-Transform Infrared (FT-IR) spectroscopy analyses were carried out using a Shimadzu IRAffinity-1S spectrometer. Samples were scanned over the range 4000-600 cm^{-1} in transmission mode.

The specific surface area measurements were performed using Micromeritics ASAP 2020 nitrogen sorption instrument. Samples were degassed overnight under high vacuum at 100 ^{o}C prior to analysis. Analysis was carried out *via* nitrogen sorption, carried out at 77 K.

Solid state NMR spectra were carried out using a Bruker Advance I 400 MHz spectrometer equipped with a widebore 9.4T magnet. Powered samples were packet into a ZrO_2 rotor and rotated at rates between 10 and 15 KHz in a 4 mm MAS probe.

2.6.3. Typical preparation of polyDVB by PP

*PolyDVB (**II-1**)*

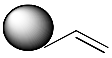

Polymer **II-I** was synthesised by modifying an existing procedure.[1-4,22] Divinylbenzene was freed from inhibitor by passage through a short column of alumina (Aluminium oxide activated, neutral, Brockmann I) prior to polymerisation. Recently purified DVB, (10.0 g, 80.0 mmol) and recrystalised AIBN (0.39 g, 2.40 mmol, 2 mol% relative to the total number of polymerisable double bonds) were placed into a 1 L Nalgene® bottle with acetonitrile (CH_3CN) and toluene as porogenic solvents. The bottle contents were sonicated for 15 min and the contents were purged with bubbling N_2 for 20 min before being sealed under N_2. The bottle was placed on a low-profile roller, which was housed inside a temperature-controlled incubator, and rolled at 30 rpm along its long axis. The temperature was ramped from room temperature to 60 °C over 1h and then held at 60 °C for further 48 h. The product was filtered off under vacuum on a 0.22 μm nylon filter membrane and then washed in sequence with 100 mL volumes of CH_3CN, toluene, methanol and acetone. The product (**II-1**), in the form of a white powder, was dried overnight at 70 °C at 1 mbar.

FT-IR: $\bar{\upsilon}$cm^{-1} 3050 (=CH str.), 2920 and 2850 (C-H str.), 1605, 1590, 1510 and 1485 (C=C str.), 1445 (CH_2 def.), 990, 905, 830, 790 and 710 (CH def.).

Isotherms:

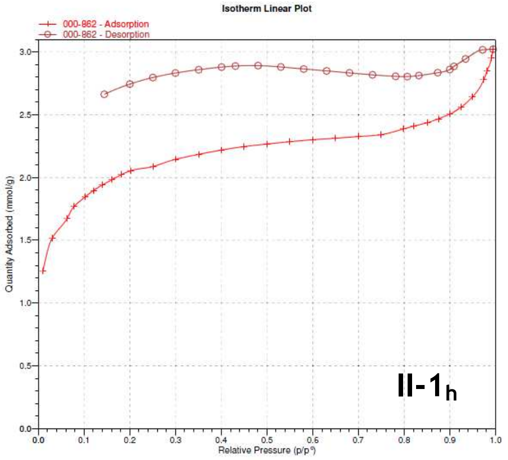

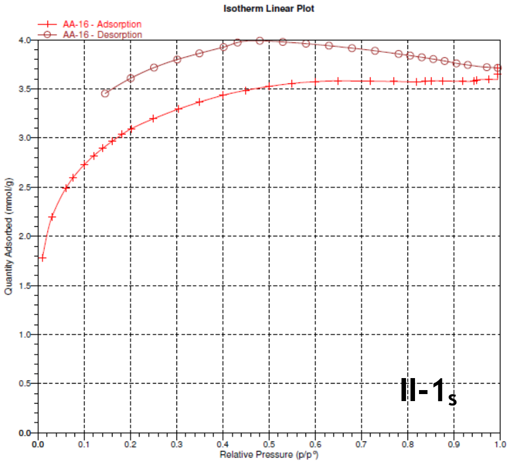

2.6.4. Bromination of polyDVB

*Dibromo polyDVB (**II-2**)*

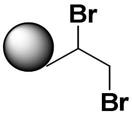

Polymer **II-1** (0.10 g, 0.77 mmol) and 0.4 mL (0.78 mmol) of a solution of bromine in chloroform (02 mL / 2 mL) were suspended at 0 ºC in chloroform (10 mL) under an argon atmosphere and stirred gently overnight. The mixture was filtered and washed with saturated aqueous sodium thiosulfate solution (100 mL), ethanol (20 mL), ethyl acetate (20 mL) and diethyl ether (20 mL) giving **II-2** as a light yellow insoluble powder (0.14 g).

2.6.5. Functionalisation of polyDVB by olefin CM

General procedure for the functionalisation of PolyDVB[(9)]

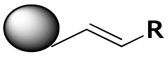

The functionalisation reactions were carried out in a 50 mL round-bottomed flask equipped with a condenser. PolyDVB was suspended in CH_2Cl_2 (15 mL) under an argon atmosphere. Second-generation Grubbs catalyst (5.0 mol%) and the coupling partner (4.0 equiv relative to the polymer) were then added to the suspension and the resulting mixture was heated under reflux overnight. The next day the reaction was allowed to cool down to room temperature and the product was filtered off under vacuum on a 0.22 µm nylon filter membrane and then washed in sequence with 15 mL volumes of dichloromethane, ethanol, ethyl acetate, petroleum ether and diethyl ether. The product, in the form of an off-white powder, was dried overnight at 70 °C at 1 mbar.

*Polymer with methyl acrylate (**II-4**)*

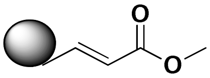

The general procedure was used with polymers **II-1**$_g$, **II-1**$_h$ (0.23 g, 1.8 mmol) and methyl acrylate, **II-3,** (0.64 mL, 7.1 mmol, 4 equiv) to give 0.23 g of **II-4**$_g$ and 0.24 g of **II-4**$_h$. The general procedure was also used with polymer **II-1**$_s$ (0.30 g, 2.3 mmol) and **II-3** (0.84 mL 9.2 mmol, 4 equiv) to give 0.28 g of **II-4**$_s$.

FT-IR: $\bar{\upsilon}cm^{-1}$ 3050 (=CH str.), 2920 and 2850 (C-H str.), 1735 (C=O str.), 1605, 1590, 1510 and 1485 (C=C str.), 1445 (CH_2 def.), 1170 (C-O-C str.), 990, 905, 830, 790 and 705 (CH def.).

*Hydrolysis of the functionalised product (**II-5**)*

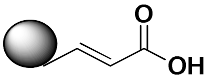

Polymer (**II-5$_s$**) was synthesised by modifying an existing procedure.(17) Polymer **II-4$_g$** (0.13 g, 0.76 mmol) was suspended in toluene (60 mL) under an argon atmosphere and then a solution of sodium hydroxide (4.5 g) in methanol (20 mL) was added to the suspension and was heated under reflux overnight. The next day the reaction was allowed to cool down to room temperature, and the pH was adjusted to 5 with concentrated HCl. The product (**II-5$_g$**), in the form of an off-white powder, was filtered off under vacuum, washed with water (30 mL) and methanol (30 mL) and dried overnight at 70 °C at 1 mbar (0.60 g, 52 %). The same procedure was followed with polymers **II-1$_h$** (0.090 g) and **II-1$_s$** (0.24 g) to give 0.71 g (85%) of polymer **II-5$_h$** and 0.16 g (76%) of polymer **II-5$_s$**.

FT-IR: $\bar{\upsilon}$cm^{-1} 3600 (OH str.), 3050 (=CH str.), 2920 and 2850 (C-H str.), 1710 (C=O str.), 1605, 1590, 1510 and 1485 (C=C str.), 1445 (CH_2 def.), 990, 905, 830, 790 and 705 (CH def.).

*Polymer with acrylic acid (**II-5'**)*

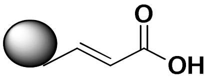

The general procedure was used with polymers **II-1$_e$, II-1$_g$, II-1$_h$** (0.023 g, 0.18 mmol) and acrylic acid, **II-6,** (0.048 mL 0.71 mmol, 4 equiv) to give 0.020 g of **II-5$_e$'** 0.020 g of **II-5$_g$'** and 0.026 g of **II-5$_h$'**. The general procedure was also used with polymer **II-1$_s$** (0.30 g, 2.3 mmol) **II-6** (0.63 mL 9.2 mmol, 4 equiv) to give 0.3 g of **II-5$_s$'**.

FT-IR: $\bar{\upsilon}$cm^{-1} 3600 (OH str.), 3050 (=CH str.), 2920 and 2850 (C-H str.), 1705 (C=O str.), 1605, 1590, 1510 and 1485 (C=C str.), 1445 (CH_2 def.), 990, 905, 830, 790 and 705 (CH def.).

*Polymer with dimethyl vinylphosphonate (**II-8**)*

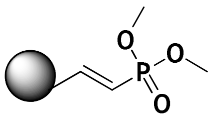

The general procedure was used starting with 0.080 g (0.61 mmol) of polymer **II-1$_h$** and with 0.29 mL (2.4 mmol) of dimethyl vinylphosphonate, **II-7**, to give 0.084 g of **II-8$_h$**.

FT-IR: $\bar{\upsilon}$cm^{-1} 3050 (=CH str.), 2920 and 2850 (C-H str.), 1605, 1590, 1510 and 1485 (C=C str.), 1445 (CH_2 def.), 1370 (O-P-O str.), 1255 (P=O str.), 1175 (C-O-P str.), 990, 905, 830, 790 and 705 (CH def.).

*Hydrolysis of the functionalised product (**II-9**)*

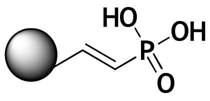

Polymer **II-9$_h$** was synthesised by modifying an existing procedure.(17) Polymer **II-8$_h$** (0.022 g) was suspended in toluene (5.0 mL) under an argon atmosphere and then a solution of sodium hydroxide (0.36 g) in methanol (1.8 mL) was added to the suspension and it was heated under reflux overnight. The next day after cooling down the reaction to room temperature, the pH was adjusted to 5 with concentrated HCl. and the product **II-9$_h$**, a white powder, was filtered, washed with water (10 mL) and methanol (10 mL) and dried overnight at 70 °C at 1 mbar (0.012 g, 67%). The general procedure was also used with polymer **II-30$_s$** (0.12 g, 0.60 mmol) suspended in 60 mL of toluene with a solution of sodium hydroxide (4.5 g) in methanol (20 mL) to give 0.07 g (71%) of polymer **II-9$_s$.**

FT-IR: $\bar{\upsilon}$cm^{-1} 3600 (OH str.), 3050 (=CH str.), 2920 and 2850 (C-H str.), 2320 (P-OH str.), 1605, 1590, 1510 and 1485 (C=C str.), 1445 (CH_2 def.), 1370 (O-P-O str.), 1220 (P=O str.), 990, 905, 830, 790 and 705 (CH def.).

*Polymer with Fmoc-protected homoallylamine (**II-14**)*

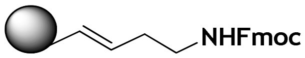

The general procedure was used starting with 0.80 g (0.61 mmol) of polymer **II-1**$_h$ with 0.72 g (2.4 mmol) of Fmoc-protected homoallylamine, **II-13**, to give 0.13 g of **II-14**$_h$**.** The general procedure was also used starting with 0.21 g (1.6 mmol) of polymer **II-1**$_s$ and with 1.6 g (5.4 mmol) of **II-13** to give 0.22 g of **II-14**$_s$**.**

FT-IR: $\bar{\upsilon}$cm^{-1} 3050 (=CH str.), 2920 and 2850 (C-H str.), 1700 (C=O str.) 1605, 1590, and 1485 (C=C str.), 1510 (NH def.), 1445 (CH_2 def.), 1320 (C-O str.), 990, 905, 830, 790 and 705 (CH def.).

*Polymer with Fmoc-protected allylglycine (**II-16**)*

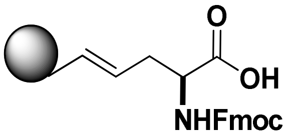

The general procedure was used starting with 0.050 g (0.38 mmol) of polymer **II-1**$_h$ and with 0.52 g (1.5 mmol) of Fmoc-protected allylglycine, **II-15**, to give 0.10 g of **II-16**$_h$**.** The general procedure was also used starting with 0.20 g (1.5 mmol) of polymer **II-1**$_s$ and with 1.5 g (5.4 mmol) of **II-15** to give 0.20 g of **II-16**$_s$**.**

FT-IR: $\bar{\upsilon}$cm^{-1} 3050 (=CH str.), 2920 and 2850 (C-H str.), 1715 and 1695 (C=O str.) 1605, 1590 and 1485 (C=C str.), 1520 (NH def.), 1445 (CH_2 def.), 1290 (C-O str.), 1270 (CN str.), 990, 905, 830, 790 and 705 (CH def.).

*Polymer with Fmoc-protected 4-allyloxyproline (**II-20**)*

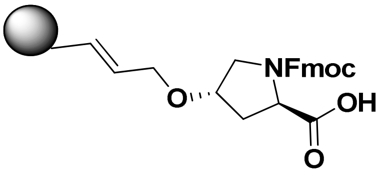

The general procedure was used starting with 0.43 g (0.33 mmol) of polymer **II-1**$_h$ and with 0.52 g (1.3 mmol) of Fmoc-protected 4-allyloxyproline,**II-19**, to give 0.032 g of **II-20**$_h$**.** The general procedure was also used starting with 0.25 g (1.9 mmol) of polymer **II-1**$_s$ and with 2.8 g (7.7 mmol) of **II-19** to give 0.20 g of **II-20**$_s$**.**

FT-IR: $\bar{\upsilon}$cm^{-1} 3050 (=CH str.), 2920 and 2850 (C-H str.), 1712 (C=O str.) 1605, 1590, 1510 and 1485 (C=C str.), 1445 (CH$_2$ def.), 1300 (C-O str.), 1230 and 1030 (CN str.), 1170 (C-O-C str.), 990, 905, 830, 790 and 705 (CH def.).

*Polymer with allyl bromide (**II-28**)*

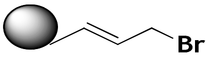

The general procedure was used with polymer **II-1**$_s$ (0.30 g, 2.3 mmol) and 0.8 mL of allyl bromide, **II-27**, to give 0.29 g of **II-28**$_s$**.**

*Polymer with diethyl vinylphosphonate (**II-30**)*

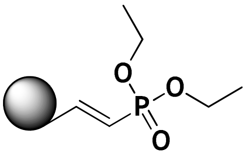

The general procedure was used starting with 0.15 g (1.2 mmol) of polymer **II-1**$_s$ and with 0.7 mL (4.6 mmol) of diethyl vinylphosphonate, **II-29**, to give 0.15 g of **II-30**$_s$**.**

FT-IR: $\bar{\upsilon}$cm^{-1} 3050 (=CH str.), 2920 and 2850 (C-H str.), 1605, 1590, 1510 and 1485 (C=C str.), 1445 (CH$_2$ def.), 1365 (O-P-O str.), 1260 (P=O str.), 1160 (C-O-P str.), 990, 905, 830, 790 and 705 (CH def.).

Isotherms of polymer II-1$_s$ after functionalisation reactions by CM:

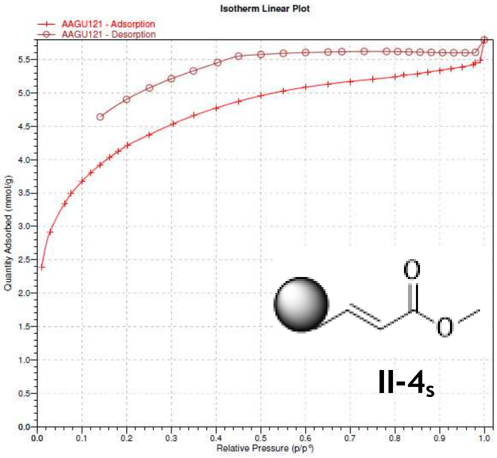

II-4$_s$

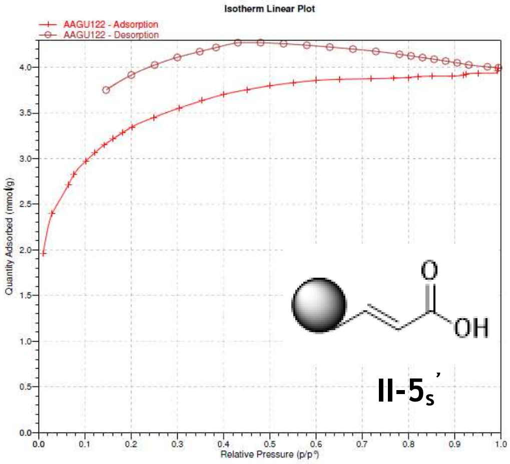

II-5$_s$'

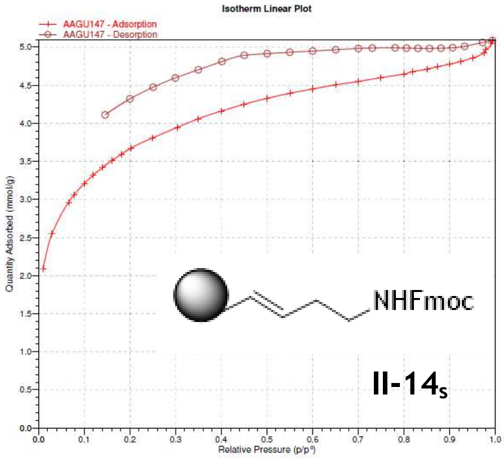

II-14$_s$

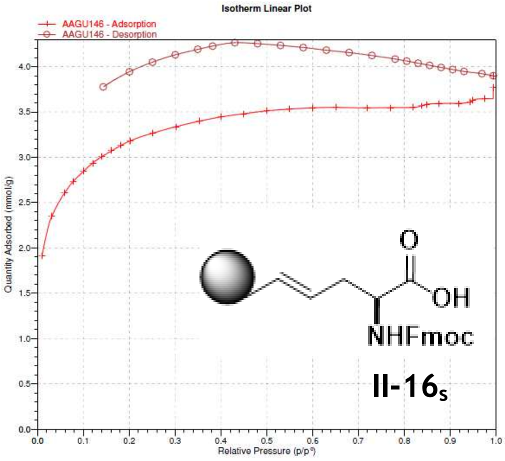

II-16$_s$

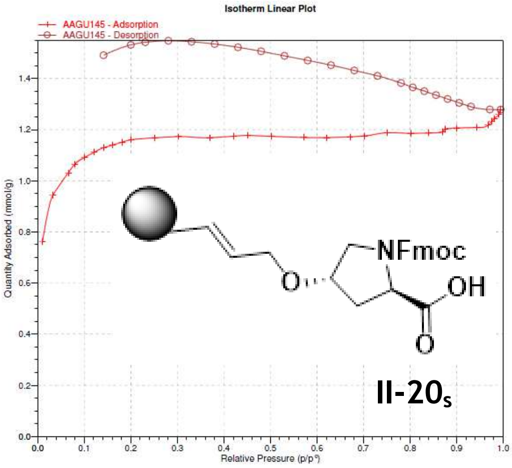

II-20$_s$

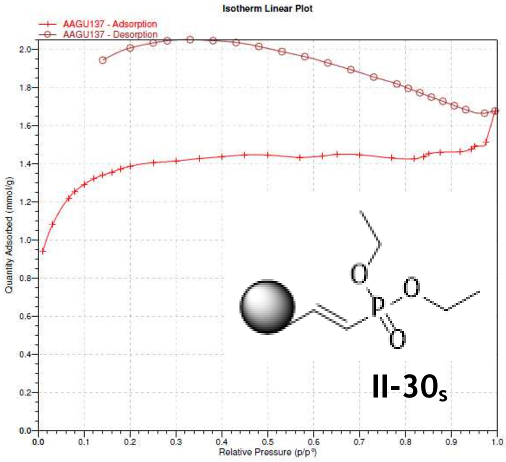

II-30$_s$

2.6.6. Synthesis of Fmoc-homoallylamine

*2-(But-3'-enyl)isoindoline-1,3-dione (**II-11**)*

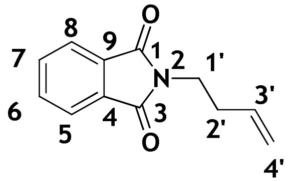

Compound **II-11** was synthesised by modifying an existing procedure.(13) DIAD (10.7 mL, 54.1 mmol, 1.30 equiv) was added dropwise in the dark to a solution of 3-buten-1-ol, **II-10** (3.60 mL, 53.7 mmol), phthalimide (7.90 g, 53.7 mmol, 1.29 equiv) and Ph_3P (14.1 g, 57.7 mmol 1.29 equiv) in anhydrous THF (150 mL) at r.t. After stirring the mixture for 5 h, H_2O (200 mL) was added and the aqueous phase was extracted with PE (3 x 200 mL). The combined organic extracts were dried ($MgSO_4$), filtered and concentrated *in vacuo*. Silica gel column chromatography [EtOAc/PE (1:9)] gave **II-11** as a light yellow powder, (8.30 g, 100%).

R*f* 0.4 (EtOAc/PE 1:9)

^{1}H NMR (400 MHz, $CDCl_3$) δ = 7.80 (2H, dd, *J* = 5.4, 3.0 Hz, H-(5,8)), 7.65 (2H, dd, *J* = 5.4, 3.0 Hz, H-(6,7)), 5.74 (1H, ddt, *J* = 17.1, 10.2, 6.9 Hz, H-3'), 5.00 (1H, dq, *J* = 17.0, 3.1 Hz, H-4'a), 4.95 (1H, dq, *J* = 10.3, 3.1 Hz, H-4'b), 3.70 (2H, t, *J* = 7.0 Hz, H-1'), 2.38 (2H, dt, *J* = 7.0, 2.4 Hz, H-2').

^{13}C NMR (100 MHz, $CDCl_3$) δ = 168.3 (C-(1,3)), 134.5 (C-3'), 133.9 (C-(6,7), 132.1 (C-(4,9)), 123.2 (C-(5,8)), 117.5 (C-4'),37.3 (C-1'), 32.8 (C-2').

HRMS (CI) *m/z* $(M+H)^+$ $C_{12}H_{12}NO_2$ Calcd.: 202.0868. Found: 202.0717.

m.p. 52 °C

*3-butenylamine hydrochloride (**II-12**)*$^{(25)}$

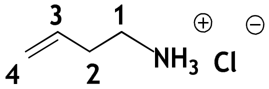

Compound **II-12** was synthesised using an existing procedure.$^{(25)}$ Compound **II-11** (2.00 g, 10.0 mmol) was dissolved in ethanol (100 mL) and the resulting solution was heated to 50 °C. Hydrazine monohydrate (98%) (2.40 mL, 50.0 mmol, 5 equiv) was then added to the mixture, which was stirred under an argon atmosphere for 1h. After that time, a white suspension was formed and the reaction suspension was quenched with 2 N aqueous HCl (10.0 mL). The resulting suspension was stirred for another 10 min. The white solid was filtered off and **II-12** was obtained as a white solid, which was carried onto the next step without purification.

^{1}H NMR (400 MHz, $CDCl_3$) δ = 5.60 (1H, ddt, *J* = 17.1, 10.3, 7.0 Hz, H-3), 5.10 (1H, dq, *J* = 17.2, 1.5 Hz, H-4a), 5.08 (1H, dq, *J* = 10.1, 1.5 Hz, H-4b), 2.96 (2H, t, *J* = 6.8 Hz, H-1), 2.31 (2H, tt, *J* = 6.9, 1.5 Hz, H-2).

*N-(9-Fluorenyl-6'-methoxycarbonyl)-3'-butenylamine (**II-13**)*

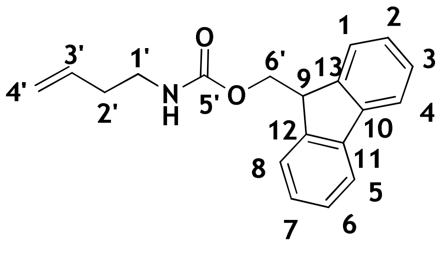

Compound **II-13** was synthesised by modifying an existing procedure.$^{(15)}$ Compound **II-12** was dissolved in water (50 mL) and the pH was set to 9 with TEA. Fmoc hydroxysuccinimide (6.3 g, 21 mmol, 1.1 equiv) was then dissolved in CH_3CN (50 mL) and added to the basic solution. The reaction mixture was stirred at room temperature and the pH was kept at pH 9 with TEA. After 1.5 h the reaction was completed and CH_3CN was evaporated *in vacuo*. The mixture was acidified with 1 N aqueous H_2SO_4 to pH 1 and extracted with EtOAc. The organic layer was dried over $MgSO_4$, filtered and concentrated in *vacuo*. The crude product was purified by silica gel column chromatography [EtOAc/PE (2:8)] giving **II-13** as a light yellow powder, (1.8 g, 61%).

R*f* 0.3 (EtOAc/PE 2:8)

^{1}H NMR (400 MHz, $CDCl_3$) δ = 7.79 (2H, dt, *J* = 7.5, 1.3 Hz, H-(4,5)), 7.61 (2H, d, *J* = 7.4 Hz, H-(1,8)), 7.42 (2H, tt, *J* = 7.4, 1.3 Hz, H-(3,6)), 7.37-7.31 (2H, td, *J* = 7.4, 1.2 Hz, H-(2,7)), 5.86-5.73 (1H, ddt, *J* = 17.2, 10.1, 6.9 Hz, H-3’), 5.17 (1H, dd, *J* = 17.3, 1.2 Hz, H-4’a), 5.15 (1H, dd, *J* = 9.9, 1.2 Hz, H-4’b), 4.82 (1H, t, *J* = 7.0 Hz, NH), 4.44 (2H, d, *J* = 7.0 Hz, H-6’), 4.26 (1H, t, *J* = 7.0 Hz, H-9), 3.32 (2H, appq, *J* = 6.4 Hz, H-1’), 2.31 (2H, q, *J* = 7.0 Hz, H-2’).

^{13}C NMR (100 MHz, $CDCl_3$) δ = 156.4 (C-5’), 144.0(C-(12, 13)), 141.3 (C-(10, 11)), 135.1 (C-3’), 127.7 (C-(3, 6)), 127.0 (C-(4, 5)), 125.1 (C-(2, 7)), (120.0 (C-(1, 8)), 117.4 (C-4’), 66.6 (C-6’), 47.3 (C-9), 40.1 (C-1’), 34.2 (C-2’).

HRMS (ESI) *m*/*z* $(M+Na)^+$ $C_{19}H_{19}NO_2Na$ Calcd: 316.1308. Found: 316.1305.

FT-IR: $\bar{\upsilon}$cm^{-1} 3420 (NH str.), 3080 (=CH str.), 2910 and 2870 (C-H str.), 1704 (C=O str.) 1620 and 1450 (C=C str.), 1520 (NH def.), 1420 (CH_2 def.), 1290 (C-O str.), 1090 (CN str.), 920 and 750 (CH def.), 720 (NH def.).

m.p. 83 – 85 °C

2.6.7. Synthesis of Fmoc-4-allyloxyproline

*1-(((9H-fluoren-9-yl)methoxy)carbonyl)-4-hydroxypyrrolidine-2-carboxylic acid (**II-18**)*

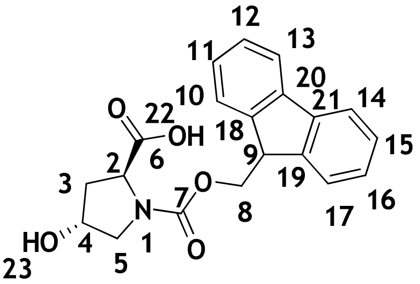

Compound **II-18** was synthesised by modifying an existing procedure.(15) *trans*-4-Hydroxy-*L*-proline, **II-17**, (3.6 g, 27mmol) was dissolved in water (40 mL) and the pH was set to 9 with TEA. Fmoc hydroxysuccinimide (9.2 g, 30 mmol, 1.1 equiv) was dissolved in CH_3CN (40 mL) and added to the basic solution. The reaction mixture was stirred at room temperature and the pH was kept at pH 9 with TEA. After 1.5 h the reaction was complete and CH_3CN was evaporated *in vacuo*. The mixture was acidified with 1 N aqueous H_2SO_4 to pH 1 and extracted with EtOAc (3 x 100 mL). The organic layer was dried with $MgSO_4$, filtered and concentrated *in vacuo*. The crude product was purified by silica gel column chromatography [EtOAc/PE (1:9)] giving **II-18** as a light yellow powder (8.5 g, 89%).

R*f* 0.3 (EtOAc/PE 1:9)

^{1}H NMR (500 MHz, $CDCl_3$) δ = 7.79-7.70 (2H, m, H-(13,14)), 7.62-7.52 (2H, m, H-(10,17)), 7.40 (2H, td, *J* = 7.5, 2.0 Hz H-(12,15)), 7.31 (2H, td, *J* = 7.4, 2.1 Hz, H-(11,16)), 5.19-5.15 (2H, m, H-8), 4.41 (1H, t, *J* = 7.9 Hz, H-9),4.30 (1H, t, *J* = 6.9, H-2), 3.50 (1H, dd, *J* = 10.9, 4.3 Hz, H-5a), 3.45 (1H, dd, *J* = 11.0, 4.2 Hz, H-5b), 3.40-3.39 (1H, m, H-23), 3.37 (1H, tt, *J* = 4.3, 1.5 Hz, H-4), 2.20 (1H, dt, *J* = 11.2, 1.6 Hz, H-3a), 2.15 (1H, dt, *J* = 11.1, 1.5 Hz, H-3b).

^{13}C NMR (100 MHz, CDCl3) δ = 172.4 (C-6), 156.3 (C-7), 143.6 (C-(18, 19)), 141.3 (C-(20,21)), 127.8 (C-(11,16)), 127.2 (C-(12,15)), 125.0 (C-(13,14)), 120.0 (C-(10,17)), 69.8 (C-4), 68.2 (C-8), 60.5 (C-2), 58.1 (C-5), 47.1 (C-9), 37.6 (C-3).

HRMS (ESI) *m/z* $(M+Na)^+$ $C_{20}H_{19}NO_5Na$ Calcd: 376.1161. Found: 376.1147.

m.p. 186-196 °C

*Synthesis of 1-(((9H-fluoren-9-yl)methoxy)carbonyl)-4-Allyloxypyrrolidine-2-carboxylic acid (**II-19**)*

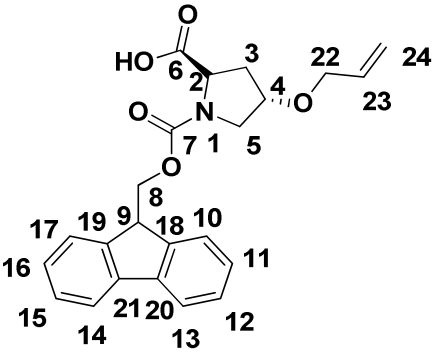

Compound **II-19** was synthesised by modifying an existing procedure.(16,18) To a stirred suspension of sodium hydride (0.18g, 7.4 mmol 2.6 equiv) in anhydrous DMF (10 mL) was added a solution of **II-18** (1.0 g, 2.8 mmol) in anhydrous DMF (20 mL) at room temperature under argon. After 30 min, allyl bromide (0.62 mL, 7.1 mmol, 2.5 equiv) was added to the mixture. After 19 h, 20 mL of water and aqueous hydrochloric acid (3 N) were added to quench and acidify the mixture until pH 4. The mixture was extracted with Et_2O (3 x 130 mL) and the combined organic phases were washed with brine. The combined organic extracts were dried over $MgSO_4$, filtered and concentrated *in vacuo*. The obtained solid (1.2 g) was dissolved in CH_2Cl_2 (4 mL) and TFA (14 mL) and the mixture was stirred at room temperature for 2 h under argon. The reaction was quenched by bubbling argon (to eliminate any volatile compounds) and water (20 mL), and it was extracted with CH_2Cl_2 (3 x 30 mL). The combined organic layers were dried with $MgSO_4$, filtered and concentrated *in vacuo*. The crude product was purified by silica gel column chromatography [EtOAc/PE (1:9)] giving **II-19** as a brown oil (0.67 g, 60%).

R_f 0.2 (EtOAc/PE 1:9)

^{1}H NMR T $_{50 \rightarrow 25\ °C}$ (400 MHz, $CDCl_3$) δ = 7.75 (2H, d, *J* = 7.5 Hz, H-(13,14)), 7.68-7.53 (2H, m, H-(10,17)), 7.39 (2H, t, *J* = 7.4 Hz, H-(12,15)), 7.35 (2H, t, *J* = 7.4 Hz, H(11,16)), 6.00-5.77 (1H, m, H-23), 5.33 (1H, dd, *J* = 17.2, 5.3 Hz, H-24a), 5.20 (1H, dd, *J* = 10.8, 5.3 Hz, H-24b), 4.73-4.67 (2H, m, H-8), 4.63 (1H, t, *J* = 7.5 Hz, H-9), 4.47-4.40 (1H, m, H-2), 4.39-4.21 (2H, m, H-(22a,22b)), 4.20-4.05 (1H, m, H-5b), 3.85-3.50 (2H, m, H-(4,5a)), 2.47-2.27 (1H, m, H-3a), 2.05-2.17 (1H, m, H-3b).

^{13}C NMR (100 MHz, $CDCl_3$) δ = 172.3 (C-6), 155.3 (C-7), 143.7 C-(18,19)), 141.9 (C-(20,21)), 131.9 (C-23), 127.8 (C-(12,15)), 127.1 (C-(11,16)), 125.2 (C-(13,14)), 120.1 (C-(10,17)), 118.9 (C-24), 69.3 (C-4), 67.8 (C-22), 65.9 (C-8), 58.1 (C-2), 55.0 (C-5), 47.3 (C-9), 38.9 (C-3).

HRMS (CI) *m/z* $(M+H)^+$ $C_{23}H_{24}NO_5$ Calcd: 394.1649. Found: 394.1654.

FT-IR: $\bar{\upsilon}$cm^{-1} 3450 (OH str.), 3050 (=CH str.), 2920 and 2850 (C-H str.), 1750 and 1680 (C=O str.) 1605, 1590 and 1485 (C=C str.), 1420 (CH_2 def.), 1350 (C-O str.), 1180 (C-O-C str.), 910, and 750 (CH def.).

2.6.8. Synthesis of Fmoc-allylcysteine

*Synthesis of 2'-(((9H-fluoren-9-yl)methoxy)carbonylamino)-3'-mercaptopropanoic acid (**II-24**)*

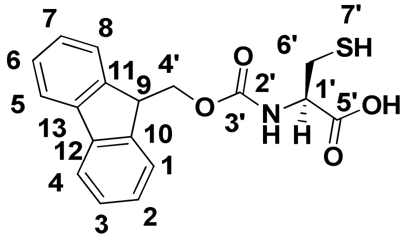

Compound **II-24** was synthesised by modifying an existing procedure.$^{(26)}$ 9-Fluorenylmethoxycarbonyl-S-trityl-*L*-cysteine, **II-23**, (2.0 g, 3.4 mmol) was dissolved in TFA (8.0 mL). Triethylsilane (1.1 mL, 6.8 mmol, 2 equiv) was then added to the solution and the reaction was stirred at 23 °C for 1.5 h under argon atmosphere. The reaction was quenched by bubbling argon (to eliminate any volatile compounds) and water (20 mL). The solid was filtered and washed with Et_2O (30 mL). The product obtained (**II-24**) was pure (0.50 g). Alongside, the filtrate was extracted with Et_2O and the combined organic phases were dried with $MgSO_4$, filtered and concentrated *in vacuo* obtaining additional product. Purification of the combined products was performed by silica gel column chromatography [EtOAc/PE/AcOH (4.3:5.6:0.1)] giving **II-24** as a white powder, (0.70 g, total yield: 98%).

R_f 0.3 (EtOAc/PE/AcOH 4.3:5.6:0.1)

^{1}H NMR (400 MHz, $CDCl_3$) δ = 7.81 (2H, dd, *J* = 7.5, 0.9 Hz, H-(4,5)), 7.64 (2H, dd, *J* = 7.5, 1.0 Hz, H-(1,8)), 7.45 (2H, tt, *J* = 7.5, 0.9 Hz, H-(3,6)), 7.36 (2H, tt, *J* = 7.5, 1.0 Hz, H-(2,7)), 5.70 (1H, d, *J* = 7.5 Hz, H-2'), 4.76 (1H, dt, *J* = 7.5, 3.3 Hz, H-1'), 4.50 (2H, m, H-4'), 4.28 (2H, t, *J* = 6.6 Hz, H-9), 3.18-3.00 (1H, dd, *J* = 13.5, 7.5 Hz, H-6a'), 3.05-2.97 (1H, dd, *J* = 13.5, 3.3 Hz, H-6b'), 1.49 (1H, t, *J* = 8.8 Hz, H-7').

^{13}C NMR (100 MHz, $CDCl_3$) δ = 176.9 (C-5'), 155.8 (C-3'), 144.5 (C-(10,11)), 141.3 (C-(12,13)), 134.8 (C-(3,6)), 134.2 (C-(4,5)), 124.5 (C-(2,7)), 53.4 (C-1'), 120.3 (C-(1,8), 67.1 (C-4'), 47.1 (C-9), 22.4 (C-6').

HRMS (ESI) *m/z* (M-H)$^-$ $C_{18}H_{16}NO_4S$ Calcd: 342.0806. Found: 342.079.

m.p. 109-115 °C

2.6.9. Fmoc deprotection reaction and free amine test

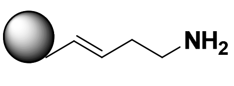

II-31

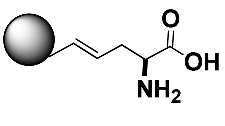

II-32

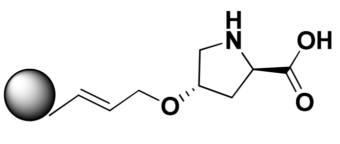

II-33

Fmoc deprotection

Fmoc deprotection reaction was carried out following a known protocol.(27) In a round-bottomed flask, 30 mg of resin (**II-14, II-16** and **II-20**) was suspended in 20% piperidine in CH_2Cl_2 or DMF (10 mL) for 1 h. The mixture was stirred very gently for 2 h at room temperature under argon. The resin was filtered off (**II-31, II-32, II-33**) and the solvent was evaporated in *vacuo* to recover the fulvene-piperidine adduct and measure the absorbance.[28]

The Beer-Lambert Law (Equation 2.4) was used to calculate the loading of the Fmoc group in the polymer. The samples were diluted in methanol until the absorbance fell within the range of the spectrometer (625 times), the volume of the samples were 5 mL and the weight of the samples used were 0.28, 0.48 and 0.40 g (**II-31, II-32, II-33**).

$$\text{Loading in mmolg}^{-1} = \left(\frac{\text{Absorbance}}{7800}\right) \times \text{ dilution } \times \left(\frac{\text{Flask volume (mL)}}{\text{wt. of sample (g)}}\right)$$

Equation 2.4 Beer-Lambert Law equation.

Ninhydrin test

The unprotected resin (**II-14, II-16** and **II-20**) was suspended in a small amount of ninhydrin/EtOH (0.09g/25 mL) solution and it was heated at 100 ^{o}C for 15 mins.

Bromophenol blue test

The unprotected resin (**II-14, II-16** and **II-20**) was placed in a clean Eppendorf tube. 10-15 drops of a solution of 0.05% bromophenol blue in DMA were added to the resin. Beads were inspected immediately.

2.7. REFERENCES

(1) Fitch, R. M. *Elastoplastics* **1971**, *3*, 146–156.

(2) Li, K.; Stöver, H. D. H. *J. Polym. Sci. Part A Polym. Chem.* **1993**, *31*, 3257–3263.

(3) Li, W.; Stöver, H. D. H. *J. Polym. Sci. Part A Polym. Chem.* **1997**, *36*, 1543–1551.

(4) Downey, J. S.; Frank, R. S.; Li, W.; Stöver, H. D. H. *Macromolecules* **1999**, *32*, 2838–2844.

(5) Goh, E. C. C.; Stöver, H. D. H. *Macromolecules* **2002**, *35*, 9983–9989.

(6) Radhakrishnan, R.; Underhill, P. T. *Soft Matter* **2012**, *8*, 6991–7003.

(7) Wang, R.; Wang, Z. G. *Macromolecules* **2012**, *45*, 6266–6271.

(8) Christian, G. D. *Analytical chemistry*, Fifth Edit.; J. Wiley and Sons: New York, 1994.

(9) Chatterjee, A. K.; Choi, T. L.; Sanders, D. P.; Grubbs, R. H. *J. Am. Chem. Soc.* **2003**, *125*, 11360–11370.

(10) Connon, S. J.; Blechert, S. *Angew. Chem. Int. Ed.* **2003**, *42*, 1900–1923.

(11) Li, W.; Sto, H. D. H. *Macromolecules* **2000**, *33*, 4354–4360.

(12) Law, R. V; Sherrington, D. C.; Snape, C. E. *Macromolecules* **1997**, *9297*, 2868–2875.

(13) Sen, S. E.; Roach, S. L. *Synthesis* **1994**, 756–758.

(14) McNaughton, B. R.; Bucholtz, K. M.; Camaaño-Moure, A.; Miller, B. L. *Org. Lett.* **2005**, *7*, 733–736.

(15) Ghalit, N.; Poot, A. J.; Fu, A.; Rijkers, D. T. S.; Liskamp, R. M. J. *Org. Lett.* **2005**, *7*, 2961–2964.

(16) Kyle, D. J.; Blake, P. R.; Smithwick, D.; Green, L. M.; Martin, J. A.; Sinsko, J. A.; Summers, M. F. *J. Med. Chem.* **1993**, *36*, 1450–1460.

(17) Baines, F. C.; Bevington, J. C. *J. Polym. Chem. Part A Polym. Chem.* **1968**, *6*, 2433–2440.

(18) DiGioia, L. M.; Leggio, A.; Liguori, A.; Perri, F.; Siciliano, C.; Viscomi, M. C. *Amino Acids* **2010**, *38*, 133–143.

(19) Huck, C. W.; Bonn, G. K. *J. Chromatogr. A* **2000**, *885*, 51–72.

(20) Fritz, J. S.; Dumont, P. J.; Schmidt, L. W. *J. Chromatogr. A* **1995**, *691*, 133–140.

(21) Puig, D.; Barceló, D. *J. Chromatogr. A* **1996**, *733*, 371–381.

(22) Limé, F.; Irgum, K. *Macromolecules* **2009**, *42*, 4436–4442.

(23) Bratkowska, D.; Marcé, R. M.; Cormack, P. A. G.; Sherrington, D. C.; Borrull, F.; Fontanals, N. *J. Chromatogr. A* **2010**, *1217*, 1575–1582.

(24) Cormack, P. A. G.; Davies, A.; Fontanals, N. *React. Funct. Polym.* **2012**, *72*, 939–946.

(25) McNaughton, B. R.; Bucholtz, K. M.; Camaaño-Moure, A.; Miller, B. L. *Org. Lett.* **2005**, *7*, 733–736.

(26) Pearson, D. A.; Blanchette, M.; Baker, L.; Guindon, C. A. *Tetrahedron Lett.* **1989**, *30*, 2739–2742.

(27) Fields, G. B. *CHAPTER 2 Methods for Removing the Fmoc Group*; Pennington, M. W., Dunn, B. M., Eds.; Humana press inc: Totowa, NJ, 1994; Vol. 35.

(28) Kimmins, S. D.; Wyman, P.; Cameron, N. R. *Polymer* **2014**, *55*, 416–425.

CHAPTER 3

SYNTHESIS, CHARACTERISATION AND FUNCTIONALISATION BY OLEFIN CROSS METATHESIS OF POLYDIVINYLBENZENE COPOLYMERS

3.1. INTRODUCTION

3.1.1. Copolymerisation processes

The process in which two or more monomers with different molecular structures are reacted to form macromolecules is called a copolymerisation reaction.(1) The nature of the products obtained, the copolymers, will vary depending on:

- The different kinds of monomers chosen.
- The relative concentrations of the monomers present in the reaction.
- The distribution of the monomers in the polymer chain during the polymerisation reaction, which is determined by their intrinsic reactivity and relative concentration.

Due to these factors, the copolymerisation technique is the ideal method to obtain polymers presenting useful physicochemical properties for some specific applications. A wide range of industrial copolymers are known, which have been modified to alter substantially their solubility, mechanical properties, thermal properties, *etc*. Polystyrene is the most characteristic example. Polystyrene presents poor mechanical and thermal properties, and it is highly soluble in many organic solvents. However, when polystyrene it is copolymerised with Divinylbenzene (DVB), its mechanical and thermal properties are improved and its solubility in organic solvent decreases. If polystyrene is copolymerised with 1,3-butadiene, a material with elastic properties is obtained. Therefore, if 1,3-butadiene and DVB are copolymerised with polystyrene, the thermal, mechanical and elastic properties of polystyrene increase and its solubility in organic solvents decreases.(2)

The role of copolymers is also very important with natural polymers, specifically in the case of polysaccharides and proteins in which their properties are highly dependent on the sugar and amino acids sequences. Usually, a copolymerisation reaction can be represented as follows (**Scheme 3.1**):

$$xA + yB \rightarrow - A - A - B - A - A - A - B - B - B - B - A - B - A -$$

Scheme 3.1 Typical copolymerisation reaction scheme.

The composition of the polymer formed has two different monomer units (A and B) randomly assigned or following a regular structure depending on the structure of the monomers used, the initiator type used, the solvent, the temperature, *etc*. Copolymers can also be classified according to the arrangement of the monomers into the polymer chain as follows:(2)

Statistical copolymers:

These kinds of copolymers are formed when the monomer units (A and B) are randomly arranged in the polymer chain.(1,2) One example of this kind of copolymerisation is the one between styrene and DVB.(3) The polymer formed receives the name poly(styrene-*co*-DVB)(4) and the arrangement is presented in **Scheme 3.2.**

- A - B - A - A - B - A - A - A - B - B - A - B - A - A -

Scheme 3.2 Structure of statistical copolymers.

Alternating copolymers:

The monomers A and B tend to arrange in an alternating way along the polymer chain (Scheme 3.3).(1,2) One example of this kind of polymer could be the copolymerisation reaction between DVB and maleic anhydride (MA) monomers.(5) The name of the polymer formed is poly(DVB-*alt*-MA).(4)

- A - B - A - B - A - B - A - B - A - B - A - B - A -

Scheme 3.3 Structure of alternating copolymers.

Block copolymers:

Block copolymers or sequential copolymers are polymers in which all the A and B monomer units form separated, homogeneous sequences linked by covalent bonds (**Scheme 3.4**). Block copolymers with two, three or four distinct blocks are called diblocks, triblocks or tetrablocks respectively.(2)

A______(A)$_n$______A-B______(B)$_n$______B or

B______(B)$_n$______B-A______(A)$_m$______A-B______(B)$_j$______B

Scheme 3.4 Structure of block copolymers.

One example of a block copolymers is poly(styrene-*b*-methyl methacrylate).(4,6) The polymer is formed by polymerising first styrene and then by subsequently polymerising methyl methacrylate from the reactive end of the polystyrene chain. Block copolymers are used in chemical catalysis, oil recovery, as models for some enzymatic reactions, to obtain small colloidal particles, *etc.*(2)

Graft copolymers:

The previously mentioned block polymers were linear polymers but branched copolymers can also be formed (**Scheme 3.5**).(2) In these polymers the B monomer branches can be distributed statistically or regularly along the main A polymer chain. The nomenclature for this kind of graft polymers is poly(A-*g*-B)(4) (**Scheme 3.5**).

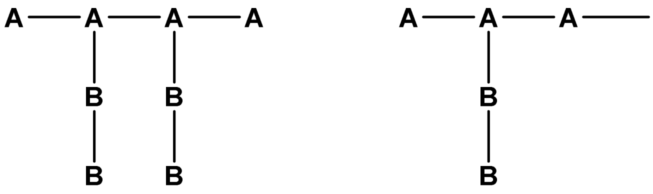

Scheme 3.5 Structure of graft polymers.

Graft polymers can also be a mixture of block and grafted polymers (**Scheme 3.6**). One example of graft polymers is ABS resin (structure in **Scheme 3.6**b), which is obtained by copolymerising acrylonitrile and styrene in the presence of polybutadiene. This reaction forms poly [butadiene-(styrene-*co*-acrylonitrile)]. These polymers can be obtained by radical, ionic or cationic polymerisations. Nevertheless, radical polymerisation is the most widely used polymerisation in industry.(2,7)

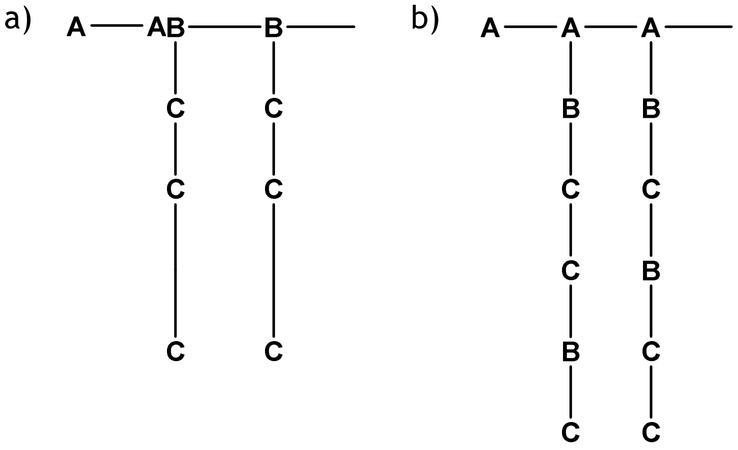

Scheme 3.6 Structures of mixed graft and block copolymers a) Poly[A-*b*(B-*g*-C)], b) Poly[A-*g*(B-*co*-C)].

3.2. AIM OF THE RESEARCH

In the previous chapter, a general functionalisation method was developed for the first time to install several different functional groups into porous polyDVB microspheres by olefin cross metathesis. The mild conditions employed with this technique maintained the integrity of the polymer beads and retained a olefin in the functionalised polymer. Thus, the polymer could be further functionalised providing an extra functionality to the polymer. One of the main possible applications for these polymers could be as SPE sorbents. However, the surface areas and the IECs obtained were lower than commercially available SPE sorbents, which are shown in **Table 3.1**.(8-10)

Resins	*Brand*	*Properties*	*Applications*
SCX	Waters Oasis®	IEC: 1 mmol g^{-1} pKa: <1 Particle size: 30-60 µm	Herbicides Pharmaceuticals Biological compounds
	Phenomenex Strata™	IEC: 1 mmolg $^{-1}$ pKa: 0 Particle size: 33 µm	Pharmaceuticals Drugs of abuse Biological compounds
WCX	Waters Oasis®	IEC: 0.7 mmol g^{-1} pKa: ~5 Particle size: 5-30-60 µm	Human pharmaceuticals Veterinary antibiotics
	Phenomenex Strata™	IEC: 0.8 mmol g^{-1} pKa: ~9 Particle size: 33 µm	Pharmaceuticals + Drugs abuse Antibiotics
SAX	Waters Oasis®	IEC: 0.25 mmol g^{-1} pKa: >18 Particle size: 30-60 µm	Pharmaceuticals Biological compounds
	Phenomenex Strata™	IEC: 0.25 mmol g^{-1} pKa: ~14 Particle size: 33 µm	Pharmaceuticals Biological compounds
WAX	Waters Oasis®	IEC: 0.6 mmol g^{-1} pKa: ~6 Particle size: 5-30-60 µm	Fluor. whitening agents Perfluorinated steroids Pharmaceuticals
	Phenomenex Strata™	IEC: 1 mmol g^{-1} pKa: ~9 Particle size: 33 µm	Natural organic matter

Table 3.1 Properties and applications of commercially available SPE sorbents.

To tackle the problems described previously, in this chapter, copolymerisation reactions using a divinyl co-monomer were carried out in order to increase the specific surface area and the IEC of the synthesised polymers. The choice of the divinyl co-monomer was made carefully, and monomers with pendent allylic groups, such as allyl maleimide (AMI) and allyl methacrylate (AMA), were used in the copolymerisation reactions. These divinyl co-monomers will have a pendent allyl group which will remain unreacted during the polymerisation reaction. The radical formed on this pendent double bond, will not be stabilised by resonance with the carbonyl group in the case of AMI and AMA or the phenyl ring in the case of DVB. The presence of this unreacted allyl groups will increase the number of reacting sites available for post-polymerisation CM reactions. In addition to the increase of binding sites, the polymer will be more robust, the swelling capacity higher, and therefore the surface area of the polymer will increase.

3.3. RESULTS AND DISCUSION

It is well known(11,12) that alternating copolymers can be prepared by a copolymerisation reaction between a strong electron-accepting monomer, such as MA, and an electron-donating monomer such as DVB. Furukawa reported, in 1975, that according to the nature of the monomer alternating or random copolymers were formed. Acrylic monomers are thought to act as weak electron-acceptor monomers, and therefore random copolymerisation is favoured.(13)

3.3.1. Precipitation copolymerisation of DVB and AMI

AMI was first tested as co-monomer in a precipitation copolymerisation reaction. The choice of AMI was made in order to obtain alternating copolymers (as it follows the structure of the well-known monomer MA) with larger surface areas and easier access to the pendent unreacted double bonds.

Poly(DVB-alt-AMI) starting with AMI as co-monomer

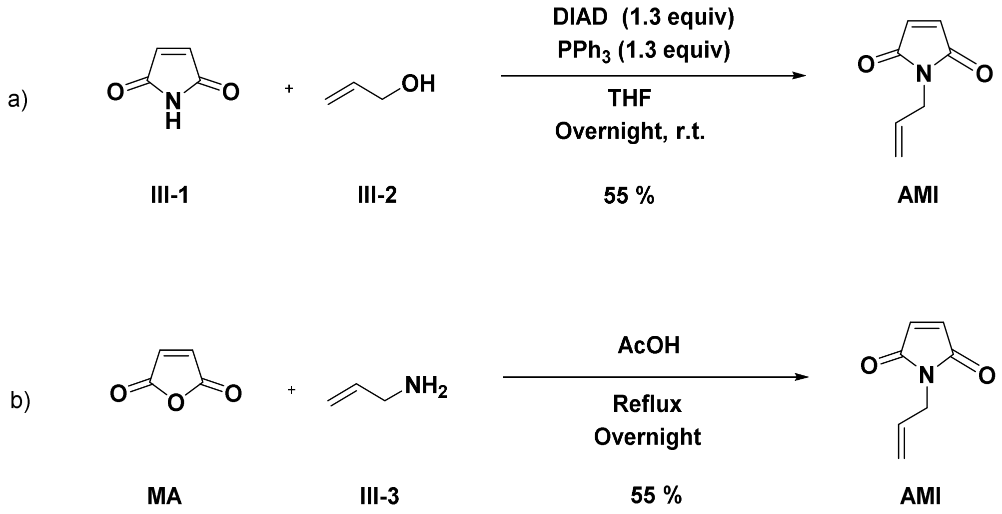

Figure 3.1 Two distinct routes for the synthesis of AMI.

The synthesis of AMI was carried out using two different strategies (Figure 3.1). The first route involved starting from maleimide (**III-1**) and a Mitsunobu⁽¹⁴⁾ reaction was carried out to synthesise AMI. Different conditions were attempted to obtain AMI. Some of them are summarised in Table 3.2. The first attempt was carried out using the conditions optimised in the previous chapter, but additionally leaving the reaction overnight. Unfortunately, only a 6% yield of the product was obtained as the maleimide remained unreacted. In order to increase the yield, the amount of allyl alcohol (**III-2**) was doubled, and so was the reaction time leaving the reaction over 2 nights, which increased the yield of the reaction to 48%. Attempting to reduce the reaction time, the alcohol amount was again increased to 3 equivalents, but no product was obtained. The last attempt to synthesise AMI was carried out following another procedure from the literature,(15) which gave AMI in 55% yield. A new route was used in order to improve the reaction yields (Figure 3.1). The new strategy(16) started from MA which was reacted with allylamine (**III-3**) to give AMI**.** Unfortunately, the yield was not improved.

Entry	***Reaction equivalents***				***Time***	***Yield***
	Maleimide	**AllOH**	**PPh_3**	**DIAD**	***(h)***	***(%)***
1	1.3	1.0	1.3	1.3	24	6
2	1.0	2.0	1.0	1.0	48	42
3	1.0	3.0	1.3	1.3	24	0
4	1.1	1.0	1.1	1.2	24	55

Table 3.2 Different reaction conditions used in Mitsunobu reaction.

Precipitation copolymerisation reactions with DVB and AMI were carried out in order to obtain porous polymer particles. Table 3.3 summarises all the conditions attempted in order to obtain poly(DVB-alt-AMI). The first attempt was carried out using typical precipitation polymerisation conditions, but aggregated particles were formed. When solids are used as monomers, problems may occur during the polymerisation. The presence of solids can result in poor solubility of the growing polymer network in certain solvents and can be particularly problematic during the initial nucleation stages of a polymerisation. In order to avoid the problem mentioned before, delayed addition of AMI was carried out.

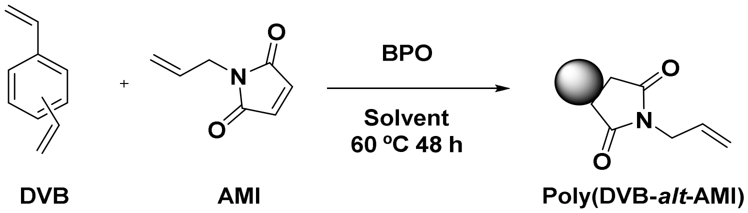

Figure 3.2 Precipitation copolymerisation of DVB with AMI.

The first attempt was carried out using AIBN as initiator (Table 3.3, entry **III-4$_a$**), but no particles were obtained. It was then decided to change the initiator to benzoyl peroxide (BPO), as this would facilitate the calculation of the polymer's composition by measuring the N% in elemental microanalysis, which was not possible with the nitrogen-containing AIBN. In order to obtain different alternating copolymers, the monomer ratios between DVB and AMI were varied (Table 3.3, entries **III-5**, **III-4$_a$**, **III-6** and **III-7**).(11-13) Unfortunately, no particles were obtained (Figure 3.3a) so another procedure with a different solvent system was followed.(17) Acetic acid and methyl ethyl ketone (MEK) were chosen as solvents (Table 3.3, entry **III-4$_c$**) but the monomer was not soluble in the media.

In 2002, Stöver and coworkers reported the synthesis of alternating copolymers derived from DVB and MA, in heptane and MEK.(18) The same conditions (but following a delayed addition of the monomer) were used (Table 3.3 entry **III-8$_a$**) to obtain poly(DVB-*alt*-AMI) particles. However, chemical aggregation was observed, which could not be avoided (Figure 3.3b). In order to eliminate the chemical aggregation, heptane was maintained as the primary solvent and different co-solvents were used (Table 3.3 entries **III-8$_b$** and **III-8$_c$**). Unfortunately, chemical aggregation was not eliminated with toluene as co-solvent (Figure 3.3c), and coagulums were formed (Figure 3.3d) when chloroform was used as co-solvent. The last attempt was carried out using acetonitrile and chloroform as solvent system (Table 3.3 entry **III-8$_d$**), but the change from heptane to acetonitrile resulted in no particles being formed (Figure 3.3e).

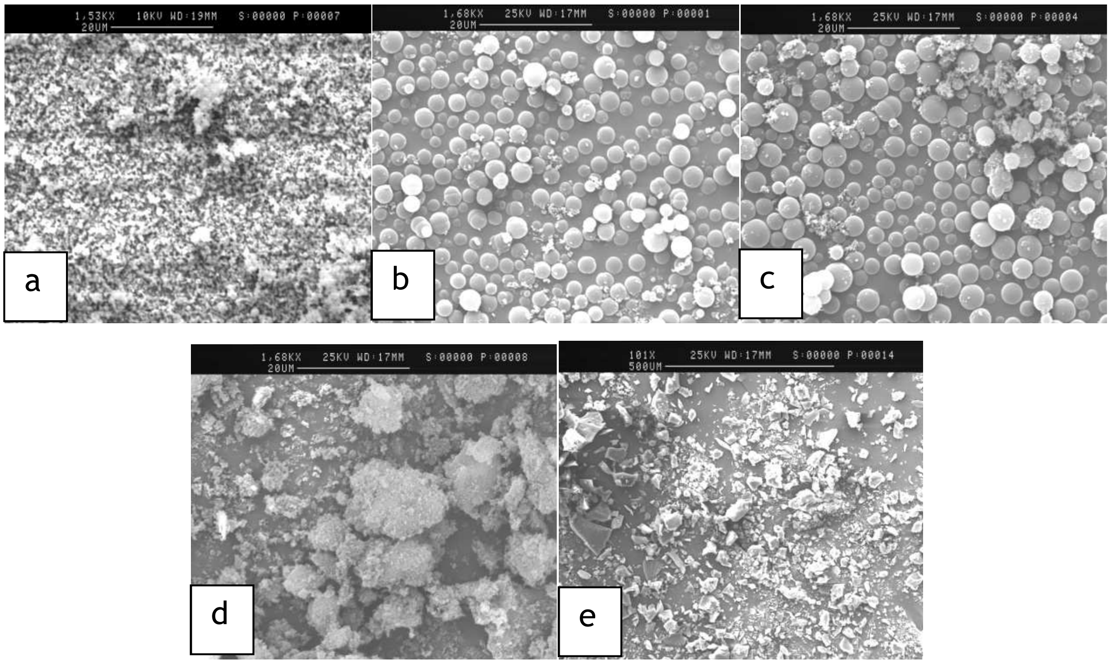

Figure 3.3 SEM micrographs of: a) III-4$_b$, b) III-8$_a$, c) III-8$_b$, d) III-8$_c$, e) III-8$_d$.

Polym ref.	*DVB*	*DVB/AMI wt./wt.*	*Mon./solv. (%wt./v)*	*Total scale (g)*	*BPO (mg)*	*CH_3CN (%)*	*Tol. (%)*	*AcOH (%)*	*Heptane (%)*	*MEK (%)*	*$CHCl_3$ (%)*	*Yield (g)*	*Yield (%)*
III-4$_a$	80	9/1	4	10	43[a]	80	20	-	-	-	-	9.6	93
III-5	80	9.5/0.5	4	10	65	80	20	-	-	-	-	7.3	70
III-4$_b$	80	9/1	4	10	63	80	20	-	-	-	-	9.2	89
III-6	80	8/2	4	10	60	80	20	-	-	-	-	9.1	87
III-7	80	7/3	4	10	57	80	20	-	-	-	-	9.5	92
III-4$_c$	80	9/1	4	0.31	30	-	-	80	-	20	-	-	-
III-8$_a$	55	6/4	9.5	2.4	28[b]	-	-	-	60	40	-	1.9	79
III-8$_b$	55	6/4	9.5	2.4	28[b]	-	40	-	60	-	-	2.1	86
III-8$_c$	55	6/4	9.5	2.4	28[b]	-	-	-	60	-	40	2.1	87
III-8$_d$	55	6/4	9.5	2.4	28[b]	60	-	-	-	-	40	2.2	90

Table 3.3 Different conditions used for precipitation copolymerisation reactions of DVB and AMI. [a]AIBN was used as initiator. [b] The amount of initiator used was 0.5 mol% relative to the total number of polymerisable double bonds.

The FT-IR spectrum of polymer **III-8$_a$** (Figure 3.4) shows DVB-derived peaks at 1600 cm^{-1} (C=C str.) and 830 cm^{-1} (CH def.) and the appearance of the AMI-derived bands at 1695 cm^{-1} (C=O str.), 1370 cm^{-1} (C-N str.) and 1345 cm^{-1} (C-O str.), strongly suggesting that the polymerisation was successfully carried out. The difference in the intensities of DVB and AMI peaks suggest that chemical aggregations can be formed by polymerised AMI, and therefore, it cannot be dissolved or eliminated from the polymer. Due to the problems obtained using AMI as a monomer, it was decided to synthesise poly(DVB-*alt*-AMI) following a two-step strategy to avoid the possible polyAMI formation.

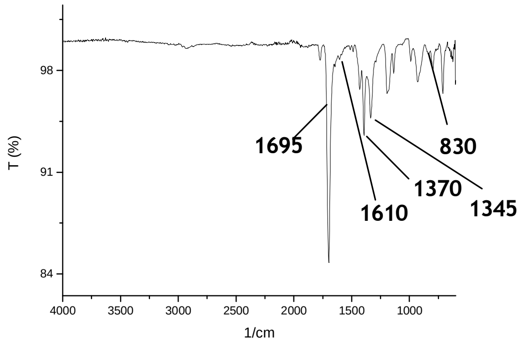

Figure 3.4 FT-IR spectrum of polymer III-8$_a$.

Poly(DVB-alt-AMI) starting with MA as co-monomer

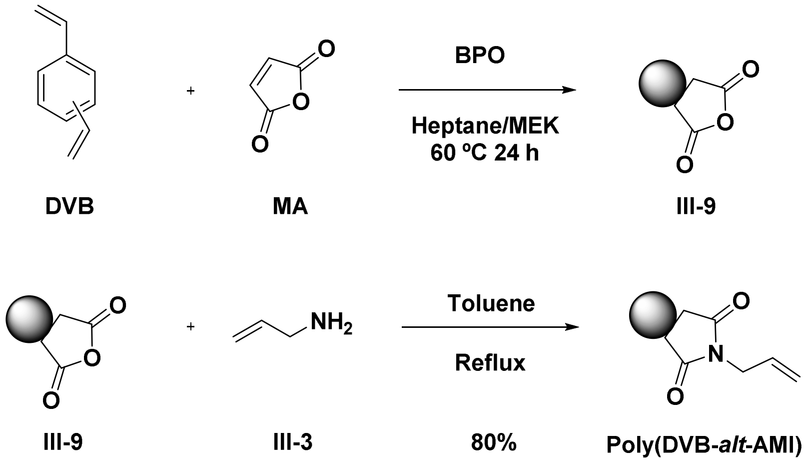

Figure 3.5 New strategy to obtain poly(DVB-*alt*-AMI).

A new strategy following the previously mentioned protocol by Stöver and coworkers(18) to obtain mondodisperse poly(DVB-*alt*-MA) particles was carried out (Figure 3.5). The first step of the synthesis was the polymerisation of DVB-55 and MA to obtain poly(DVB-55-*co*-MA) (**III-9**). Polymer **III-9$_a$** was synthesised following the best results reported by Stöver and coworkers; the results are shown in Table 3.4. The amount of initiator was changed from 0.5 mol% to 2 mol% to ensure the spherical shape of the particles giving polymer **III-9$_b$** in similar yield.

Polym ref.	*DVB/MA wt.%*	*Mon. Scale (g)*	*Mon./solv. (%wt./v)*	*BPO (mg)*	*MEK (%)*	*Hept. (%)*	*Yield (g)*	*Yield (%)*
III-9$_a$	6/4	0.97	9.5	13	40	60	0.86	88
III-9$_b$	6/4	0.97	9.5	52	40	60	0.88	89

Table 3.4 Conditions used in the formation of Poly(DVB-*alt*-MA).

SEM micrographs show that the particles obtained in both reactions had a narrow size distribution, and that no chemical aggregation was apparent (Figure 3.6). Statistical analysis performed by image J on polymer **III-9$_a$** (mean diameter: 0.8 *μm* SD: 0.06 *μm* CV: 7%) and compound **III-9$_b$** (mean diameter: 0.7 *μm* SD: 0.04 *μm* CV: 6%) confirms that quasi-monodisperse particles were obtained in both cases.

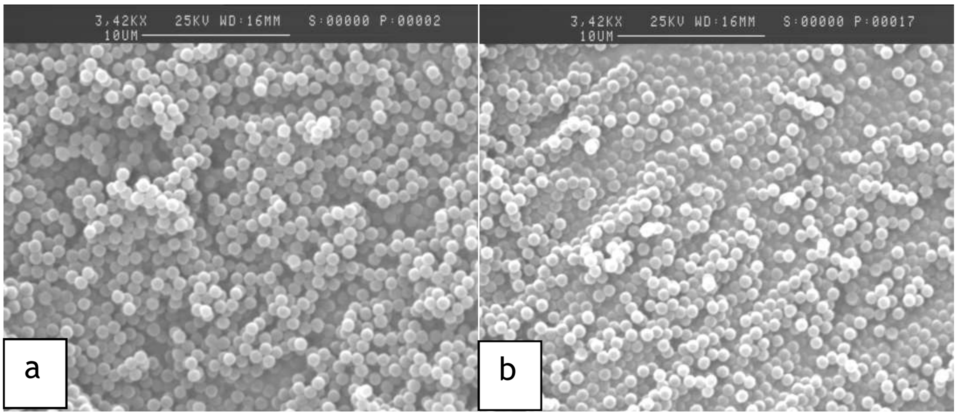

Figure 3.6 SEM micrographs of: a) III-9$_a$ and b) III-9$_b$.

For the second part of the synthesis, the polymer was swollen in anhydrous toluene for 1 h. The swelling of the polymer previous to the reaction was performed in order to access to every available MA unit. When the polymer had swollen, allylamine was added and the mixture was refluxed overnight to give **III-8$_e$** in a 78% yield (precursor: **III-9$_a$**) and **III-8$_f$** in **an** 80% yield (precursor **III-9$_b$**).

The success of the reaction was monitored by elemental microanalysis (Table 3.5) in which the N content indicates that the allylamination was successful. Assuming that the conversion of the reaction was 100%, calculations of the real polymer composition were carried out and are also shown in Table 3.5. These new ratios suggested that the anhydride was incorporated preferentially into the polymer during polymerisation.

Polymer ref.	*Elemental microanalysis (wt.%)*			*Calcd. ratios (wt.%)*	
	C	*H*	*N*	*DVB*	*AMI*
III-8$_e$	70.4	6.7	5.4	4.7	5.3
III-8$_f$	70.7	6.8	5.5	4.4	5.6

Table 3.5 Elemental microanalysis of III-8$_e$ and III-8$_f$.

The SEM micrographs (Figure 3.7) of **III-8$_e$** and **III-8$_f$** showed that the particles were not destroyed and that no chemical aggregates were formed as a result of the reaction with allylamine. Statistical analysis of the particles of **III-8$_e$** (mean diameter: 0.7 *μm* SD: 0.2 *μm* CV: 20%) and **III-8$_f$** (mean diameter: 0.8 *μm* SD: 0.1 *μm* CV: 13%) shows that after the allylamination reaction the dispersity of the particles was increased due to the insertion of the allyl group.

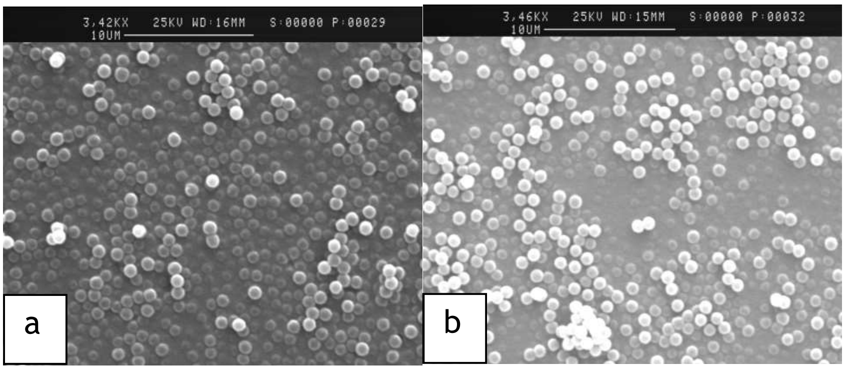

Figure 3.7 SEM micrographs of: a) III-8$_e$, b) III-8$_f$.

Nitrogen sorption analysis (Table 3.6) shows that none of the polymers obtained were porous. The size of the particles after the insertion of the allyl group was maintained lower than 1 μm and thus, the obtained surface area was low. Consequently, it was decided not to attempt CM reactions involving polymer **III-8$_e$**.

Polymer ref.	Specific surface area (m^2/g)		Specific pore vol. (cm^3/g)	Av. pore diameter (nm)
	BET	Langmuir		
III-9$_a$	-	10	-	-
III-9$_b$	10	-	-	-
III-8$_e$	-	5	-	-
III-8$_f$	10	-	-	-

Table 3.6 Nitrogen sorption analysis data.

3.3.2. Precipitation copolymerisation of DVB and AMA

Due to the problems with forming poly(DVB-*alt*-AMI) particles and functionalisation reactions thereon, AMA was used as co monomer with DVB (Figure 3.8). The allyl group of the AMA would remain unreacted after precipitation copolymerisation reactions, which would lead to an increase of the double bonds available for CM. AMA is a low viscosity liquid monomer with dual allylic and methacrylate functionalities, and it offers excellent chemical and heat resistance, adhesion, hardness, and low shrinkage to the formed copolymer.

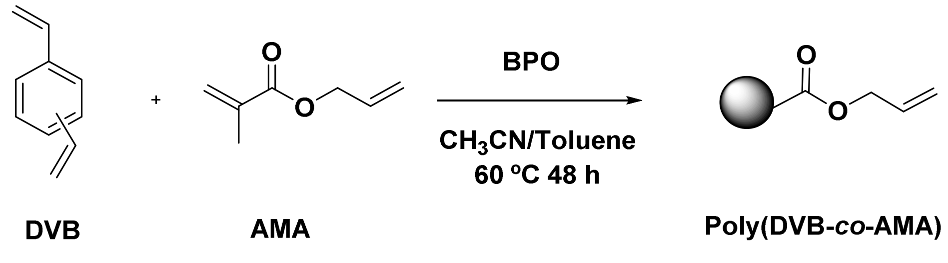

Figure 3.8 Precipitation copolymerisation of DVB and AMA.

Table 3.7 summarises all the conditions used during precipitation copolymerisation of DVB with AMA. Different ratios of DVB and AMA were attempted to increase the amount of unreacted double bonds as much as possible for CM reaction. Polymers **III-10**$_a$ and **III-10**$_c$ were synthesised using AIBN (2 mol%) as initiator, but it was decided to change from AIBN as initiator to BPO in order to avoid nitrogen in the polymer backbone for future loading calculations. The amount of toluene was also changed in order to increase the porosity of the polymer particles, giving larger yields (in most cases) when 40% of toluene was used, as the phase separation occurred later. THF was used as porogenic solvent in the synthesis of **III-12**$_b$ and **III-12**$_c$, but chemical aggregation was observed (Figure 3.9d).

Polym. ref.	*DVB/AMA wt.%*	*DVB*	*Mon./solv. (%wt./v)*	*BPO (g)*	*CH_3CN (%)*	*Tol. (%)*	*Yield (g)*	*Yield (%)*
III-10$_a$	9/1	80	4	0.43[a]	80	20	6.1	59
III-10$_b$		80	4	0.64	80	20	6.9	66
III-10$_c$		55	4	0.41[a]	75	25	4.6	45
III-10$_d$		80	4	0.64	70	30	7.6	73
III-10$_e$		55	4	0.55	70	30	6.6	64
III-10$_f$		80	4	0.64	60	40	8.2	79
III-10$_g$		55	4	0.55	60	40	5.9	57
III-11$_a$	8/2	80	4	0.61	80	20	7.4	71
III-11$_b$		55	4	0.54	70	30	6.0	58
III-11$_c$		55	4	0.54	60	40	5.2	50
III-12$_a$	7/3	80	4	0.58	80	20	7.2	70
III-12$_b$		80	4	0.58	80	20[b]	8.8	85
III-12$_c$		55	4	0.52	80	20[b]	7.2	70
III-12$_d$		80	4	0.58	70	30	7.2	70
III-12$_e$		55	4	0.52	70	30	6.5	63
III-12$_f$		80	4	0.58	60	40	6.9	67
III-12$_g$		55	4	0.52	60	40	6.9	67
III-13$_a$	1/1	80	4	0.53	80	20	5.2	51
III-14$_a$	2.5/7.5	80	4	0.46	80	20	6.2	61
III-15$_a$	1/9	80	4	0.41	80	20	8.2	80

Table 3.7 Different conditions os poly(DVB-*co*-AMA). [a] **2 mol% of AIBN as initiator.** [b] **THF as porogen.**

Figure 3.9 shows the most representative SEM micrographs of poly(DVB-*co*-AMA), the synthetic details for which are detailed in Table 3.7. Figure 3.9c shows that by using a large amount of toluene (40%) the phase separation occurred too late, particles grew and because of that, the colloidal stability of the particles failed resulting in coagulum or monolith formation. Figure 3.9f also shows that the coagulum formation started when the DVB/AMA ratio was 1/1, therefore the AMA concentration has to be kept low to retain stability and avoid coagulum formation. Figure 3.9a, b and e show poly(DVB-*co*-AMA) polydisperse particles which have the maximum amount of porogenic solvent.

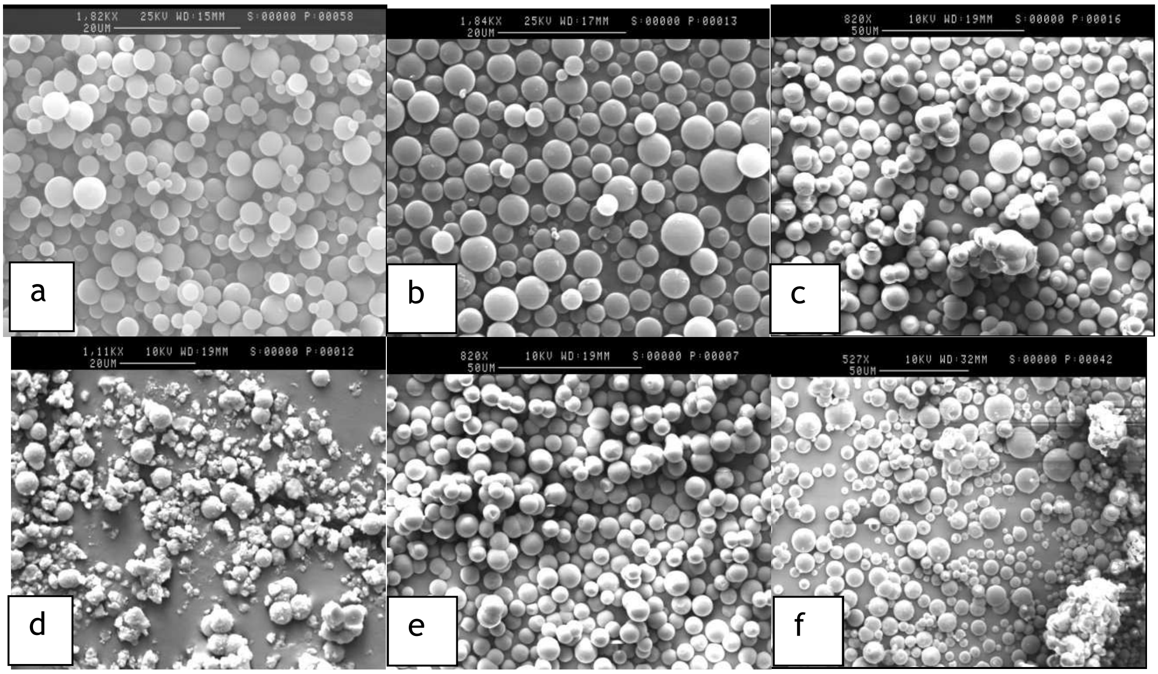

Figure 3.9 SEM micrographs of: a) III-10$_e$, b) III-11$_b$, c) III-11$_c$, d) III-12$_c$, e) III-12$_e$ and f) III-13$_a$.

Statistical analysis of polymer **III-10$_e$** (mean diameter: 2.9 *μm* SD: 0.89 *μm* CV: 31%), polymer **III-11$_b$** (mean diameter: 3.6 *μm* SD: 1.2 *μm* CV: 34%) and polymer **III-12$_e$** (mean diameter: 5.1 *μm* SD: 1.1 *μm* CV: 22%) catalogues the obtained particles as polydisperse. The analysis also shows that only polymer **III-12$_e$** was able to form particles with a mean diameter acceptable for SPE.

FT-IR spectra of the polymers (Figure 3.10) show that the obtained products are clearly poly(DVB-*co*-AMA). The appearance of the AMA peaks at 1730 cm^{-1} (C=O str.) and 1180 cm^{-1} (C-O-C str.), and the appearance of the DVB peaks at 1610 cm^{-1} (C=C str.), 1450 cm^{-1} (CH_2 def.) and 830 cm^{-1} (CH def.), proves the success of the copolymerisation. Figure 3.10 also shows that by increasing the amount of AMA in the reaction, the intensity of the FT-IR peaks of the AMA monomer increased relative to the peaks of DVB, confirming that AMA monomer is well integrated with DVB in the final polymer.

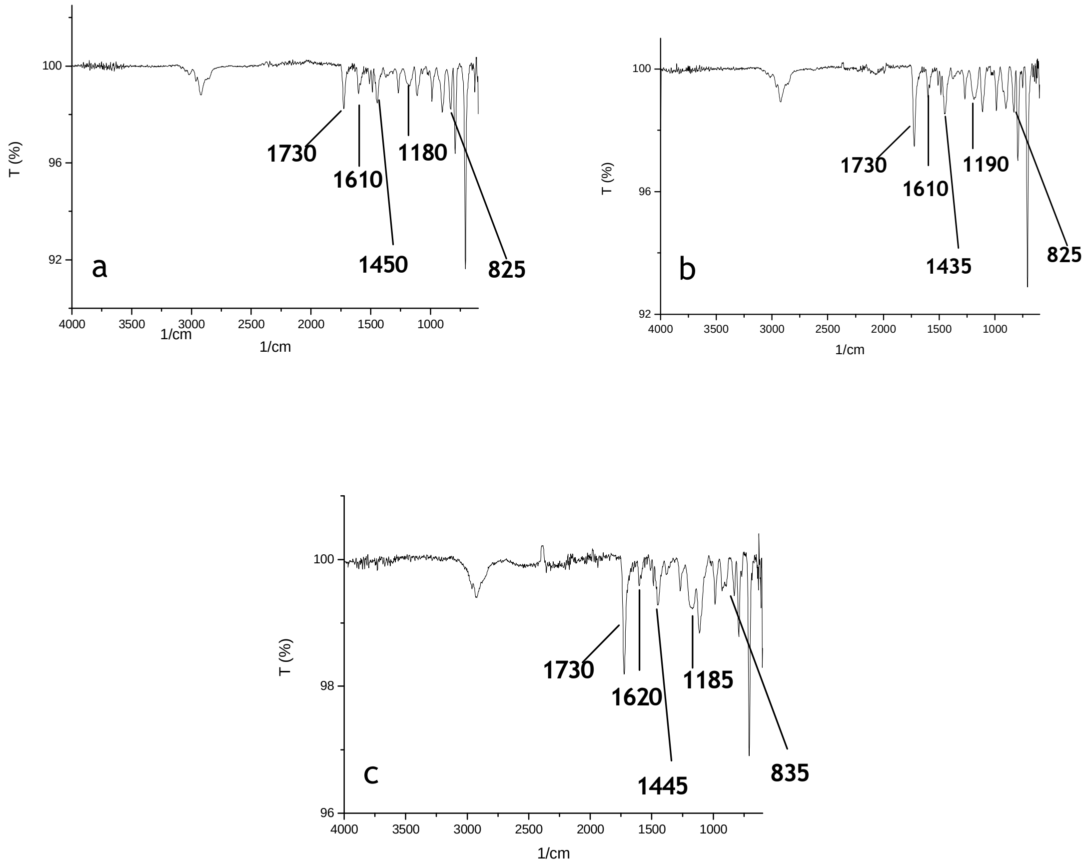

Figure 3.10 FT-IR spectra of: a) III-10$_e$, b) III-11$_b$, c) III-12$_e$.

Elemental microanalysis of the polymers was carried out in order to determine the actual composition of the polymers (Table 3.8). The differences between the expected and the experimental results indicate that the monomer ratios with which the polymers were fed, were not the same in the obtained polymers. Table 3.8 also shows the actual ratios of the polymers **III-10$_e$**, **III-11$_b$** and **III-12$_e$**, which are close to the feed ratios so, polymers **III-10$_e$**, **III-11$_b$** and **III-12$_e$** were used for functionalisation by CM reaction.

Polymer ref.	*Expected elemental microanalysis (wt.%)*		*Found elemental microanalysis (wt.%)*		*Real monomer ratios (wt.%)*	
	C	*H*	*C*	*H*	*DVB*	*AMA*
III-10$_e$	89.0	8.3	88.5	8.2	8.8	1.2
III-11$_b$	86.6	8.3	86.4	8.0	7.9	2.1
III-12$_e$	84.1	8.2	83.2	8.1	6.7	3.3

Table 3.8 Elemental microanalysis of polymers III-10$_e$, III-11$_b$ and III-12$_e$.

Nitrogen sorption analysis was performed for all the polymers synthesised. However, only data from polymers **III-10$_e$**, **III-11$_b$** and **III-12$_e$** are shown (Table 3.9) as these were the best quality particles. Table 3.9 shows that only polymer **III-10$_e$** was porous, although the surface area was smaller than the surface area obtained for polyDVB homopolymer in Chapter 2. To increase the porosity and therefore the surface area, larger amounts of toluene should be used. Unfortunately, the amount of toluene used for the synthesis of the polymers was the maximum amount allowed to avoid the formation of coagulums. Nevertheless, CM reactions were performed with these polymers.

Polymer ref.	*Specific surface area (m^2/g)*		*Specific pore vol. (cm^3/g)*	*Av. pore diameter (nm)*
	BET	*Langmuir*		
III-10$_e$	160	-	0.09	2.2
III-11$_b$	-	30	-	-
III-12$_e$	-	3	-	-

Table 3.9 Nitrogen sorption analysis data.

3.3.3. Functionalisation of poly(DVB-co-AMA) by CM

Functionalisation of poly(DVB-*co*-AMA) was carried out *via* CM reactions. With this reaction, the functionalisation is performed under very mild conditions and a wide range of coupling partners can be used whilst retaining the integrity of the polymer beads. A noteworthy advantage of this method is the retention of an olefin in the functionalised polymers, which can be used for further functionalisation.

CM involving polymers **III-10$_e$**, **III-11$_b$** and **III-12$_e$** with Fmoc-allylamine were carried out in order to test the reactivity of the polymers with CM (Figure 3.11). Fmoc-allylamine was chosen as coupling partner for the functionalisation reaction to quantify the loading of the nitrogen on the polymer by elemental microanalysis and to be used as WAX after the removal of the Fmoc group.

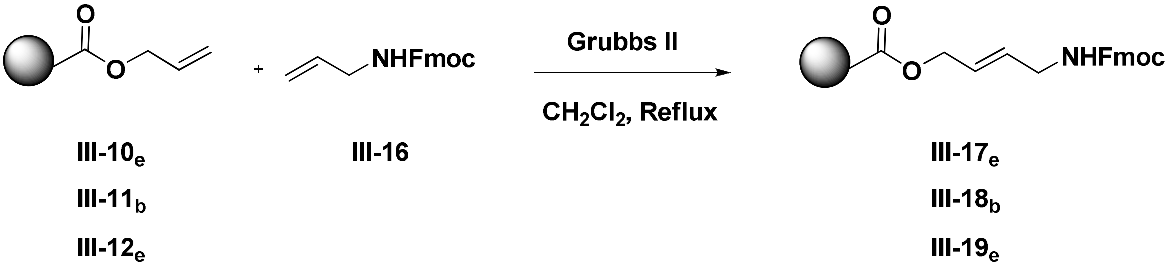

Figure 3.11 CM reaction of polymers III-10$_e$, III-11$_b$ and III-12$_e$ with Fmoc-allylamine.

Table 3.10 shows the elemental microanalysis results of the polymers after CM reaction. Polymers **III-17$_e$** and **III-18$_b$** did not undergo the CM reaction (as expected); no nitrogen was observed in the elemental microanalysis (Table 3.10). On the other hand, the functionalisation reaction was successful with polymer **III-12$_e$**, as nitrogen was detected in the elemental microanalysis of polymer **III-19$_e$**, and the absolute loading of the functional group could be established (0.42 mmolg^{-1}).

Polymer ref.	*Elemental microanalysis (wt.%)*			*N loading (mmolg^{-1})*
	C	*H*	*N*	
III-17$_e$	88.3	8.0	0/traces	-
III-18$_b$	86.2	8.3	0/traces	-
III-19$_e$	82.1	7.6	0.59	0.42

Table 3.10 Elemental microanalysis of polymers III-17$_e$, III-18$_b$ and III-19$_e$.

Due to the results obtained in the functionalisation of the polymers **III-10$_e$**, **III-11$_b$** and **III-12$_e$**, swelling tests were carried out (Figure 3.12) in order to understand the success of the functionalisation reaction with the non-porous polymer (**III-12$_e$**) and not with the porous polymer (**III-10$_e$**). **Figure 3.12** shows that, when packing 1 mL of the polymers (**III-10$_e$**, **III-11$_b$** and **III-12$_e$**) in a measuring cylinder, and adding 5 mL of CH_2Cl_2, polymer **III-12$_e$** swelled more than the other polymers (**III-10$_e$:** 1.3 mL, **III-11$_b$:** 1.4 mL and **III-12$_e$:** 1.5 mL) thereby favouring the CM reaction. The swelling capacity is directly linked with the amount of AMA on the polymer, as by decreasing the amount of DVB, less crosslinked polymer would be obtained. These results suggested that polymer **III-12$_e$** could be a gel-type polymer, as it is not porous in the dry state but swells in the presence of a good solvent, which means that functionalisation reactions can be performed.

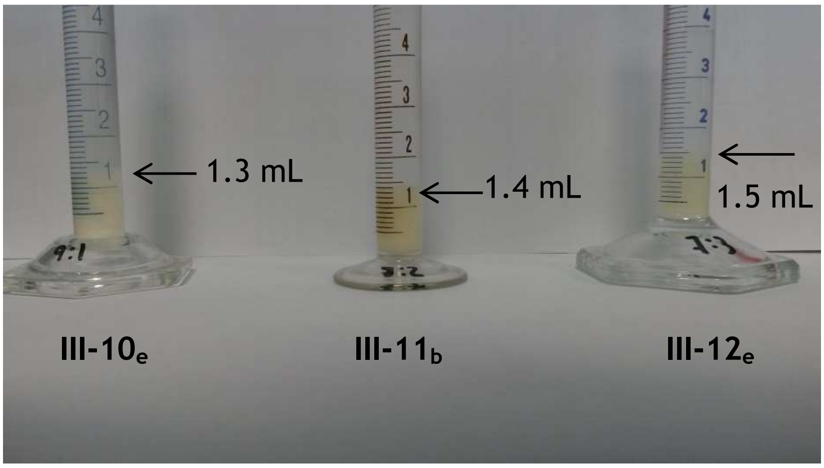

Figure 3.12 Swelling tests on polymers III-10$_e$, III-11$_b$ and III-12$_e$.

Functionalisation reactions involving polymer **III-12$_e$** were also carried out with other coupling partners (Figure 3.13). Allyl bromide (**II-27**) was chosen as coupling partner to quantify the amount of bromine immobilised on the polymer by elemental microanalysis. Diethyl vinyl phosphonate (**II-29**) was used to measure by elemental microanalysis the phosphorous loading.

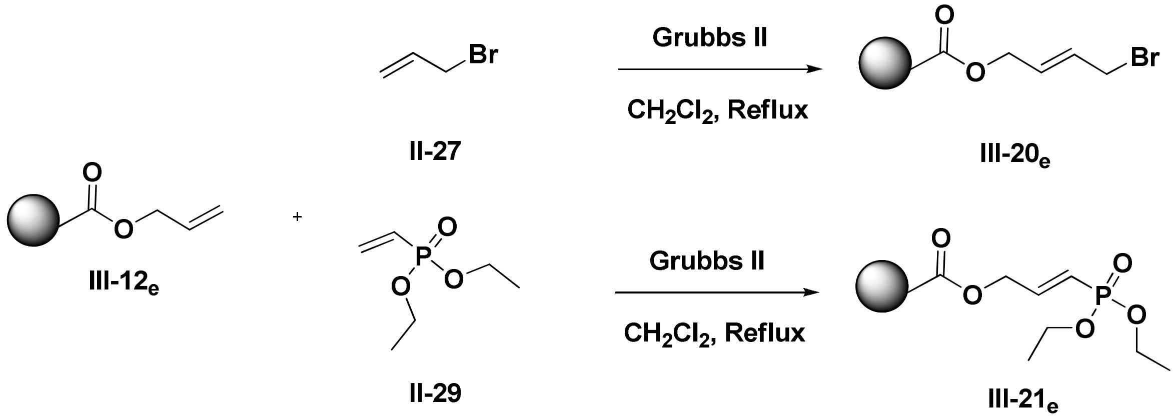

Figure 3.13 CM reactions of polymer III-12$_e$.

Elemental microanalysis of polymer **III-20$_e$** (*81.9% C, 7.0% H, 3.1% Br*) and polymer **III-21$_e$** (*80.4% C, 7.8% H, 1.0% P*) suggested the success of the functionalisation reaction and established a bromine loading of 0.39 mmolg^{-1} and a phosphorous loading of 0.34 mmolg^{-1}.

SEM micrographs (Figure 3.14) of polymers **III-19$_e$**, **III-20$_e$** and **III-21$_e$** showed that no chemical aggregation occurred during CM reactions. Statistical analysis of the particles of polymer **III-19$_e$** (mean diameter: 5.6 *μm* SD: 0.83 *μm* CV: 15%), polymer **III-20$_e$** (mean diameter: 5.4 *μm* SD: 0.84 *μm* CV: 15%) and polymer **III-21$_e$** (mean diameter: 5.5 *μm* SD: 0.8 *μm* CV: 15%) shows that the obtained particles were quasi-monodisperse. The increase in the size of these particles produced by the success of the CM reaction, leads to a lower difference between the SD and the mean diameter and thus, the CV value decreases.

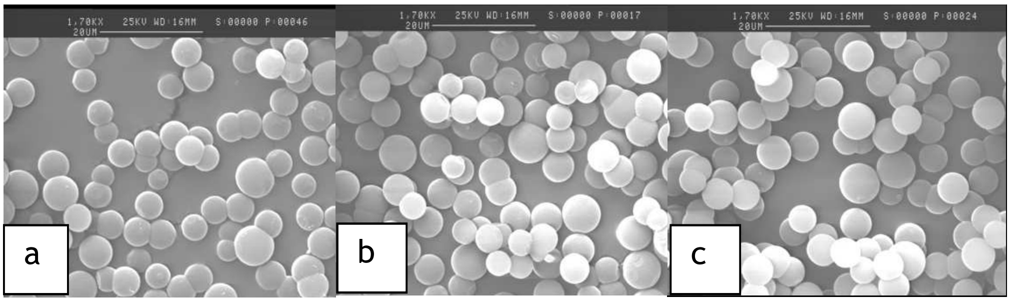

Figure 3.14 SEM micrographs of polymers a) III-19$_e$, b) III-20$_e$ and c) III-21$_e$.

Nitrogen sorption analysis of the functionalized polymers (Table 3.11) was carried out in order to see whether the polymers became porous after the immobilization of different groups. As it was expected, Table 3.11 shows that no porous materials were obtained after the functionalization reactions and instead, functionalised gel-type polymers were produced.

Polymer ref.	*Specific surface area (m^2/g)*		*Specific pore vol. (cm^3/g)*	*Av. pore diameter (nm)*
	BET	*Langmuir*		
III-19$_e$	7	-	-	-
III-20$_e$	-	5	-	-
III-21$_e$	-	2	-	-

Table 3.11 Nitrogen sorption analysis of polymers III-19$_e$, III-20$_e$ and III-21$_e$.

3.4. CONCLUSIONS

Precipitation copolymerisation reactions of DVB with a divinyl co-monomer produced good quality particles. Different conditions with different solvents were carried out but obtaining porous polymer particles proved to be extremely complicated.

Due to the reactivity of the synthesised allyl maleimide in the synthesis of poly(DVB-*alt*-AMI), it was not possible to remove the chemical aggregation, which were suspected to be poly(AMI). In order to solve this problem, a new strategy was followed beginning with copolymerising DVB with MA. After allylamination of poly(DVB-*alt*-MA), quasi-monodispersed particles were obtained, but their small size made post-functionalisation impossible. This is thought to be due to the steric hindrance of the unreacted vinyl groups of AMI. Poly(DVB-*co*-AMA) was synthesised by conventional precipitation polymerisation with toluene and acetonitrile as co-solvents. The ratio of DVB and AMA was changed in order to increase the functional group loading. However, in order to form porous polymer microspheres, a high proportion of toluene had to be used, which led to aggregation of the particles, and the formation of coagulums.

CM reactions were performed with gel-type poly(DVB-*co*-AMA) polymers and quasi-monodispersed particles were obtained. Furthermore, the insertion of the divinyl co-monomer led to an increase of the loading level of the immobilised functional group, which renders them suitable for different applications like protein immobilisation, solid-phase peptide synthesis or as metal scavenger resins.

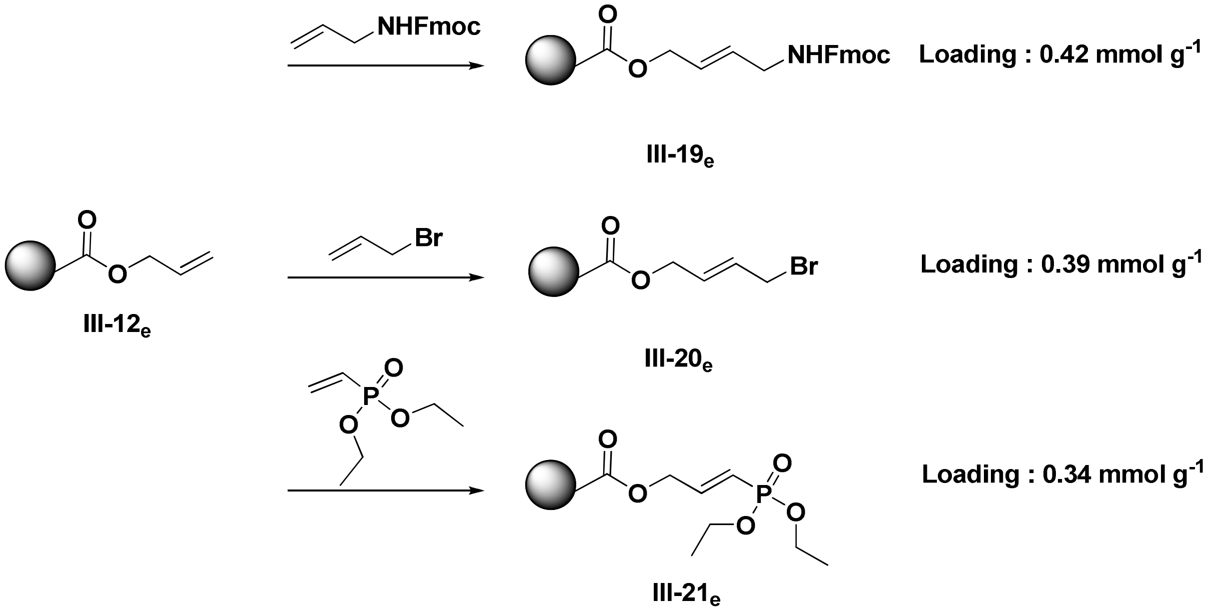

Figure 3.15 Functionalisation reactions of poly(DVB-*co*-AMA).

3.5. FUTURE WORK

Different precipitation copolymerisation conditions were used thorough this work. The insertion of a divinyl co-monomer during precipitation polymerisation was performed in order to increase the amount of unreacted double bonds available for CM reactions. In the future, precipitation copolymerisation reactions to lower the DVB/AMA concentrations in the solvent could be attempted. Lower concentrations of the monomers in the solvent can help to prevent aggregation when large amounts of co-monomer are used.

In order to obtain porous polymer particles, large amounts of the porogenic solvents are needed. However, the increment of the porogenic solvent leads to aggregation of the particles, and therefore coagulums or monoliths are formed. Thus, different solvent systems can be attempted in the future to obtain porous polymer particles.

Finally, to increase the size of the poly(DVB-*alt*-MA) particles, the MEK amount can be increased in order to form larger particle nuclei leading to later precipitation in the media. Stöver and coworkers (18) reported that by increasing the concentration of the monomers in the solvent system, larger particles were obtained. Therefore, monomer concentration can be increased to obtain larger particles.

3.6. EXPERIMENTAL

3.6.1. Materials

For the synthesis of copolymers, divinylbenzene-80 (mixture of isomers, 80.0% grade), divinylbenzene-55 (mixture of isomers, 55.0% grade) and allyl methacrylate were purchased from Sigma Aldrich and purified prior to use through a column of neutral alumina. 2,2'-Azo*bis*(isobutyronitrile), AIBN, (97.0%) was purchased from BDH and Luperox® A75, Benzoyl peroxide (BPO) was purchased from Sigma Aldrich and both were recrystalised from acetone at low temperature. HPLC grade acetonitrile was purchased from Rathburn Chemicals and was used as received. 2nd generation Grubbs catalyst, maleimide and allyl alcohol were purchased from Sigma Aldrich and were used as received. Allylbromide, diisopropyl azodicarboxylate, triphenylphosphine, Fmoc-hydroxysuccinimide and allyl amine were all purchased from Acros Organics and were also used as received. Diethyl vinylphosphonate was purchased from Fisher Scientific and was of high purity, so was used as received.

The solvents employed (toluene, hexane, acetone, methanol, tetrahydrofuran, petroleum ether [b.p. 30-40 ^{o}C], ethyl acetate, diethyl ether, glacial acetic acid, sodium bicarbonate, anhydrous 1,4-dioxane, heptane, methyl ethyl ketone (MEK) and chloroform) were purchased from Sigma Aldrich as standard laboratory reagent grade.

Dry solvents were obtained from an in-house purification system. Column chromatography sorbent EMD Guduran silica gel 60 was used and Merck silica 60 covered with aluminium sheets were used as TLC plates.

3.6.2. Equipment

Precipitation copolymerisation reactions were carried out using a Stuart Scientific S160 incubator (Surrey, UK) and a Stovall low profile roller system (NC, USA). The polymerisations were performed in Nalgene® plastic bottles. When required, samples were dried in Townson & Mercer Limited (England) vacuum ovens set to either 40 °C or 70 °C, at 60 mbar pressure.

Elemental microanalysis was performed by the University of Strathclyde Elemental Microanalysis service. C, H and N elemental microanalyses were carried out simultaneously using a Perkin Elmer 2400 Series II analyser, while halogen and phosphorous contents were determined by standard titration methods.

The optical compound microscope employed was a Olympus Vanox microscope. Scanning electron microscopy (SEM) was carried out using a Cambridge Instruments Stereoscan 90. Samples were coated in gold prior to SEM imaging. SEM statistical data was obtained by Image J.

Fourier-Transform Infrared (FT-IR) spectroscopy analyses were carried out using a Shimadzu IRAffinity-1S spectrometer. Samples were scanned over the range 4000-600 cm^{-1} in transmission mode.

The specific surface area measurements were performed using Micromeritics ASAP 2020 nitrogen sorption instrument. Samples were degassed overnight under high vacuum at 100 ^{o}C prior to analysis. Analysis was carried out *via* nitrogen sorption, carried out at 77 K.

3.6.3. Synthesis of AMI monomer

1-Allyl-1H-pyrrole-2,5-dione (III-3)(16)

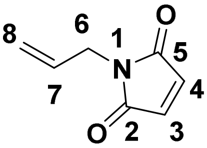

AMI was synthesised by modifying an existing procedure.(15) DIAD (20 mL, 0.10 mol, 1.2 equiv) was added dropwise, in the dark, to a solution of maleimide, **III-2,** (9.0 g, 0.093 mol, 1.1 equiv), allyl alcohol, **III-1,** (5.7 mL, 0.084 mol) and Ph_3P (24 g, 0.093 mmol 1.1 equiv) in anhydrous THF (300 mL) at room temperature. After stirring the mixture for 19 h, the solvent was evaporated in *vacuo*. Ph_3PO was precipitated in a mixture of hexane/Et_2O (1:1) and filtered off. Silica gel column chromatography [EtOAc/PE (3:7)] gave AMI as a light yellow powder (7.0 g, 55%).

R*f* 0.3 (EtOAc/PE 3:7)

AMI was also synthesised by modifying another existing procedure.(16) Glacial acetic acid (10 mL) was added dropwise to allylamine, **III-3**, (1.3 mL, 17 mmol) at 0 °C. A solution of maleic anhydride, MA, (3.0 g, 31 mmol, 1.8 equiv), in glacial acetic acid (20 mL) was then added to the allylamine solution and the mixture was refluxed overnight under an argon atmosphere. The next day the reaction was allowed to cool down to room temperature and acetic acid was removed under reduced pressure. Then, 10 mL of CH_2Cl_2 and 20 mL of water were added to the formed brown oil. The organic layer was separated and the aqueous phase was extracted with CH_2Cl_2 (3 x 10 mL). The combined organic layers were dried with Na_2SO_4, filtered and evaporated in *vacuo*. Silica gel column chromatography [EtOAc/PE (1:9)] gave AMI as a light yellow powder, (1.3 g, 55%).

R_f 0.4 (EtOAc/PE 1:9)

^{1}H NMR (500 MHz, $CDCl_3$) δ = 6.71 (2H, s, H-(3,4)), 5.78 (1H, ddt, *J* = 15.9, 10.6, 7.6, Hz, H-7), 5.12 (1H, dd, *J* = 16.0, 1.3 Hz, H-8a), 5.09 (1H, dd, *J* = 10.4, 1.2 Hz, H-8b), 4.10 (2H, dt, *J* = 5.7, 1.4 Hz, H-(6a,6b)).

^{13}C NMR (100 MHz, $CDCl_3$) δ = 170.0 (C-(2,5)), 134.2 (C-7), 131.6 (C-(3,4)), 117.7 (C-8), 39.9 (C-6).

HRMS (CI) *m/z* $(M+H)^+$ $C_7H_8NO_2$ Calcd.: 138.0550 g/mol. Found: 138.0555 g/mol.

FT-IR: $\bar{\upsilon}$cm^{-1} 3070 (=CH str.), 2980 and 2940 (C-H str.), 1690 (C=O str.) 1640 and 1440 (C=C str.), 1395 (CN str.), 1345 (C-O str.), 1120 (C-O-C str.).

m.p. 42-45 °C (lit, 42-43 °C)

3.6.4. Typical precipitation copolymerisation of DVB with AMI

General procedure of poly(DVB-co-AMI)

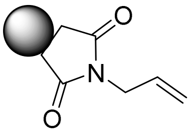

Poly(DVB-*co*-AMI) was synthesised by modifying an existing procedure.(19-21) Divinylbenzene was freed from inhibitor by passage through a short column of alumina (activated aluminium oxide, neutral, Brockmann I) prior to polymerisation. Recently purified DVB, AMI and recrystalised BPO (2 mol% relative to the total number of polymerisable double bonds) were placed into a 1 L Nalgene® bottle with acetonitrile (CH_3CN) and toluene as porogenic solvent. The bottle contents were sonicated for 15 min and the contents were purged with bubbling N_2 for 20 min before being sealed under N_2. The bottle was placed on a low-profile roller, which was housed inside a temperature-controlled incubator, and rolled at 30 rpm along its long axis. The temperature was ramped from room temperature to 60 °C over 1 h and then held at 60 °C for a further 48 h. The mixture was then allowed to cool down to room temperature. The product was filtered off under vacuum on a 0.22 µm nylon filter membrane and then washed in sequence with 100 mL volumes of CH_3CN, toluene, methanol and acetone. The product, in the form of a white fluffy powder, was dried overnight at 70 °C at 1 mbar.

FT-IR: $\bar{\nu}$/cm^{-1} 3050 (=CH str.), 2924 (C-H str.), 1700 (C=O str.) 1602, 1510 and 1485 (C=C str.), 1444 (CH_2 def.), 1390 (CN str.), 1330 (C-O str.), 1150 (C-O-C str.), 827 (CH def.), 800 and 715 (CH def.) and 630 (CN def.).

General procedure of delayed addition of AMI

Poly(DVB-*co*-AMI) was synthesised by modifying an existing procedure.(19-21) Divinylbenzene was freed from inhibitor by passage through a short column of alumina (activated aluminium oxide, neutral, Brockmann I) prior to polymerisation. Recently purified DVB and recrystalised BPO (2 mol% relative to the total number of polymerisable double bonds) were placed into a 1 L Nalgene® bottle with CH_3CN and toluene as porogenic solvents. The bottle contents were sonicated for 15 min and the contents were purged with bubbling N_2 for 20 min before being sealed under N_2. The bottle was placed on a low-profile roller, which was housed inside a temperature-controlled incubator, and rolled at 30 rpm along its long axis. The temperature was ramped from room temperature to 60 °C over 1 h and then held at 60 °C. After the nucleation stage has started (1 h after the incubator reached 60 °C), AMI was added in one portion to the Nalgene bottle, and the reaction was left for 48 h. The mixture was then allowed to cool down to room temperature. The product was filtered off under vacuum on a 0.22 μm nylon filter membrane and then washed in sequence with 100 mL volumes of CH_3CN, toluene, methanol and acetone. The product, in the form of a white fluffy powder, was dried overnight at 70 °C at 1 mbar.

FT-IR: $\bar{\nu}/cm^{-1}$ 3050 (=CH str.), 2924 (C-H str.), 1690 (C=O str.) 1602, 1510 and 1485 (C=C str.), 1444 (CH_2 def.), 1395 (CN str.), 1345 (C-O str.), 1120 (C-O-C str.), 829 (CH def.), 794 and 709 (CH def.) and 620 (CN def.).

3.6.5. Synthesis of poly(DVB-alt-AMI)

Poly(DVB-alt-MA)(22)

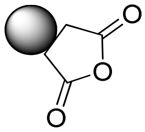

III-9$_a$ and **III-9$_b$** were synthesised by modifying an existing procedure.(13,14,18) DVB was freed from inhibitor by passage through a short column of alumina (activated aluminium oxide, neutral, Brockmann I) prior to polymerisation. Recently purified DVB (0.58 g), MA (0.38 g) and recrystalised BPO (**III-9$_a$**: 0.5 mol% and **III-9$_b$**: 2 mol% relative to the total number of polymerisable double bonds) were placed into a 20 mL Kimax tube with heptane (6.0 mL) and MEK (4.0 mL) as porogenic solvents. The contents were sonicated for 5 min and purged with bubbling N_2 for 15 min before being sealed under N_2. The tube was placed on a low-profile roller, which was housed inside a temperature-controlled incubator, and rolled at 30 rpm along its long axis. The temperature was ramped from room temperature to 60 °C over one hour and then held at 60 °C for a further 24 h. The mixture was then allowed to cool down to room temperature. The product was filtered off under vacuum on a 0.22 μm nylon filter membrane and then washed in sequence with 100 mL volumes of CH_3CN, toluene, methanol and acetone. The product, in the form of a white powder, was dried overnight at 70 °C at 1 mbar (**III-9$_a$** 0.86 g, 88%, **III-9$_b$** 0.88 g, 89%).

Isotherms:

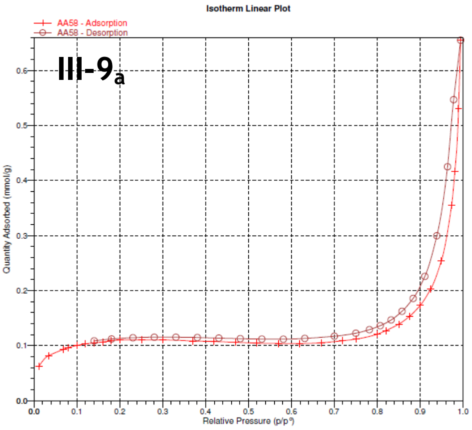

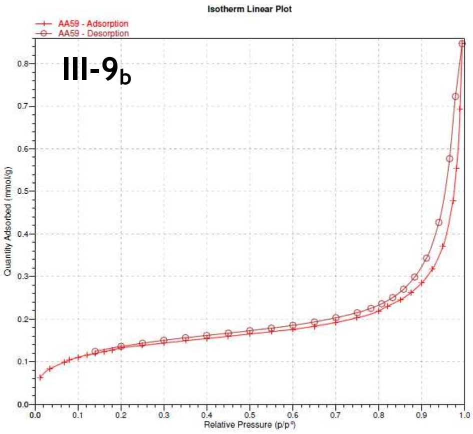

Poly(DVB-alt-AMI)

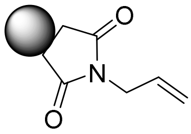

III-8$_e$ was synthesised by modifying an existing procedure.(23) Polymer **III-9$_a$** (0.44 g, 4.8 mmol) was swollen in 15 mL of anhydrous toluene for 1 h under argon. After that time, allylamine (0.36 mL, 4.8 mmol, 1.0 equiv) was added to the suspension and the mixture was refluxed overnight under argon. The next day the reaction was allowed to cool down to room temperature and the product was filtered off under vacuum on a 0.22 μm nylon filter membrane and then washed in sequence with 100 mL volumes of CH_3CN, toluene, methanol and acetone. Compound **III-8$_e$**, in the form of a white powder, was dried overnight at 70 °C at 1 mbar (0.53 g, 78%).

The same procedure was followed with polymer **III-9$_b$** (0.76 g, 8.3 mmol) and allylamine (0.62 mL, 8.3 mmol, 1.0 equiv) to give 0.95 g (80%) of polymer **III-8$_e$.**

FT-IR: $\bar{\nu}$/cm^{-1} 3030 (=CH str.), 2930 (C-H str.), 1690 (C=O str.) 1640 and 1560 1440 (CH$_2$ def.), 1390 (CN str.), 1330 (C-O str.), 1200 (C-O-C str.), 920 (CH def.), 835 (CH def.), 780 and 715 (CH def.) and 630 (CN def.).

Isotherms:

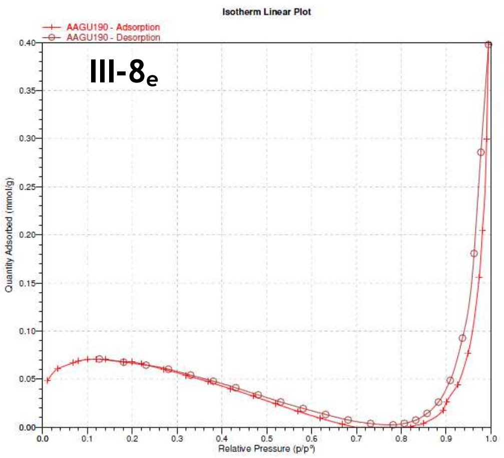

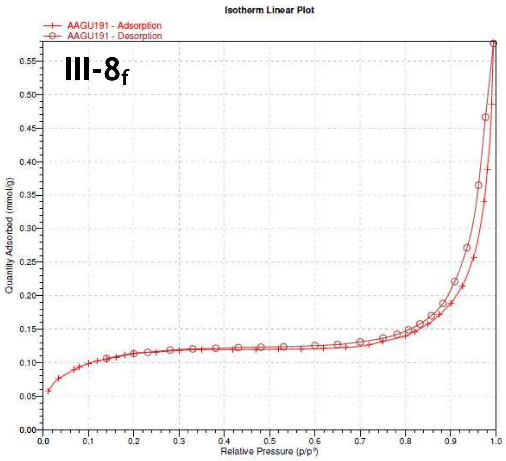

3.6.6. Typical precipitation copolymerisation of DVB with AMA

General procedure of poly(DVB-co-AMA)

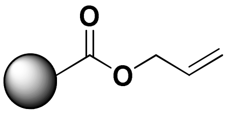

Poly(DVB-*co*-AMA) was synthesised by modifying an existing procedure.$^{(19-21)}$ Divinylbenzene was freed from inhibitor by passage through a short column of alumina (activated aluminium oxide, neutral, Brockmann I) prior to polymerisation. Recently purified DVB, AMA and recrystalised BPO (2 mol% relative to the total number of polymerisable double bonds) were placed into a 1

L Nalgene® bottle with acetonitrile (CH_3CN) and toluene as porogenic solvents. The bottle contents were sonicated for 15 min and purged with bubbling N_2 for 20 min before being sealed under N_2. The bottle was placed on a low-profile roller, which was housed inside a temperature-controlled incubator, and rolled at 30 rpm along its long axis. The temperature was ramped from room temperature to 60 °C over 1 h and then held at 60 °C for a further 48 h. The mixture was then allowed to cool down to room temperature. The product was filtered off under vacuum on a 0.22 µm nylon filter membrane and then washed in sequence with 100 mL volumes of CH_3CN, toluene, methanol and acetone. The product, in the form of a white powder, was dried overnight at 70 °C at 1 mbar.

FT-IR: $\bar{\nu}/cm^{-1}$ 3050 (=CH str.), 2900 (C-H str.), 1725 (C=O str.) 1600, 1510 and 1485 (C=C str.), 1444 (CH_2 def.), 1180 (C-O str), 1115 (C-O-C str.), 830 (CH def.), 795 and 710 (CH def.).

Isotherms:

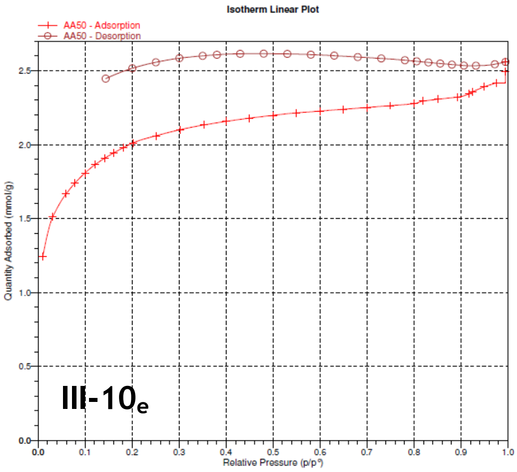

III-10$_e$

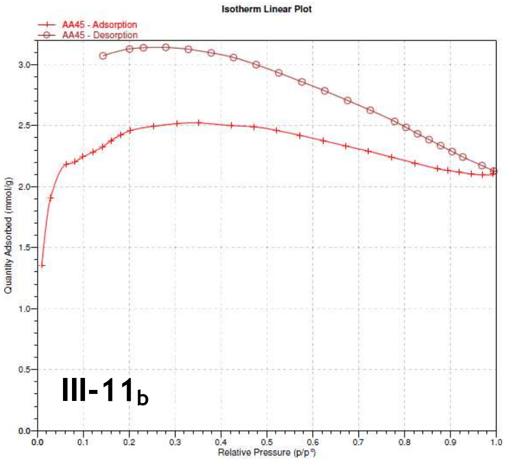

III-11$_b$

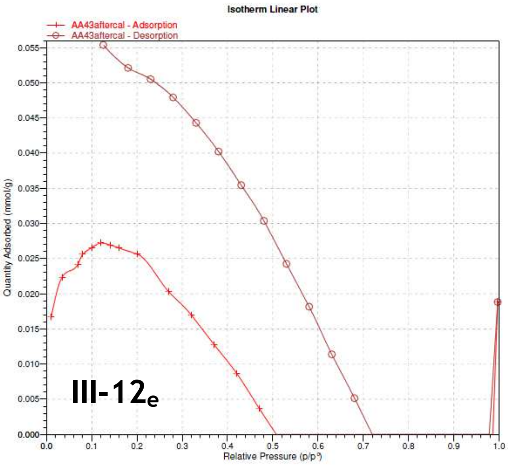

III-12$_e$

3.6.7 General procedure for the functionalisation of poly(DVB-co-AMA)

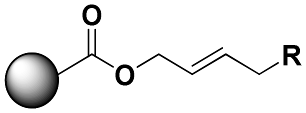

The functionalisation reactions$^{(24)}$ were carried out in a 50 mL round-bottomed flask equipped with a condenser. Polymer **III-12$_e$** was suspended in 10 mL of CH_2Cl_2 under an argon atmosphere. Second-generation Grubbs catalyst (5.0 mol%) and coupling partner (4.0 equiv) were then added to the suspension and the resulting mixture was heated under reflux overnight. The next day the reaction was allowed to cool down to room temperature and the product was filtered off under vacuum on a 0.22 µm nylon filter membrane and then washed in sequence with 15 mL volumes of dichloromethane, ethanol, ethyl acetate, petroleum ether and diethyl ether. The product, in the form of an off-white powder, was dried overnight at 70 °C at 1 mbar.

Polymer with Fmoc-protected allylamine

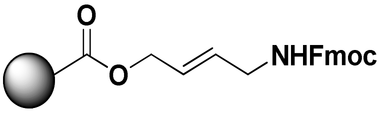

The general procedure was used starting with polymer **III-12$_e$** (0.20 g, 1.5 mmol) and 1.7 g (6.2 mmol, 4 equiv) of Fmoc-protected allylamine (**III-16**) to give 0.21 g of polymer **III-19$_e$.**

FT-IR: $\bar{\nu}$/cm^{-1}, 3020 (=CH str.), 2900 (C-H str.), 1730 and 1690 (C=O str.) 1600, 1580, and 1477 (C=C str.), 1530 (NH def.), 1440 (CH_2 def.), 1350 and 1260 (C-O str.), 1120 (C-O-C str.), 830 (CH def.), 800 and 700 (CH def.).

Polymer with allyl bromide

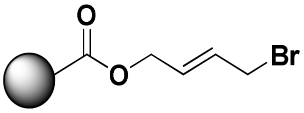

The general procedure was used starting with polymer **III-12$_e$** (0.30 g, 2.3 mmol) and 9.8 mL (9.3 mmol, 4 equiv) of allyl bromide (**II-27**) to give 0.28 g of polymer **III-20$_e$.**

Polymer with diethyl vinylphosphonate

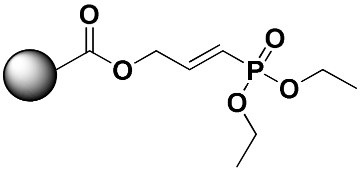

The general procedure was used starting with polymer **III-12$_e$** (0.30 g, 2.3 mmol) and 1.4 mL (9.3 mmol, 4 equiv) of diethyl vinylphosphonate (**II-29**) to give 0.29 g of polymer **III-21$_e$.**

FT-IR: $\bar{\nu}$/cm^{-1}, 3020 (=CH str.), 2980 and 2920 (C-H str.), 1725 (C=O str.) 1610, and 1477 (C=C str.), 1440 (CH_2 def.), 1350 and 1260 (C-O str.), 1390 (O-P-O str.), 1275 (P=O str.), 1150 (C-O-P str.), 1080 (C-O-C str.), 820 (CH def.), 780 and 690 (CH def.).

Isotherms of polymer III-12$_e$ after functionalisation reactions by CM:

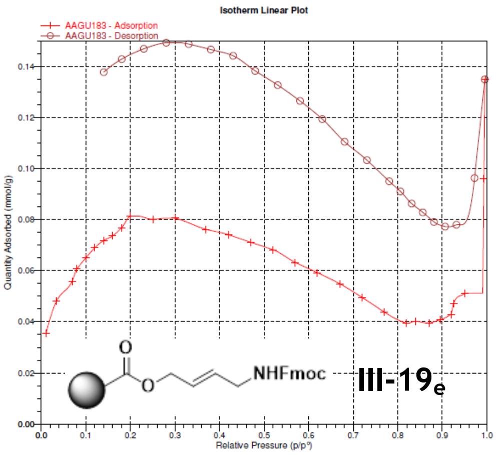

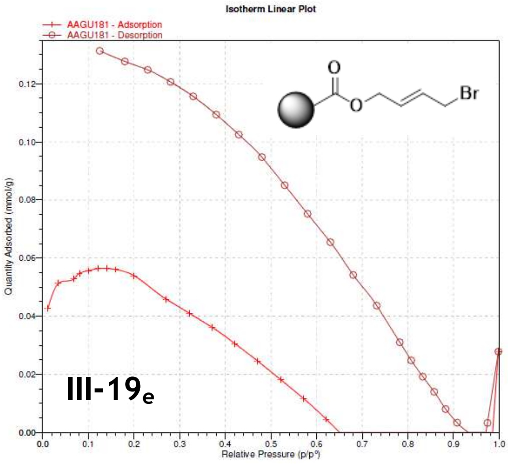

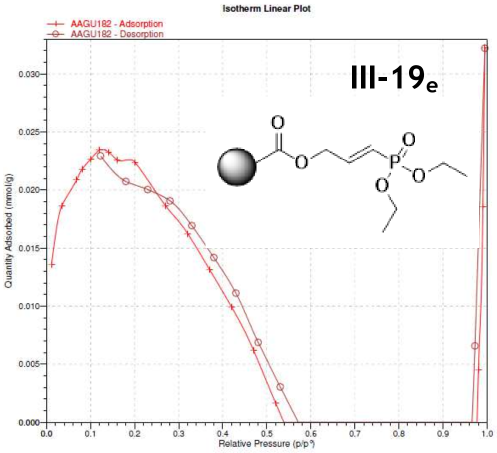

3.6.8 Synthesis of Fmoc allylamine

*(9H-fluoren-9-yl)methyl allylcarbamate (**III-20**)*(25)

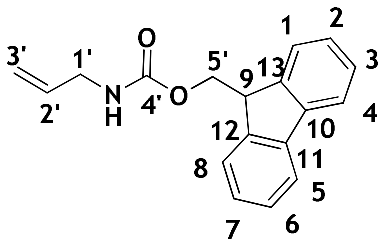

Compound **III-16** was synthesised by modifying an existing procedure.(25) Allylamine, **III-3**, (0.85 mL, 11 mmol, 1.5 equiv) was dissolved in dioxane (70 mL) at 0 °C. Then, $NaHCO_3$ (1.9 g, 23 mmol, 3 equiv) and Fmoc hydroxysuccinimide (2.6 g, 7.6 mmol) were added to the solution and the mixture was stirred for 30 min at 0 °C and then at r.t. overnight. The next morning, 50 mL of saturated aqueous $NaHCO_3$ was added to quench the reaction and the mixture was extracted with EtOAc (3 x 50 mL). The combined organic layers were then washed with saturated aqueous $NaHCO_3$ (50 mL), brine (3 x 50 mL) and water (3 x 50 mL), dried over $MgSO_4$, filtered and concentrated *in vacuo*. The crude product was purified by recrystalisation from hot ethanol giving compound **III-16** as a white powder (2.0 g, 93%).

^{1}H NMR (400 MHz, $CDCl_3$) δ = 7.60 (2H, dt, *J* = 7.5, 1.0 Hz, H-(4,5)), 7.45 (2H, d, *J* = 7.5 Hz, H-(1,8)), 7.24 (2H, t, *J* = 7.5, H-(3,6)), 7.15 (2H, td, *J* = 7.5, 1.0 Hz, H-(2,7)), 5.65 (1H, ddt, *J* = 15.7, 10.6, 5.4 Hz, H-2'), 5.00 (1H, d, *J* = 15.8 Hz, H-3'a), 4.96 (1H, d, *J* = 10.5 Hz, H-3'b), 4.83 (1H, t, *J* = 6.9 Hz, NH), 4.26 (2H, d, *J* = 6.8 Hz, H-5'), 4.06 (1H, t, *J* = 6.8 Hz, H-9), 3.65 (2H, t, *J* = 5.6 Hz, H-1').

^{13}C NMR (100 MHz, $CDCl_3$) δ = 156.5 (C-4'), 144.0(C-(12,13)), 141.5 (C-(10,11)), 134.6 (C-2'), 127.8 (C-(3,6)), 127.0 (C-(4,5)), 125.8 (C-(2,7)), (120.0 (C-(1,8)), 116.1 (C-3'), 66.7 (C-5'), 47.2 (C-9), 43.5 (C-1').

FT-IR: $\bar{\upsilon}$cm^{-1} 3310 (NH str.), 3060 (=CH str.), 2940 and 2890 (C-H str.), 1695 (C=O str.) 1640 and 1445 (C=C str.), 1545 (NH def.), 1245 (C-O str.), 1133 (CN str.).

3.7. REFERENCES

(1) Jenkins, A. D.; Kratochvíl, P.; Stepto, R. F. T.; Suter, U. W. *Pure Appl. Chem.* **1996**, *68*, 2287–2311.

(2) Katime, I.; Katime, O.; Katime, D. *Introduction to polymer science: synthesis and characterisation*; UPV/EHU, Ed.; UPV/EHU: Zarautz, Gipuzkoa, Basque Country, 2010.

(3) Viklund, C.; Nordstrom, A.; Irgum, K. *Macromol.* **2001**, *34*, 4361–4369.

(4) Wilks, E. S. *J. Chem. Inf. Comput. Sci.* **1997**, *2338*, 193–208.

(5) He, J.; Chen, D.; Fan, X.; Wang, L.; Deng, J.; Yang, W. *Chinese Chem. Lett.* **2013**, *24*, 970–974.

(6) Meena, J. S.; Chu, M.; Singh, R.; Wu, C.; Chand, U.; You, H.-C.; Liu, P.-T.; Shieh, H.-P. D.; Ko, F.-H. *RSC Adv.* **2014**, *4*, 18493.

(7) Grabowski, T. S.; Va, V. W. Blends of polycarbonates with polybutadiene, styrene, acrylonitrile graft copolymers, 1964.

(8) Bratkowska, D.; Fontanals, N.; Borrull, F.; Cormack, P. A. G.; Sherrington, D. C.; Marcé, R. M. *J. Chromatogr. A* **2010**, *1217*, 3238–3243.

(9) Waters Oasis Catalogue http://www.waters.com/webassets/cms/library/docs/lcSP.pdf (accessed Apr 14, 2016).

(10) Phenomenex Strata Catalogue http://phenomenex.blob.core.windows.net/documents/97f08011-7ff9-4343-8310-ee5f27ae707a.pdf (accessed Apr 14, 2016).

(11) Furukawa, J.; Iseda, Y.; Haga, K.; Kataoka, N. *J. Polym. Sci. Part A Polym. Chem.* **1970**, *8*, 1147–1163.

(12) Furukawa, J.; Kobayashi, E.; Iseda, Y.; Arai, Y. *Poly. J.* **1970**, *1*, 442–449.

(13) Furukawa, J. *J. Polym. Sci. Part A Polym. Chem.* **1975**, *51*, 105–118.

(14) Sen, S. E.; Roach, S. L. *Synthesis* **1994**, 756–758.

(15) Walker, M. A. *Tetrahedron Lett.* **1994**, *35*, 665–668.

(16) Gómez-SanJuan, A.; Sotomayor, N.; Lete, E. *Eur. J. Org. Chem.* **2013**, 6722–6732.

(17) Yan, Q.; Zhao, T.; Bai, Y.; Zhang, F.; Yang, W. *Phys. Chem.* **2009**, *113*, 3008–3014.

(18) Frank, R. S.; Downey, J. S.; Yu, K.; Stöver, H. D. H. *Macromolecules* **2002**, *35*, 2728–2735.

(19) Downey, J. S.; Frank, R. S.; Li, W.; Stöver, H. D. H. *Macromolecules* **1999**, *32*, 2838–2844.

(20) Li, W.; Stöver, H. D. H. *J. Polym. Sci. Part A Polym. Chem.* **1997**, *36*, 1543–1551.

(21) Baines, F. C.; Bevington, J. C. *J. Polym. Chem. Part A Polym. Chem.* **1968**, *6*, 2433–2440.

(22) Goh, E. C. C.; Stöver, H. D. H. *Macromolecules* **2002**, *35*, 9983–9989.

(23) Cava, M. P.; Deana, A. A.; Muth, K.; Mitchell, M. J. *Org. Synth.* **1961**, *41*, 93.

(24) Chatterjee, A. K.; Choi, T. L.; Sanders, D. P.; Grubbs, R. H. *J. Am. Chem. Soc.* **2003**, *125*, 11360–11370.

(25) Eto, K.; Yoshino, M.; Takahashi, K.; Ishihara, J.; Hatakeyama, S. *Org. Lett.* **2011**, *13*, 5398–5401.

CHAPTER 4

HYPERCROSSLINKING OF GEL-TYPE POLYDIVINYLBENZENE-BASED POLYMERS BY RING-CLOSING METATHESIS

4.1. INTRODUCTION

4.1.1 Hypercrosslinked polymers

Hypercrosslinked (HXL) polymers are a new generation of permanently porous polymeric resins. Their ultra-high specific surface areas (> 1000 m^2g^{-1}) and their high micropore content (~0.6 mLg^{-1}) makes them particularly suitable for separation processes.(1) HXL polymeric materials were first developed by Davankov *et al.* in 1974 and are sometimes referred to as Davankov resins.(2,3)

Hypercrosslinking process

Hypercrosslinking is a process in which microporosity can be introduced into polymers increasing their specific surface area. The increase in the surface area is accompanied by enhanced solvent sorption characteristics. The methodology developed by Davankov *et al.*(2,3) started from the post-polymerisation crosslinking reaction of linear polystyrene or poly(styrene-*co*-DVB) chains in its highly swollen gel state. This crosslinking reaction required a thermodynamically good solvent such as anhydrous 1,2-dichloroethane, a Lewis acid, and a crosslinking agent to produce hypercrosslinked styrenic materials. The role of the crosslinking agent, which can take the form of either an 'internal' or 'external' electrophile, is the formation of rigid bridges joining adjacent aromatic rings in the swollen gel. One of the most common 'internal' electrophile methods uses vinylbenzylchloride (VBC), which can be introduced into the polymer as co-monomer during polymerisation reaction. The presence of the chloromethyl groups in VBC can readily react with the Lewis acid by Friedel-Crafts type reaction. 'External' crosslinking agents, on the other hand, are introduced during the crosslinking reaction and contain at least two separate reactive groups reacting and forming a bridge with two aromatic rings present in the polymer (Figure 4.1).(4)

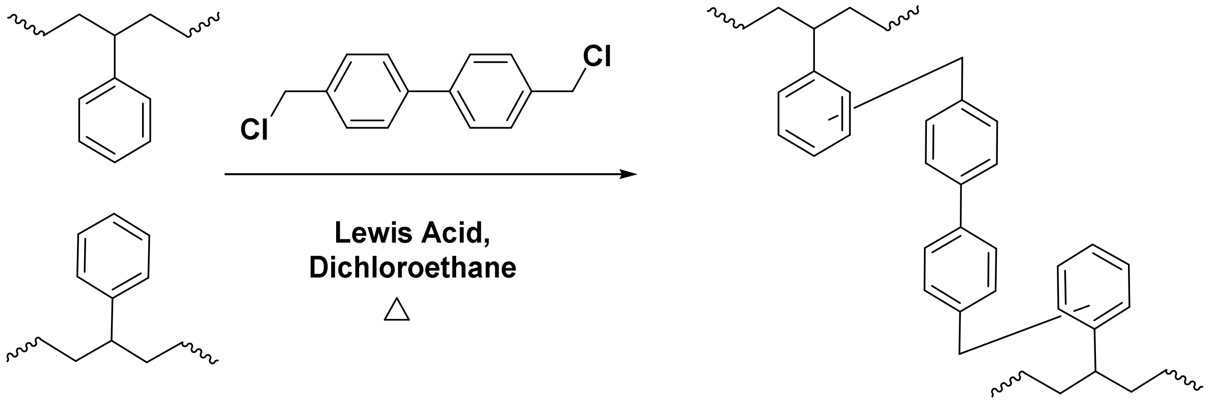

Figure 4.1Hypercrosslinking reaction by using 4,4′-*Bis*(chloromethyl)-1,1′-biphenyl (BCMBP) as external crosslinker.

Lewis acids or a protonic acid such as HF can be used in the hypercrosslinking reaction. Theoretically, all Lewis acids can potentially promote the reaction, *i.e.*, $AlCl_3$, $FeCl_3$, $SnCl_4$, etc. However, in practice, Sherrington and coworkers(5) found that $FeCl_3$ is more active than other Lewis acids as higher specific surface areas were obtained. They hypothesised that the poor solubility of $AlCl_3$ and steric bulk of $SnCl_4$ may limit the hypercrosslinking reaction; therefore $FeCl_3$ offers the best compromise in terms of solubility and size. Figure 4.2 shows how steric bulk may affect the second crosslink. After the first crosslink formed, the access to the second chloromethyl moiety is reduced and thus, larger Lewis acids cannot complete the second crosslink. Formation of the second crosslink is thought to be extremely favourable as the aromatic ring, due to the double alkylation, is electron rich. Additionally, the first crosslink brings the chloromethyl group closer to the aromatic ring and the resultant cyclisation results in a highly stable six-membered ring.(6)

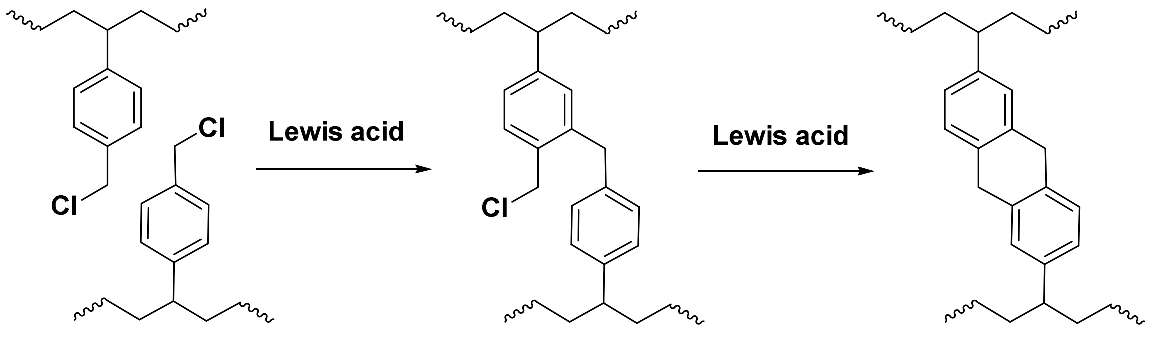

Figure 4.2 Hypercrosslinking reaction of Poly(DVB-*co*-VBC) *via* an internal electrophile.(5)

Although Davankov developed the hypercrosslinking methodology(2,3) in linear polystyrene, his methodology has been applied to hypercrosslink different styrenic precursors synthesised by suspension,(7) emulsion,(8) non-aqueous dispersion,(9) and precipitation polymerisation.(10) Thus, Davankov-type methodology can be applied to produce particles with ultra-high surface area with different particle sizes.

Use of HXL polymers

The insertion of micropores into polymer structures by Davankov methodology leads to different uses.(11) The most common use of HXL polymers is for the extraction of compounds from aqueous solution. The high specific surface areas have improved retention capabilities and chemical functionalisation enhanced the selectivity of the sorbents.

HXL polymer microspheres are commercially available but the diameters of the particles have several hundred microns. One example of commercially available resins are Hypersol-Macronet resins.(12) These resins are HXL polystyrene microspheres with diameters between 0.3-1.2 mm and specific surface areas of 800-1000 m^2g^{-1}. They can exist unmodified or modified with weak base anion-exchangers for the removal of phenolic compounds, aniline(13) etc. Another commercially available resin, Lewatit VP OC 1163 HXL, was first modified by Zhan and coworkers(14) with dimethylamine (WAX) and trimethylamine (SAX). The modified resins had a surface area of 700 m^2g^{-1} and were also used for the removal of phenolic compounds from aqueous solutions. Additionally, Barlas and coworkers(15) showed that the resins could also be used in the removal of pesticides and herbicides from aqueous solutions. Although HXL resins can be accessed commercially, many groups choose to prepare HXL resins within their own laboratories.

Within our group, HXL polymer microspheres prepared by precipitation polymerisation of DVB and VBC monomers, followed by a Friedel-Crafts catalysed crosslinking reaction, have been functionalised and used as selective SPE sorbents for pharmaceutical analysis from water samples. Bratkowska *et al.*(16)

synthesised more hydrophilic microspheres for the extraction of polar contaminants from water by introducing hydroxyethyl methacrylate (HEMA) as third monomer during the initial polymerisation. Introduction of WAX(17,18) and SAX(10,19,20) functionality also allowed for the selective extraction of acidic and basic pharmaceutical compounds from complex environmental water samples.

Li *et al.*(21) showed that microporous materials could be better adsorbents for metal ions than mesoporous and macroporous materials, due to comparable size of pores and metal ions. They modified the HXL polymers with a sulfonation reaction in order to improve the hydrophilicity and to improve the interaction with toxic metals (Pb^{2+}, Cu^{2+}, Cr^{3+} and Ni^{2+}) for the removal from aqueous solutions.

HXL polymers can also be used as gas storage and capture sorbents. In 2006 Svec *et al.*(22) investigated HXL poly(DVB-*co*-VBC), prepared *via* suspension polymerisation, as hydrogen storage materials. HXL polymers with surface areas of up to 1900m^2g^{-1} stored 1.5 wt.% hydrogen at 0.15 MPa and 77.3 K. The results obtained were comparable to the commercially available HXL polymer Hypersol-Macronet MN200 (1.3 wt.% hydrogen at 0.12 MPa). Unfortunately the materials failed when the level of hydrogen storage was raised to 6 wt.% established by the U.S. Departments of Energy for hydrogen storage materials. More recently in 2016, Chang *et al.*(23) synthesised HXL indolo[3,2-b]carbazole-based microporous polymers by Friedel-Crafts alkylation of indolo[3,2-b]carbazole-based monomers. HXL polymers with surface areas up to 1400 m^2g^{-1} were able to storage 1.7 wt.% hydrogen at 1.13 bar and 77.3 K. The CO_2 capture capacity of these HXL polymers can reach up to 3.58 $mmolg^{-1}$ at 1.13 bar and 273 K, which is comparable with other organic porous adsorbents. Furthermore the high selectivity of HXL indolo[3,2-b]carbazole towards CO_2 over N_2 (29:1) makes it a promising material for CO_2 separation.

4.2. AIM OF THE RESEARCH

HXL polymers are a new generation of permanently porous, polymeric resins. Due to their high micropore contents and ultra-high surface areas (~2000 m^2g^{-1}) the analyte retention has been enhanced.(18) However, the selectivity of these polymers is limited, $FeCl_3$ removal sometimes requires large amounts of solvents and they present a brown/red colour, making unlikely their use for separation chemistry.

To tackle all the drawbacks mentioned before, we focused upon the development of olefin metathesis-based methods for the hypercrosslinking of gel-type materials. Herein we report a hypercrosslinking method of gel-type poly(DVB-*co*-AMA) polymers under very mild conditions and employing low amounts of solvents where poly(DVB-*co*-AMA) was prepared by precipitation polymerisation (PP).(24,25) One of the goals was to introduce porosity in the crosslinked polymers by using ring-closing metathesis (RCM) reaction as a new hypercrosslinking method.

4.3. RESULTS AND DISCUSSION

In chapter 3, different ratios of acetonitrile and toluene were used in order to obtain porous poly(DVB-*co*-AMA) microspheres to further functionalise by cross metathesis (CM) reaction. However, CM reaction was only successful with a solvent ratio in which gel-type polymers were obtained. With the obtainment of gel-type poly(DVB-*co*-AMA) the attractive idea of increasing the surface area by performing a RCM reaction was explored. This hypercrosslinking offers the advantages of mild conditions and low amount of solvents. In addition to this it should increase the selectivity of the polymers as the olefin would remain in the polymer for further functionalisation and colourless product would be obtained.

4.3.1. Synthesis of gel-type polymer microspheres by precipitation copolymerisation

Precipitation copolymerisation reactions of DVB-55 or DVB-80 with AMA were carried out in neat acetonitrile, using benzoyl peroxide (BPO) as thermal initiator (Figure 4.3). Toluene was removed from the reaction media in order to obtain gel-type materials. Furthermore, precipitation polymerisation in neat acetonitrile leads to a greater control over the dispersity of the particles, as phase separation occurs earlier and no particle aggregations are formed.

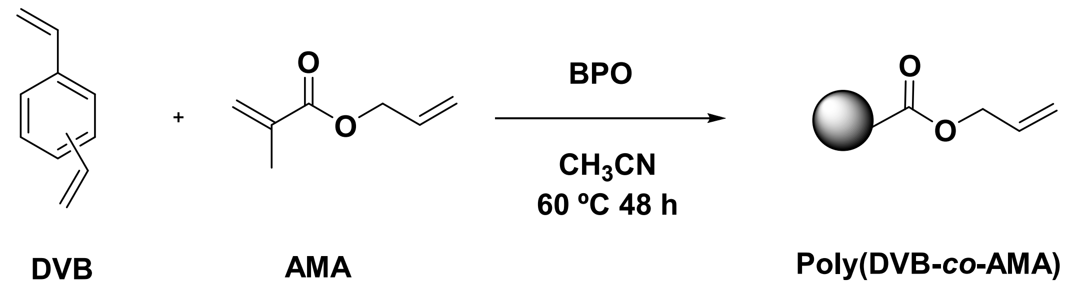

Figure 4.3 Precipitation copolymerisation of DVB and AMA.

Precipitation copolymerisation reactions using different ratios of DVB-80 or DVB-55 with AMA were attempted. Table 4.1 shows that reactions involving DVB-80 gave larger yields than reactions carried out with DVB-55. The yield difference is due to the amount of vinyl groups present in the monomers. DVB-80 has a greater amount of vinyl groups than DVB-55 and thus, the yields are higher. Besides the difference in the yields due to the different types of DVB used, Table 4.1 also shows that by increasing the amount of AMA, lower yields were obtained since the amount of reactive double bonds of the DVB were reduced.

Polym. ref.	*DVB*	*DVB/MA wt.%*	*Scale (g)*	*Mon./solv. (%wt./v)*	*BPO (mg)*	*Time (h)*	*Yield (g)*	*Yield (%)*
IV-1	80	9/1	4.5	2	0.29	48	2.3	49
IV-2	55	9/1	4.5	2	0.25	48	2.2	47
IV-3	80	7.5/2.5	4.5	2	0.27	48	2.6	56
IV-4	55	7.5/2.5	4.5	2	0.24	48	1.9	40
IV-5	80	5/5	4.5	2	0.24	48	2.1	45
IV-6	55	5/5	4.5	2	0.22	48	1.8	40
IV-7	80	2.5/7.5	10	2	0.46	48	5.0	48
IV-8	55	2.5/7.5	10	2	0.41	48	4.7	45
IV-9	80	1/9	10	2	0.41	48	4.4	43
IV-10	55	1/9	4.5	2	0.18	48	1.8	38

Table 4.1 Precipitation copolymerisation conditions used in the synthesis of poly(DVB-*co*-AMA).

Elemental microanalysis of the polymers (Table 4.2) was carried out in order to confirm that the polymers obtained were poly(DVB-co-AMA). Table 4.2 also shows that the amount of the monomers added did not match with the final composition of the polymers obtained. The small differences between the monomer feed and the experimental ratios could be due to a partial evaporation of the monomers during the degassing step or during the transfer of the monomers to the Nalgene® bottles.

Polymer ref.	*Expected elemental microanalysis (wt.%)*		*Found elemental microanalysis (wt.%)*		*Real monomer ratios (wt.%)*	
	C	**H**	**C**	**H**	**DVB**	**AMA**
IV-1	89.4	8.0	87.9	7.8	8.4	1.6
IV-2	89.1	8.3	88.2	8.1	8.7	1.3
IV-3	85.6	8.0	85.5	7.9	7.5	2.5
IV-4	85.3	8.3	85.0	8.1	7.4	2.6
IV-5	79.3	8.0	81.2	7.8	5.8	4.2
IV-6	79.1	8.2	80.2	8.1	5.4	4.6
IV-7	73.0	8.0	75.4	8.0	3.5	6.6
IV-8	72.9	8.1	74.8	7.8	3.3	6.8
IV-9	69.2	8.0	70.0	7.7	1.3	8.7
IV-10	69.1	8.0	70.2	8.2	1.4	8.6

Table 4.2 Elemental microanalysis of different Poly(DVB-*co*-AMA).

Statistical analysis of the particles was carried out using image J program (Table 4.3). Small particles (< 5 μm) were obtained after precipitation copolymerisation in absence of toluene as particle desolvation was not delayed by the porogenic solvent and they precipitate earlier. DVB composition also affected the size of the particles since DVB-55 presents a greater amount of ethyl styrene and therefore the particles were more swollen. Polymers **IV-1**, **IV-2**, **IV-3** and **IV-4** (Table 4.3) have more crosslinked particles than the rest of the polymers, as higher amounts of DVB were used. Polymers **IV-1** and **IV-3**, made from DVB-80, reacted more with AMA and the particles obtained were more mechanically robust than DVB-55 based particles, due to the degree of polymerisation and the amount of available double bonds. However, when the amount of AMA was increased, less crosslinked polymers were obtained and thus polymers made of DVB-55 have in general greater diameters. Table 4.3 also shows that by keeping the amount of DVB high or very low, quasi-monodispersed particles were obtained. On the other hand, polydispersed particles were obtained when similar ratios of DVB and AMA were used due to the random co-polymerisation of DVB and AMA.

Polym. ref.	*Mean diameter (μm)*	*SD (μm)*	*Min (μm)*	*Max (μm)*	*CV (%)*
IV-1	1.2	0.19	0.77	1.6	17
IV-2	1.1	0.19	0.80	1.6	17
IV-3	2.5	0.32	1.6	3.2	13
IV-4	2.1	0.25	1.5	2.9	12
IV-5	2.5	0.39	1.7	3.7	16
IV-6	3.5	1.0	1.9	7.1	29
IV-7	1.7	0.63	0.67	3.2	38
IV-8	2.2	0.89	0.75	6.5	40
IV-9	2.5	1.0	0.66	3.7	41
IV-10	3.5	0.44	2.3	4.3	12

Table 4.3 Image J analysis of synthesised poly(DVB-*co*-AMA).

SEM micrographs (Figure 4.4) of the polymers show that spherical microspheres were obtained. Figure 4.4 also shows that by decreasing the amount of DVB, the colloidal stability of the particles started to fail and particles started to aggregate. Hardness of the particles was also affected by decreasing the amount of DVB and rough surfaces of the particles were observed (Figure 4.4).

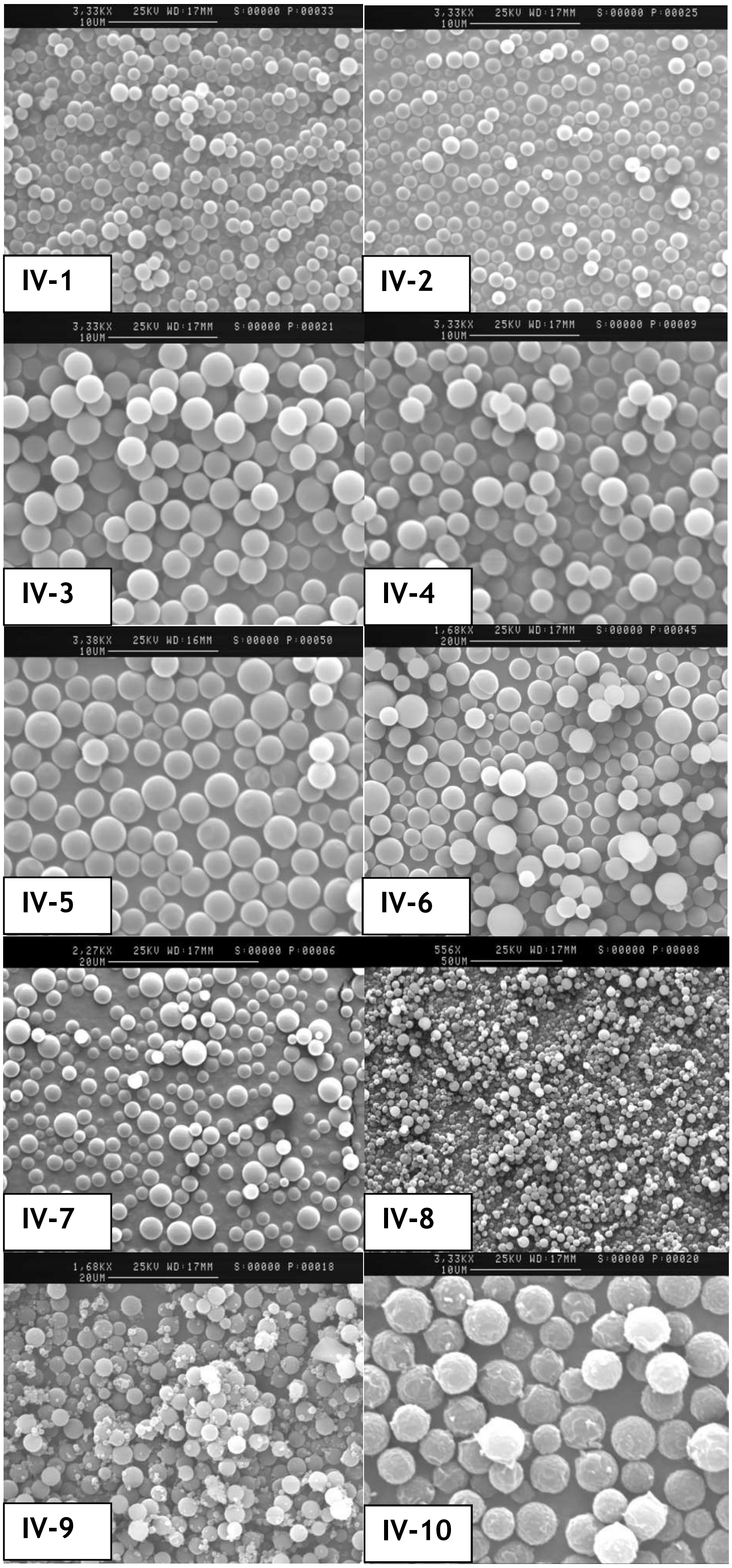

Figure 4.4 SEM micrographs of synthesised poly(DVB-*co*-AMA).

In order to confirm that gel-type polymers were formed, nitrogen sorption porosimety analysis was carried out. Table 4.4 shows that only polymers **IV-6**, **IV-**

8 and **IV-10** follow the BET method and adsorbed the nitrogen in several distinct layers. The change in sorption mode could be due to the high crosslinking level of DVB-80 or by the large amounts of DVB used in addition to the lack of the porogenic solvent. As a consequence, the amount of nitrogen that can access each pore has been reduced and therefore it can form a single layer in the space provided. Table 4.4 also suggests that due to the low surface areas, the synthesis of gel-type polymers was successful.

Polymer ref.	*Specific surface area (m^2/g)*		*Specific pore vol. (cm^3/g)*	*Av. pore diameter (nm)*
	BET	*Langmuir*		
IV-1	-	90	-	-
IV-2	-	20	-	-
IV-3	-	70	-	-
IV-4	-	3	-	-
IV-5	-	20	-	-
IV-6	2	-	-	-
IV-7	4	-	-	-
IV-8	2	-	-	-
IV-9	-	1	-	-
IV-10	3	-	-	-

Table 4.4 Nitrogen sorption porosimetry analysis of poly(DVB-AMA) polymers.

Solvent uptake test was carried out in all the polymers to identify the more suitable solvent to perform the RCM reaction (Graph 4.1). The test was carried out in dichloromethane since it is the solvent in which olefin metathesis in general gives the best efficiency, and in toluene where previous polymers swell the most (chapter 3 polymers). Graph 4.1 shows that polymers can uptake more toluene than dichloromethane, therefore toluene was chosen to perform the RCM reactions.

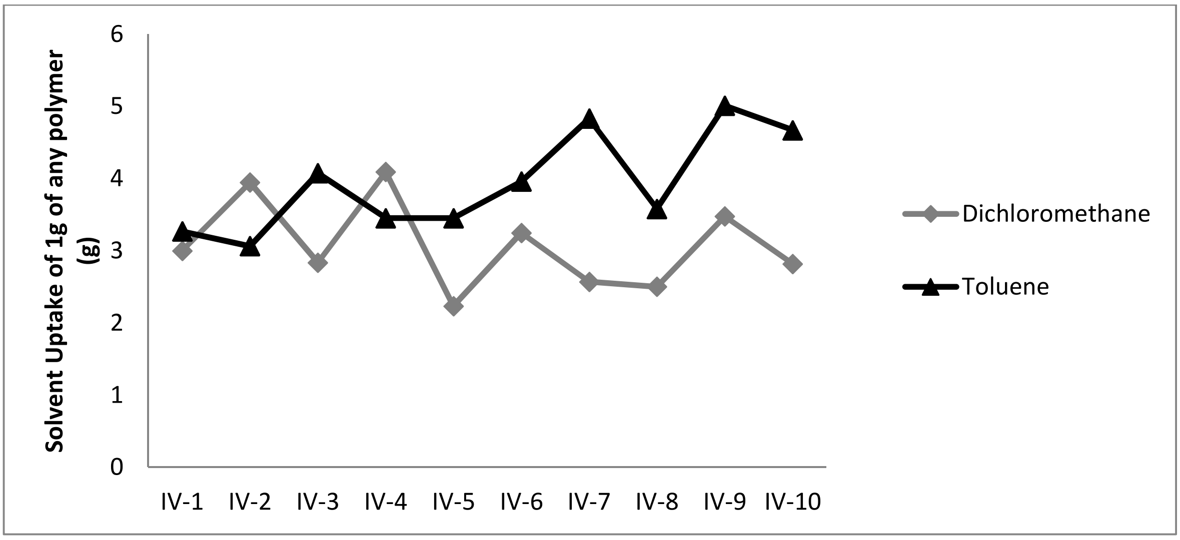

Graph 4.1 Solvent uptake test of polymers in dichloromethane and in toluene.

A swelling test was also carried out in order to see the swelling behaviour of the polymers for RCM reaction. Polymer **IV-7** and **IV-10** were selected and 1.2 mL were packed into a measuring cylinder. When 5 mL of toluene were added, polymer **IV-7** swelled from 1.2 mL to 1.7 mL and polymer **IV-10** from 1.2 mL to 1.9 mL. Volumes were checked after 1 h and 24 h but no changes were observed, indicating that swelling of the polymers occurred immediately.

4.3.2. Hypercrosslinking reaction of gel-type poly(DVB-co-AMA) polymers by RCM

After the selection of the appropriate solvent, RCM was carried out with all the synthesised polymers (Figure 4.5). It is believed that two different allyl groups can undergo the RCM easier than a vinyl group (from DVB) with an allyl group since vinyl groups could be more hindered. However, both metathesis can occur and the cyclisation will insert porosity into the polymers and therefore the surface area will be larger.

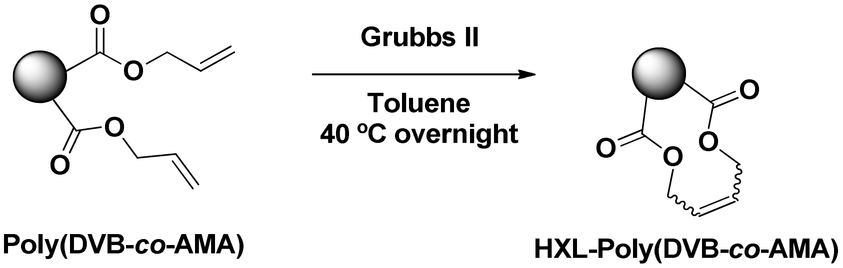

Figure 4.5 RCM of poly(DVB-*co*-AMA) to form HXL-poly(DVB-*co*-AMA).

Nitrogen sorption porosimetry analysis was carried out as confirmation of the success of the RCM reaction. Table 4.5 shows that RCM only occurred in polymers **IV-7** and **IV-10.** Taking into account the solvent uptake test (Graph 4.1), it was not surprising that only polymers **IV-7** and **IV-10** could undergo the RCM reaction as both polymers (as well as polymer **IV-9)** could uptake more solvent and therefore swell the most. On the other hand, coagulums were formed in polymer **IV-9** after RCM reaction, although its solvent uptake capacity was greater than in polymer **IV-7** and **IV-10** (Figure 4.6). Nitrogen sorption porosimetry data of Polymer **HXL-IV-7** shows that nitrogen adsorption happened in a single layer fitting the Langmuir isotherm. However, polymer **HXL-IV-10** followed the BET method and adsorbed the nitrogen in several distinct layers. The change in the sorption mode it is strongly related with the type of DVB used as well as with the ratios of DVB used. Since DVB-80 has less amount of ethyl styrene and therefore, more binding sites than DVB-55, polymers made with DVB-80 are more crosslinked, pores are smaller and thus, nitrogen cannot be adsorbed trough the pores. A larger surface area was obtained with polymer **HXL-IV-7** due to the higher amount of double bonds that reacted during the RCM reaction. However, the pore volume and the average pore diameter of polymer **HXL-IV-10** are larger as DVB-55 was used as monomer and therefore, a less crosslinked polymer with greater pore sizes was obtained.

Polymer ref.	*Specific surface area (m^2/g)*		*Specific pore vol. (cm^3/g)*	*Av. pore diameter (nm)*
	BET	*Langmuir*		
HXL-IV-1	11	-	-	-
HXL-IV-2	9	-	-	-
HXL-IV-3	-	29	-	-
HXL-IV-4	5	-	-	-
HXL-IV-5	-	12	-	-
HXL-IV-6	-	4	-	-
HXL-IV-7	-	479	0.22	2.5
HXL-IV-8	-	5	-	-
HXL-IV-9	5	-	-	-
HXL-IV-10	356	-	0.23	3.5

Table 4.5 Nitrogen sorption porosimetry after RCM reaction.

Elemental microanalysis of polymers **HXL-IV-7** (*74.7% C, 7.7% H)* and **HXL-IV-10** (*68.8% C, 7.7% H*) indicated the success of the hypercrosslinking reaction. The amounts of hydrogen and carbon have been significantly reduced due to the loss of ethylene in the RCM reaction. SEM micrographs (Figure 4.6) show that particles were not destroyed by the hypercrosslinking reaction. Statistical analysis of the particles of polymers **HXL-IV-7** (mean diameter: 2.2 *μm*, SD: 0.72 *μm*, CV: 32%)) and **HXL-IV-10** (mean diameter: 3.6 *μm*, SD: 0.53 *μm*, CV: 15%) also suggested that RCM worked, as the mean diameter of the particles was larger than the diameters of polymers **IV-7** and **IV-10** (Table 4.3). Statistical analysis also shows that particles of polymer **HXL-IV-10** were still quasi-monodispersed.

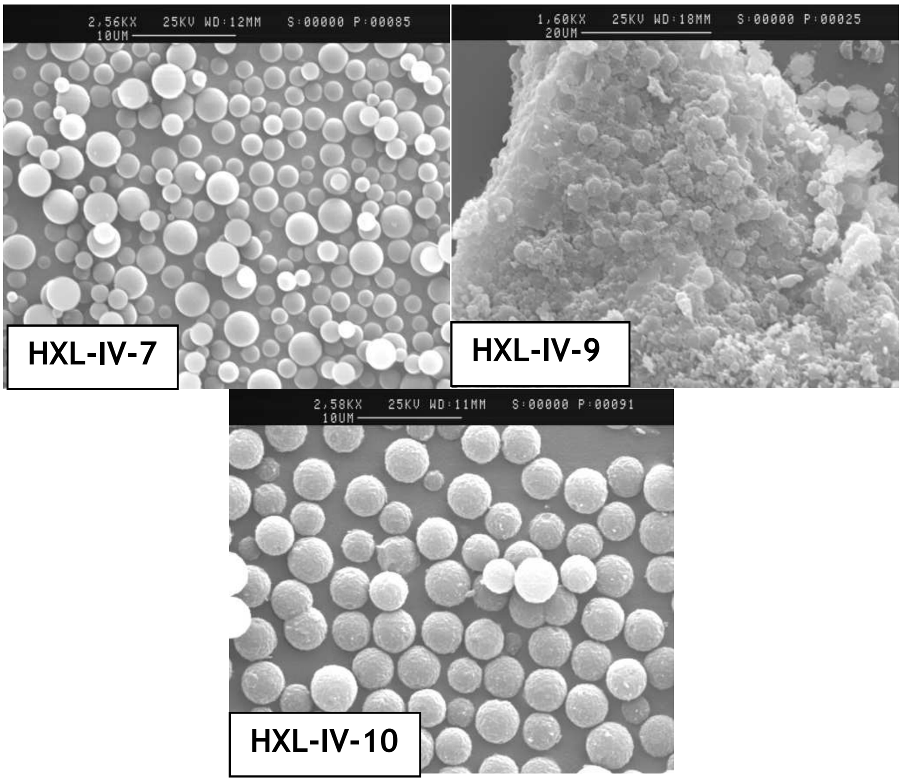

Figure 4.6 SEM micrographs of HXL-IV-7, HXL-IV-9 and HXL-IV-10.

4.3.1. Synthesis and hypercrosslinking reaction of Poly(DVB-alt-AMI)

After the success of the RCM in poly(DVB-*co*-AMA) polymers, the previously synthesised poly(DVB-*alt*-AMI) (**III-8$_f$**) was used to undergo the RCM reaction. Due to the small size of the particles (< 1 µm), non-porous polymer microspheres were obtained (BET surface area: 10 m^2g^{-1}).

RCM was performed with the synthesised poly(DVB-*alt*-AMI) particles to obtain HXL porous polymer particles. RCM reaction could occur in two different ways; between two different ally groups of allyl maleimide (AMI) or between the allyl groups with the vinyl groups from the DVB. The alternating character of the polymer could suggest that RCM might occur between the vinyl group from the DVB and an allyl group but due to the rigidity of the maleimide, it is most likely to occur between both allyl groups (Figure 4.7).

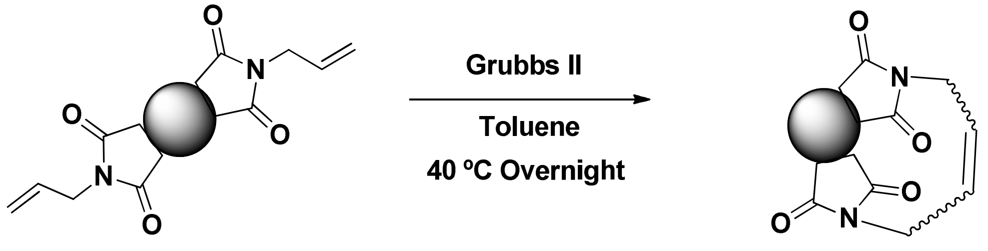

III-8f **HXL-IV-11**

Figure 4.7 RCM reaction of poly(DVB-*alt*-AMI).

Nitrogen sorption porosimetry analysis was carried out to assess the success of the reaction. Unfortunately, the Langmuir surface area of the polymer was still 10 m^2g^{-1}, which indicates that the polymer did not undergo the RCM. Elemental microanalysis of polymer **HXL-IV-11** (*70.9% C, 6.7% H, 5.1% N*) also suggests that no RCM reactions were occurred as polymer **III-8**$_f$ (*70.7% C, 6.8% H, 5.5% N*) has similar amounts of carbon, hydrogen and nitrogen. It was thought that because the particles were very small and rigid, RCM was not successful.

4.4. CONCLUSIONS

Precipitation copolymerisation reactions of poly(DVB-*co*-AMA) in neat acetonitrile were carried out in order to obtain gel-type polymer microspheres. The absence of toluene as co-solvent reduced the dispersity of the particles and quasi-monodispersed particles were obtained with high amounts of DVB or AMA. However, when similar amounts of DVB and AMA were used, dispersity of the particles increased. This might suggest that since AMA is a less reactive monomer than DVB, reactivity rates are different and therefore desolvation of the particles may occur later or the capture of the AMA occurred in the growth stage.

The solvent uptake test showed that polymers with large amounts of AMA (polymers **IV-7**, **IV-9** and **IV-10**) can uptake more solvent and therefore swell the most. The swelling test revealed that the swelling of these polymers occurred immediately after the addition of the solvent, indicating that RCM can be carried out without swelling the polymers before addition of the catalyst.

RCM reaction was carried out in all poly(DVB-*co*-AMA) polymers and only polymers with a high solvent uptake and swelling capacity underwent the hypercrosslinking reaction (polymer **HXL-IV-7** and **HXL-IV-10**). Nitrogen sorption porosimetry analysis showed that surface areas of around 400 m^2g^{-1} for DVB-55 based polymers and around 500 m^2g^{-1} for DVB-80 based polymers were obtained. Unfortunately, the surface areas obtained were not as large as by using the Davankov methodology (around 2000 m^2g^{-1}). However, using RCM as hypercrosslinking method, the selectivity of the polymers will be greater as the olefin is still present in the polymer and can be further functionalised. Additionally, mild conditions and low amounts of solvents were used during the reaction and purification of the polymer and the polymers remained colourless after the hypercrosslinking, which makes them better alternatives for separation chemistry.

In order to insert porosity into non-porous poly(DVB-*alt*-AMI), RCM was carried out. Unfortunately, due to the rigid character of the maleimide and the small size of the particles (< 1μm), hypercrosslinking was not successful.

4.5. FUTURE WORK

Different precipitation copolymerisation reactions were carried out in neat acetonitrile in order to obtain gel-type polymers to hypercrosslink and obtain ultra-high surface areas. However, surface areas below 500 m^2g^{-1} were obtained. In order to increase the surface area of these polymers, solvent mixtures of toluene and a less polar solvent such as heptane can be used in the RCM reaction. According to the solvent uptake and swelling tests, the swelling of the polymers is higher in non-polar solvents than in polar solvents. Therefore, in heptane the polymer should swell more than in toluene and thus, the catalyst would reach the inner double bonds easier increasing the surface area of the polymer. To ensure the solubility of the catalyst, a small amount of toluene should be added to the reaction.

The introduction of a terpolymer such as hydroxyethyl methacrylate (HEMA) could be another alternative in order to increase the surface area of the polymers. With the use of HEMA, more crosslinked polymer will be obtained with larger particles and a greater amount of double bonds. By keeping the ratio of DVB-55 and HEMA low, HXL polymers should be obtained with larger surface areas.

Styrene can also be used in the formation of gel-type polymers to hypercrosslink *via* RCM. The bulky benzene ring will let to the polymer swell more and therefore, the access to the double bonds will be easier. In addition to that, longer bridges will be formed, increasing the surface area of the polymers.

4.6. EXPERIMENTAL

4.6.1. Materials

For the synthesis of copolymers, divinylbenzene-80 (mixture of isomers, 80.0% grade), divinylbenzene-55 (mixture of isomers, 55.0% grade) and allyl methacrylate were purchased from Sigma Aldrich and purified prior to use through a column of neutral alumina. Luperox® A75, Benzoyl peroxide (BPO) was purchased from Sigma Aldrich and was recrystalised from acetone at low temperature. HPLC grade acetonitrile was purchased from Rathburn Chemicals and was used as received. Second-generation Grubbs catalyst, maleimide and allyl alcohol were purchased from Sigma Aldrich and were used as received. Ally amine was purchased from Acros Organics and was also used as received.

The solvents employed (toluene, acetone, methanol, tetrahydrofuran, ethanol, petroleum ether [b.p. 30-40 °C], ethyl acetate, diethyl ether, heptane, methyl ethyl ketone (MEK) and chloroform) were purchased from Sigma Aldrich as standard laboratory reagent grade. Dry solvents were obtained from an in-house purification system.

4.6.2. Equipment

Precipitation copolymerisation reactions were carried out using a Stuart Scientific S160 incubator (Surrey, UK) and a Stovall low profile roller system (NC, USA). The polymerisations were performed in Nalgene® plastic bottles. When required, samples were dried in Townson & Mercer Limited (England) vacuum ovens set to either 40 °C or 70 °C, at 60 mbar pressure.

Elemental microanalysis was performed by the University of Strathclyde Elemental Microanalysis service. C, H and N elemental microanalyses were carried out simultaneously using a Perkin Elmer 2400 Series II analyser, while halogen and phosphorous contents were determined by standard titration methods.

Scanning electron microscopy (SEM) was carried out using a Cambridge Instruments Stereoscan 90. Samples were coated in gold prior to SEM imaging. SEM statistical data was obtained by Image J.

Fourier-Transform Infrared (FT-IR) spectroscopy analyses were carried out using a Shimadzu IRAffinity-1S spectrometer. Samples were scanned over the range 4000-600 cm^{-1} in transmission mode.

The specific surface area measurements were performed using Micromeritics ASAP 2020 nitrogen sorption instrument. Samples were degassed overnight under high vacuum at 100 ^{o}C prior to analysis. Analysis was carried out *via* nitrogen sorption, carried out at 77 K.

Solvent uptake data was obtained using centrifuge tubes fitted with 0.2 µm modified nylon 500 µL centrifugal filter inserts (VWR, North America). The centrifuge used was an Eppendorf Centrifuge 5804 (Hamburg, Germany).

4.6.3. Typical precipitation copolymerisation reaction of DVB with AMA

Poly(DVB-co-AMA)

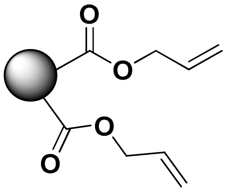

Poly(DVB-*co*-AMA) was synthesised by modifying an existing procedure.**(10)** Divinylbenzene was freed from inhibitor by passage through a short column of alumina (activated aluminium oxide, neutral, Brockmann I) prior to polymerisation. Recently purified DVB, AMA and recrystalised BPO (2 mol% relative to the total number of polymerisable double bonds) were placed into a 1 L Nalgene® bottle with acetonitrile (CH_3CN). The bottle contents were sonicated for 15 min and the contents were purged with bubbling N_2 for 20 min before being sealed under N_2. The bottle was placed on a low-profile roller, which was housed inside a temperature-controlled incubator, and rolled at 30 rpm along its long axis. The temperature was ramped from room temperature to 60 °C over 1 h and then held at 60 °C for a further 48 h. The mixture was then allowed to cool down to room temperature. The product was filtered off under vacuum on a 0.22 μm nylon filter membrane and then washed in sequence with 100 mL volumes of CH_3CN, toluene, methanol and acetone. The product, in the form of a white powder, was dried overnight at 70 °C at 1 mbar.

FT-IR: $\bar{\upsilon}$cm^{-1} 3050 (=CH str.), 2900 (C-H str.), 1725 (C=O str.) 1600, 1510 and 1485 (C=C str.), 1444 (CH_2 def.), 1180 (C-O str.), 1115 (C-O-C str.), 830 (CH def.), 795 and 710 (CH def.).

Isotherms:

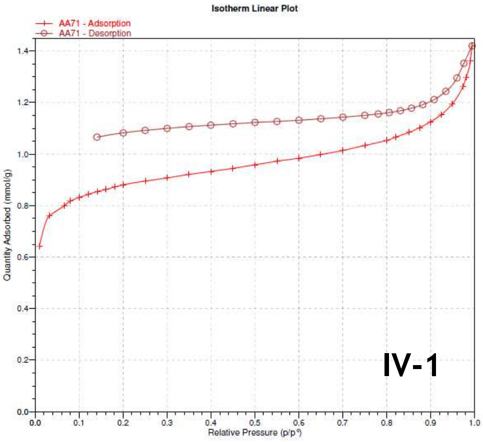

IV-1

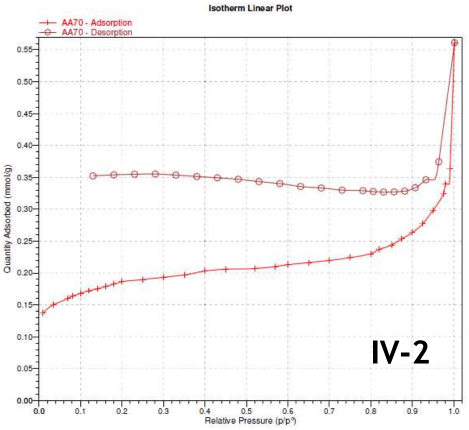

IV-2

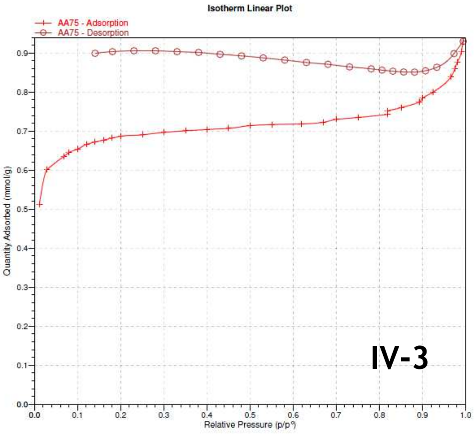

IV-3

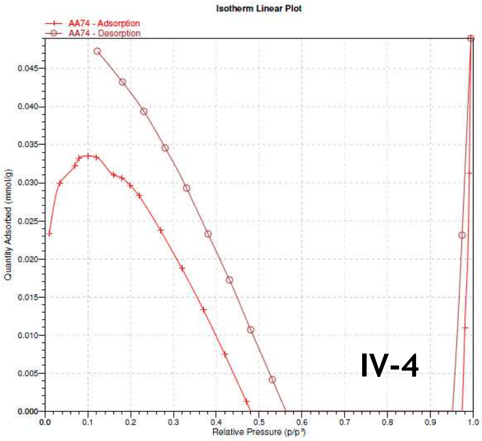

IV-4

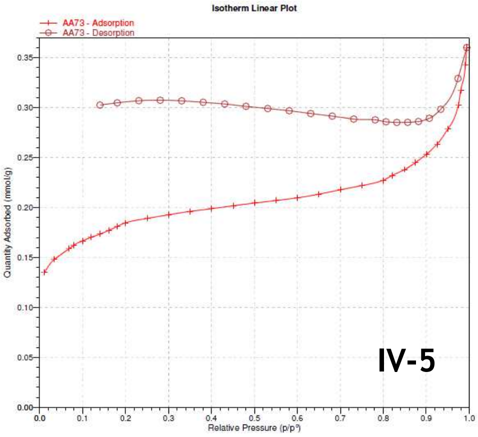

IV-5

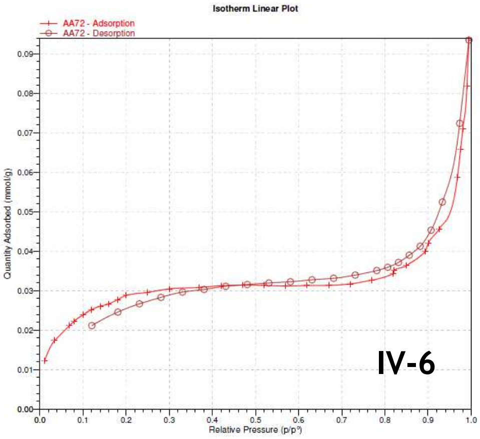

IV-6

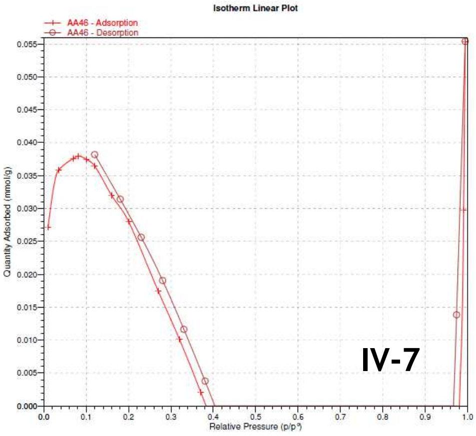

IV-7

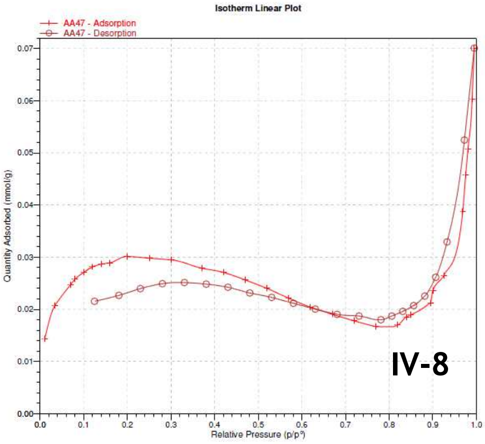

IV-8

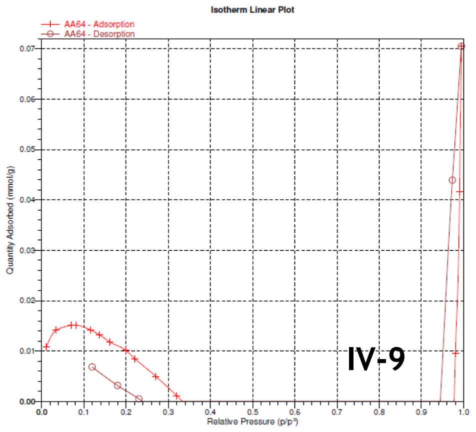

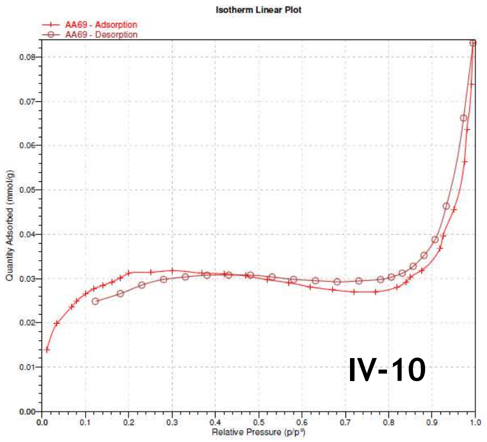

4.6.4. Typical hypercrosslinking reaction via RCM

HXL-poly(DVB-co-AMA)

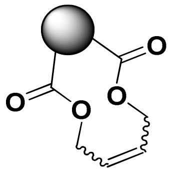

The RCM reactions were carried out in a 20 mL Kimax tube. The polymer (0.15 g) was suspended in dry toluene (5 mL). Second-generation Grubbs catalyst (5.0 mol%) was then added to the suspension and the resulting mixture was sealed under nitrogen. The tube was placed on a low-profile roller, which was housed inside a temperature-controlled incubator, and rolled at 30 rpm along its long axis. The temperature was ramped from room temperature to 40 °C over one hour and then held at 40 °C overnight. The next day the mixture was allowed to cool down to room temperature. The product was filtered off under vacuum on a 0.22 μm nylon filter membrane and then washed in sequence with 15 mL volumes of dichloromethane, ethanol, ethyl acetate, petroleum ether and diethyl ether. The product, in the form of an off-white powder, was dried overnight at 70 °C at 1 mbar.

Polymer ref.	*Starting polymer*	*Starting amount (g)*	*GII (mg)*	*Time (h)*	*Product recovered (mg)*
HXL-IV-1	**IV-1**	0.15	47	24	0.15
HXL-IV-2	**IV-2**	0.15	47	24	0.15
HXL-IV-3	**IV-3**	0.15	48	24	0.14
HXL-IV-4	**IV-4**	0.15	48	24	0.14
HXL-IV-5	**IV-5**	0.15	48	24	0.14
HXL-IV-6	**IV-6**	0.15	48	24	0.14
HXL-IV-7	**IV-7**	0.15	49	24	0.13
HXL-IV-8	**IV-8**	0.15	49	24	0.14
HXL-IV-9	**IV-9**	0.15	49	24	0.14
HXL-IV-10	**IV-10**	0.15	49	24	0.13

Table 4.6 Amounts of reagents used and obtained yields.

Isotherms after RCM:

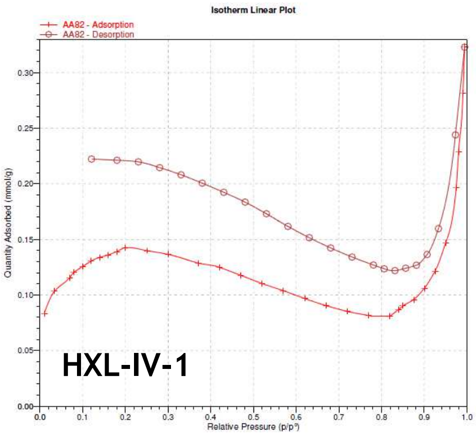

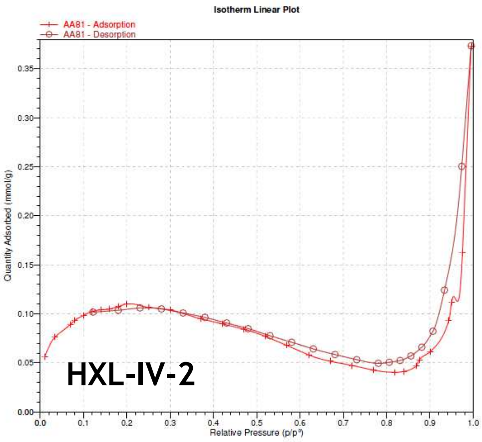

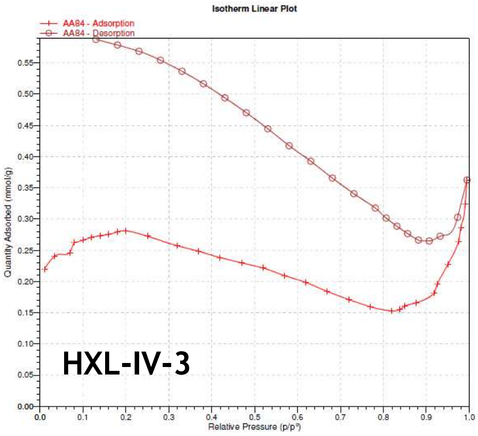

HXL-IV-3

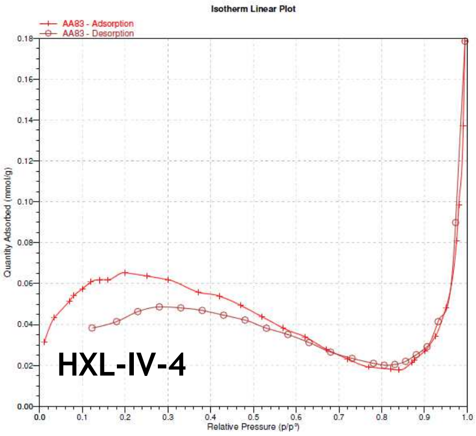

HXL-IV-4

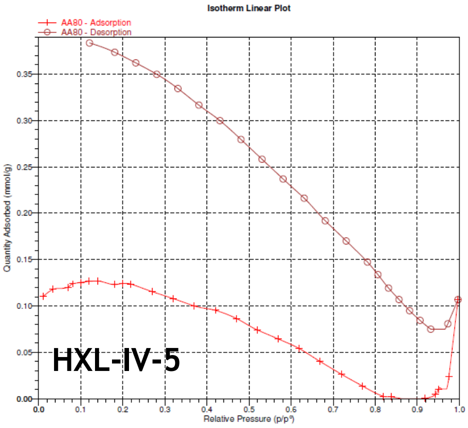

HXL-IV-5

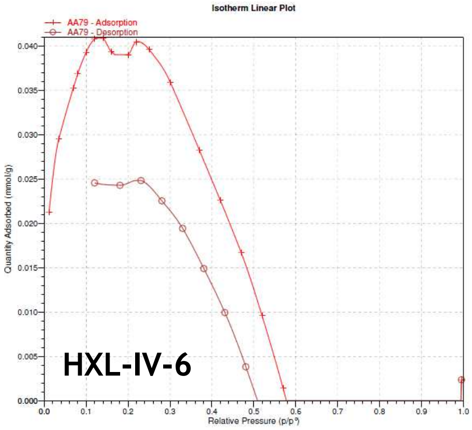

HXL-IV-6

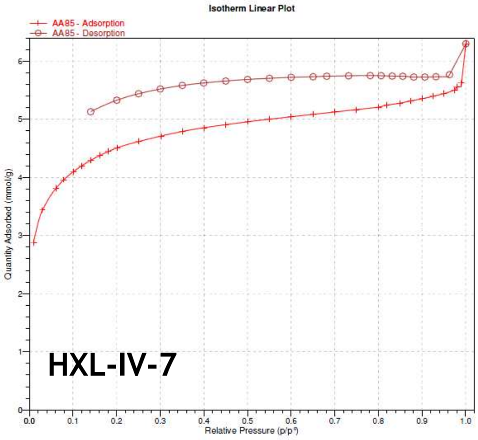

HXL-IV-7

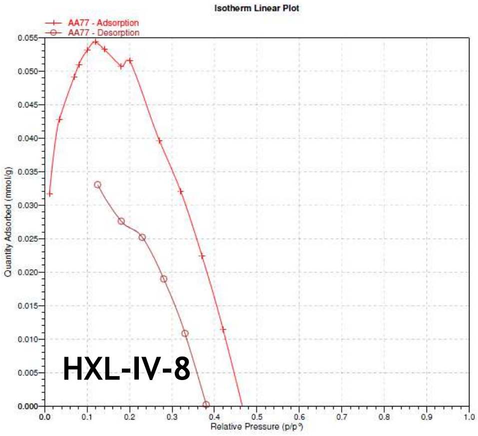

HXL-IV-8

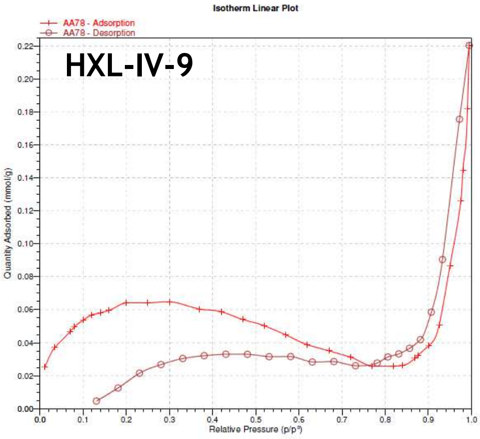

HXL-IV-9

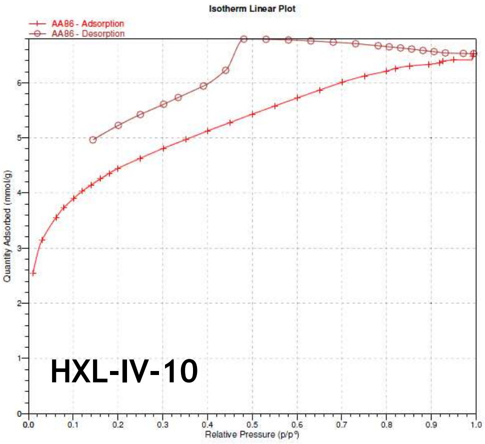

HXL-IV-10

4.7. REFERENCES

(1) Fontanals, N.; Marce, R. M.; Cormack, P. A. G.; Marc, R. M.; Sherrington, D. C.; Borrull, F. *J. Chromatogr. A* **2008**, *1191*, 118–124.

(2) Davankov, V. A; Rogoshin, S. V; Tsyurupa, M. P. *J. Polym. Sci. Part C, Polym. Symp.* **1974**, *47*, 95–101.

(3) Tsyurupa, M. P.; Davankov, V. A.; Rogozhin, S. V. *J. Polym. Sci. Part C, Polym. Symp.* **1974**, *47*, 189–195.

(4) Zhang, X.; Shen, S.; Fan, L. *J. Mater. Sci.* **2007**, *42*, 7621–7629.

(5) Ahn, J. H.; Jang, J. E.; Oh, C. G.; Ihm, S. K.; Cortez, J.; Sherrington, D. C. *Macromolecules* **2006**, *39*, 627–632.

(6) Fontanals, N.; Marcé, R. M.; Borrull, F.; Cormack, P. A. G. *Polym. Chem.* **2015**, *6* (41), 7231–7244.

(7) Fontanals, N.; Corte, J.; Galia, M.; Marce, R. M.; Cormack, P. A. G. *J. Polym. Sci. Part A Polym. Chem.* **2006**, *43*, 1718–1728.

(8) Yang, X.; Tan, L.; Xia, L.; Wood, C. D.; Tan, B. *Macromol. Rapid Commun.* **2015**, *36*, 1553–1558.

(9) Fontanals, N.; Miralles, N.; Abdullah, N.; Davies, A.; Gilart, N.; Cormack, P. A. G. *J. Chromatogr. A* **2014**, *1343*, 55–62.

(10) Cormack, P. A. G.; Davies, A.; Fontanals, N. *React. Funct. Polym.* **2012**, *72*, 939–946.

(11) Davankov, V.; Pavlova, L.; Tsyurupa, M.; Brady, J.; Balsamo, M.; Yousha, E. **2000**, *739*, 73–80.

(12) Hypersol-Macronet catalogue http://purolite.com/Customized/Uploads/MACRONET_Brochure_062503.pdf (accessed Apr 28, 2016).

(13) Valderrama, C.; Barios, J. I.; Farran, A.; Cortina, J. L. *Water. Air. Soil Pollut.* **2010**, *210*, 421–434.

(14) Jiang, Z.; Li, A.; Cai, J.; Wang, C.; Zhang, Q. *J. Environ. Sci.* **2007**, *19*, 135–140.

(15) Vergili, I.; Barlas, H. *Desalination* **2009**, *249*, 1107–1114.

(16) Bratkowska, D.; Fontanals, N.; Borrull, F.; Cormack, P. A. G.; Sherrington, D. C.; Marcé, R. M. *J. Chromatogr. A* **2010**, *1217*, 3238–3243.

(17) Fontanals, N.; Cormack, P. A. G.; Sherrington, D. C.; Marcé, R. M.; Borrull, F. *J. Chromatogr. A* **2010**, *1217*, 2855–2861.

(18) Fontanals, N.; Cormack, P. A. G.; Sherrington, D. C. *J. Chromatogr. A* **2008**, *1215*, 21–29.

(19) Bratkowska, D.; Marcé, R. M.; Cormack, P. A. G.; Sherrington, D. C.; Borrull, F.; Fontanals, N. *J. Chromatogr. A* **2010**, *1217*, 1575–1582.

(20) Bratkowska, D.; Davies, A.; Cormack, P. A. G.; Borrull, F.; Sherrington, D. C.; Marc, R. M. *J. Sep. Sci.* **2012**, *35*, 2621–2628.

(21) Li, B.; Su, F.; Luo, H. K.; Liang, L.; Tan, B. *Microporous Mesoporous Mater.* **2011**, *138*, 207–214.

(22) Germain, J.; Hradil, J.; Fréchet, J.; Svec, F. *Chem. Mater.* **2006**, *18*, 4430–4435.

(23) Chang, D.; Yu, M.; Zhang, C.; Zhao, Y.; Kong, R.; Xie, F.; Jiang, J.-X. *Microporous Mesoporous Mater.* **2016**, *228*, 231–236.

(24) Li, W.; Stöver, H. D. H. *J. Polym. Sci. Part A Polym. Chem.* **1997**, *36*, 1543–1551.

(25) Chatterjee, A. K.; Choi, T. L.; Sanders, D. P.; Grubbs, R. H. *J. Am. Chem. Soc.* **2003**, *125*, 11360–11370.

CHAPTER 5

HYPERCROSSLINKING BY OLEFIN METATHESIS OF GEL-TYPE POLY(DVB-co-AMA) POLYMER BY USING AN EXTERNAL CROSSLINKER

5.1. INTRODUCTION

5.1.1 Hypercrosslinking reaction with external crosslinkers

Originally, Davankov et al. discovered hypercrosslinked (HXL) networks *via* the post-crosslinking of polystyrenic chains in the swollen gel-state by using external crosslinkers.(1,2) The external crosslinker was installed by Friedel-Crafts reaction forming a methylene bridge between two polystyrene chains. 4,4′-*Bis*(chloromethyl)-1,1′-biphenyl (BCMBP) was used as the external crosslinker for first time by Davankov *et al.* (Figure 4.1).(1) By using an external crosslinker, together with a Lewis acid, all the aromatic rings can be crosslinked and ultra-high specific surface areas can be achieved. The formed HXL network displays a high degree of crosslinking, low packing density due to the amount of rigid spacers holding the polymer chains apart, and an extremely high specific surface area (up to around 2000 m^2g^{-1}), which is due to a large population of very small pores (2-4 nm).(2)

External crosslinkers are normally used when it is not possible to carry out internal crosslinking with the polymer precursors. Different groups started using chloromethyl ether (CME) as external crosslinker (Figure 5.1a).(3,4) However, due to the carcinogenic properties of the compound, different external crosslinkers were used. Zhang and coworkers(5) used carbon tetrachloride (Figure 5.1b) and dimethoxymethane as the external crosslinkers with linear poly-*p*-phenylenes obtaining specific surface areas of around 1000 m^2g^{-1}. Another interesting alternative to CME, is 1,2-dichloroethane, since it can be used as solvent and as crosslinker at the same time.(6,7)

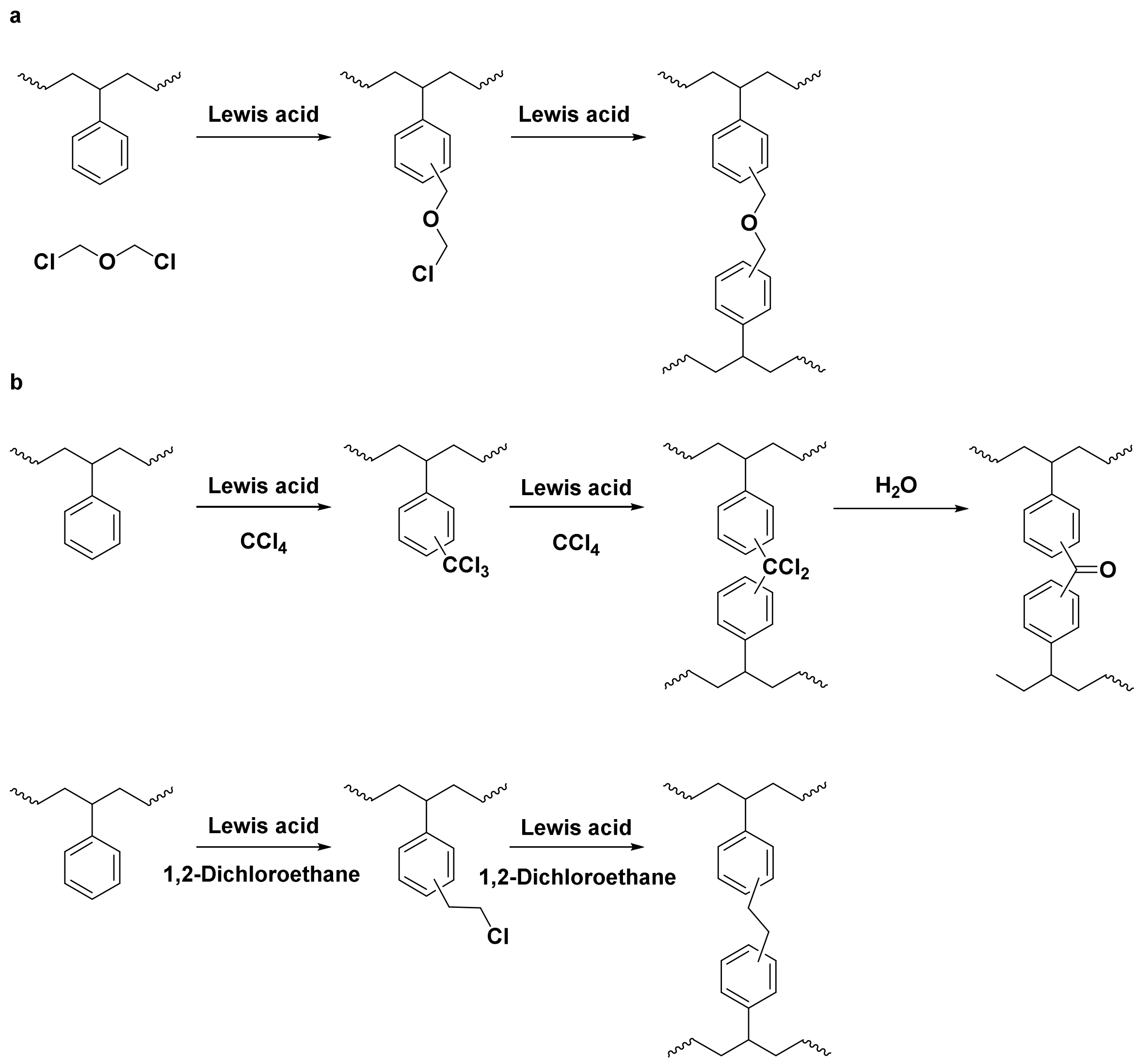

Figure 5.1 Hypercrosslinking reactions using different crosslinkers a) CME, b) CCl_4 and c) dichloroethane.

Different aspects have to be taken in consideration when selecting an external crosslinker; structural variations of the crosslinked bridge in a HXL polymer are directly connected with the porosity of the polymers as changes in the length and rigidity of the bridge will affect the morphology of the pores. Chemical modifications on the other hand, will install a moiety from the crosslinker on the polymer. Another parameter to bear in mind is the reaction kinetics. In 1998 Hradil and Králová studied the kinetics of HXL poly(styrene-co DVB) by using CCl_4 as external crosslinker. However it was found that CCl_4 reacted more slowly and lower conversions were obtained than by using CME as external crosslinker.

In 1999 Pastukhov *et al.*(8) found that 0.5 moles of cross-agent per mol of repeating unit able to crosslink were needed in order to achieve 100% of crosslinking. They also found that the higher the amount of cross-agent, the higher the specific surface areas.

Di and tri-iodoalkanes were used as cross-agents by Svec and coworkers(9,10) in order to hypercrosslink aromatic rings with electron-donating groups such as polyaniline(9) or polypyrrole(10) (Figure 5.2). The choice of diiodoalkanes over dichloro and dibromo alkanes was made in order to compensate the limited reactivity of polyaniline.(9) The introduction of boron as single-atom crosslinker was also reported by Germain *et al.*(10) as novel chemistry in the field of hypercrosslinking. All these materials were used as hydrogen storage materials as the pores were too small for nitrogen adsorption but large enough for hydrogen adsorption. However, further optimisations have to be carried out in order to compare these new materials with polystyrene-based HXL materials.

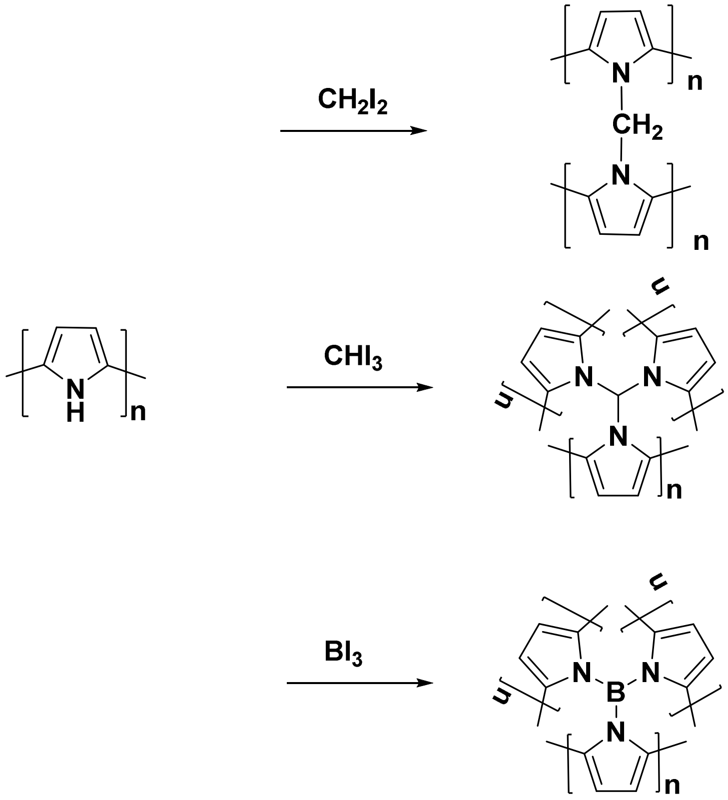

Figure 5.2 Polypyrrole hypercrosslinking by using diiodo and triiodo compounds.

A new hypercrosslinking strategy was developed by Li *et al.* in 2011,(11) which consisted in the ‘knitting’ of rigid building blocks with an external crosslinker such as formaldehyde dimethyl acetal (FDA).(11) The main advantage of using FDA as external crosslinker was that no HCl was formed as a by-product, since methanol was formed instead. Tan and coworkers(11) started this one-step approach by heating at 45 °C the solution of the aromatic monomer (including benzene, phenol or chlorobenzene), FDA as cross-agent and $FeCl_3$ as Lewis acid for 5 h and then at 80 °C for 19 h to complete the condensation (Figure 5.3). After different conditions were attempted, they obtained specific surface areas of 1400 m^2g^{-1}, 1.45 wt.% of H_2 adsorption (at 77.3 K and 1.13 bar) and 13.5 wt.% of CO_2 adsorption (at 273.15 K and 1 bar). In the following years, this approach has been used with different monomers such as aromatic heterocycles,(12) hydroxymethylated aromatic molecules,(13) aniline and benzene,(14) and tetrahedral monomers(15,16) among others.

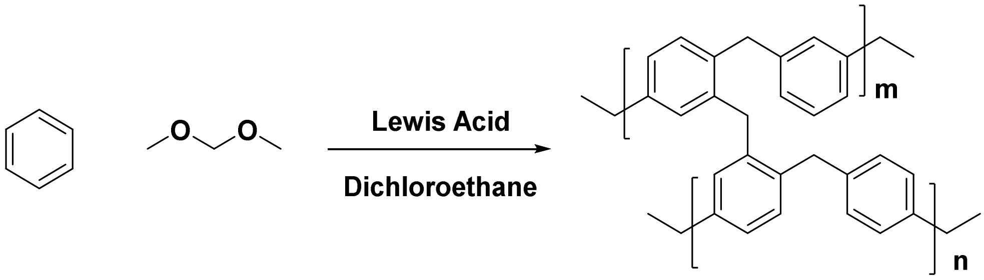

Figure 5.3 'Knitting' process developed by Tan and coworkers using FDA as cross-agent.[11]

In 2014 Maya *et al.*(17) HXL different poly(styrene-*co*-DVB) monoliths using a Friedel-Crafts reaction with $FeCl_3$ comparing different external crosslinkers: BCMBP, dichloroxylene and FDA. After optimisation of the conditions of the reaction with all three external crosslinkers, the specific surface area of the resulting monolith was higher than the specific surface area of the precursor poly(styrene-*co*-DVB), which gave benefits in terms of column efficiency. The highest specific surface area obtained was around 900 m^2g^{-1}, obtained by crosslinking the precursor with BCMBP.

5.2. AIM OF THE RESEARCH

Ultra-high specific surface areas (around 2000 m^2g^{-1}) are achieved by internal hypercrosslinking of polymer precursors. Due to steric hindrance or the rigid morphology of the polymeric precursors, sometimes the hypercrosslinking is far from trivial. When hypercrosslinking *via* internal crosslinker is not possible, external cross-agents are used. However, lower surface areas are obtained through this method and different parameters such as the structure of the bridge, chemical composition and kinetics has to be taken in consideration before the reaction.

In chapter 4, different gel-type polymers were synthesised in order to obtain HXL polymers by RCM reaction. However, only polymers with large amounts of allyl methacrylate (AMA) underwent the hypercrosslinking reaction. In this work, different cross-agents with more than 2 vinyl groups were used to hypercrosslink poly(DVB-*co*-AMA) polymers by a CM/RCM reaction. One of the goals was to increase the surface areas of the polymers with these multivinyl cross-agents and at the same time increase the selectivity of the HXL products. A noteworthy advantage of the CM/RCM process is that different functionalities can be installed in the HXL product, as the olefin is still present and can be further functionalised.

5.3. RESULTS AND DISCUSSION

The choice of tetravinyl external crosslinkers such as the commercially available tetravinylsilane (TVSi) was made in order to improve the surface area of the polymers and the amount of double bonds available for functionalisation. It was believed that after CM/RCM reaction at least two of the double bonds were consumed, giving porous polymers with at least two different types of olefins. The vinyl groups used in the CM/RCM will give a less reactive Type II olefin whereas the remaining vinyl groups will still be Type I olefins. The different types of olefins would give the option of install two different functional groups (if desired) on the polymer either by CM or by any other technique.

5.3.1. Hypercrosslinking reaction of gel-type poly(DVB-co-AMA) with TVSi

In the previous chapter (chapter 4) precipitation copolymerisation reaction using different ratios of divinylbenzene (DVB-55 or DVB-80) with AMA were carried out in neat acetonitrile and using benzoyl peroxide (BPO) as thermal initiator (Table 4.1). The suppression of toluene during the polymerisations led to the formation of gel-type polymers which were non porous in the dry state (Table 4.5). Nevertheless their swelling capacity rendered them suitable to undergo RCM reaction.

The commercially available TVSi was chosen as external crosslinker in order to hypercrosslink the previously synthesised poly(DVB-*co*-AMA) polymers (Table 4.1). The polymer was first swollen overnight in order to facilitate the access to all the internal vinyl groups and then CM/RCM reaction was carried out (Figure 5.4). Second-generation Hoveyda Grubbs (HGII) catalyst was used in order to obtain higher reactivity during the CM/RCM. This catalyst was chosen since it is a phosphine free catalyst, air and moisture resistant.

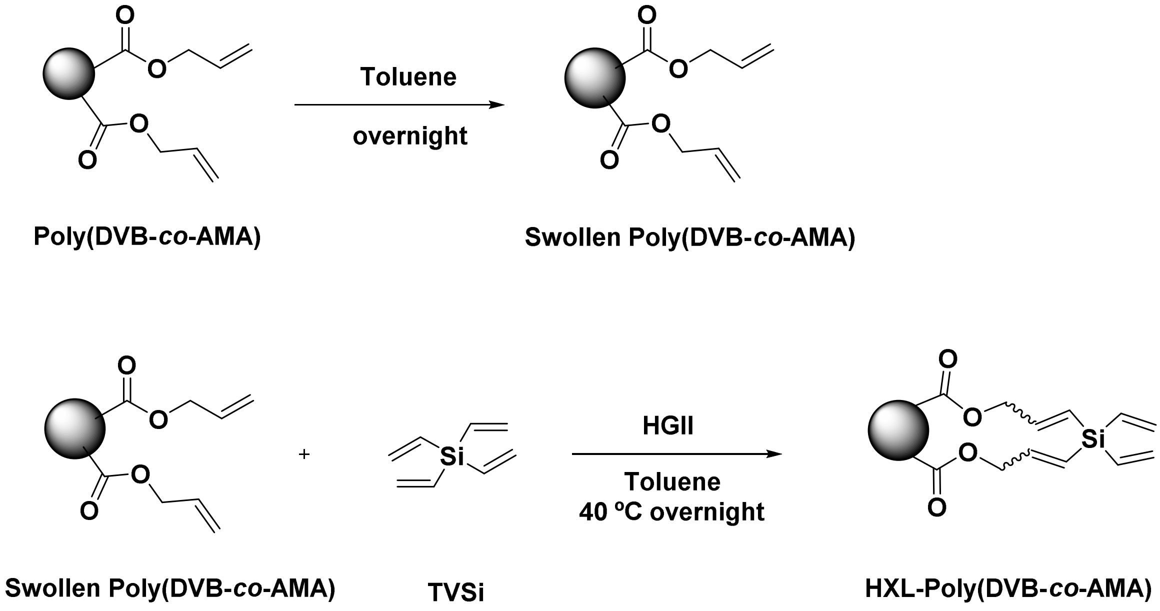

Figure 5.4 RCM reaction of poly(DVB-*co*-AMA) with TVSi.

Different conditions were attempted in order to achieve the CM/RCM reaction for hypercrosslinking reaction (Table 5.1). Second-generation Grubbs (GII) catalyst was first tested with polymer **IV-10** (Table 5.1 entry **V-1**), but due to the decrease in the recovered mass, it was believed that the reaction did not succeed. The catalyst was then changed to a more stable HGII catalyst and it was tested with polymer **IV-7** (Table 5.1 entry **V-2**) but no increase of mass was observed either. In order to push the reaction, an excess of TVSi (4 equiv) and HGII (5 mol% and 10 mol%) with polymers **IV-7** and **IV-10** (Table 5.1 entries **V-3** to **V-5**) were also attempted but in none of the cases the masses were increased.

Polym. ref.	*Starting polym.*	*Polym. (g)*	*TVSi (equiv)*	*HGII (mol%)*	*Recovered mass (g)*
V-1	**IV-10**	0.10	0.5	5*	0.078
V-2	**IV-7**	0.10	0.5	5	0.094
V-3	**IV-10**	0.12	4	5	0.11
V-4	**IV-7**	0.12	4	10	0.11
V-5	**IV-10**	0.12	4	10	0.12

Table 5.1 Conditions used for hypercrosslinking **reaction with TVSi. * Grubbs II catalyst used.**

FT-IR analysis of the functionalised polymers was carried but bands of TVSi were overlapped with the bands of the polymer before the CM/RCM reaction, hence making FT-IR analysis unreliable for the characterisation of these polymers. SEM analysis was carried out to check if particles were destroyed when RCM was carried out with TVSi. The micrographs (Figure 5.5) show that particles were not destroyed and no chemical aggregations were formed after the CM/RCM reaction with TVSi.

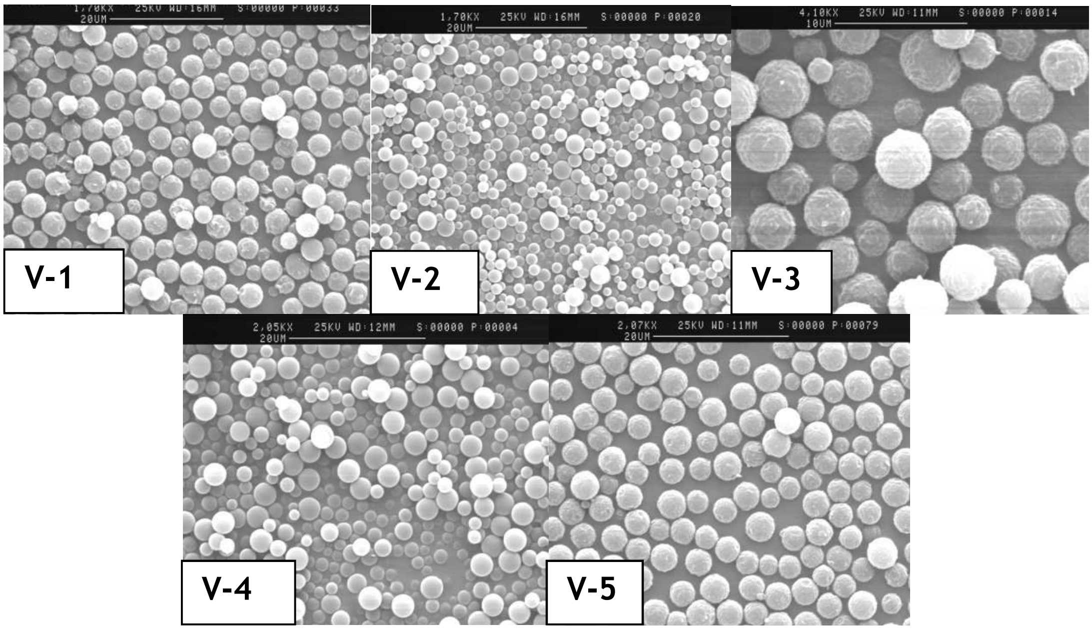

Figure 5.5 SEM micrographs of HXL-V-1, HXL-V-2, HXL-V-3, HXL-V-4 and HXL-V-5.

Statistical analysis of the particles was carried out in order to compare the sizes of the particles before and after the RCM reaction and to check the success of the reaction. Table 5.2 shows that the size of the particles had increased after the CM/RCM reaction, with TVSi indicating that metathesis reaction occurred. However, due to the small increase in the size, it was thought that CM reaction took place but not subsequent RCM.

Polym. ref.	*Mean diameter (μm)*	*SD (μm)*	*Min (μm)*	*Max (μm)*	*CV (%)*
IV-7	1.7	0.63	0.67	3.2	38
IV-10	3.5	0.44	2.3	4.3	12
V-1	3.7	0.45	2.3	4.5	12
V-2	2.0	0.63	0.79	3.6	32
V-3	3.7	0.66	1.7	5.6	18
V-4	2.4	0.72	0.75	3.7	30
V-5	3.7	0.54	2.3	4.9	15

Table 5.2 Statistical analysis of the polymers after CM reaction with TVSi.

Nitrogen sorption porosimetry analysis was carried out to check if polymers underwent CM or CM/RCM reaction. The low specific surface areas of polymers **V-1** (5 m^2g^{-1}), **V-2** (1 m^2g^{-1}), **V-3** (47 m^2g^{-1}), **V-4** (8 m^2g^{-1}) and **V-5** (6 m^2g^{-1}), confirmed that polymers only underwent the CM reaction as non-porous particles were obtained.

Energy-dispersive X-ray analysis (EDX) was carried out to identify silicon moieties in the composition of the polymers (Figure 5.6). EDX spectra show the presence of silicon in the polymers, which suggested that TVSi was used as coupling partner during the CM and not as external crosslinker as desired. Figure 5.6d shows that by using an excess of TVSi with polymer **IV-10**, CM reaction worked more effectively than in the rest of the cases as 5% of silicon was detected.

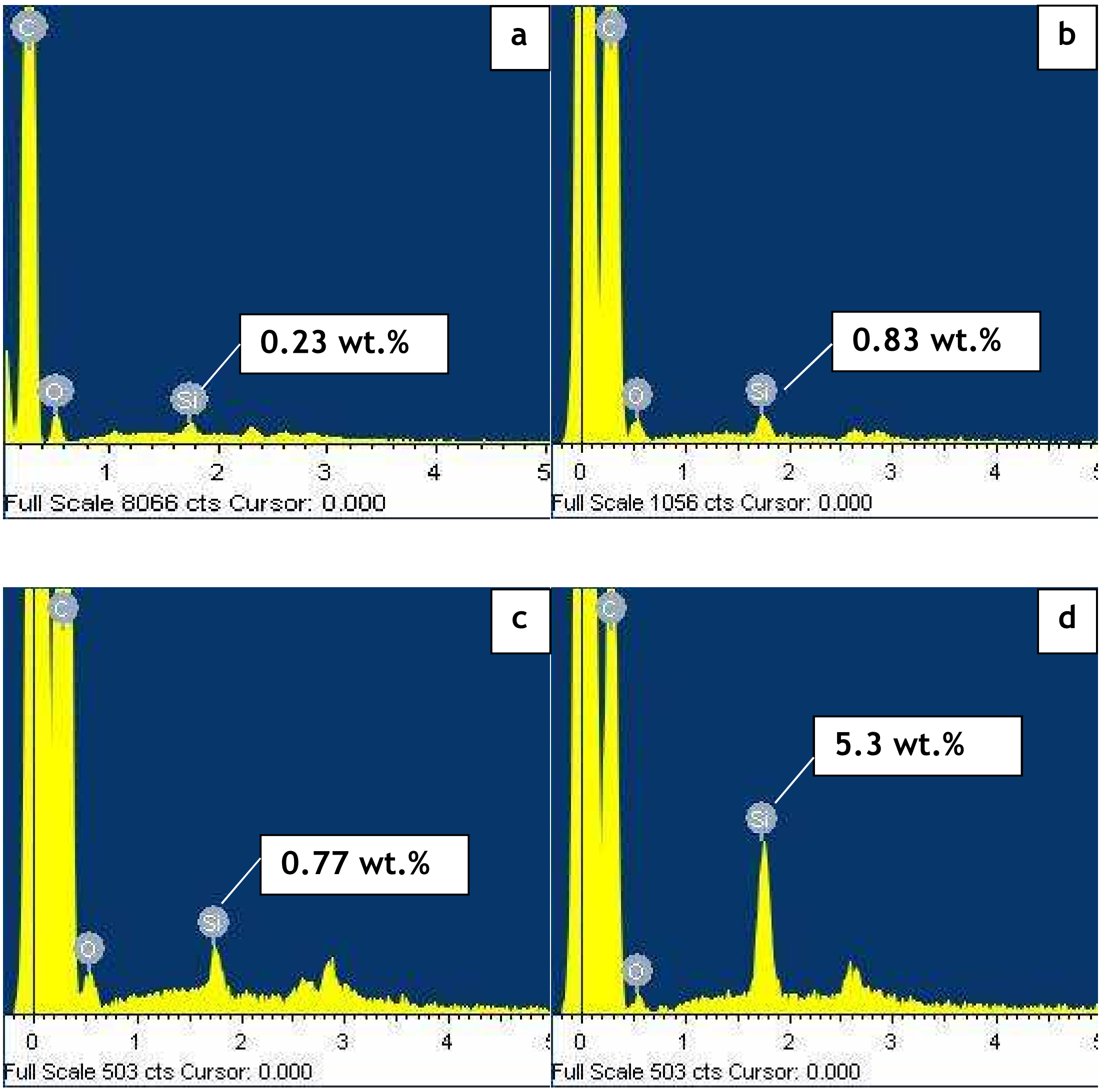

Figure 5.6 EDX spectra of a) V-1, b) V-3, c) V-4, d) V-5.

5.3.2. Hypercrosslinking reaction of gel-type poly(DVB-co-AMA) with tetraallyl orthosilicate (TAOSi)

In 2011 Young and coworkers$^{(18)}$ examined the influence of different silyl groups on the yield of RCM and CM reactions. They found that ethoxy substituents promoted the formation of the product and led to higher yields in comparison with alkyl and/or aryl substituents. In order to increase the reactivity of the hypercrosslinking reaction with an external crosslinker, the commercially available tetraallyl orthosilicate (TAOSi) was used as external crosslinker (Figure 5.7).

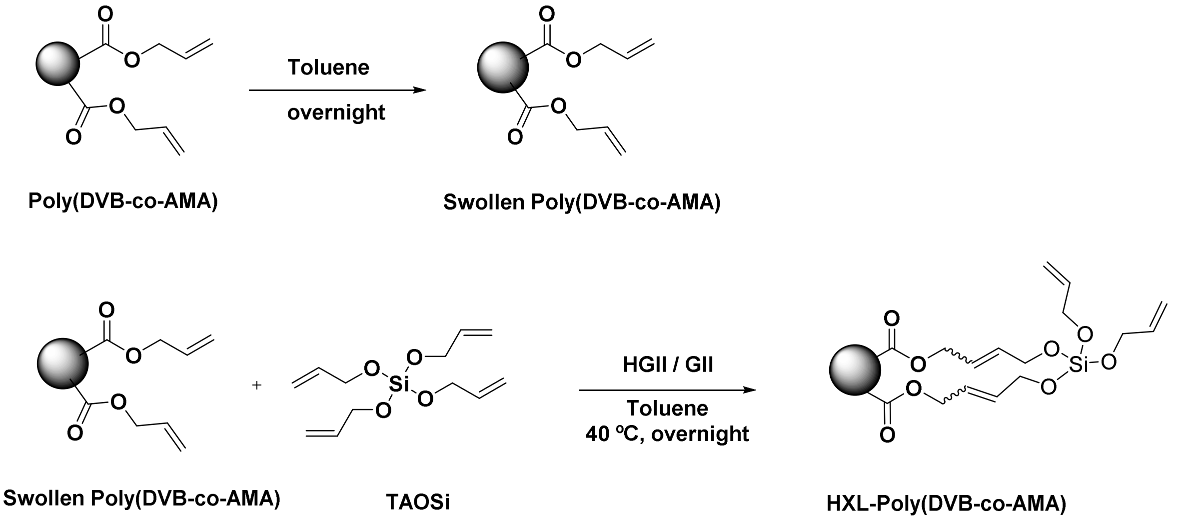

Figure 5.7 RCM reaction involving TAOSi as external crosslinker.

Polymers **IV-7** and **IV-10** were first tested using an excess of TAOSi (4 equiv) as cross partner and using 5 mol% of Grubbs II catalyst to give polymers **V-6** and **V-7,** respectively (Table 5.3 entries **V-6** and **V-7**). However, due to the high reactivity of TAOSi two different types of products were obtained after the RCM reaction. One of the products was an off-white powder, similar in appearance to the starting polymers and the other one was a brown and hard powder. When the brown product was taken out from the polymer-looked alike product, EDX analysis of the latter was performed. EDX analysis shows (Table 5.3) that homodimerisation of TAOSi occurred as traces (**V-7**) or no silicon (**V-6**) was found after the removal of the brown product.

Polym. ref.	*Starting polym.*	*Polym. (g)*	*TAOSi (equiv)*	*Cat.*	*Cat. (mol%)*	*Recovered mass (g)*	*EDX Si (wt.%)*
V-6	**IV-7**	0.12	4	GII	5	0.12+0.0042	0.00
V-7	**IV-10**	0.12	4	GII	5	0.12+0.0065	0.19
V-8	**IV-10**	0.10	0.5	GII	5	0.14	1.1
V-9	**IV-1**	0.080	0.5	HGII	5	0.094	1.1
V-10	**IV-2**	0.080	0.5	HGII	5	0.093	0.45
V-11	**IV-3**	0.080	0.5	HGII	5	0.10	1.2
V-12	**IV-4**	0.080	0.5	HGII	5	0.11	0.77
V-13	**IV-5**	0.10	0.5	HGII	5	0.12	0.35
V-14	**IV-6**	0.10	0.5	HGII	5	0.12	0.31
V-15	**IV-7**	0.10	0.5	HGII	5	0.13	1.9
V-16	**IV-8**	0.10	0.5	HGII	5	0.13	1.9
V-17	**IV-9**	0.10	0.5	HGII	5	0.13	1.6
V-18	**IV-10**	0.10	0.5	HGII	5	0.14	2.1

Table 5.3 Different conditions used and EDX analysis of metathesis reactions with TAOSi.

To avoid the homodimerisation of the cross agent, the ratio between the polymer and TAOSi was decreased to 0.5 equiv to give polymer **V-8** (Table 5.3 entry **V-8**). The increase in the recovered mass suggested that the CM/RCM reaction was successful. The SEM micrograph of polymer **V-8** (Figure 5.8) shows that no chemical aggregations were obtained after the CM/RCM. Nevertheless, a few changes in the size of the particles were observed after the measurement of the particles (mean diameter: 3.3 *µm*, SD: 0.67 *µm*, CV: 20%). The CV of the particles indicates that CM happened as they changed from quasi-monodispersed to polydispersed. Unfortunately, the particle size after CM/RCM was expected to be larger and therefore, it was thought that only CM took place. In order to clarify whether CM/RCM occurred, nitrogen sorption porosimetry analysis was performed. The low specific surface area of **V-8** (5 m^2g^{-1}) suggested that polymer **IV-10** only underwent CM reactions. EDX analysis (Table 5.3) also suggested that CM occurred between the polymer and TAOSi.

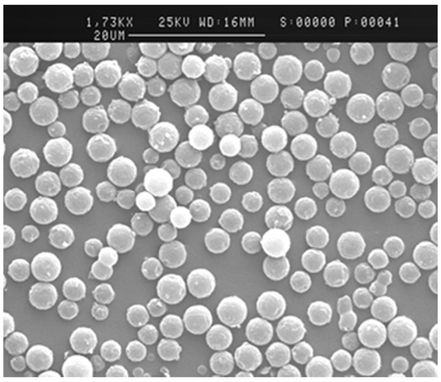

Figure 5.8 SEM micrograph of polymer V-8.

Table 5.3 shows the conditions employed using TAOSi as cross agent with all the different polymers synthesised in chapter 4 (Table 5.3 entries **V-9** to **V-18**). In order to promote the CM/RCM reaction, HGII was used instead of GII catalyst. Nevertheless, the polymer and TAOSi ratio was kept at 1/0.5 in order to avoid the homodimerisation of the external crosslinker. As the amount of recovered mass was higher than in any of the previously mentioned cases, it was believed that the polymers underwent the CM/RCM with TAOSi. Nitrogen sorption porosimetry analysis of the functionalised polymers was performed to check if the surface areas of the polymers changed after metathesis with TAOSi but surface areas lower than 5 m^2g^{-1} were obtained in all of the cases. This confirmed that the polymer only underwent CM with TAOSi, and not the subsequent RCM reaction.

Figure 5.9 shows the most representative SEM micrographs of the polymers after CM reaction with TAOSi. When the metathesis reaction with TAOSi was carried out with polymer **IV-1** (particle size around 1 µm) polydispersed particles were observed (Figure 5.9 polymer **V-9**). However, when larger particle size precursors (> 2 μm) were used for metathesis reactions, some aggregations appeared (Figure 5.9 polymer **V-12**) and more chemical aggregations, and coagulums were observed (Figure 5.9 polymer **V-18)** with larger particle sizes (>3 μm). The SEM micrograph of polymer **V-18** shows that aggregations consisted of newly formed particles during the metathesis reaction. The formation of these new particles of poly(TAOSi) suggested that a new precipitation polymerisation technique was discovered.

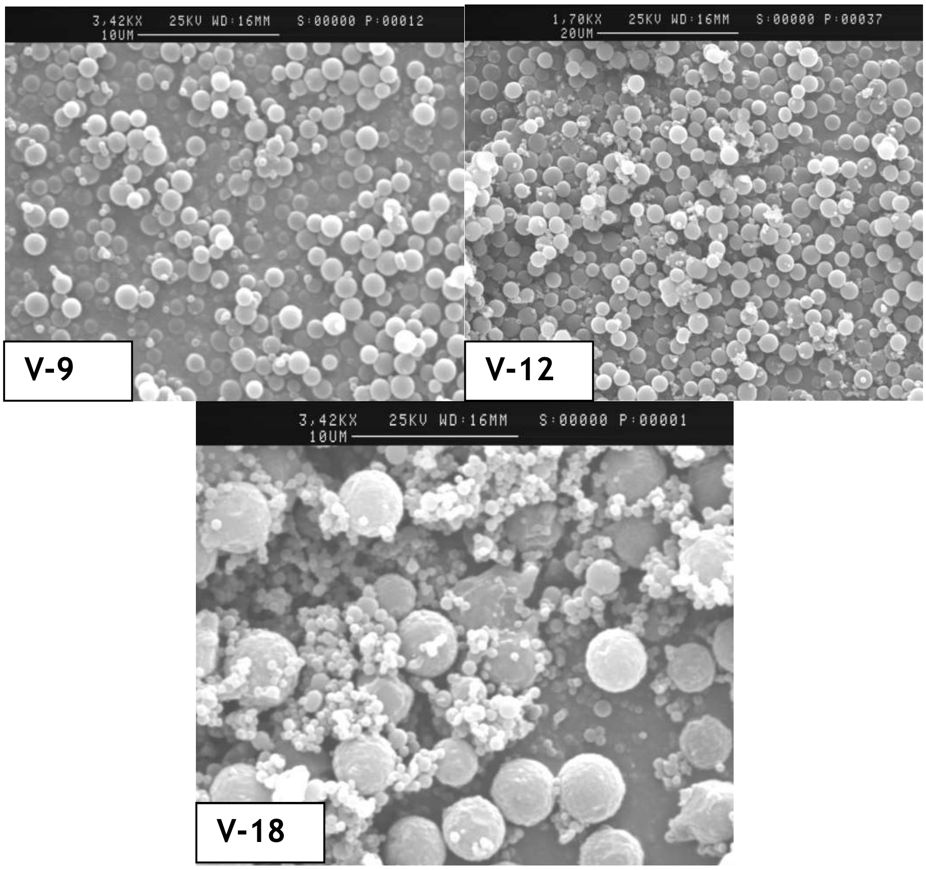

Figure 5.9 SEM micrographs of polymers V-9, V-12 and V-18.

Synthesis of poly(TAOSi)

The use of TAOSi as external crosslinker with poly(DVB-*co*-AMA) resulted in the formation of new particles. At the beginning the newly formed particles went unnoticed as they presented similar particle sizes as the polymer. The use of olefin metathesis as new precipitation polymerisation method has never been reported before, which led us to optimise this new synthetic approach. A blank experiment was first carried out in the absence of catalyst in order to determine if the particles were formed by olefin metathesis or by radical polymerisation of TAOSi. The reaction was left over 2 days in toluene at 40 °C but no product precipitated. The recovery of the starting material indicates that particle formation occurred due to the presence of HGII catalyst, which crosslinks TAOSi. Entry **V-19**$_{a}$ (Table 5.4) shows conditions used in the first attempt to obtain poly(TAOSi) particles (Figure 5.10). It was observed that precipitation occurred 5 min after being rolled at 40 °C but the reaction was left overnight to ensure that the reaction had reached full conversion.

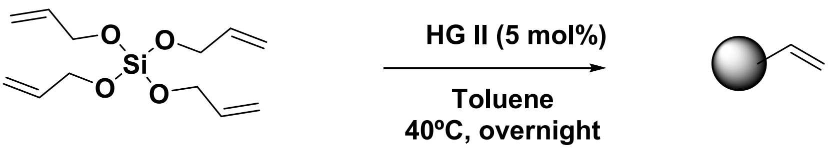

TAOSi **Poly(TAOSi)**

Figure 5.10 Poly(TAOSi) reaction by CM reaction.

The SEM micrograph shows that spherical polymer microspheres were obtained, although aggregations were formed during the reaction (Figure 5.11). This was believed to happen due to the fast nucleation and precipitation of the particles in the media.

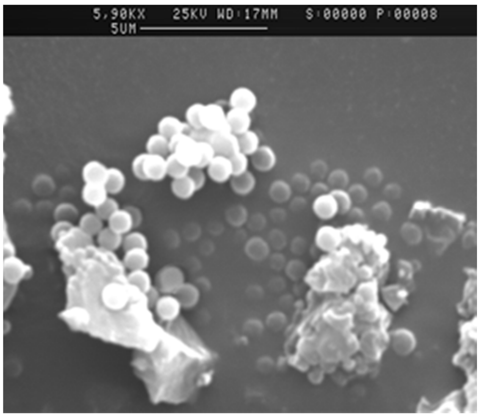

Figure 5.11 SEM micrograph of polymer V-19$_{a}$.

Table 5.4 shows some of the variations attempted in order to delay the nucleation stage of the particles and thus, the precipitation of the polymer in the media. The first attempt to delay the precipitation of the polymer was carried out by performing the reaction at r.t. Nucleation of the polymer was observed after 1 h of reaction and a higher yield was obtained (Table 5.4 entry

V-19$_b$). However, the decrease of the temperature favoured the formation of coagulums (Figure 5.12). The concentration of the monomer in the solvent was also changed with the same purpose and to avoid the aggregations. By decreasing the concentration, similar yields were obtained (Table 5.4 entries **V-19$_c$** and **V-19$_d$**), but a significant increase was observed when the solvent amount was reduced (Table 5.4 entry **V-19$_e$**). This suggests that coagulums could have been formed, as it happened in entry **V-19$_b$**.

Polym. ref.	*TAOSi (mL)*	*[TAOSi] (mol L^{-1})*	*Toluene (mL)*	*HGII (mol%)*	*Temperature (°C)*	*Yield (g)*	*Yield (%)*
V-19$_a$	0.10	0.078	5.0	5	40	0.019	25
V-19$_b$	0.10	0.078	5.0	5	r.t.	0.032	42
V-19$_c$	0.10	0.026	15	5	40	0.021	28
V-19$_d$	0.10	0.039	10	5	40	0.019	24
V-19$_e$	0.10	0.16	2.5	5	40	0.039	51

Table 5.4. Applied reaction conditions for polymer V-19.

SEM micrographs show that monoliths and coagulums were formed when the concentration was increased (Figure 5.12 entry **V-19$_e$**). On the other hand, when the concentration was reduced, spherical microspheres were obtained (Figure 5.12 entries **V-19$_c$** and **V-19$_d$**). However, the quality of the particles was not as good as the particles of polymer **V-19$_a$**, since a linkage between the particles was noticed.

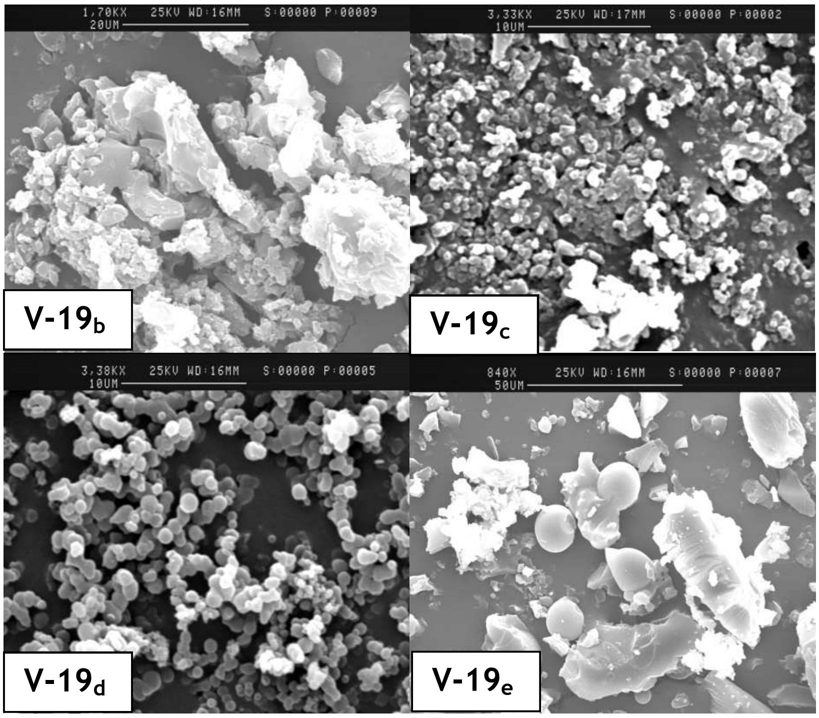

Figure 5.12 SEM micrographs of polymers V-19$_b$, V-19$_c$, V-19$_d$ and V-19$_e$.

Several solvent systems were then used to try to increase the reaction yield and to delay the precipitation of the as well as introduce porosity in the polymer network. TAOSi concentration, reaction temperature and catalyst amount were maintained as in the formation of polymer **V-19$_a$**. Acetonitrile was first used as solvent because typical precipitation polymerisations are normally carried out in neat acetonitrile, which acts as θ solvent. Unfortunately acetonitrile is not normally a good solvent for CM as nitrogen coordinates with the ruthenium and no product was obtained (Table 5.5 entry **V-19$_f$**). The toluene ratio was then raised and it was found that acetonitrile had to be eliminated for the formation of the polymer to occur (Table 5.5 entries **V-19$_g$** and **V-19$_h$**). Mixtures of toluene with other solvents such as chloroform or THF were then attempted but they gave lower yields than in neat toluene (Table 5.5 entries **V-19$_i$** and **V-19$_j$**). As TAOSi has a similar polymer backbone to polydimethylsiloxane (PDMS), it was decided to follow a table found in the literature containing the solubility and polarity parameters of different solvents in relation to PDMS.(19) The table shows that chloroform and THF have similar solubility parameters but THF has a higher dipolar moment (1.7 D) than chloroform (1.0 D). On the other hand, acetonitrile has a dipolar moment of 4.0 D and toluene a dipolar moment of 0.4 D therefore, a solvent more polar than toluene but less polar than chloroform was required. Dioxane (μ = 0.5 D) was then chosen as co-solvent and the reaction gave a high yield (Table 5.5 entry **V-19$_k$**), but non-spherical particles were formed (Figure 5.13 polymer **V-19$_k$**). As no improvement was obtained by selecting a solvent such as dioxane, a solvent less polar than toluene was used in order to improve the reaction conditions. Metathesis reactions with heptane (μ = 0.0 D) were then carried out but similar yields to reactions with toluene were obtained (Table 5.5 entries **V-19$_l$** and **V-19$_m$**).

Polym. ref.	*TAOSi (mL)*	*Solvent 1*	*Solvent 2*	*Solvent ratio*	*HGII (mol%)*	*Yield (mg)*	*Yield (%)*
V-19$_f$	0.10	CH_3CN	-	-	5	0.0	0
V-19$_g$	0.10	Toluene	CH_3CN	40:60	5	0.0	0
V-19$_h$	0.10	Toluene	CH_3CN	95:5	5	1.0	1
V-19$_i$	0.1	Toluene	$CHCl_3$	95:5	5	5.9	8
V-19$_j$	0.1	Toluene	THF	95:5	5	14	17
V-19$_k$	0.1	Toluene	Dioxane	95:5	5	63	81
V-19$_l$	0.15	Toluene	Heptane	95:5	5	14	12
V-19$_m$	0.15	Toluene	Heptane	75:25	5	42	36

Table 5.5 Different solvent systems used for polymer V-19.

SEM micrographs of polymers **V-19$_i$** to **V-19$_m$** show that none of the solvents attempted were able to give better polymer particles than with toluene (Figure 5.13). Spherical particles were obtained by combining toluene with chloroform (**V-19$_i$**) and THF (**V-19$_j$**), but particles were linked in the first case and coagulums appeared in the second one. When dioxane or heptane were used as co-solvents (polymers **V-19$_k$**, **V-19$_l$** and **V-19$_m$**), non-spherical particles and aggregations were formed.

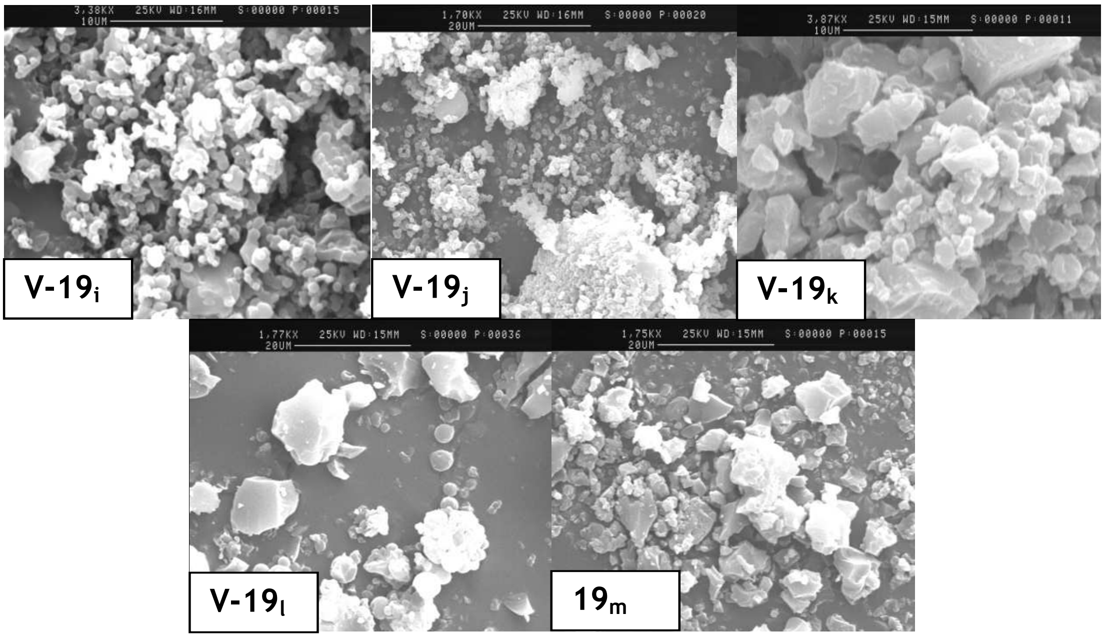

Figure 5.13 SEM micrographs of polymers V-19$_i$, V-19$_j$, V-19$_k$, V-19$_l$ and V-19$_m$.

Since it was not possible to delay the precipitation of the polymer in the media, the amount of catalyst was increased in order to improve the reaction yield. Table 5.6 shows that by increasing the amount of catalyst, larger yields were obtained. As the difference between 10 mol% and 15 mol% was not very significant, it was believed that the reaction reached the plateau state and therefore no larger amounts of catalyst were attempted.

Polym. ref.	*TAOSi (L)*	*Toluene (mL)*	*HGII (mol %)*	*Yield (mg)*	*Yield (%)*
V-19$_a$	0.10	5	5	19	25
V-19$_n$	0.10	5	10	50	65
V-19$_o$	0.1	5	15	61	79

Table 5.6 Different catalyst amounts attempted for polymer V-19.

SEM micrographs of the polymers show that until larger amounts of catalyst used, better quality particles were obtained. The best quality particles were formed when 15 mol% of HGII was used (Figure 5.14). Statistical analysis of the particles of polymer **V-19$_o$** (mean diameter: 0.53 *μm*, SD: 0.12 *μm*, CV: 23%) shows that the particles were polydisperse. Nitrogen sorption porosimetry analysis was performed in polymer **V-19$_o$** and BET surface area of 3 m^2g^{-1} was obtained.

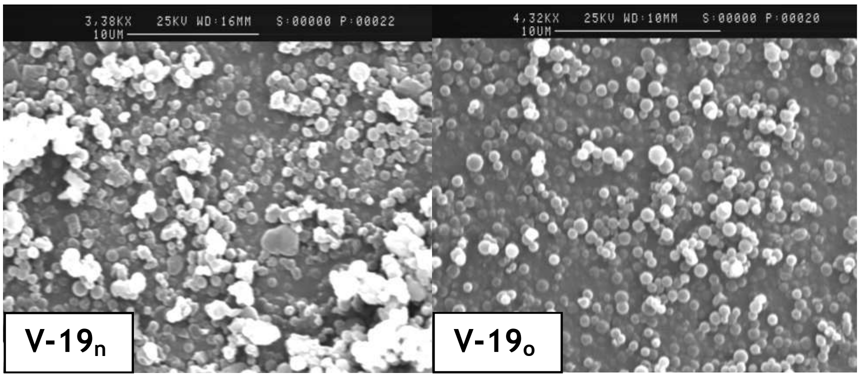

Figure 5.14 SEM micrographs of polymers V-19$_n$ and V-19$_o$.

A swelling test was also performed in polymer **V-19$_o$** to check if the polymer formed was a gel-type polymer. The polymer was packed in a measuring cylinder (1 mL) and 5 mL of toluene were added but the polymer barely swelled (0.1 mL). The polymer was left swelling overnight but no difference was observed. Therefore, non-porous polymer particles were synthesised by this kind of precipitation polymerisation.

Functionalisation of poly(TAOSi) microspheres by a secondary CM reaction

After the synthesis of poly(TAOSi) particles, the functionalisation reaction of the formed particles was first carried out by using CM reaction with methyl acrylate since it was a good CM partner (Figure 5.15). Elemental microanalysis of compound **V-20$_o$** was carried out. The difference in the carbon and hydrogen amount between compounds **V-20$_o$** (*19.9% C, 3.6% H*) and compound **V-19$_o$** (*38.6% C, 5.3% H*) indicates that the CM reaction with compound **II-3** was successful.

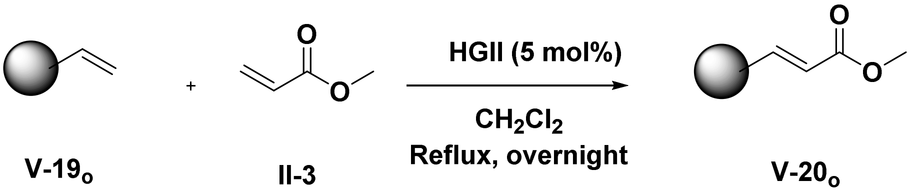

Figure 5.15 CM reaction with methyl acrylate.

FT-IR spectrum of polymer **V-20$_o$** (Figure 5.16a) suggests the success of the reaction, as the peak at 1720 cm^{-1}(C=O str.) may confirm the presence of the carbonyl peak of methyl acrylate. The SEM micrograph of compound **V-20$_o$** shows that the particles were not destroyed after the CM reaction (Figure 5.16b). Statistical analysis of the particles (mean diameter: 0.62 *μm*, SD: 0.20 *μm*, CV: 32%) indicated that particle size increased after the functionalisation reaction was performed. This suggests that the polymer underwent a secondary CM reaction.

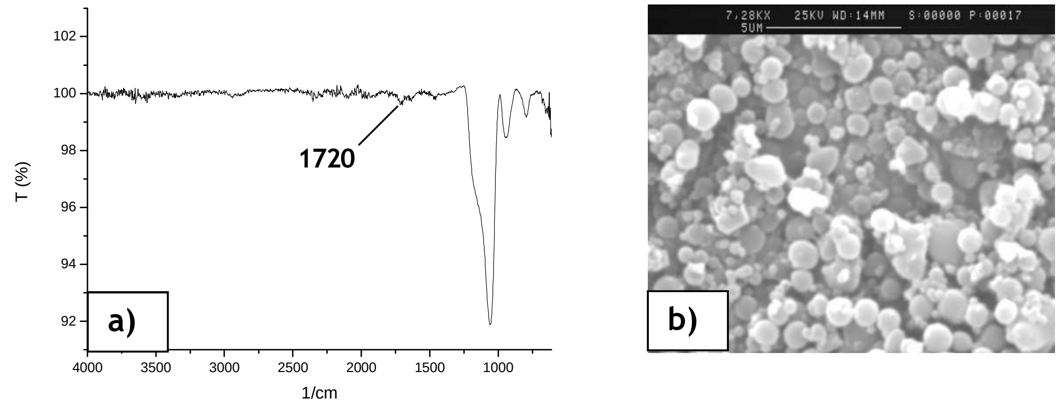

Figure 5.16 a) FT-IR spectrum b) SEM analysis of polymer V-19$_o$ after CM reaction with methyl acrylate.

In order to determine the success of the reaction with more ease, the functionalisation reaction was carried out by using allyl bromide as coupling partner. Allyl bromide was selected to quantify the amount of bromine present in the polymer after CM reaction by elemental microanalysis and thus, to establish the loading level of the functional group on the polymer (Figure 5.17).

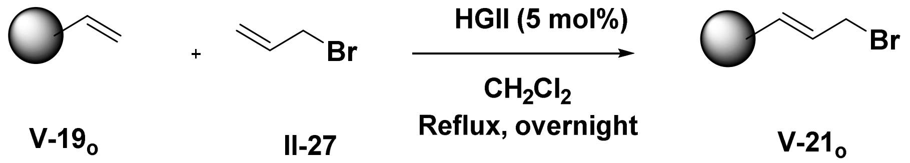

Figure 5.17 CM reaction of poly(TAOSi) with allyl bromide.

Elemental microanalysis was carried out to quantify the amount of bromine in the sample (*18.8% C, 3.6% H, nil/traces Br%*). The amount of carbon and hydrogen indicated that the polymer underwent the CM reaction with allyl bromide. However, it was not possible to quantify the amount of bromine by elemental microanalysis and therefore, a more sensitive technique such as EDX analysis was performed (Figure 5.18a). In the EDX spectrum, a bromine content of 1.03 wt.% was found, indicating that the reaction was successful. SEM analysis was also carried out to check the quality of the particles after the CM reaction with allyl bromide, which shows that the particles were not destroyed after the CM reaction.

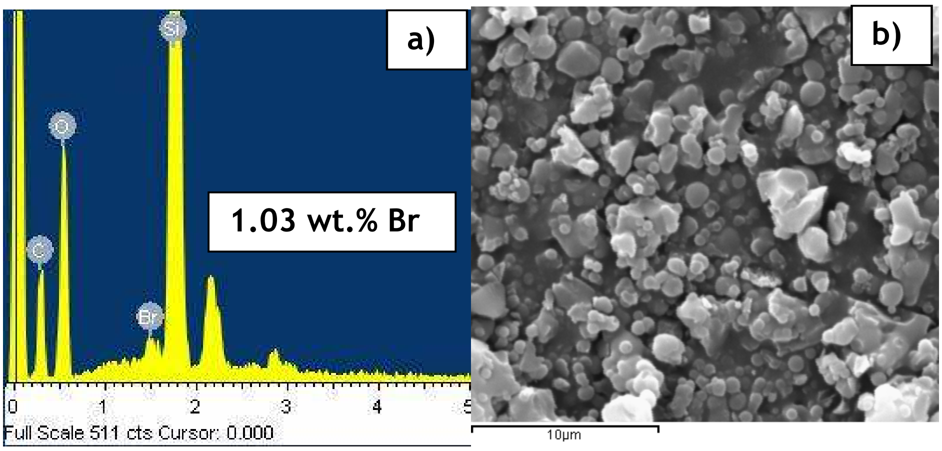

Figure 5.18 a) EDX analysis and b) SEM micrograph of polymer V-21$_o$.

After the success of the CM reactions with methyl acrylate and allyl bromide, a more interesting coupling partner was selected for the CM reaction (Figure 5.19). Compact spherical particles are used in a wide range of applications such as spacers for liquid crystal displays, immunological analysis, and radioactive particles but also are used in separation media.$^{(20)}$ Fmoc-4-allyloxyproline was chosen as coupling partner since it is a zwitterionc compound, which can be used (after the removal of Fmoc group) as a cation or anion exchanger depending on the pH used in the conditioning step of the column.

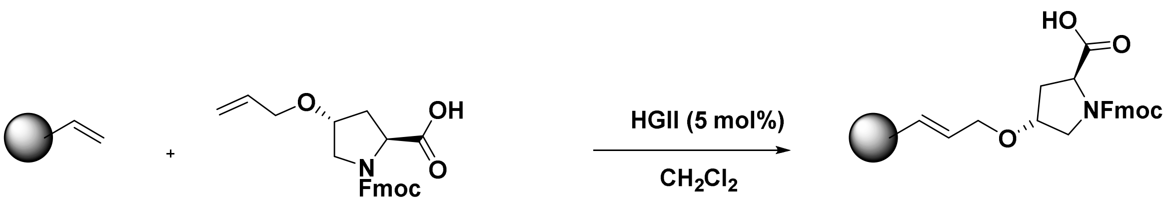

V-19$_o$ II-19 V-22$_o$

Figure 5.19 CM reaction with Fmoc-4-allyloxyproline.

Elemental microanalysis of compound **V-22$_o$** (*21.4% C, 3.3% H, nil/traces N%*) was performed, but nitrogen content was below the detection limits of the analyser and the loading level of the functional group could not be established. However, the success of the reaction was confirmed as the amount of carbon and hydrogen were lower than in poly(TAOSi). The FT-IR spectrum (Figure 5.20a) of compound **V-22$_o$** confirmed that the polymer underwent the CM reaction due to the appearance of the acid group bands at 3400 cm^{-1} (OH str.) and 1705 cm^{-1} (C=O str.). The SEM micrograph (Figure 5.20b) shows that the particles were not destroyed after the functionalisation reaction. Statistical analysis of the particles (mean diameter: 0.68 *μm*, SD: 0.20 *μm*, CV: 29%) was also carried out. The insertion of the coupling partner into the polymer led to an increase in the size of the particles, indicating that the CM reaction with compound **II-19** was successful.

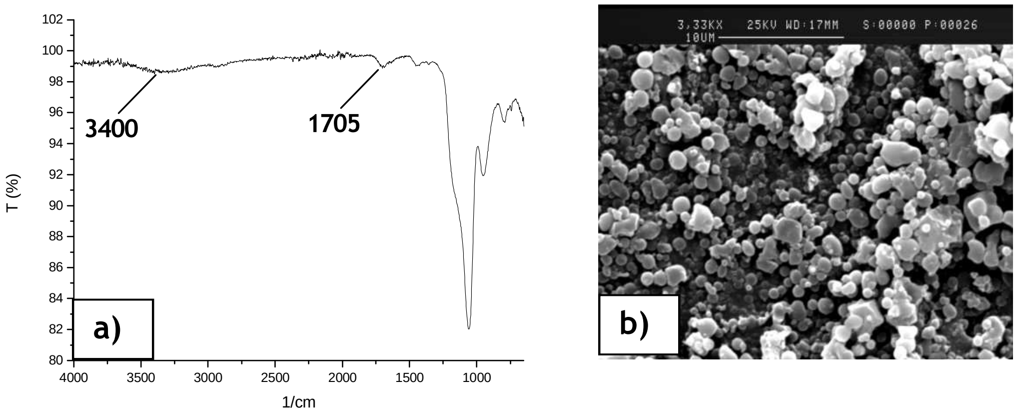

Figure 5.20 a) FT-IR spectrum and b) SEM micrograph of compound V-22$_o$.

Polarity changes in poly(TAOSi)

Upjohn dihydroxylation was performed in polymer **V-19$_o$** to form the corresponding diol moiety in order to obtain polar polymer particles (Figure 5.21). In addition to that, dihydroxylation reaction by using osmium tetroxide was chosen to see if the polymer beads could immobilise osmium by trapping the metal in the polymer network after elimination of the solvent.

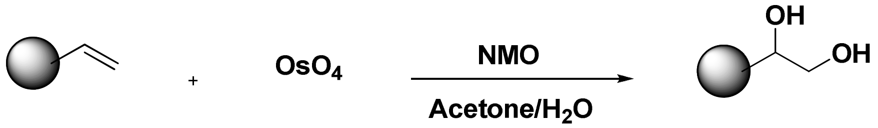

V-19$_o$ **V-23** **V-24$_o$**

Figure 5.21 Upjohn dihydroxylation reaction of polymer V-19$_o$.

The FT-IR spectrum of compound **V-24$_o$** (Figure 5.22a) suggested the success of the dihydroxylation reaction as the broad band of the alcohols appeared at 3400 cm^{-1} (OH str.). Elemental microanalysis of the compound **V-24$_o$** (*8.0% C, 1.8% H*) was also carried out to verify the success of the reaction. The low carbon content suggested that the dihydroxylation reaction was successful. However, the low carbon content registered could also suggest that osmium was immobilised in the polymer network but no more analysis were performed to ascertain the presence of the osmium in the network. The SEM micrograph (Figure 5.22b) shows that after the dihydroxylation reaction, particles aggregated and some coagulums were formed.

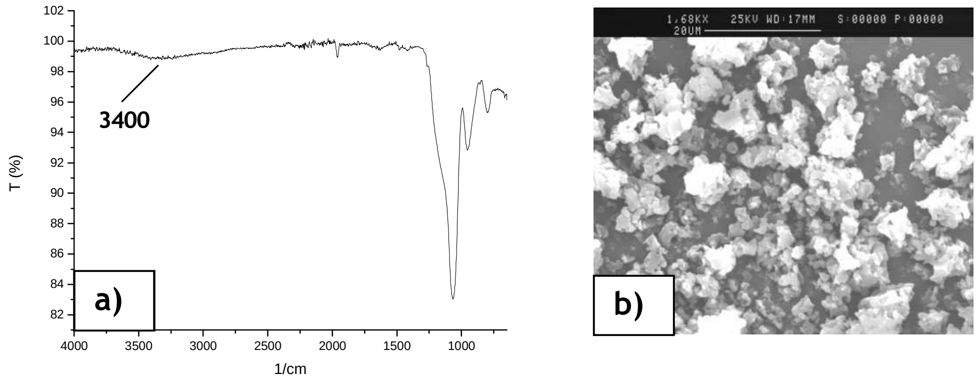

Figure 5.22 a) FT-IR spectrum and b) SEM micrograph of polymer V-24$_o$.

5.3.3. Hypercrosslinking reaction of gel-type poly(DVB-co-AMA) with Triallyloxy phenylsilane (TAPSi)

Taking in consideration the reactivity problem, a multivinyl crosslinker more reactive than TVSi and less reactive than TAOSi that presents more than 2 vinyl groups to improve the selectivity of the HXL polymer needed to be found. For this purpose, tris(allyloxy)(phenyl)silane (TAPSi) was synthesised. The synthesis started from the commercially available trichloro phenylsilane, which was allylated to give TAPSi (Figure 5.23).(21) The first attempt of this reaction was carried out at room temperature overnight but only disubsituted product was obtained after 24 h of reaction. Therefore, the temperature was increased to speed up the reaction and the trisubstituted product was obtained in 55% yield. After the synthesis of the crosslinker, the polymer (**IV-7**) was swollen overnight and then the CM/RCM reaction was performed but no increase of the mass was observed.

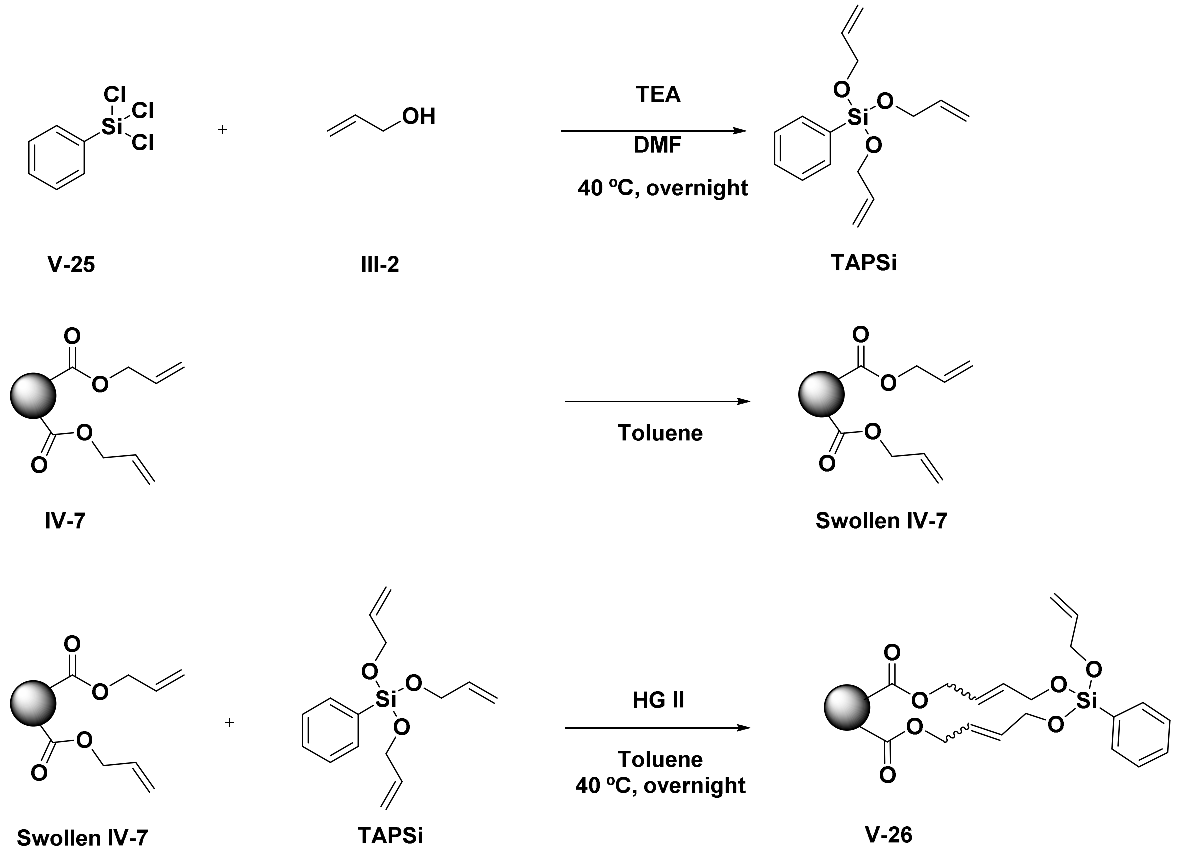

Figure 5.23 Synthesis of TAPSi and CM/RCM reaction with polymer IV-7.

The SEM micrograph of the particles shows (Figure 5.24) that no chemical aggregations or new particles were formed after the metathesis reaction. However, statistical analysis of the particles shows that polymer **V-26** particles (mean diameter: 2.0 *μm*, SD: 0.52 *μm*, CV: 26%) were larger than polymer **IV-7** particles (mean diameter: 1.7 *μm*, SD: 0.63 *μm*, CV: 38%), suggesting that metathesis reaction happened. EDX analysis was then carried out to verify whether the metathesis reaction was performed between TAPSi and polymer **IV-**

7 by quantifying the amount of silicon present in the sample. Unfortunately, no silicon moieties were detected in polymer **V-26** and therefore, nitrogen sorption porosimetry was not performed on the sample.

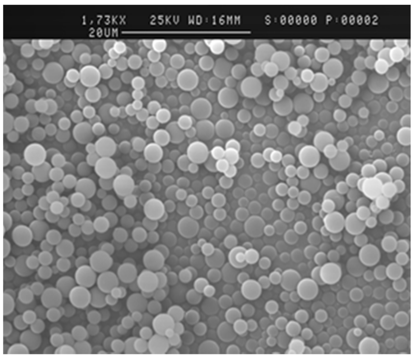

Figure 5.24 SEM micrograph of polymer V-26.

CM/RCM of TAPSi was also carried out in order to check if the monomer could form polymer particles by itself as it happened with TAOSi. However, due to the presence of the phenyl group, the reactivity of TAPSi was lower than the reactivity of TAOSi, interfering with the particles formation.

5.4. CONCLUSIONS

Different polymers were synthesised in chapter 4 with the aim to increase the surface area by using RCM as a hypercrosslinking method. However, only polymers with large amounts of AMA were able to undergo the RCM reaction. In order to increase further the surface areas obtained in chapter 4, tetravinyl compounds such as TVSI and TAOSi were purchased to be used as external crosslinkers. A noteworthy advantage of these tetravinyl compounds was that at least 2 of the olefins would be consumed by CM/RCM giving some type 2 olefins but other type 1 olefins would still remain unreacted providing extra functionality to the polymer microspheres.

Several conditions were applied with different polymers to undergo the CM/RCM reaction with these commercially available external crosslinkers. However, CM/RCM did not take place in any of the cases as the surface areas of the polymers were < 5 m^2g^{-1}. On the other hand, a new type of polymerisation using low amounts of solvent was discovered, as TAOSi underwent CM/RCM on its own and formed new particles when treated with metathesis catalyst. Optimisation of the newly formed polymer particles was carried out and it was found that toluene was the best solvent for the formation of spherical poly(TAOSi) particles. A secondary CM was then successfully carried out with different coupling partners to functionalise the poly(TAOSi) particles. In an attempt to change the polarity of these particles dihydroxylation reaction was then carried out. This result could suggest that the osmium was trapped in the polymer network, although no further analyses were carried out to confirm that due to the lack of the material.

A new external crosslinker, less reactive than TAOSi but more reactive than TVSi, was then synthesised. Unfortunately, no silicon was detected after CM reaction with the polymer was attempted and no new particles were formed either.

5.5. FUTURE WORK

Different tetravinyl monomers were used as potential external crosslinkers to hypercrosslink poly(DVB-*co*-AMA) gel-type polymers, but with no success. One of the possible solutions to increase the surface area could be to have larger alkyl chains in the crosslinking agent. With longer chains, the steric hindrance of the terminal double bonds will be lower and therefore the polymer could undergo easier the CM/RCM with the cross agent. In the future, other tetravinyl monomers could be synthesised to undergo the CM/RCM reaction.

Focusing on poly(TAOSi) polymer particles, one of the aims for the future could be to use a different solvent to delay the nucleation and the precipitation of the particles in the media, as well as to increase the particle size of the polymer. Different solvent systems could also be used in order to introduce porosity on the polymer, and to delay the nucleation of the particles. After further optimisation of this new type of polymerisation, different multivinyl monomers should be tried to generalise this new technique of precipitation polymerisation.

Dihydroxylation reaction in a higher scale should be carried out to ensure if the osmium was immobilised by the poly(TAOSi) polymer network. To ensure that osmium has been trapped on the polymer network, a basic hydrolysis of the putative osmate ester of the polymer should be carried out. Elemental microanalysis will confirm if poly(TAOSi) microspheres can be used as heavy metal scavengers.

5.6. EXPERIMENTAL

5.6.1. Materials

Methyl acrylate, Second-generation Hoveyda Grubbs catalyst, Second-generation Grubbs catalyst, allyl alcohol, allyl bromide, anhydrous DMF, anhydrous dioxane, anhydrous triethylamine, 4-methylmorpholine *N*-oxide, osmium tetroxide 2.5 wt.% in *tert*-butanol, TVSi, TAOSi and trichloro(phenyl)silane were all purchased from Sigma Aldrich and were used as received.

The solvents employed (toluene, acetone, methanol, tetrahydrofuran, chloroform, petroleum ether [b.p. 30-40 °C], ethyl acetate, diethyl ether, heptane) were purchased from Sigma Aldrich as standard laboratory reagent grade. Dry solvents were obtained from an in-house purification system.

5.6.2. Equipment

CM reactions were carried out using a Stuart Scientific S160 incubator (Surrey, UK) and a Stovall low profile roller system (NC, USA). The polymerisations and the functionalisation reactions were performed in Kimax® centrifuge tubes. When required, samples were dried in Townson & Mercer Limited (England) vacuum ovens set to either 40 °C or 70 °C, at 60 mbar pressure.

Elemental microanalysis was performed by the University of Strathclyde Elemental Microanalysis service. C, H and N elemental microanalyses were carried out simultaneously using a Perkin Elmer 2400 Series II analyser, while halogen contents were determined by standard titration methods.

Scanning electron microscopy (SEM) was carried out using a Cambridge Instruments Stereoscan 90. Samples were coated in gold prior to SEM imaging. SEM statistical data was obtained by Image J.

Fourier-Transform Infrared (FT-IR) spectroscopy analyses were carried out using a Shimadzu IRAffinity-1S spectrometer. Samples were scanned over the range 4000-600 cm^{-1} in transmission mode.

The specific surface area measurements were performed using Micromeritics ASAP 2020 nitrogen sorption instrument. Samples were degassed overnight under high vacuum at 100 ^{o}C prior to analysis. Analysis was carried out *via* nitrogen sorption, carried out at 77 K.

EDX analysis was carried out using a XL30 ESEM microscope equipped with an Oxford instrument 10 mm2SDD detector X-act. Samples were coated in palladium prior to SEM imaging.

5.6.3. General hypercrosslinking reaction by using external crosslinkers

The CM/RCM reactions(22) were carried out in a 20 mL Kimax® tube. The polymer was suspended in dry toluene (5 mL) and was left under nitrogen atmosphere overnight to reach the maximum swelling of the polymer. The next day, Second-generation Grubbs catalyst or Second-generation Hoveyda-Grubs catalyst and the external crosslinker were added to the suspension and the resulting mixture was sealed under nitrogen. The tube was placed on a low-profile roller, which was housed inside a temperature-controlled incubator, and rolled at 30 rpm along its long axis. The temperature was ramped from room temperature to 40 °C over one hour and then held at 40 °C overnight. The next day the mixture was allowed to cool down to room temperature. The product was filtered off under vacuum on a 0.22 μm nylon filter membrane and then washed in sequence with 15 mL volumes of dichloromethane, methanol, ethyl acetate, petroleum ether and diethyl ether. The product, in the form of an off-white powder, was dried overnight at 70 °C at 1 mbar.

General FT-IR spectrum of poly(DVB-*co*-AMA) with TVSi: $\bar{\upsilon}\mathrm{cm}^{-1}$ 3050 (=CH str.), 2980, 2900 and 2865 (C-H str.), 1730 (C=O str.) 1600, 1520 and 1460 (C=C str.), 1425 (CH_2 def.), 1270-930 (Si-CH str. and C-O-C str.), 825 (CH def.), 790 and 710 (CH def.).

General FT-IR spectrum of poly(DVB-*co*-AMA) with TAOSi: $\bar{\upsilon}\mathrm{cm}^{-1}$ 3050 (=CH str.), 2980, 2900 and 2865 (C-H str.), 1730 (C=O str.) 1600, 1500 and 1465 (C=C str.), 1425 (CH_2 def.), 1270-920 (Si-CH str., Si-O-C str. and C-O-C str), 830 (CH def.), 790 and 700 (CH def.).

General FT-IR spectrum of poly(DVB-*co*-AMA) with TAPSi: $\bar{\upsilon}\mathrm{cm}^{-1}$ 3050 (=CH str.), 2980, 2900 and 2865 (C-H str.), 1725 (C=O str.) 1600, 1515 and 1465 (C=C str.), 1435 (CH_2 def.), 1270-930 (Si-CH str., Si-O-C str. and C-O-C str), 830 (CH def.), 790 and 700 (CH def.).

5.6.4. Precipitation polymerisation of poly(TAOSi) by CM/RCM reaction

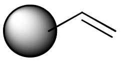

Poly(TAOSi)

Polymerisation reactions(22) were carried out in a 20 mL Kimax® tube. TAOSi (0.1 mL) was dissolved in toluene (5 mL). Second-generation Hoveyda-Grubbs catalyst was then added to the solution and the resulting mixture was sealed under nitrogen. The tube was placed on a low-profile roller, which was housed inside a temperature-controlled incubator, and rolled at 30 rpm along its long axis. The temperature was ramped from room temperature to 40 °C over 30 min and then held at 40 °C overnight. The next day the mixture was allowed to cool down to room temperature. The product was filtered off under vacuum on a 0.22 μm nylon filter membrane and then washed in sequence with 15 mL volumes of acetone, dichloromethane, methanol, ethyl acetate, petroleum ether and diethyl ether. The product, in the form of a light-yellow powder, was dried overnight at 70 °C at 1 mbar.

General FT-IR spectrum of poly(TAOSi): $\bar{\upsilon}$cm^{-1} 3020 (=CH str.), 2930 and 2875 (C-H str.), 1480 (C=C str.), 1415 (CH_2 def.), 1270 (Si-CH str.), 1070 (Si-O-C str.), 915 (C-O def.) and 860 (C-Si str.).

5.6.5. General post-functionalisation reactions of poly(TAOSi)

The functionalisation reactions$^{(22)}$ were carried out in a 50 mL round-bottomed flask equipped with a condenser. Polymer **V-19$_o$** was suspended in dichloromethane (10 mL) under an argon atmosphere. Second-generation Hoveyda-Grubbs catalyst and coupling partner (4 equiv) were then added to the suspension and the resulting mixture was heated under reflux overnight. The next day the reaction was allowed to cool down to room temperature and the product was filtered off under vacuum on a 0.22 µm nylon filter membrane and then washed in sequence with 15 mL volumes of dichloromethane, ethanol, ethyl acetate, petroleum ether and diethyl ether. The product, in the form of a light-yellow powder, was dried overnight at 70 °C at 1 mbar.

Methyl acrylate

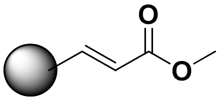

V-20$_o$

The general procedure was used starting with polymer **V-19$_o$** (0.040 g, 0.15 mmol) and with 0.056 mL (0.62 mmol, 4 equiv) of methyl acrylate (**II-3**) to give 0.023 g of polymer **III-20$_o$.**

FT-IR: $\bar{\upsilon}$cm^{-1} 3020 (=CH str.), 2930 and 2875 (C-H str.), 1720 (C=O str.), 1480 (C=C str.), 1415 (CH_2 def.), 1270 (Si-CH str.), 1060 (Si-O-C str.), 950 (C-O def.) and 800 (C-Si str.).

Allyl bromide

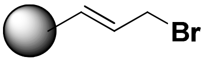

V-21$_o$

The general procedure was used starting with polymer **V-19$_o$** (0.040 g, 0.15 mmol) and with 0.054 mL (0.62 mmol, 4 equiv) of allyl bromide (**II-27**) to give 0.022 g of polymer **III-21$_o$.**

Fmoc-4-allyloxyproline

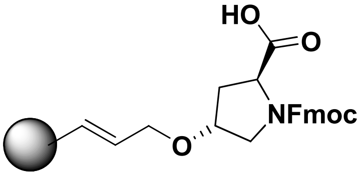

V-22$_o$

The general procedure was used starting with polymer **V-19$_o$** (0.030 g, 0.12 mmol) and with 0.184 mg (0.47 mmol, 4 equiv) of Fmoc-4-allyloxyproline (**II-19**) to give 0.018 g of polymer **III-22$_o$.**

FT-IR: $\bar{\upsilon}$cm^{-1} 3400 (OH str.), 2930 and 2875 (C-H str.), 1700 (C=O str.), 1450 (C=C str.), 1390 (CH$_2$ def.), 1270 (Si-CH str.), 1050 (Si-O-C str.), 950 (C-O def.) and 780 (C-Si str.).

5.6.6. Upjohn dihydroxylation

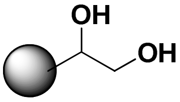

V-24$_o$

Upjohn dihydroxylation was carried out by modifying an existing procedure.(23) Polymer **V-19$_o$** (0.013 g, 0.051 mmol) was suspended in a mixture of acetone and water in 1:1 ratio (13 mL). NMO (0.030 g, 0.25 mmol, 5 equiv) was then added to the suspension and was cooled down to 0 °C for 5 min swirling the flask occasionally. A solution of osmium tetroxide 2.5 wt.% in *tert*-butanol (0.026 mL, 5 mol%) was then added dropwise to the suspension and the mixture was left overnight swirling the flask occasionally. The next day the reaction was quenched with a saturated aqueous solution of Na_2SO_3 and then the product was filtered off under vacuum on a 0.22 µm nylon filter membrane. The product was washed in sequence with 15 mL volumes of acetone, water, dichloromethane, methanol, ethyl acetate, petroleum ether and diethyl ether. The product, in the form of a light-yellow powder (5 mg), was dried overnight at 70 °C at 1 mbar.

FT-IR: $\bar{\upsilon}$cm^{-1} 3400 (OH str.), 2930 and 2875 (C-H str.), 1420 (CH_2 def.), 1270 (Si-CH str.), 1060 (Si-O-C str.), 950 (C-O def.) and 800 (C-Si str.).

5.6.7. Synthesis of tris(allyloxy)(phenyl)silane

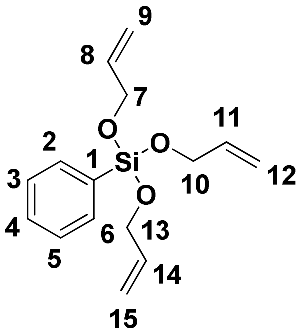

TAPSi

TAPSi was synthesised by modifying an existing procedure.(21) Compound **III-2** (4.3 mL, 63 mmol, 5.0 equiv) and anhydrous TEA (6.1 mL, 44 mmol, 3.5 equiv) were dissolved in anhydrous DMF (10 mL). Compound **V-25** (2.0 mL, 13 mmol) was then added dropwise to the mixture and the reaction was stirred at 40 °C overnight. The reaction was quenched with water (30 mL), extracted with EtOAc (3 x 30 mL) and the combined organic phases were washed with brine (4 x 20 mL) and water (2 x 30 mL). The combined organic extracts were dried with Na_2SO_4, filtered and concentrated *in vacuo*. The crude product was purified by silica gel column chromatography [EtOAc/PE (1:9)] giving TAPSi as a colourless liquid (1.8 g, **55** %).

R*f* 0.8 (EtOAc/PE 1:9)

^{1}H NMR (500 MHz, $CDCl_3$) δ = 7.59 (2H, td, *J* = 7.2, 1.2 Hz, H-(3,5)), 7.29 (1H, tt, *J* = 7.3, 1.2 Hz, H-4), 7.26 (2H, tt, *J* = 7.2, 1.2 Hz, H-(2,6)), 5.99–5.78 (3H, ddt, *J* = 16.9, 10.3, 4.8 Hz, H-(8,11,14)), 5.21 (3H, dq, *J* = 17.0, 1.6 Hz, H-(9a,12a,15a)), 5.00 (3H, dq, *J* = 10.4, 1.6 Hz, H-(9b,12b,15b)), 4.25 (6H, dt, *J* = 4.8, 1.6 Hz, H-(7,10,13).

^{13}C NMR (100 MHz, $CDCl_3$) δ = 136.4 (C-1), 134.9 (C-(2,6)), 134.7 (C-(8,11,14)), 130.7 (C-4), 130.1 (C-(3,5)), 128.0 (C-(9,12,15)), 64.0 (C-(7,10,13)).

HRMS (ESI) *m/z* $(M\text{-}Na)^+$ $C_{15}H_{20}NaO_3Si$ Calcd: 299.1079. Found: 299.1062.

FT-IR: $\bar{\upsilon}$cm^{-1} 3070 (=CH str.), 2980, 2920 and 2865 (C-H str.), 1600 and 1460 (C=C str.), 1425 (CH_2 def.), 1263 (Si-CH str.), 1130-1060 (Si-O-C str.).

5.7. REFERENCES

(1) Davankov, V. A.; Rogoshin, S. V; Tsyurupa, M. P. *J. Polym. Sci. Part C, Polym. Symp.* **1974**, *47*, 95–101.

(2) Fontanals, N.; Marcé, R. M.; Borrull, F.; Cormack, P. A. G. *Polym. Chem.* **2015**, *6*, 7231–7244.

(3) Law, R. V; Sherrington, D. C.; Snape, C. E.; Ando, I.; Kurosu, H. *Macromolecules* **1996**, *29*, 6284–6293.

(4) Joseph, R.; Ford, W. T.; Zhang, S.; Tsyurupa, M. P.; Pastukhov, A. V; Davankov, V. A. *J. Polym. Sci. Part A Polym. Chem.* **1996**, *35*, 695–701.

(5) Zhang, D.; Tao, L.; Ju, J.; Wang, Y.; Wang, Q.; Wang, T. *Polymer* **2015**, *60*, 234–240.

(6) Lee, J.-Y.; Wood, C. D.; Bradshaw, D.; Rosseinsky, M. J.; Cooper, A. I. *Chem. Commun.* **2006**, *25*, 2670–2672.

(7) Hubbard, K. L.; Finch, J. A.; Darling, G. D. *React. & Funct. Polym.* **1999**, *39*, 207–225.

(8) Pastukhov, A. V.; Tsyurupa, M. P.; Davankov, V. A. *J. Polym. Sci. Part B Polym. Phys.* **1999**, *37*, 2324–2333.

(9) Germain, J.; Fréchet, J. M. J.; Svec, F. *J. Mater. Chem.* **2007**, *17*, 4989–4997.

(10) Germain, J.; Fréchet, J. M. J.; Svec, F. *Chem. Commun.* **2009**, *12*, 1526–1528.

(11) Li, B.; Su, F.; Luo, H. K.; Liang, L.; Tan, B. *Microporous Mesoporous Mater.* **2011**, *138*, 207–214.

(12) Luo, Y.; Li, B.; Wang, W.; Wu, K.; Tan, B. *Adv. Mater.* **2012**, *24*, 5703–5707.

(13) Luo, Y.; Zhang, S.; Ma, Y.; Wang, W.; Tan, B. *Polym. Chem.* **2013**, *4*, 1126–1131.

(14) Dawson, R.; Ratvijitvech, T.; Corker, M.; Laybourn, A.; Khimyak, Y. Z.; Cooper, A. I.; Adams, D. J. *Polym. Chem.* **2012**, *3*, 2034.

(15) Yao, S.; Yang, X.; Yu, M.; Zhang, Y.; Jiang, J.-X. *J. Mater. Chem. A* **2014**, *2*, 8054.

(16) Dawson, R.; Stöckel, E.; Holst, J. R.; Adams, D. J.; Cooper, A. I. *Energy Environ. Sci.* **2011**, *4*, 4239.

(17) Maya, F.; Svec, F. *Polymer* **2014**, *55*, 340–346.

(18) Wang, Y.; Jimenez, M.; Hansen, A. S.; Raiber, E. A.; Schreiber, S. L.; Young, D. W. *J. Am. Chem. Soc.* **2011**, *133*, 9196–9199.

(19) Lee, J. N.; Park, C.; Whitesides, G. M. *Anal. Chem.* **2003**, *75*, 6544–6554.

(20) Christensen, B. E.; Myhr, M. H.; Aune, O.; Hagen, S.; Berge, A.; Ugelstad, J. *Carbohydr. Polym.* **1996**, *29*, 217–223.

(21) Waser, J.; Nambu, H.; Carreira, E. M. *J. Am. Chem. Soc.* **2005**, *127*, 8294–8295.

(22) Chatterjee, A. K.; Choi, T. L.; Sanders, D. P.; Grubbs, R. H. *J. Am. Chem. Soc.* **2003**, *125*, 11360–11370.

(23) VanRheenen, V.; Kelly, R. C.; Cha, D. Y. *Tetrahedron Lett.* **1976**, *23*, 1973–1976.

CHAPTER 6

GENERAL CONCLUSIONS AND ADDITIONAL FUTURE WORK

6.1. GENERAL CONCLUSIONS AND ADDITIONAL FUTURE WORK

In conclusion, olefin metathesis to chemically modify polymer microspheres has been shown to be a facile, versatile and mild method, for both post-polymerisation chemical modification reactions with a wide range of interesting coupling partners and as hypercrosslinking process.

Porous poly(DVB-55) microspheres were first synthesised by using a mixture of acetonitrile and toluene as solvents. However, due to the large amount of toluene needed for the functionalisation, polydisperse particles with broad size distribution were obtained and therefore, it was decided to change the co-solvent. By using THF as co-solvent, narrow size distribution particles were obtained.

The pendent vinyl groups that remained unreacted after the polymerisation of DVB-55 were subjected to cross metathesis. A wide range of interesting and useful functional groups were installed on the polymer under mild conditions, maintaining the unsaturation for possible further functionalisation. The intrinsic porosity and the well-defined physical format of the microspheres render them eminently suitable for a range of potential application.

In order to increase the surface area of the microspheres and the loading level of the functional groups, it was decided to use a secondary divinyl monomer for precipitation copolymerisation reaction with DVB and AMA was selected. The choice of the solvent proved difficult as the amount required for functionalisation resulted in aggregation of the particles. Toluene was used as porogenic solvent but gel-type poly(DVB-*co*-AMA) particles were obtained. These particles were then subjected to functionalisation *via* CM reaction with different coupling partners and functionalised polymer particles with higher loadings of the functional groups were obtained.

After the gel-type polymers were obtained, toluene was eliminated from the system and precipitation copolymerisation reactions between DVB-55 and DVB-80 to use ring-closing metathesis as an internal hypercrosslinking method. It was observed that only polymers with large amounts of AMA were capable to undergo the RCM reaction, giving surface areas of almost 500 m^2g^{-1}.

Multivinyl external crosslinkers such as tetravinysilane, tetraallylorthosilicate and tris(allyl)phenyl silane were utilised as coupling partners for CM/RCM reaction for the external hypercrosslinking of the gel-type poly(DVB-*co*-AMA) polymers. No hypercrosslinking was observed in any of the cases although new polymer particles composed of only tetrallylorthosilicate were discovered. This new discovery was optimised and quasi-monodispersed particles were obtained by precipitation polymerisation reaction *via* CM/RCM reaction. These particles were also functionalised by a secondary CM reaction with some interesting compounds such as 4-allyloxy proline. UpJohn dihydroxylation was also carried out to change the polarity of the particles. The dihydroxylation was successful but further analysis needs to be carried out as it is suspected that the osmate ester was trapped within the polymer network.

Given the success of olefin metathesis methods for the functionalisation of polymer microspheres, in the future, this methodology could be extended to the functionalisation of linear or branched polymers such as poly(AMA) by CM with different coupling partners. In addition to that, crosslinking of the linear or branched polymer could also be attempted either internally or externally in order to form polymer microspheres by using RCM or CM/RCM reactions.